CENTRAL RESEARCH LIBRARY
DOCUMENT COLLECTION

ORNL-2396
Chemistry-General
TID-4500 (14th ed.)

MARTIN MARIETTA ENERGY SYSTEMS LIBRARIES
3 4456 0350544 6

cy. 4

GUIDE TO THE PHASE DIAGRAMS OF THE FLUORIDE SYSTEMS

J. E. Ricci

CENTRAL RESEARCH LIBRARY
DOCUMENT COLLECTION
LIBRARY LOAN COPY
DO NOT TRANSFER TO ANOTHER PERSON
If you wish someone else to see this document, send in name with document and the library will arrange a loan.

OAK RIDGE NATIONAL LABORATORY
operated by
UNION CARBIDE CORPORATION
for the
U.S. ATOMIC ENERGY COMMISSION

Printed in USA. Price $2.75 cents. Available from the

Office of Technical Services
U. S. Department of Commerce
Washington 25, D. C.

LEGAL NOTICE

This report was prepared as an account of Government sponsored work. Neither the United States, nor the Commission, nor any person acting on behalf of the Commission:

A. Makes any warranty or representation, express or implied, with respect to the accuracy, completeness, or usefulness of the information contained in this report, or that the use of any information, apparatus, method, or process disclosed in this report may not infringe privately owned rights; or

B. Assumes any liabilities with respect to the use of, or for damages resulting from the use of any information, apparatus, method, or process disclosed in this report.

As used in the above, "person acting on behalf of the Commission" includes any employee or contractor of the Commission to the extent that such employee or contractor prepares, handles or distributes, or provides access to, any information pursuant to his employment or contract with the Commission.

ORNL-2396
Chemistry-General
TID-4500 (14th ed.)

Contract No. W-7405-eng-26

REACTOR PROJECTS DIVISION

GUIDE TO THE PHASE DIAGRAMS OF THE FLUORIDE SYSTEMS

J. E. Ricci

Consultant to Oak Ridge National Laboratory from New York University, Department of Chemistry

DATE ISSUED

NOV 13 1958

OAK RIDGE NATIONAL LABORATORY
Oak Ridge, Tennessee
operated by
UNION CARBIDE CORPORATION
for the
U.S. ATOMIC ENERGY COMMISSION

MARTIN MARIETTA ENERGY SYSTEMS LIBRARIES

3 4456 0350544 6

PREFACE

A comprehensive study of fused-salt phase equilibria has been in progress at the Oak Ridge National Laboratory for several years in connection with reactor technology. In the course of that study, several complex fused-salt ternary systems have become well enough understood that nearly complete phase diagrams of the systems could be constructed.[1] Detailed discussion of the phase equilibria occurring in those systems is included herein.

Except for the $LiF-BeF_2-UF_4$ and $NaF-BeF_2-UF_4$ systems, each of the diagrams of ternary systems included in this discussion was derived at ORNL in the Fused Salt Chemistry Section, under the direction of W. R. Grimes.

Because it was felt that this collection of fluoride phase diagrams might prove more valuable if accompanied with a discussion of some of the types of phase relations illustrated in them, the following treatment was prepared. The purpose is to present some general principles and explanations which should aid in the reading, interpretation, and use of the actual diagrams in the collection and of other similar diagrams which may still be determined. While the relations are usually explicitly shown, at least as far as they are known, in the temperature-composition diagrams of the binary systems, the corresponding relations are not always equally apparent in the usual "phase diagram" of a ternary system of any complexity. In either case, moreover, the diagram does not show the actual data and observations upon which the diagram itself, essentially an inference, is based, nor does it give any idea of the amount of work, in experimentation and in thought, underlying the construction of the diagram. This aspect of the diagrams, however, is something best presented and treated by the investigators themselves.

All the diagrams in the collection represent "condensed systems": i.e., they show the temperature-composition relations between solid and liquid phases under one atmosphere of open pressure. For chemical reasons the atmosphere was actually helium or argon. No two-liquid equilibria were encountered. Limited miscibility of solids is involved in some of the diagrams, but there are no critical solution (or consolute) points for solid solution. The discussion will deal only with types of phase equilibria actually represented in the systems.

We shall treat first the essentials involved in the binary diagrams of the collection, and then, more extensively, the essential relations for the several ternary diagrams. The last sections will consider specifically the ternary systems and their constituent binary systems.

---

[1] R. E. Thoma (ed), *Phase Diagrams of Nuclear Reactor Materials*, ORNL-2548 (to be published).

CONTENTS

PREFACE iii

LIST OF FIGURES vii

PART I. GENERAL PRINCIPLES

1. BINARY DIAGRAMS 3
   - 1.1. Pure Components as Solid Phases 3
   - 1.2. Pure Compounds 3
     - Relation Between Congruence and Incongruence of Melting for a Binary Compound 4
   - 1.3. Solid Solution 4
     - Continuous Solid Solution 4
     - Miscibility Gap in Solid Solution 5
     - Solid Solution and Polymorphism 5
2. TERNARY EQUILIBRIUM OF LIQUID AND ONE SOLID (SURFACES) 7
   - 2.1. Fixed Solid 8
   - 2.2. Variable Solid (Solid Solution) 8
     - Fractionation Path 9
     - Equilibrium Path 9
3. TERNARY EQUILIBRIUM OF LIQUID AND TWO SOLIDS (CURVES) 11
   - 3.1. Reaction Types 11
   - 3.2. Maximum and Minimum Temperature Points 12
   - 3.3. Equilibrium Crystallization Process for Liquid on a Two-Solid Curve 12
4. TERNARY CONDENSED INVARIANT POINTS (FOUR PHASES) 14
   - 4.1. Binary Decompositions in Presence of Ternary Liquid 14
     - "Pure" Solids 14
     - Effect of the Third Component Entering into Solid Solution 14
   - 4.2. Types of Ternary Invariants 15
     - Type A Invariant: Triangular or Terminal Type of Invariant 15
     - Type B Invariant: Quadrangular, Diagonal, or Metathetical Type of Invariant 15
   - 4.3. Relations of the Three Liquid Curves at Their Invariant Intersection 15
   - 4.4. Congruent and Incongruent Crystallization End Points 17
   - 4.5. Melting Points of Ternary Compounds 19
   - 4.6. Invariants Involving Solids Only 19
5. CRYSTALLIZATION PROCESS WITH PURE SOLIDS 20
6. CYRSTALLIZATION PROCESS WITH CONTINUOUS BINARY SOLID SOLUTION 25
   - 6.1. Fractionation Process 26
   - 6.2. Equilibrium Process 26
7. CRYSTALLIZATION PROCESS WITH SOLID SOLUTIONS AND SEVERAL INVARIANTS 29
   - 7.1. The Phase Diagram 29
   - 7.2. Equilibrium Crystallization Process 30
   - 7.3. Process of Crystallization with Perfect Fractionation 32
   - 7.4. Ternary Solid Solution in Compound D_1 33

PART II. THE ACTUAL DIAGRAMS

8. SYSTEM $X-U-V$: $LiF-UF_4-BeF_2$ 37

9. SYSTEM $Y-U-V$: $NaF-UF_4-BeF_2$ 40

10. SYSTEM $Y-U-R$: $NaF-UF_4-RbF$ 44

11. SYSTEM $Y-Z-R$: $NaF-ZrF_4-RbF$ 47

11.1. The System According to Figure 11.3 and Neglecting Solid Solution 47

11.2. Consideration of Solid Solution Formation 49

11.3. The Region for Compounds G and H of System $R-Z$ 49
The Region As Shown in Figures 11.6 and 11.7 49
The Region As Shown in Figures 11.8 and 11.9 51

11.4. The Region Involving Compounds B and D of System $Y-Z$ 52

12. SYSTEM $Y-Z-X$: $NaF-ZrF_4-LiF$ 55

12.1. Subsystem $Y-A-G-X$ 56

12.2. Subsystem $E-Z-H$ 58

12.3. Subsystem $A-E-H-G$ 59

12.4. Subsolidus Decompositions of Compounds G and I 60
Decomposition of Compound I 60
Decomposition of Compound G 61

13. SYSTEM $Y-U-X$: $NaF-UF_4-LiF$ 64

13.1. The Invariants P_A, P_C, P_G, and P_E 64
The Invariant P_A 64
The Invariant P_C 65
The Invariant P_G 66
The Invariant P_E 66

13.2. The Region DUH 68

13.3. The Region $YDHX$ 71

13.4. Fractionation Process on the Solid Solution Fields 73

14. SYSTEM $Y-U-Z$: $NaF-UF_4-ZrF_4$ 75

14.1. General Characteristics 75

14.2. Subsystem $Y-A-G$ 75

14.3. Subsystem $A-D-K-G$ 79
The Region Involving A, B, C, and D 80
The Region Involving G, H, I, and K 87
Fractionation Processes in the Subsystem $A-D-K-G$ 89
Subsolidus Reactions Involving Compounds A, H, and J 90

14.4. Subsystem $D-U-Z-K$ 91
Equilibrium Crystallization Along Curves 91
Fractionation Processes in the Subsystem $D-U-Z-K$ 94
Equilibrium Crystallization in the U_s Field 95
Subsolidus Compounds E and F 96

15. SYSTEM $Y-W-Z$: $NaF-ThF_4-ZrF_4$ 97

LIST OF FIGURES

1.1. Pure components as solids 3
1.2. Retrograde solubility curve 3
1.3. Binary compounds 3
1.4. "Inverse" fusion of binary compound 5
1.5. Singular point between congruence and incongruence of melting 5
1.6. Continuous solid solution without maximum or minimum 5
1.7. Continuous solid solution with minimum 5
1.8. Discontinuous solid solution, eutectic case 6
1.9. Discontinuous solid solution, peritectic case 6
1.10. Elevation of transition temperature, involving liquid 6
1.11. Elevation of transition temperature, subsolidus 6
1.12. Depression of transition temperature, involving liquid 6
1.13. Depression of transition temperature, subsolidus 6
1.14. Depression of transition temperature, lower form pure 6

2.1. Liquidus surface for pure solid A 8
2.2. Fractionation path on surface for liquid in equilibrium with A–B solid solution 9
2.3. Relation between equilibrium path and fractionation paths: for ternary solid solution 10
2.4. Relation between equilibrium path and fractionation paths: for binary solid solution 10

3.1. Change from even to odd reaction: two solid solutions 11
3.2. Change from odd to even reaction: two solid solutions 11
3.3. Change from odd to even reaction: two pure solids 11
3.4. Temperature maximum in reaction L – calories $\longrightarrow S_1 + S_2$ 12
3.5. Temperature minimum in reaction $L + S_1$ – calories $\longrightarrow S_2$ 12
3.6. Three-phase triangle on curve for L – calories $\longrightarrow S_1 + S_2$ 12

4.1. Type A invariant 16
4.2. Type B invariant 16
4.3. Arrangement of curves at a eutectic 16
4.4. Arrangement of curves for case (a) and case (b) 16
4.5. Arrangement of curves for case (c) and case (d) 16
4.6. Impossible angles of intersection 17
4.7. Eutectic triangle contains only the eutectic "point" E 17
4.8. Eutectic triangle also contains several peritectic "points" 17
4.9. Invariant, case (a) 19
4.10. Invariant, case (d) 19
4.11. Invariant, case (c) 19
4.12. Invariant, case (b) 19
4.13. Semicongruent melting point of ternary compound M_2 19

5.1. Two three-solid arrangements for two binary compounds 20
5.2. Necessary arrangement of curves and invariants for the two cases in Fig. 5.1 20
5.3. Hypothetical ternary system with three binary compounds 21
5.4. The section A–D_2 of Fig. 5.3 21
5.5. Isotherm between p_1 and r 21
5.6. Isotherm between r and m 23
5.7. Isotherm above P_3 and still above E_1 and E_2 24
5.8. Isotherm at P_3 24
5.9. The section D_1–D_2 24
5.10. The section D_3–D_2 24
5.11. The section C–D_3 24
5.12. The section D_1–B 24

6.1. Ternary system with continuous A–B solid solution and pure C 25
6.2. The binary system A–B of Fig. 6.1 25
6.3. Arbitrary section, from C to the AB side 25
6.4. Fractionation paths for the solid solution surface 26
6.5. Equilibrium paths and inflection point of fractionation path 28

7.1. Ternary system with discontinuous A–B solid solution and two binary compounds 29
7.2. Binary system A–B of Fig. 7.1 29
7.3. The invariant reaction planes of Fig. 7.1 30
7.4. The section D_2–S_m 30
7.5. Isotherm above p 31
7.6. Isotherm just below p 31
7.7. Isotherm below m but above P_1 and above E_3 31
7.8. The section D_1–D_2 32
7.9. The section D_1–B 32
7.10. The section A–D_2 32
7.11. Portion of Fig. 7.3, with some ternary solid solution at D_1 33
7.12. Isotherm for Fig. 7.11, between p and P_1 33
7.13. Isotherm just above P_1 33
7.14. Part of the section D_1–D_2, for Fig. 7.11 33

8.1. System X–U: LiF–UF_4 37
8.2. System U–V: UF_4–BeF_2 37
8.3. System X–V: LiF–BeF_2 37
8.4. System X–U–V: LiF–UF_4–BeF_2 38
8.5. Isotherm involving the invariant P_A 39
8.6. Isotherm above P_2 and P_1 39
8.7. The section C–V: $LiF{\cdot}4UF_4$–BeF_2 39
8.8. The section B–V: $7LiF{\cdot}6UF_4$–BeF_2 39

8.9. The section B–D: $7LiF \cdot 6UF_4$–$2LiF \cdot BeF_2$ 39
8.10. The section A–D: $4LiF \cdot UF_4$–$2LiF \cdot BeF_2$ 39

9.1. System Y–U: NaF–UF_4 40
9.2. System Y–V: NaF–BeF_2 40
9.3. System Y–U–V: NaF–UF_4–BeF_2 41
9.4. Isotherms involving compounds E and F ($NaF \cdot 2UF_4$ and $NaF \cdot 4UF_4$) 42
9.5. The section F–V: $NaF \cdot 4UF_4$–BeF_2 42
9.6. The section E–V: $NaF \cdot 2UF_4$–BeF_2 42
9.7. The section D–V: $7NaF \cdot 6UF_4$–BeF_2 43
9.8. The section B–H: $2NaF \cdot UF_4$–$2NaF \cdot BeF_2$ 43
9.9. The section D–H: $7NaF \cdot 6UF_4$–$2NaF \cdot BeF_2$ 43

10.1. System R–U: RbF–UF_4 44
10.2. System Y–R: NaF–RbF 44
10.3. System Y–U–R: NaF–UF_4–RbF 45
10.4. The section D–N: $7NaF \cdot 6UF_4$–$RbF \cdot 6UF_4$ 46
10.5. The section D–M: $7NaF \cdot 6UF_4$–$RbF \cdot 3UF_4$ 46
10.6. The section D–K: $7NaF \cdot 6UF_4$–$2RbF \cdot 3UF_4$ 46
10.7. The section D–I: $7NaF \cdot 6UF_4$–$7RbF \cdot 6UF_4$ 46
10.8. The section B–H: $2NaF \cdot UF_4$–$2RbF \cdot UF_4$ 46
10.9. The section Y–Q: NaF–$NaF \cdot RbF \cdot UF_4$ 46
10.10. The section Q–G: $NaF \cdot RbF \cdot UF_4$–$3RbF \cdot UF_4$ 46

11.1. System Y–Z: NaF–ZrF_4 48
11.2. System R–Z: RbF–ZrF_4 48
11.3. System Y–Z–R: NaF–ZrF_4–RbF 49
11.4. The partial section M_1–Z: $NaF \cdot RbF \cdot ZrF_4$–$ZrF_4$ 50
11.5. Divisions of Fig. 11.3 50
11.6. Detail of binary system Z–R: ZrF_4–RbF 50
11.7. Region involving compounds H and G: $5NaF \cdot 2ZrF_4$ and $3NaF \cdot ZrF_4$ 51
11.8. Detail of system Z–R, for H ($5NaF \cdot 2ZrF_4$) assumed pure 52
11.9. Region involving H and G, for H pure: $5NaF \cdot 2ZrF_4$ (pure) and $3NaF \cdot ZrF_4$ 52
11.10. Region involving solid solutions in Y–Z (NaF–ZrF_4) system 53

12.1. System X–Z: LiF–ZrF_4 55
12.2. System Y–X: NaF–LiF 55
12.3. System Y–Z–X: NaF–ZrF_4–LiF 56
12.4. Region below section A–G ($3NaF \cdot ZrF_4$–$3LiF \cdot ZrF_4$) 57
12.5. The section A–G ($3NaF \cdot ZrF_4$–$3LiF \cdot ZrF_4$) 57
12.6. Region above section E–H ($7NaF \cdot 6ZrF_4$–$2LiF \cdot ZrF_4$) 58
12.7. The section F–I ($3NaF \cdot 4ZrF_4$–$3LiF \cdot 4ZrF_4$) 58

12.8. Middle region of system *Y–Z–X*: $NaF–ZrF_4–LiF$ 59
12.9. Decomposition of compound *I* ($3LiF·4ZrF_4$) 60
12.10. The section *F–I* ($3NaF·4ZrF_4–3LiF·4ZrF_4$) 61
12.11. Decomposition of compound *G* ($3LiF·ZrF_4$) 62
12.12. The section *A–G* ($3NaF·ZrF_4–3LiF·ZrF_4$) 63

13.1. System *X–U*: $LiF–UF_4$ 64
13.2. System *Y–U–X*: $NaF–UF_4–LiF$ 65
13.3. The section *D–H* ($7NaF·6UF_4–7LiF·6UF_4$) 66
13.4. Decomposition of compound *C* ($5NaF·3UF_4$) 67
13.5. Decomposition of compound *G* ($4LiF·UF_4$) 68
13.6. Formation of compound *E* ($NaF·2UF_4$) 69
13.7. Region above section *D–H* ($7NaF·6UF_4–7LiF·6UF_4$) 70
13.8. The section *E–H* ($NaF·2UF_4–7LiF·6UF_4$) 71
13.9. Region below section *D–H* ($7NaF·6UF_4–7LiF·6UF_4$) 72
13.10. The section *B–G* ($2NaF·UF_4–4LiF·UF_4$) 73
13.11. Detail of Fig. 13.2, near compound *C* ($5NaF·3UF_4$) 74

14.1. System *Y–Z*: $NaF–ZrF_4$ 76
14.2. System *U–Z*: $UF_4–ZrF_4$ 76
14.3. System *Y–U–Z*: $NaF–UF_4–ZrF_4$ 77
14.4. The section *A–G* ($3NaF·UF_4–3NaF·ZrF_4$) 78
14.5. The section *D–K* ($7NaF·6UF_4–7NaF·6ZrF_4$) 78
14.6. The section between *Y* (NaF) and the point on *UZ* that represents the composition $1UF_4–1ZrF_4$ 78
14.7. Subsystem *Y–A–G*: $NaF–3NaF·UF_4–3NaF·ZrF_4$ 79
14.8. Subsystem *Y–A–G* ($NaF–3NaF·UF_4–3NaF·ZrF_4$): fractionation paths 79
14.9. Subsystem *A–D–K–G*: system $NaF–UF_4–ZrF_4$, region between 3:1 and 7:6 solid solutions 79
14.10. Scheme I for compound *C* ($5NaF·3UF_4$) 81
14.11. Sequence of isotherms for Scheme I 82–83
14.12. The section between *C* ($5NaF·3UF_4$) and the point on *YZ* that represents the composition $5NaF–3ZrF_4$, in Scheme I 84
14.13. Scheme II for compound *C* ($5NaF·3UF_4$) 86
14.14. Sequence of isotherms for Scheme II 87
14.15. The section between *C* ($5NaF·3UF_4$) and the point on *YZ* that represents the composition $5NaF–3ZrF_4$, in Scheme II 88
14.16. Lower part of subsystem *A–D–K–G*: the $NaF–ZrF_4$ side of Fig. 14.9 89
14.17. Solids left after complete solidification, in region *YDK* ($NaF–7NaF·6UF_4–7NaF·6ZrF_4$) 90
14.18. Decomposition of compound *A* ($3NaF·UF_4$) 91
14.19. Transition in compound *H* ($5NaF·2ZrF_4$) 92

14.20. Appearance of compound J ($3NaF \cdot 2ZrF_4$) 93
14.21. Subsystem $D-U-Z-K$: system $NaF-UF_4-ZrF_4$ between the 7:6 solid solution and the UF_4-ZrF_4 solid solution 93
14.22. Subsystem $D-U-Z-K$: temperature contours 93
14.23. Subsystem $D-U-Z-K$: fractionation paths 94
14.24. Appearance of compounds E and F ($NaF \cdot 2UF_4$ and $NaF \cdot 4UF_4$) 96

15.1. System $Y-W$: $NaF-ThF_4$ 97
15.2. System $W-Z$: ThF_4-ZrF_4 97
15.3. System $Y-W-Z$: $NaF-ThF_4-ZrF_4$ 98
15.4. System $Y-W-Z$: $NaF-ThF_4-ZrF_4$ (revised) 99
15.5. Middle region of system $Y-W-Z$ ($NaF-ThF_4-ZrF_4$) 100
15.6. Subsolidus transition in compound B ($5NaF \cdot 2ZrF_4$) 101
15.7. $W-Z$ region of system $Y-W-Z$ (ThF_4-ZrF_4 region of system $NaF-ThF_4-ZrF_4$) 102
15.8. Fractionation paths for the solid solution surface of system $Y-W-Z$ ($NaF-ThF_4-ZrF_4$) 103

PART I

GENERAL PRINCIPLES

1. BINARY DIAGRAMS

1.1 PURE COMPONENTS AS SOLID PHASES

With the pure components as the only solid phases in a binary system (Fig. 1.1), the melting points (T_A and T_B) are lowered and the system is always eutectic in type. In Fig. 1.1 the eutectic e involves the high-temperature form of A (A_α) and the low-temperature form of B (B_β); at the temperature of e the phase reaction is:

$$L(e) - \text{calories} \rightleftharpoons A_\alpha + B_\beta \ .$$

If T'_A is the transition temperature for the forms of A, then the two-solid mixture consists, at equilibrium, of A_α and B_β above T'_A and of A_β and B_β below T'_A. If T'_B is the transition temperature for the polymorphic forms of B, there will be a break in the freezing-point curve (or solubility curve) of the B solid at the temperature T'_B, unaffected by the A if both forms of the B solid are pure. Above T'_B, the liquid is in equilibrium with B_α, below T'_B with B_β. If the transition $B_\alpha \rightarrow B_\beta$ fails to occur on cooling, a metastable eutectic e(m) is possible, for liquid in (metastable) equilibrium with A_α and B_α.

(It is possible for a solubility curve to show a "retrograde" temperature effect, even down to the eutectic, in which case we would have Fig. 1.2. Retrograde changes of solubility with temperature were not encountered in the present systems, whether binary or ternary, but reference will be made to this question later.)

Liquids with composition between A and e, such as point a (Fig. 1.1), give A_α as primary crystallization product when cooled to the curve $T_A e$. At the temperature T_x the equilibrium mixture consists of solid A_α and liquid l in the ratio (by weight or by moles, depending on the units of the diagram) xl/xs. When the temperature of e (eutectic) is reached, the remaining liquid freezes invariantly to a secondary crystallization product of a mixture of A_α and B_β crystals in the proportion ev/eu. For liquids between b and B in composition the primary solid will be B_α, changing to B_β at T'_B, and followed by the eutectic mixture at e.

In a two-phase region such as $T_A ue$, the coexisting equilibrium phases are joined by horizontal tie lines (also called conjugation lines, conodes, joins) running in this case between the liquidus curve $T_A e$ and the solidus curve $T_A u$. With pure solid A, the solidus is here a vertical line, the edge of the diagram. The horizontal line uev is also sometimes considered part of the solidus of the diagram.

1.2. PURE COMPOUNDS

Figure 1.3 shows three binary compounds (C, D, E) in the system A–B:

1. Compound C melts congruently at C_c; it has a congruent melting point. It is stable as a solid phase until it melts to a liquid of its own chemical (analytical) composition. Points e_1 and e_2 are eutectics for solids A and C_α and for C_α and D, respectively. At T'_C, the higher-temperature form C_α undergoes transition to C_β. At T_C, C_β decomposes on cooling into the solids A and D.

2. Compound D melts incongruently at the temperature D_i. It decomposes as a solid phase

UNCLASSIFIED
ORNL-LR-DWG 24748

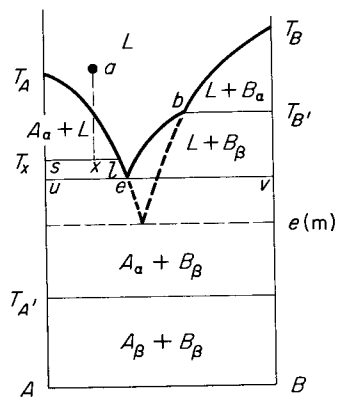

Fig. 1.1.

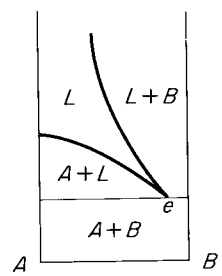

Fig. 1.2.

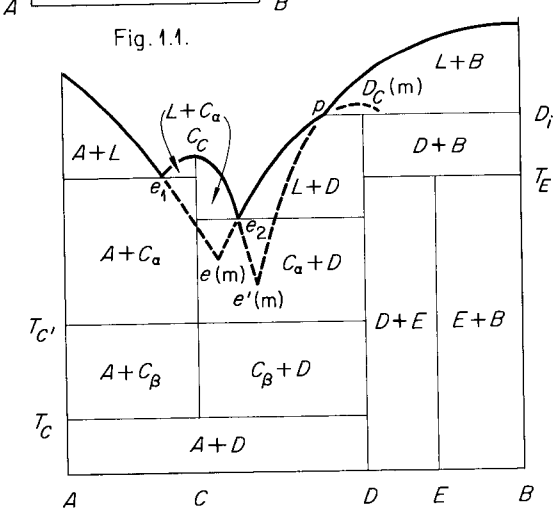

Fig. 1.3.

(into liquid p and solid B) before reaching its own melting point [the metastable or submerged congruent melting point D_c(m)]. In contrast to a eutectic point (e_1, e_2), the point p is called a peritectic point (also meritectic, sometimes) and the reaction:

$$D + \text{calories} \rightleftharpoons L(p) + B$$

is a peritectic reaction.

3. Compound E decomposes as a solid phase, into D and B, at the temperature T_E, before it reaches any equilibrium with liquid. Such a solid phase is sometimes called "subsolidus."

Figure 1.3 shows a metastable eutectic, e(m), between solids A and D, possible if compound C fails to form on cooling; e'(m) is a similar metastable eutectic for solids C_α and B.

It is also possible for a compound to undergo incongruent melting on cooling (inverse peritectic, or inverse fusion), as shown in Fig. 1.4. No example is found in the actual binary systems studied, but the relation will be referred to under the ternary systems. In Fig. 1.4, T_1 is the usual incongruent melting point of C; T_2 is its inverse fusion point:

$$C - \text{calories} \rightleftharpoons L(p') + B \ .$$

Relation Between Congruence and Incongruence of Melting for a Binary Compound

The flatness of the freezing-point curve of a compound at the maximum, whether exposed and stable as at C_c in Fig. 1.3 or submerged and metastable as at D_c(m), depends on the degree of dissociation of the compound in the liquid state. If the compound C is not dissociated at all, the maximum is a pointed intersection of two unrelated curves: on one side the freezing-point curve of the compound in the binary system A–C, on the other side the freezing-point curve of the compound in the unrelated binary system C–B. Only when the maximum is such a sharp intersection may the whole diagram be said, strictly, to consist of two adjacent binary systems. If there is any dissociation of C into A and B in the liquid state, the curve is rounded, and its maximum is lowered, because the liquid, even at the maximum itself, is not pure C (in the molecular sense) but C plus A and B. The greater the degree of dissociation, the flatter and lower is the maximum. Hence, whether the melting point of the compound will be exposed or submerged relative to the freezing-point curves of adjacent solid phases depends on the "true" melting point of the compound without decomposition and on its degree of dissociation in the melt.

In a comparison of corresponding compounds of given formula, such as $A{\cdot}B$ in a series of homologous binary systems with A fixed and B varied, the congruence or incongruence of the melting point of the compound will be a function of three variables: the melting point of the second component (B, B', B'', . . .), the "true" melting point of the compound ($A{\cdot}B$, $A{\cdot}B'$, etc.), and the degree of dissociation of the compound in the melt.

For a given specific binary system, moreover, the relation may vary with the pressure, because of several effects. Pressure causes some change in the relative melting points of all three solids of the system (A, C, B); it causes corresponding changes in the compositions of the intervening isothermally invariant liquid solutions (e, p, etc.); and it causes changes in the dissociation of the compound. The melting point of the compound may therefore be exposed (congruent) at one pressure and submerged (incongruent) at a different pressure. At some particular or singular value of the pressure, therefore, the diagram would pass through the configuration in Fig. 1.5. When a system at arbitrary pressure seems to give such a diagram, however, it is reasonable to suppose that the maximum is actually either just exposed or just submerged.

1.3. SOLID SOLUTION

Continuous Solid Solution

In a binary system with continuous solid solution, the usual relation is either an ascending one as in Fig. 1.6, without minimum or maximum, or, as in Fig. 1.7, one with a minimum. Continuous solid solution with a maximum is very rare. The space $L + S$ between the liquidus and solidus curves represents, at equilibrium, two-phase mixtures, the L and S compositions being joined by a horizontal tie line at any temperature. In Fig. 1.6 L and S have the same composition only for the pure components. In Fig. 1.7 the L and S curves touch at the minimum; they touch tangentially, however, and the two parts of the diagram are not strictly like two binary systems side by side.

Except for the pure components or for the composition m, a given composition has a definite temperature range of freezing or melting, for

UNCLASSIFIED
ORNL-LR-DWG 24749

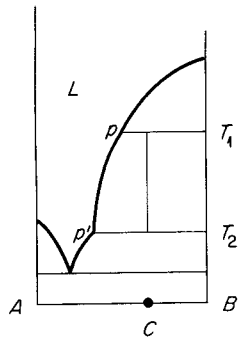

Fig. 1.4.

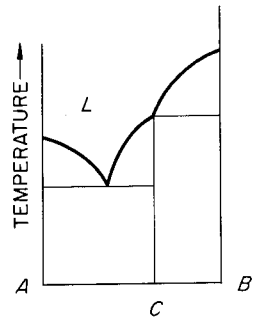

Fig. 1.5.

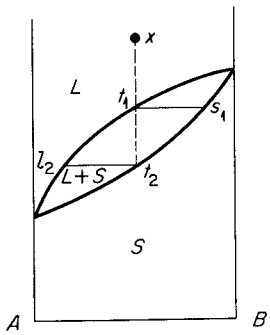

Fig. 1.6.

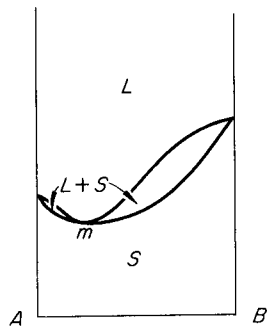

Fig. 1.7.

equilibrium conditions. Liquid x (Fig. 1.6) begins to freeze at t_1, and the solid starts with composition s_1. As the temperature falls, the L and S compositions adjust themselves, always on the ends of a tie line, and the solid reaches the composition x at temperature t_2, the last trace of liquid that solidifies having the composition l_2. Such a crystallization process assumes complete equilibrium all along, with the time for diffusion in the solid that is formed being sufficient for the solid to remain of uniform composition and in equilibrium with the liquid.

As the opposite limiting extreme we may speak of crystallization with perfect fractionation, in which no diffusion at all is assumed to be permitted to occur in the solid. The first trace of solid formed is assumed to be effectively removed from the reaction (as in removal of vapor in distillation), and becomes merely the core of a growing particle with a layered structure, one with infinitesimal layers with infinitesimally changing composition, each layer being taken out of the equilibrium as it is deposited. In such a process the liquid x (Fig. 1.6) begins to freeze at t_1, forming solid s_1, but now, with removal of B-rich solid, the remaining liquid continues to fall in freezing point and approaches the melting point of A as limit. The solid formed has a core with composition near s_1 and an outermost layer approaching A in composition. As in azeotropic distillation, such fractionation in the case of Fig. 1.7 is limited by the minimum m.

Miscibility Gap in Solid Solution

Figure 1.8 shows limited solid solubility in a system with minimum melting point. The eutectic of this system:

$$L(e) - \text{calories} \rightleftharpoons a + b$$

is similar to that in Fig. 1.1 except that the solids (a, b) are not pure. They represent the limits of solid miscibility at the temperature e. The change of this solid solubility with temperature is then shown by the curves aa' and bb', joined by tie lines indicating the compositions of conjugate solid solutions. In Fig. 1.9 the miscibility gap impinges on a system without minimum melting point. The relation:

$$a + \text{calories} \rightleftharpoons L(p) + b \ ,$$

is called peritectic, being analogous to the incongruent melting point of a compound (D in Fig. 1.3).

Solid Solution and Polymorphism

We consider only a few simple relations for the effect of B (in solid solution) on a polymorphic transition point of A. Unlike Fig. 1.1, if B dissolves in solid A, then the transition temperature for:

$$A_\beta + \text{calories} \rightleftharpoons A_\alpha$$

is either raised or lowered:

1. It is raised if B is more soluble in the lower form than in the upper form of A (Figs. 1.10, 1.11). The region x represents equilibrium between α phase and β phase, and with the B content in β greater than the B content in α, the transition temperature is raised, from T_A to T_A'. In Fig. 1.10 the phase reaction at T_A' is:

$$A_\beta + \text{calories} \rightleftharpoons A_\alpha + L(p) \ .$$

In Fig. 1.11:

$$A_\beta + \text{calories} \rightleftharpoons A_\alpha + B_s \ ,$$

the B_s phase being a solid solution.

UNCLASSIFIED
ORNL-LR-DWG 24750

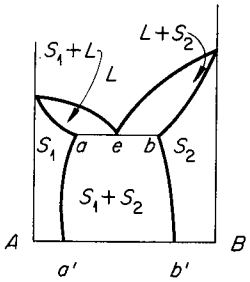

Fig. 1.8.

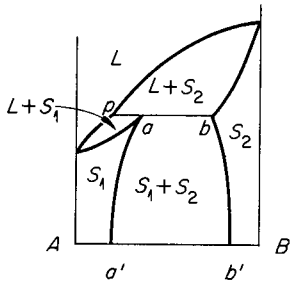

Fig. 1.9.

UNCLASSIFIED
ORNL-LR-DWG 24751

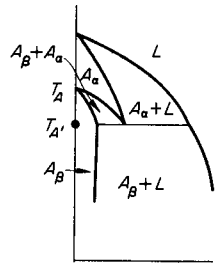

Fig. 1.12.

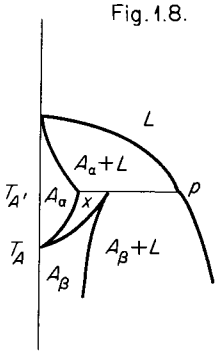

Fig. 1.10.

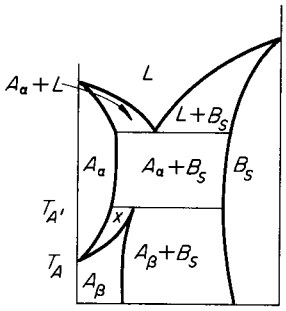

Fig. 1.11.

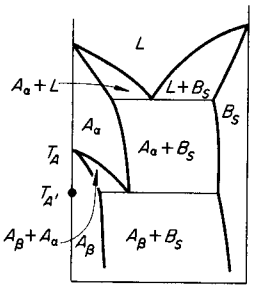

Fig. 1.13.

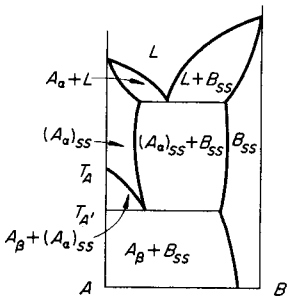

Fig. 1.14.

2. It is lowered if B is more soluble in the upper form; it is, therefore, always lowered if the lower form is pure A_β (Figs. 1.12, 1.13, and 1.14).

Polymorphic transitions of this sort apply to solid solutions of binary compounds, as well as to solid solutions of the components themselves. These are only a few of the relations possible in transitions of solid solutions, but they suffice for the systems under consideration. In particular, these systems involve no case of a congruently melting binary compound dissolving adjacent solids on both sides; such a relation always involves the possibility of nonstoichiometric maxima and Berthollide compounds.

2. TERNARY EQUILIBRIUM OF LIQUID AND ONE SOLID (SURFACES)

The ternary diagrams under consideration deal with temperature-composition (T vs c) relations in additive ternary systems, each with three fluorides as components. The special problems of representation met with for reciprocal ternary systems, those containing two cations and two anions, are not involved.

The relations could presumably be completely and explicitly shown in a transparent, "explodable" and sectionable three-dimensional triangular prism model, in which the various phase spaces and the two-, three-, and four-phase equilibria are distinguished. The two-phase spaces contain horizontal (isothermal) tie lines joining the compositions of coexisting phases (liquid and solid, or two solids). The three-phase equilibria occupy spaces triangular in isothermal section – spaces generated by isothermal three-phase triangles, the corners of which move along continuous curves with changing temperature. The four-phase equilibria (isobarically invariant) constitute isothermal planes defined by the four phases of the equilibrium.

The relations in the three-dimensional T vs c prism are usually represented and discussed by means of plane diagrams which are either projections or sections of the prism.

The only type of projection used in the present discussion is the polythermal projection of the liquidus surfaces. This is a projection parallel to the temperature axis, upon the triangular composition plane, showing, therefore, the various parts of the liquidus surface or surfaces as viewed from the direction of high temperature. The resulting "phase diagram" thus consists of fields (projected surfaces) for liquid saturated with a single solid, of the boundary curves between surfaces, for liquid saturated with two solids, and of points for the intersection of these curves, three at a time, for liquid in equilibrium with three solids. The direction of temperature change can be shown by arrows on the curves, and some actual temperatures can be shown by means of isothermal contours.

Such a polythermal projection shows directly which surface will be reached by a liquid of known composition upon cooling, and hence what the nature, if not the composition, of the primary crystallization product will be. The diagrams under consideration give this information (where it is known) unambiguously in every case because they involve no solid phase with a retrograde effect of temperature on its solubility (Fig. 1.2), so that there is no overlapping, in polythermal projection, of primary phase fields. This restriction is understood in all the subsequent discussion. The absence of retrograde effect means, moreover, that the amount of liquid always diminishes on cooling, while the total amount of solid (or solids) always increases.

The T vs c prism is further studied and analyzed by means of plane sections, which may be vertical T vs c sections through two particular binary compositions, or may be horizontal isothermal sections which then amount to isothermal solubility diagrams of the ternary system.

We shall now consider the crystallization equilibrium of liquid and one solid (the surfaces of the liquidus); in the immediately following sections we shall consider the equilibrium of liquid with two solids (the boundary curves) and the equilibrium of liquid with three solids (the "condensed invariants" of the system).

The "surface" (the field, in projection) is variously referred to as crystallization surface, freezing-point surface, solubility surface, primary phase region, or primary phase field.

When a liquid is cooled to one of these surfaces it deposits one solid on cooling, as long as the liquid is still on the surface ("on the surface" means anywhere short of a boundary curve). Every point on the surface represents equilibrium between that particular liquid (point) and a particular solid composition, and the liquid and solid compositions or points are joined by a tie line (isothermal). If the surface is cut in isothermal section, the isothermal solubility curve is then joined by a series of nonintersecting tie lines to the composition of the saturating solid. If the solid is one of fixed, constant composition, all the tie lines, at any and all temperatures of the surface, meet at the fixed composition of the solid phase. Otherwise the tie lines, at any temperature, simply join the liquidus and solidus curves; the solidus "curve" may be a straight line.

The direction of falling temperature at any point of the surface is away from the composition of the separating solid in equilibrium with the liquid at that point. If the solid is one of fixed composition, therefore, straight lines radiating from its composition are lines of falling temperature, in every direction, and they cut contours of lower temperature, progressively.

2.1. FIXED SOLID

In Fig. 2.1, the region Ae_1Ee_2 is the (projected) surface for saturation with pure solid A. The arrows on the boundaries indicate the direction of falling temperature, and the curves $T_1, \ldots, T_4$ are isothermal contours ($T_1 > \ldots > T_4$). If the liquid x, with composition falling on this surface, is cooled, it begins to precipitate solid A at T_1. The crystallization path of the liquid, the path followed by the liquid on the A surface while it is being cooled and while it is precipitating A, is then a straight line extended from A through x. Removal of A from the liquid makes its composition proceed in a straight line from the corner A. The crystallization paths for a field of a solid of fixed composition are therefore simply straight lines radiating from the composition of the solid. The composition of the liquid starting at x, while precipitating A, will therefore be l_2, l_3, l_4, etc., at the successive temperatures shown, and the ratio of solid to liquid is given by xl_2/xA, etc., at each temperature. The quantity of liquid is always diminishing, but the liquid is never completely consumed while it is still on the A surface. Some liquid must reach one of the boundary curves of the field.

These relations hold, moreover, whether the solid A is kept in contact with the liquid while it is being cooled, or whether the solid is continually removed as produced.

UNCLASSIFIED
ORNL-LR-DWG 24752

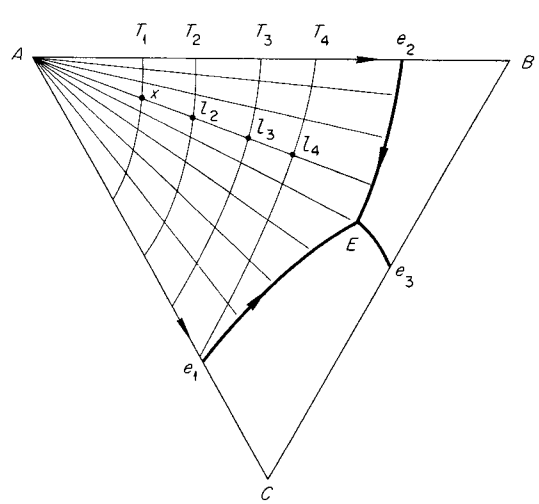

Fig. 2.1.

2.2. VARIABLE SOLID (SOLID SOLUTION)

If the solid is a ternary solid solution, there is a solidus surface, representing solid solutions which are in equilibrium (point for point) with liquids on the liquidus surface. The solidus surface lies everywhere beneath the liquidus surface in temperature, and it will not be represented at all in the usual "phase diagram." Any point on the liquidus is connected by an isothermal tie line with one individual point on the solidus, representing the solid composition with which it is in equilibrium. These tie lines never anywhere intersect. The space between the two surfaces is the two-phase space in which mixtures consist, at equilibrium, of liquid and the solid solution.

These surfaces are in contact at the composition of a pure component (if the solid phase includes the composition of the pure component), and otherwise only at absolute maxima or absolute minima of temperature, which may be at the binary sides or in the ternary system: only at points, in other words, and not along a whole ridge or trough (valley). [The "absolute" maximum or minimum of a liquidus surface is a point "on" the surface – and this means, it must be recalled, not on any one of its boundaries with another surface. The absolute maximum or minimum may be at a unary point (composition of a component), at a binary point (side of the triangle), or at a ternary point, as at the dome of a continuous ternary liquidus. The surface, moreover, may have more than one absolute maximum (or minimum).]

The equilibrium process of the freezing of a liquid now involves a definite temperature range, the vertical distance along the temperature axis, in the T vs c prism, between the liquidus and solidus surfaces. A liquid of composition x, let us say, begins to freeze at T_1 (the liquidus temperature at x) and is completely solidified at T_2 (the solidus temperature for the same composition x). The composition s_1 of the solid, as it just begins to form at T_1, is different from x. As the crystallization proceeds, however, with falling temperature, and if the liquid and solid phases maintain complete equilibrium with each other, both phases change in composition, so that at T_2 the final solid has the original composition x and the last trace of liquid to solidify has still a different composition l_2. Between T_1 and T_2 each phase has followed a separate, three-dimensional curve with respect to temperature and

composition, one along the liquidus surface and one along the solidus surface, but such that the two compositions were always joined by an equilibrium tie line, at each temperature, passing through the total composition x.

The path followed by the liquid, on the liquidus, in such a process, is called its "equilibrium path": the path followed by the composition of the liquid during cooling, if the whole of the solid phase is at every moment in complete equilibrium with the liquid. Such a process can be attained only as a limit, perhaps, with extremely slow cooling, since the interior of the growing solid can be kept uniform with the surface layer only through diffusion in the solid.

At the opposite extreme of behavior we may specify that no diffusion whatever takes place in the growing solid. The first infinitesimal amount of solid now acts simply as an unchanging core for a growing layered structure, each layer differing infinitesimally in composition from the preceding one, and each layer, because of the absence of diffusion, being effectively removed from the equilibrium as it is formed. In such a process there is no longer a definite freezing range for the liquid. As the solid produced is being effectively removed, the remaining liquid tends toward some temperature minimum of the surface before being consumed. The path followed by the liquid in such a limiting process of perfect fractionation we shall call a "fractionation path."

(When the separating solid is of fixed composition, as in Fig. 2.1, there is no distinction between "equilibrium path" and "fractionation path"; hence the one term, "crystallization path.")

Fractionation Path

The surface may be considered to be covered by a family of curves (fractionation paths), following the course of falling temperature and hence cutting contours in the order of falling temperature, and all originating at some absolute maximum of the surface. If there is an absolute minimum on the surface, then these paths, after fanning out, converge again at that minimum. All the cases in the systems under consideration concern solid solution surfaces having one or two absolute maxima (in some cases the maximum is submerged or metastable); there are no solid solution surfaces with an absolute minimum. Hence the fractionation paths in these systems do not converge with falling temperature, but end, each at a separate point, at the various boundaries (for liquid in equilibrium with two solids) of the surface. With two absolute maxima on a surface, there are two families of crystallization paths, one originating at each maximum.

At any point on the surface, such a path starts with a direction given by the L–S tie line at that point of the surface, but the direction immediately changes because, as the temperature changes, the separating solid also changes. The direction of motion for the liquid composition is away from the composition of the separating solid. The fractionation path is therefore such that its tangent at any point is the L–S tie line at that point (Fig. 2.2). Here the curve Bf is a fractionation path on a surface for precipitation of an A–B solid solution; and the lines $l_1 s_1$, $l_2 s_2$, . . . , $l_4 s_4$ are L–S tie lines on this surface at temperatures $T_1 > T_2 > T_3 > T_4$.

UNCLASSIFIED
ORNL-LR-DWG 32546

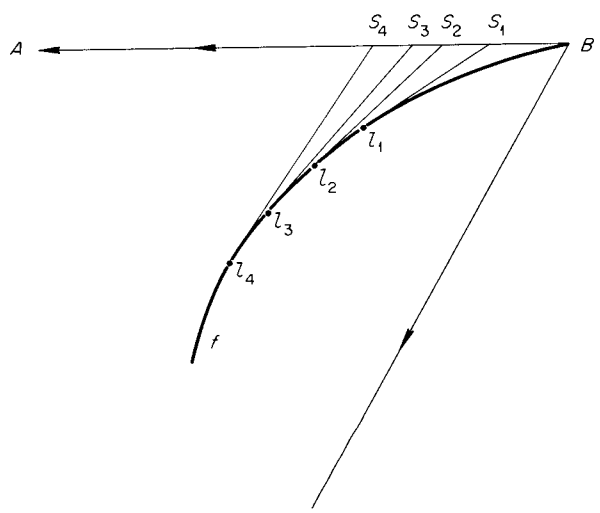

Fig. 2.2.

Equilibrium Path

The composition x in Fig. 2.3 is liquid above temperature t_1 and solid below t_5. When cooled to t_1, it just begins to produce solid of composition s_1; s_1 is a point on the solidus surface in equilibrium with the point l_1 (or x) on the liquidus surface. The line $s_1 l_1$ is therefore the S–L tie line for l_1 at t_1. With precipitation of s_1, the liquid tends to move on the liquidus in the direction of this tie line (i.e., it tends, with

removal of the solid phase, to follow the fractionation path p_1, to which the tie line $s_1 l_1$ is tangent at l_1), but its motion is restricted by the condition that the line joining solid and liquid compositions must always pass through the fixed point x, at each temperature, and that this line must always be an equilibrium tie line. These successive tie lines are $s_2 l_2$, $s_3 l_3$, etc. The solid follows the curve $s_1 s_2 \ldots s_5$ (s_5 being the same as x), and the liquid follows the curve (its equilibrium path) $l_1 l_2 \ldots l_5$ (l_1 being the same as x). At t_5 the sample is completely solidified, l_5 being the composition of the last trace of liquid. Since the lines $s_2 l_2$, $s_3 l_3$, etc., are tie lines, they are tangent, at the liquid points, to the fractionation paths ($p_2 \ldots p_5$) through these points.

It is thus seen that the equilibrium path of the liquid x (its path on the liquidus surface) is one which crosses, with falling temperature, successive fractionation paths at points where the tangent to the path passes through the point x. The equilibrium path crosses the fractionation paths from the convex to the concave side. If a fractionation path should be a straight line, it is not crossed by an equilibrium path; it is itself an equilibrium path, as in the case of precipitation of pure solid.

In the general case of Fig. 2.3, the solid is a ternary solid solution, and the liquid may completely solidify, as assumed in Fig. 2.3, before it reaches a boundary curve of the surface. If, as in Fig. 2.2, the solid solution is binary, it is impossible for a ternary liquid precipitating the solid solution to solidify completely before it reaches a boundary curve of the surface, where a solid involving the third component may also precipitate. But although, with binary solid solution, the curve $s_1 s_2 \ldots s_5$ becomes a straight line, the relations between equilibrium path and fractionation paths developed in Fig. 2.3 still hold (Fig. 2.4). At t_4 the mixture is not all solid; it still consists of liquid and solid in the ratio $s_4 x / x l_4$.

Returning to Fig. 2.3, any total composition, like x itself, on the particular tie line $s_3 l_3$ will consist, at t_3, of the phases s_3 and l_3. Hence the equilibrium path of any total composition between s_3 and l_3 will pass through one common point, namely, l_3. Consequently, while there is but one fractionation path passing through any single point of the surface, there will be an infinite number of equilibrium paths passing through the same point. A surface may therefore be described by the family or families of fractionation paths on it, but not by equilibrium paths.

UNCLASSIFIED
ORNL-LR-DWG 24753

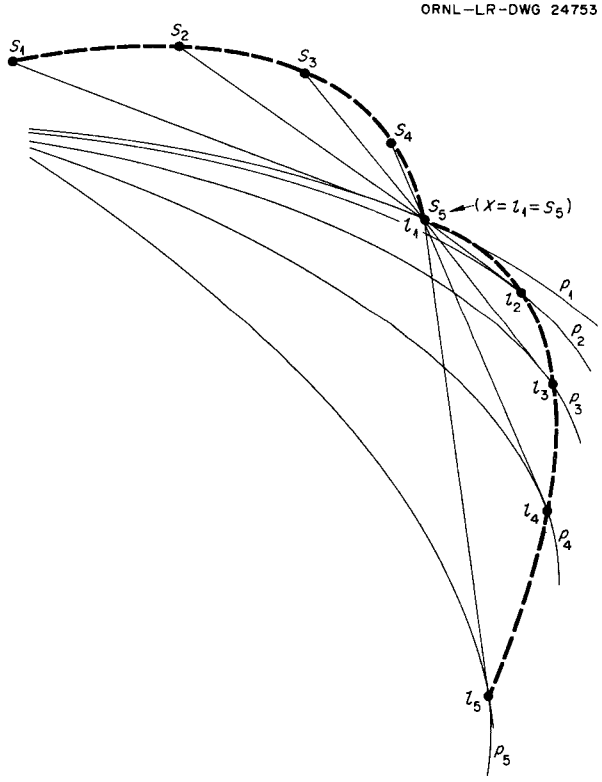

Fig. 2.3

UNCLASSIFIED
ORNL-LR-DWG 24754

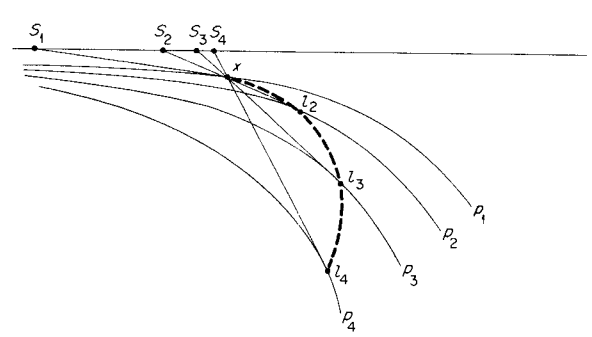

Fig. 2.4.

3. TERNARY EQUILIBRIUM OF LIQUID AND TWO SOLIDS (CURVES)

We now consider the crystallization process for a liquid in equilibrium with two solids, S_1 and S_2: liquid on a curve of twofold saturation (boundary curve, field boundary).

3.1. REACTION TYPES

The curve constituting the boundary between the surface for S_1 and the surface for S_2 represents liquid in equilibrium with both solids, but not necessarily precipitating both solids upon cooling. If the liquid does precipitate both solids on cooling, and the reaction is:

$$L - \text{calories} \rightleftharpoons S_1 + S_2 \ ,$$

the crystallization is said to be positive for both solids, $S_1(+)$, $S_2(+)$, and the curve is said to be one of even reaction. [With retrograde temperature effects it is possible to have both solids dissolving on cooling, with negative crystallization for both, so that the reaction may still be even: $S_1(-)$, $S_2(-)$.] The curve is one of odd reaction (a transition curve) if one solid (S_1, let us say) is dissolving in or reacting with the liquid and the other, S_2, is precipitating during cooling. The crystallization is now $S_1(-)$, $S_2(+)$, and the reaction is:

$$L + S_1 - \text{calories} \rightleftharpoons S_2 \ .$$

The sign of the reaction at a particular point on the two-solid curve involves the direction of the tangent to the curve at that point in relation to the compositions of the two solid phases in equilibrium with the liquid at that point. The liquid is at any point simply one corner L of a three-phase triangle. In the general case, in which all three phases are variable in composition, each equilibrium phase follows its own composition curve in the phase diagram, but the usual polythermal phase diagram shows only the curve for the liquid composition. If the solids S_1 and S_2 are of fixed composition, then the S_1–S_2 leg of the triangle is a fixed line and only the L–S_1 and L–S_2 legs move, with L on the liquid curve; if one of the solids is a binary solid solution, then the curve for that solid is a straight line; etc. In any case the liquid curve on the ordinary phase diagram represents simply one corner of the three-phase triangle of the equilibrium, and the whole triangle may in general be moving, with its corners changing in composition, as the temperature changes.

Figures 3.1, 3.2, and 3.3 show three cases: Figs. 3.1 and 3.2, cases with curves for both S_1 and S_2, both of which are therefore ternary solid solutions; Fig. 3.3, a case with fixed solids for S_1 and S_2. The arrows on the curves indicate the direction of falling temperature. The surface on the left of the L curve is that for liquid depositing S_1 on cooling; that on the right is for liquid depositing S_2 on cooling.

UNCLASSIFIED
ORNL-LR-DWG 24755

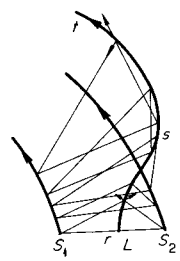

Fig. 3.1.

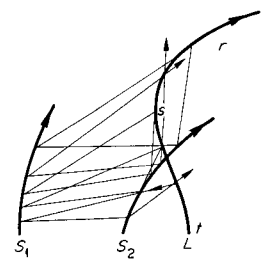

Fig. 3.2.

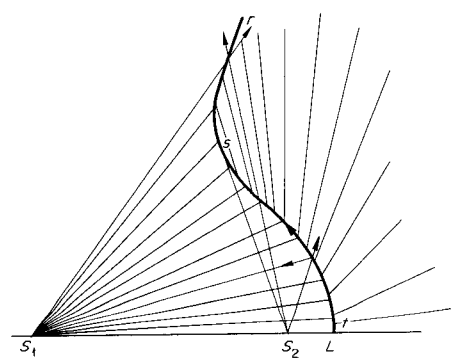

Fig. 3.3.

Positive crystallization (precipitation) of a solid from a liquid corresponds to a direction vector for the motion of the liquid away from the composition of the separating solid; for negative crystallization or dissolving of a solid in a liquid, the direction vector for the motion of the liquid is toward the solid. The resultant of the direction vectors must make the liquid move in the direction of falling temperature on the L curve. Examination of the direction vectors, in Figs. 3.1, 3.2, and 3.3, required to give the indicated motion

on the L curve, shows that the reaction is even, in every case, between r and s [$S_1(+)$, $S_2(+)$], and odd between s and t [$S_1(-)$, $S_2(+)$]. Equivalent to this procedure is the test of the tangent to the curve at any point. If the tangent extends between the compositions of the equilibrium solids, i.e., if the tangent cuts the S_1-S_2 leg of the three-phase triangle, the curve is even [$S_1(+)$, $S_2(+)$]; otherwise it is odd. The sign of the reaction changes at point s, where the tangent to the curve passes through the composition of one of the solids (S_2 for the cases illustrated); i.e., where one of the $L-S$ legs of the triangle is tangent to the L curve.

A curve originating at a binary eutectic (presumably as in Fig. 3.1), whether entering the ternary system with falling or with rising temperature, always starts as an even curve, while one originating at a binary peritectic (Figs. 3.2 and 3.3) starts as odd. But in all cases the sign may change as the curve proceeds on its course, both because of changing direction of the L curve and because of variation in solid compositions. Hence if "eutectic curve" or "peritectic curve" refers simply to the origin of the curve, the expression does not necessarily describe the type of reaction later on along the curve. Since the type of reaction at any point on a curve is an important property of the curve, it is better to speak of "even" and "odd" curves in order to distinguish curves for the precipitation of two solids from transition curves.

The sign of the reaction on a liquid-solid curve is, then, quite clear, on the ordinary phase diagram, if the solids are of fixed composition; but, when the solids are variable, the type of reaction (precipitation of two solids or transition) is often unknown, for it is necessary at any point to know the compositions of the saturating solids in order to test the tangent at that point.

Since the direction of falling temperature on a surface is always away from the composition of the separating solid, it turns out that a two-solid curve of even reaction can be reached from either side, but if the reaction is odd [$S_1(-)$, $S_2(+)$] it can be reached only from the S_1 side. Both the fractionation paths and the equilibrium paths lead to the odd curve from the S_1 surface, and away from it on the S_2 surface. This is at once clear in Fig. 3.3, where all the crystallization paths on the S_1 surface radiate as straight lines from the point S_1, and those on the S_2 surface are straight lines radiating from the point S_2.

3.2. MAXIMUM AND MINIMUM TEMPERATURE POINTS

A twofold saturation curve may pass through a maximum or a minimum of temperature. This is possible only if at least one of the solids is variable in composition. At the maximum or minimum the three-phase triangle becomes a line: the three phases (L, S_1, and S_2) have collinear compositions, all lying on one straight line of the diagram. Figure 3.4 shows the case of a maximum on a curve of even reaction, and Fig. 3.5 a minimum on a curve of odd reaction.

The leading corner of the three-phase triangle (in the direction of falling temperature) may be said to be the liquid. The collinearity corresponds to the relations at a binary origin of such an equilibrium, which is always a maximum or a minimum for the equilibrium, and where of necessity the three phases are on one straight line, which then opens up into a triangle on entering the ternary diagram.

3.3. EQUILIBRIUM CRYSTALLIZATION PROCESS FOR LIQUID ON A TWO-SOLID CURVE

When the liquid is on a two-solid curve, the fixed total composition x of the sample being cooled must lie inside the three-phase triangle (Fig. 3.6). The mixture consists of three phases,

UNCLASSIFIED
ORNL-LR-DWG 24756

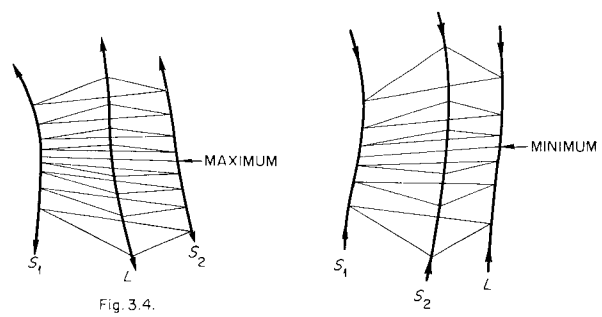

Fig. 3.4.

Fig. 3.5.

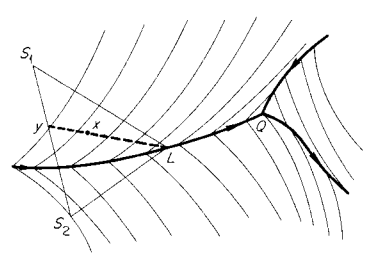

Fig. 3.6.

such that the ratio of the total solids to liquid is xL/xy, and the ratio of S_1 to S_2 is yS_2/yS_1.

As the temperature falls and L travels down the curve, the whole three-phase triangle moves with it, S_1 and S_2 in general following their own composition curves. Since the point x is fixed, it is therefore possible (but not necessary) that one of the three sides of the triangle may come to sweep through x. When this happens, the mixture becomes a two-phase mixture, the third phase having been consumed in the crystallization process. In the sketch in Fig. 3.6, if the general configuration remains the same while the triangle moves to the right, the amount of solid increases and the liquid diminishes (as always), and when the side S_1S_2 sweeps through x, the liquid vanishes, leaving S_1 and S_2. The solidification process would then be completed while L is still on the curve, or before L reaches the end of the curve, Q. But if the triangle twists and changes shape as L moves down the curve, the point x may come to be swept by the S_1L leg (S_2 vanishing) or by the S_2L leg (S_1 vanishing). If S_2 vanishes and the liquid is left saturated with only S_1, the liquid leaves the curve to travel on the S_1 field; if S_1 is consumed, the liquid, saturated with S_2 alone, moves off the curve onto the S_2 field.

Some of the possible variations of behavior are the following:

1. Curve of even reaction:
   (*a*) If the solids are not variable, no phase is consumed while L is on the curve. The liquid diminishes, but some reaches the end of the curve; L does not leave the curve.
   (*b*) If S_1 is variable and S_2 constant, either liquid or S_2 may be consumed, but not S_1. Solidification may be complete on the curve, or L may leave the curve for the S_1 field, or it may reach the end of the curve.
   (*c*) If both solids are variable, any one of the three phases may be consumed. Solidification may be complete on the curve, or L may leave the curve on either side, or L may reach the end of the curve.
2. Curve of odd reaction [$S_1(-)$, $S_2(+)$]: Now S_1 may always be consumed, whatever the nature of the solids.
   (*a*) With fixed solids, only S_1 can be consumed. The liquid may leave the curve for the S_2 field, or it may reach the end. Solidification cannot be completed with L on the curve.
   (*b*) If S_1 is variable (S_2 fixed or variable), then any one of the three phases may be consumed. Solidification may be completed on the curve, L may leave the curve for either side, or it may reach the end of the curve.

A transition curve (odd reaction) is traveled (L moves along the curve) only if complete equilibrium is maintained between the liquid and the dissolving, or reacting, solid. If this solid (S_1) is effectively out of the equilibrium (i.e., if it is removed as formed, if its surface is covered by deposition of S_2, or if the process is too rapid), then a liquid which reaches such a curve by deposition of S_1 merely crosses the curve. It begins to precipitate S_2 without consuming any S_1; it undergoes a change in direction and enters at once upon the S_2 surface. The new solid S_2 is merely deposited upon the first (S_1) in a nonequilibrium mixture.

4. TERNARY CONDENSED INVARIANT POINTS (FOUR PHASES)

Ternary condensed invariant points are generally the points of intersection of three curves, each for a liquid in equilibrium with two solids, resulting in the equilibrium of a liquid with three solids. In addition we shall have to consider reactions involving four solids, below temperatures of equilibrium with liquid.

The four phases of the (isobarically) invariant equilibrium are arranged either as a triangle, with one phase inside (type A), or as a quadrangle (type B). The special case which may appear to be the limit between triangle and quadrangle, with the fourth phase on a side of the triangle (i.e., with three of the four phases on a straight line), is strictly a binary three-phase invariant, and the fourth phase, while present, is not involved in the phase reaction. We shall discuss this case before considering the true ternary invariant reactions.

4.1. BINARY DECOMPOSITIONS IN PRESENCE OF TERNARY LIQUID

Given the four coexisting phases arranged as follows:

$$\begin{array}{ccccc} \mathrm{Ph}_1 & — & \mathrm{Ph}_2 & — & \mathrm{Ph}_3 \\ & \diagdown & & \diagup & \\ & & \mathrm{Ph}_4 & & \end{array}$$

with Ph_1, Ph_2, and Ph_3 collinear, then the equilibrium:

$$\mathrm{Ph}_2 \rightleftharpoons \mathrm{Ph}_1 + \mathrm{Ph}_3 \pm \text{calories}$$

does not involve Ph_4. Such a situation arises for the interaction of three solids (collinear) in the presence of a liquid phase:

$$\begin{array}{ccccc} B & — & C & — & D \\ & \diagdown & | & \diagup & \\ & & L & & \end{array}$$

the liquid being saturated with all three. In the usual examples found, the three solids are on a binary side of the ternary diagram, but sometimes they are on a line inside the ternary system.

"Pure" Solids

If B, C, and D are three successive solids in the binary system A–E, and if they are "pure" in the sense that, although they may involve binary solid solution among themselves, they nevertheless do not take into (ternary) solid solution the third component F, then the temperature (always at constant pressure) of the equilibrium:

$$C \rightleftharpoons B + D + \text{calories}$$

is unchanged by the presence of a liquid, containing F, in which these solids are dissolved to saturation. The liquid may even contain more than one such foreign component. Provided that the three solids themselves remain pure in respect to any of the foreign components (F, G, . . .) in the liquid phase, the temperature of the phase reaction is the same as that in the binary system A–E itself.

Not only is the temperature independent of the composition of the liquid phase, but, since the liquid is not involved in the phase reaction, the very amount of the liquid phase is constant (complete equilibrium being assumed) during the phase reaction.

Such strictly binary invariant points will be distinguished with a subscript identifying the decomposing solid phase, such as P_{S_2}, or P_C, in the above examples. A similar invariant would be that of the transition of a binary solid solution in presence of a ternary liquid (points T'_A in Figs. 1.10 to 1.14).

Effect of the Third Component Entering into Solid Solution

If a foreign component enters any of the three solids, forming a solid solution, the temperature of the phase reaction is changed, and it now varies with the composition of the solid solution (or solid solutions). If C alone forms such a solid solution with the foreign component, then the decomposition temperature is raised if the reaction is:

$$C + \text{calories} \rightleftharpoons B + D \ ,$$

and lowered if

$$C - \text{calories} \rightleftharpoons B + D \ .$$

If C remains "pure" while either or both of the other solids form a solid solution with the added component, then the decomposition temperature is lowered if the reaction is:

$$C + \text{calories} \rightleftharpoons B + D \ ,$$

and raised if

$$C - \text{calories} \rightleftharpoons B + D \ .$$

If both C and one (or both) of its products form such a solid solution, then the temperature of decomposition may be either raised or lowered, and it may even pass through a maximum or a minimum.

Finally, however, when such ternary solid solution is involved in one or more of the three solids, their compositions are no longer collinear. The invariant reaction now involves all four phases, it is no longer binary but ternary, and it will pertain to one or other of the ternary types now to be discussed.

4.2. TYPES OF TERNARY INVARIANTS

Type A Invariant: Triangular or Terminal Type of Invariant

In the case of a type A invariant (Fig. 4.1), the phase reaction is terminal with respect to the interior phase. The phase reaction is:

$$4 \pm \text{calories} \rightleftharpoons 1 + 2 + 3 \ .$$

On one side of the invariant temperature we have the three equilibria involving 1, 2, and 4; 2′, 3′, and 4′; and 1″, 3″, and 4″; and on the other side only the equilibrium of 1‴, 2‴, and 3‴. The interior phase, 4, exists only on one side, and its stable existence is terminated at the type A invariant.

If the interior phase is a liquid and the others are solids, the invariant is a eutectic. All four phases may be solids, and then the invariant is the decomposition of solid 4 into three solids. The liquid may be an exterior phase, and then the invariant is an incongruent melting point of the interior ternary solid 4; two cases arise. Case (*a*):

$$4 + \text{calories} \rightleftharpoons 1 + 2 + L$$

is a ternary analog of the incongruent melting point of a binary solid into liquid and another solid. Case (*b*):

$$4 - \text{calories} \rightleftharpoons 1 + 2 + L$$

is an inverse peritectic or inverse fusion point, like one found in rare cases in binary systems (Fig. 1.4), and (possibly) in one case in the present ternary systems (solid phase C in system Y–U–Z, Fig. 14.10).

Type B Invariant: Quadrangular, Diagonal, or Metathetical Type of Invariant

In the case of a type B invariant (Fig. 4.2), the phase reaction is:

$$1 + 3 \pm \text{calories} \rightleftharpoons 2 + 4 \ ,$$

not terminal for any phase. On one side of the invariant temperature we have the equilibria involving 1, 2, and 3 and 1′, 3′, and 4′, and on the other side the equilibria involving 1″, 2″, and 4″ and 2‴, 3‴, and 4‴. This invariant is related to double decomposition reactions, even when occurring in additive ternary systems. The combination 1 and 3 is stable only on one side of the invariant temperature, and the combination 2 and 4 only on the other side. The stable diagonal of the quadrangle changes from 1-3 to 2-4; hence the term "diagonal reaction."

4.3. RELATIONS OF THE THREE LIQUID CURVES AT THEIR INVARIANT INTERSECTION

On the liquidus diagram the only invariants we see are those involving a liquid phase and three solids, and they occur as intersections of three curves of liquid in equilibrium with two solids. Hence, unless the locations of the three solids are known, relative to the position of the invariant liquid (commonly this position is called "the invariant point," but the invariant is not a point but a plane, either triangular or quadrangular), we cannot always know the type of invariant involved.

If, as in Fig. 4.3, all three liquid curves fall in temperature to their intersection, the invariant is a eutectic (type A). The phase reaction is terminal for the liquid, which is inside the three-solid triangle:

$$L - \text{calories} \rightleftharpoons S_1 + S_2 + S_3 \ .$$

Conversely, if the liquid of the intersection is known to be inside the three-solid triangle, then the temperature must fall to the intersection on all three curves, and the intersection is a eutectic, the temperature minimum for the liquidus in the area of the three-solid triangle.

UNCLASSIFIED
ORNL-LR-DWG 24757

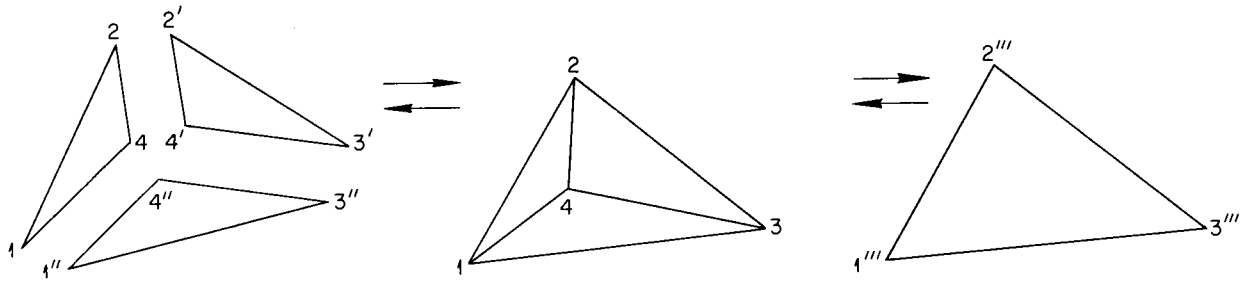

Fig. 4.1.

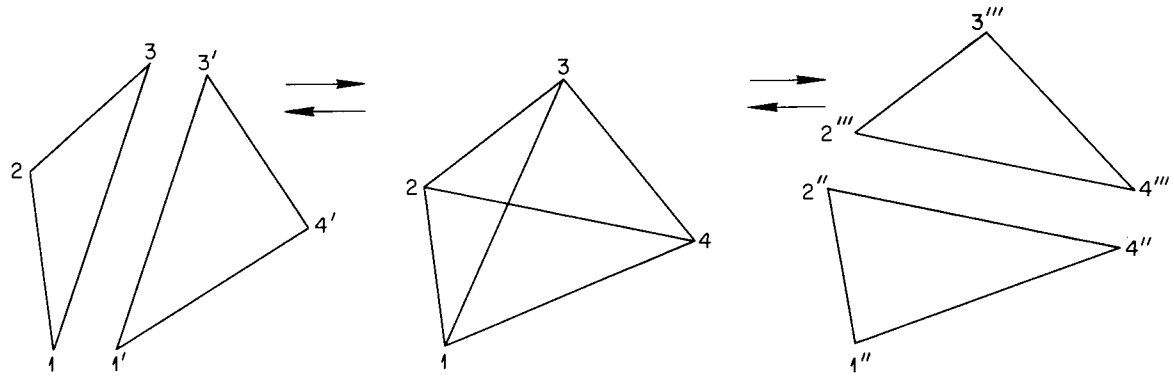

Fig. 4.2.

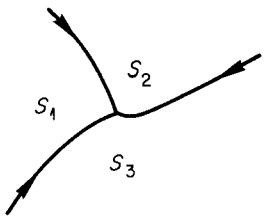

Fig. 4.3.

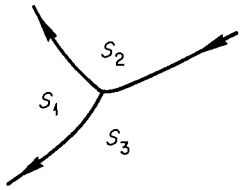

Fig. 4.4.

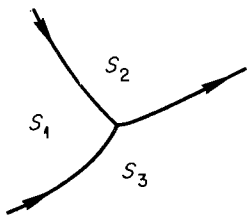

Fig. 4.5.

But any other arrangement of temperature fall of the three curves may mean either a type A or a type B invariant. Thus, the arrangement in Fig. 4.4 may mean either of the following reactions:

(*a*) Type A: $S_1 + \text{calories} \rightleftharpoons S_2 + S_3 + L$.

(*b*) Type B: $S_1 + L + \text{calories} \rightleftharpoons S_2 + S_3$.

That in Fig. 4.5 may be either of the following:

(*c*) Type A: $S_1 - \text{calories} \rightleftharpoons S_2 + S_3 + L$.

(*d*) Type B: $S_1 + L - \text{calories} \rightleftharpoons S_2 + S_3$.

These four invariants involving liquid (*a*, *b*, *c*, *d*) are usually called simply "ternary peritectics" as distinct from the eutectic reaction.

Moreover, the curves meeting at a eutectic are usually all three of even reaction, but they need not be; one may be odd in reaction. For invariants (*a*) and (*b*) (Fig. 4.4) one of the curves proceeding from the invariant to lower temperature must be odd. For invariants (*c*) and (*d*) (Fig. 4.5) no restrictions of reaction sign hold.

For all invariant intersections of three liquid curves, no angle of the intersection can be greater than 180°. This requirement holds both for the truly ternary invariants (types A and B) and for those explained as binary invariants with the three solids on one straight line. This restriction means that the metastable extension of each curve must extend into the field of the third solid. The metastable extension of the curve for liquid in equilibrium with S_1 and S_2, for example, must penetrate to temperatures below the surface for liquid in equilibrium with S_3, and this requirement cannot be satisfied, for all three curves simultaneously, if any angle of the intersection is greater than 180°. Thus, in Fig. 4.6, the extension ia' of the curve for liquid in equilibrium with S_2 and S_3, which is a boundary of the surface for liquid in equilibrium with S_3, would have to penetrate beneath the S_3 surface itself, an impossibility in the absence of retrograde temperature effects, here excluded. The same contradiction would hold for the extension ib' of the curve for liquid in equilibrium with S_1 and S_3, which is also a boundary of the S_3 surface. Only the metastable extension ic' of the curve for liquid in equilibrium with S_1 and S_2 would behave correctly.

4.4. CONGRUENT AND INCONGRUENT CRYSTALLIZATION END POINTS

In Figs. 4.7 and 4.8, E represents a eutectic liquid in equilibrium with the three solids S_1, S_2, and S_3; (S_1), (S_2), and (S_3) represent the fields for liquid in equilibrium with each of the three solid phases. With complete equilibrium always maintained during cooling, the point E must be reached, along one or another of the three curves meeting at E, by liquid from any total composition in the triangle $S_1S_2S_3$, no matter how many other invariant points may be traversed on the way; and, with complete equilibrium, only liquids from original compositions in the triangle $S_1S_2S_3$ will reach E. Liquids with original composition x in the triangle $S_1S_2S_3$ cannot dry up, or they cannot be completely solidified, until some liquid finally reaches E. Since liquid E is inside the triangle of its three solids, so that the composition of the liquid E is accountable in terms of its three solids, it is said to dry up congruently; i.e., E is the congruent crystallization end point for compositions in the triangle $S_1S_2S_3$. Also, when the liquid

UNCLASSIFIED
ORNL-LR-DWG 24758

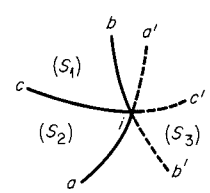

Fig. 4.6

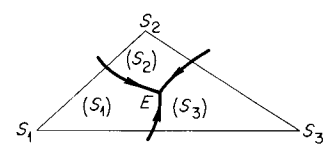

Fig. 4.7

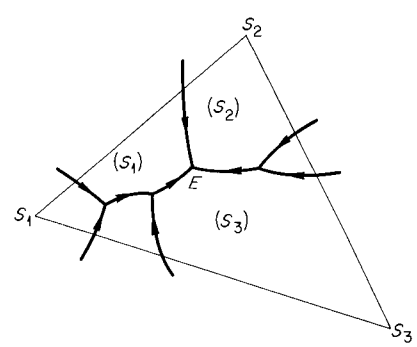

Fig. 4.8

reaches E, it is always entirely consumed; it never leaves E. This is so whether the solids involved in the reaction are removed as formed or not. (Exceptions, of course, would occur if there is supercooling with respect to some solid phase; in such a case the liquid, approaching an invariant point along a two-solid curve, simply continues on the metastable extension of that curve until the metastability is relieved.)

Invariant points other than eutectics [peritectic points (*a*) and (*d*), Sec 4.3] may be crystallization end points for some compositions, but they are then, in contrast, incongruent crystallization end points. The liquid in these cases is not inside the triangle of its three solids, and its composition is not accountable in terms of these solids.

The following consideration of these invariants assumes complete equilibrium in all processes.

Case (*a*): Reaction of type A (Fig. 4.9):

$$L + S_2 + S_3 - \text{calories} \rightleftharpoons S_1 \ .$$

Here point P is reached by liquids traveling down in temperature along the curve LS_2S_3, provided the original total composition x is in the triangle PS_2S_3. Then S_1 appears in the invariant reaction, and if x is in the triangle $S_1S_2S_3$ the liquid is consumed, leaving the three solids. Point P is therefore the incongruent crystallization end point for the composition triangle $S_1S_2S_3$. As for the rest of the quadrangle: with x in the triangle PS_1S_2, the solid S_3 is consumed, leaving liquid, S_1, and S_2, and the liquid enters upon the curve LS_1S_2; for x in the triangle PS_1S_3, S_2 is consumed, and L leaves along the curve LS_1S_3.

This invariant is seen to be the incongruent melting point of the interior phase S_1, which may be either a fixed ternary compound or a ternary solid solution. Upon heating, it decomposes or melts incongruently, at the temperature of the invariant, to produce liquid of composition P, S_2, and S_3.

Case (*d*): Reaction of type B (Fig. 4.10):

$$S_1 + L - \text{calories} \rightleftharpoons S_2 + S_3 \ .$$

Liquid P is reached on cooling for x in the quadrangle $S_1S_2PS_3$, along the curve LS_1S_2 if x is in the triangle S_1S_2P and along curve LS_1S_3 for x in the triangle S_1S_3P. If x is in the triangle S_2PS_3, S_1 is consumed and L proceeds along curve LS_2S_3. But if x is in the triangle $S_1S_2S_3$, the liquid is consumed, leaving the solids S_1, S_2, and S_3. Point P is thus the incongruent crystallization end point for the composition triangle $S_1S_2S_3$.

The invariants (*b*) and (*c*), on the other hand, are never crystallization end points in a cooling process.

Case (*c*): Reaction of type A (Fig. 4.11):

$$S_1 - \text{calories} \rightleftharpoons S_2 + S_3 + L \ .$$

This is the inverse incongruent melting point of the solid S_1 (a fixed ternary compound or a ternary solid solution), decomposing or melting incongruently, on cooling, into liquid of composition P, S_2, and S_3; it is somewhat like that in Fig. 1.4 for a binary system. Liquids saturated with S_1 and S_3, along curve LS_1S_3, reach P on cooling if x is in triangle S_1S_3P; and liquids on curve LS_1S_2, saturated with S_1 and S_2, reach P if x is in triangle S_1S_2P. Then at P, solid S_1 decomposes, and when all of it is consumed, the liquid proceeds on the curve LS_2S_3. This case is encountered later in Fig. 14.10, in system Y–U–Z. For x in triangle $S_1S_2S_3$, the system is completely solid before the temperature falls to P; but at P the liquid phase reappears in the invariant reaction, as a result of the decomposition of S_1, and L then proceeds along curve LS_2S_3.

Case (*b*): Reaction of type B (Fig. 4.12):

$$S_2 + S_3 - \text{calories} \rightleftharpoons S_1 + L \ .$$

At this invariant temperature the combination of solids S_2 and S_3 reacts, on cooling, to produce liquid of composition P and S_1. Liquid saturated with S_2 and S_3, along curve LS_2S_3, reaches P on cooling if x is in triangle PS_2S_3. Then if x is above the diagonal PS_1, S_3 is consumed in the invariant reaction, leaving liquid, S_2, and S_1, and L then moves away on the curve LS_1S_2; for x below the diagonal, S_2 is consumed, and L leaves upon the curve LS_1S_3. In this invariant, the cooling of two solids, S_2 and S_3, leads to the formation of liquid and the solid S_1, a situation encountered later in Fig. 13.6, in system Y–U–X. For x in triangle $S_1S_2S_3$, the system is completely solid before the temperature falls to P; but at P the liquid phase reappears in the invariant reaction, either S_2 or S_3 is consumed completely, and L then proceeds along one of the curves falling away from P.

UNCLASSIFIED
ORNL-LR-DWG 24759

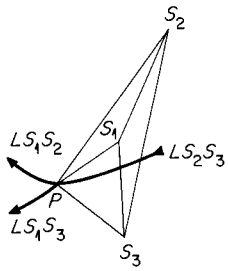

Fig. 4.9.

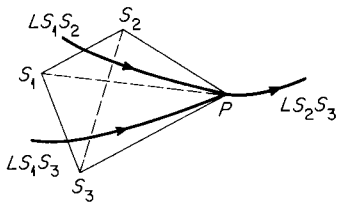

Fig. 4.10.

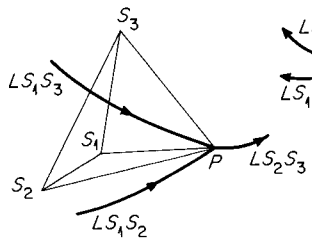

Fig. 4.11.

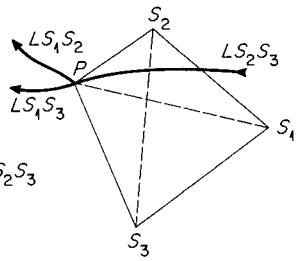

Fig. 4.12.

With complete equilibrium, therefore, a liquid reaching point P may be completely solidified at that point in case (*a*) or case (*d*), but never in case (*b*) or case (*c*).

In the absence of complete equilibrium, however, or if the liquid is not given time to react as required with the solid phases at the invariant temperature, the liquid reaching P does not stop there at all, but travels on down in temperature; along one of the issuing two-solid curves if there is an even curve to lower temperature, or onto a surface, of liquid in equilibrium with one solid, if there is no even curve leaving P for lower temperature. Such crystallization processes will be completed in various ways: on a solid solution liquidus surface (the last crystallization product being a single solid), on a curve of even reaction (the last product being a mixture of two solids), or at a eutectic (the last crystallization product being a mixture of three solids).

4.5. MELTING POINTS OF TERNARY COMPOUNDS

There are three types of melting points of ternary compounds.

1. Congruent melting point: The solid ternary compound here melts to a ternary liquid of the same composition. This will occur at an absolute maximum of the surface for liquid in equilibrium with the compound, not at a boundary of that surface. The compound is here said to possess an "open" or "exposed" maximum.

2. Semicongruent melting point: In this case the ternary compound M_2 decomposes to a liquid L_y and another solid M_1, with all three compositions, M_1, M_2, and L_y, lying on a straight line in the ternary diagram. This temperature will be a maximum (y, in Fig. 4.13) on the boundary curve between the surface $(L + M_1)$ and the surface $(L + M_2)$, and hence on curve LM_1M_2. The temperature on curve LM_1M_2 falls away from y in both directions, but, while the temperature on the surface $(L + M_1)$ falls toward y, the temperature on the surface $(L + M_2)$ falls away from y.

3. Incongruent melting point: In this case the ternary compound S_T decomposes to a liquid P and two other solids, in an invariant reaction in which the ternary compound is the interior phase of a triangle; case (*a*) above (Fig. 4.9).

4.6. INVARIANTS INVOLVING SOLIDS ONLY

Invariant reactions both of type A and of type B may involve simply four solid phases, below temperatures of liquid equilibrium. The usual case would be some double decomposition of type B. The type A reaction would apply for the decomposition, on heating or cooling, of one solid into three others, as already mentioned. Both types will be encountered later.

UNCLASSIFIED
ORNL-LR-DWG 24760

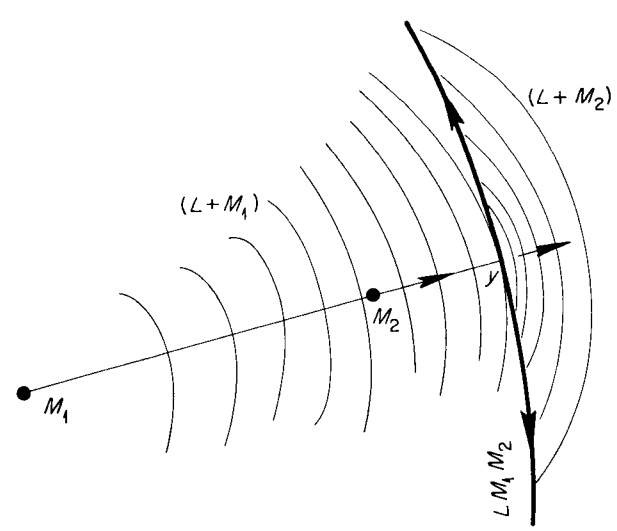

Fig. 4.13.

5. CRYSTALLIZATION PROCESS WITH PURE SOLIDS

In this and in the next two sections we shall consider some of the relations met with in typical ternary systems, first in systems involving only pure solid phases and then in systems involving solid solutions.

The ternary system of Fig. 5.1 contains two binary compounds, D_1 and D_2, stable at the liquidus temperature and not decomposing on cooling. Any ternary liquid, upon complete solidification, must, if complete equilibrium is maintained throughout, consist finally of a mixture of three of the five solids of the system – A, B, C, D_1, and D_2. But there are two arrangements of the five solids possible: scheme (*a*) and scheme (*b*). We know in advance that one of the three-solid combinations will be A, D_1, and D_2, but to determine whether the coexistence of solids in the system is (*a*) or (*b*), experiment is required. In (*a*) the pair of solids D_1 and B is an unstable combination, and it would react to produce D_2 and C (plus excess of either D_1 or B), while in (*b*) the pair D_2 and C is unstable and would react to produce D_1 and B. For this reason the three-solid coexistence triangles shown in either scheme are sometimes called "compatibility triangles." Theoretically, a single experiment, upon a liquid composition at the intersection of the lines D_1B and D_2C, would suffice to establish the coexistence relations, provided that the final solids obtained upon complete crystallization represented true equilibrium. In scheme (*a*) the experiment would yield the pair D_2 and C as sole solids, and in scheme (*b*) the opposite pair. Such an experiment is an application of what is known as Guertler's *Klärkreuzverfahren*.

In either case, the phase diagram will have five fields and three invariant points of liquid in equilibrium with three solids, each functioning as a crystallization end point, congruent or incongruent, for one of the three-solid triangles. The curves of liquid in equilibrium with two solids will be joined by three intersections, as in Figs. 5.2 (*a*) and (*b*), corresponding respectively to Figs. 5.1 (*a*) and (*b*). The invariants are numbered to correspond to the three-solid triangles in Fig. 5.1.

In either case, at least one of these invariants must be a eutectic, with the invariant liquid inside the three-solid triangle of corresponding number, while the other two points may be either eutectics or peritectics, together or separately. Scheme (*a*) thus comes to have nine possible arrangements of the three invariant points:

Triangle I	Triangle II	Triangle III
E_1	E_2	E_3
E_1, P_2	--	E_3
E_1	--	P_2, E_3
E_1	E_2, P_3	--
--	P_1, E_2	E_3
E_1, P_2, P_3	--	--
E_1, P_2	P_3	--
--	P_1, E_2, P_3	--
--	--	P_1, P_2, E_3

The entry "E_1, P_2 P_3 --" in line 7 means, for example, that the first two intersections are in triangle I and the third in triangle II, so that the first is a eutectic and the other two are peritectics.

Although each of the curves for liquid in equilibrium with two solids enters the ternary diagram with falling temperature, the temperature direction on the two interior curves depends on the nature

UNCLASSIFIED
ORNL-LR-DWG 24761

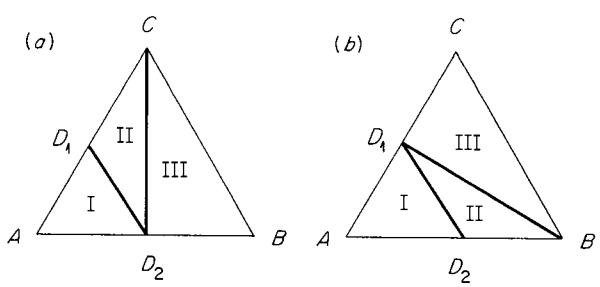

Fig. 5.1.

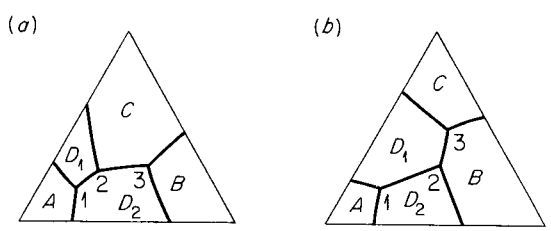

Fig. 5.2.

of the invariant points involved, for only a eutectic is a temperature minimum.

Moreover, each of the nine possibilities enumerated for scheme (*a*) will have several variations depending on the congruence or incongruence of the melting points of the binary compounds in their binary systems, with further subvariations (for incongruence) depending on whether the peritectic and eutectic solutions for the incongruent compound are on the side of one or of the other component in its binary system. With a congruent melting point, the composition of the compound will be on the binary side of its ternary field, at the maximum temperature of the surface, and the crystallization paths radiate from its composition. The composition point of an incongruently melting compound will be outside its field, but the composition point still represents the (metastable) maximum of its surface, and the crystallization paths radiate, by extension, from its composition.

In Fig. 5.3, with three binary compounds, D_2 melts congruently, and e_5 and e_6 are both binary eutectics:

$$L(e_5) \rightarrow B + D_2 \ ,$$

$$L(e_6) \rightarrow C + D_2 \ .$$

(Note: reactions are written for the cooling process.) The compounds D_1 and D_3 both melt incongruently, and p_1 and p_3 are the peritectic liquids of the respective binary systems:

$$L(p_1) + C \rightarrow D_1 \ ,$$

$$L(p_3) + A \rightarrow D_3 \ .$$

There are six fields, projections of surfaces for liquid saturated with a single solid: A, D_1, C, D_2, B, and D_3, in clockwise order.

The system has four ternary invariant points, corresponding to the four three-solid triangles. Three of the invariants are eutectics (temperature minima); however, one, P_3, is not, since its liquid, saturated with the solids of triangle III, falls in triangle IV. The temperature along the curve E_1E_2, for liquid saturated with D_1 and D_2, has a maximum value at m, the intersection of the boundary curve with the line joining the two solids. This is a "collinear equilibrium," and the three-phase triangle for liquid in equilibrium with D_1 and D_2, starting as the straight line D_1mD_2, expands, with falling temperature, to end as the triangle $D_1E_1D_2$ at E_1 and as the triangle $D_1E_2D_2$ at E_2. The line D_1mD_2, joining the compositions of the solids and intersecting the boundary curve between their adjacent fields, is known as an Alkemade line. With the temperature falling toward m on both adjacent surfaces (for liquid in equilibrium with D_1 and for liquid in equilibrium with D_2), while the temperature falls away from m on the E_1E_2 curve, the point m is a saddle point on the curve.

The line $Am'D_2$ is another Alkemade line, and m' another saddle point, a minimum in temperature on the surfaces between A and D_2 but a maximum of temperature on the curve E_2P_3. The triangle for liquid in equilibrium with A and D_2 expands, with falling temperature, from the line $Am'D_2$ to the triangle AE_2D_2 and, also with falling temperature, to the triangle AP_3D_2.

The section of the diagram through the line $Am'D_2$, moreover, is a quasi-binary section. The vertical section of the T vs c prism through this line is altogether like the T vs c diagram of a simple binary system (Fig. 5.4). Such a section

UNCLASSIFIED
ORNL-LR-DWG 24762

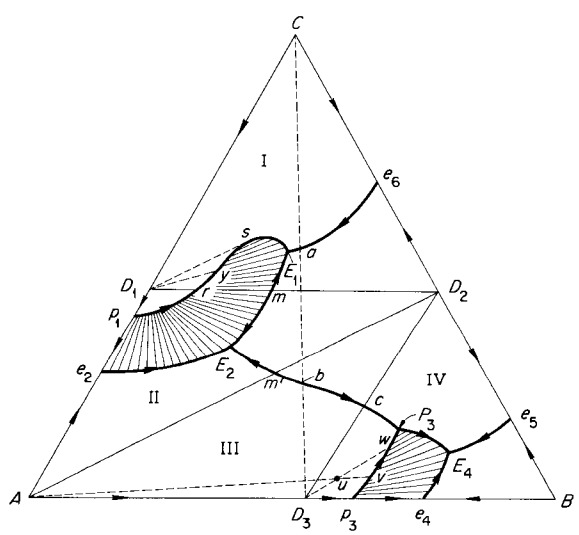

Fig. 5.3.

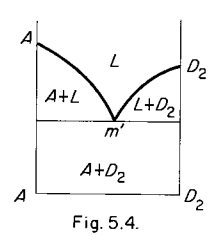

Fig. 5.4.

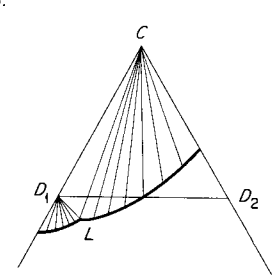

Fig. 5.5.

divides the actual ternary system A–B–C into two separate subsystems, A–C–D_2 and A–D_2–B. The section through the line D_1mD_2, on the other hand, although also containing a saddle point very similar to m', is not quasi-binary; one of the solid phases involved in the equilibria traversed on this section is C (between D_1 and point r), so that the phase equilibria along line D_1mD_2 are not describable on the basis of a binary system with D_1 and D_2 as components.

From this point on, phase reactions involving one or two or three solids will be written always as occurring in the direction of falling temperature, or in the direction of removal of heat, unless otherwise specified. The equation:

$$L \rightarrow S_1 + S_2 \ ,$$

therefore, means:

$$L - \text{calories} \rightarrow S_1 + S_2 \ .$$

The reactions along the boundary curves of Fig. 5.3 are as follows:

e_2E_2: $L \rightarrow D_1 + A$;
p_3P_3: $L + A \rightarrow D_3$ (reaction odd);
e_4E_4: $L \rightarrow D_3 + B$;
e_5E_4: $L \rightarrow B + D_2$;
e_6E_1: $L \rightarrow D_2 + C$;
p_1E_1: reaction odd from p_1 to s: $L + C \rightarrow D_1$; reaction even from s to E_1: $L \rightarrow C + D_1$ (the line D_1s is tangent to the curve);
E_1mE_2: $L \rightarrow D_1 + D_2$;
E_1mP_3: $L \rightarrow A + D_2$;
P_3E_4: $L \rightarrow D_3 + D_2$.

The invariant reactions are:

E_1: $L \rightarrow D_1 + C + D_2$;
E_2: $L \rightarrow A + D_1 + D_2$;
P_3: $L + A \rightarrow D_2 + D_3$;
E_4: $L \rightarrow D_3 + D_2 + B$.

Liquids with original composition x in triangle I must reach E_1 for complete solidification; those in triangle II must reach E_2; those in triangle III must reach P_3; and those in triangle IV must reach E_4.

The peritectic P_3 is reached by all liquids with x in the quadrangle $AD_2P_3D_3$. For x in the region $m'D_2P_3$, the liquid precipitates D_2 as the first solid, reaches curve $m'P_3$, and then proceeds to P_3 carrying A and D_2 as solids. For x in the region $Am'P_3$, the liquid reaches curve $m'P_3$ after precipitating A, and also reaches P_3 carrying A and D_2. Liquids with x in the region AP_3D_3, and hence on the A surface, precipitate A and reach the curve p_3P_3, which is then followed while some A reacts with liquid to form D_3. At P_3:

$$L + A \rightarrow D_3 + D_2 \ .$$

Now for x in triangle III, the liquid is consumed, leaving A, D_3, and D_2 (complete solidification). But for x in the triangle $D_3D_2P_3$, A is consumed and the liquid proceeds on curve P_3E_4.

The eutectic E_4 is reached by all liquids with x in triangle IV. Those from the triangle $D_3D_2P_3$ reach P_3, as already explained. Those in the quadrangle $P_3D_2e_5E_4$ precipitate D_2 as the first solid, reach one of the boundary curves, and then proceed to E_4, either along curve P_3E_4 precipitating D_3 and D_2, or along curve e_5E_4 precipitating D_2 and B. Those from the B field behave similarly, reaching E_4 either along curve e_4E_4 with D_3 and B as solids or along curve e_5E_4 with D_2 and B as solids. Those falling upon the D_3 field, $p_3P_3E_4e_4$, precipitate D_3 as first solid, and reach E_4 along either curve P_3E_4 or curve e_4E_4. Original compositions in the region $D_3P_3p_3$, such as point u, give A as first solid and reach the transition curve p_3P_3 on a straight line from A, as at point v. They then travel on the curve, toward P_3, but solid A is consumed before P_3 is reached, as at point w, on a straight line through D_3 and u. At this point the liquid is saturated only with D_3, and it therefore leaves the curve and travels across the D_3 field to one of its boundaries, P_3E_4 or e_4E_4, finally to reach E_4.

The transition curve p_3P_3 is therefore left behind, after some travel along the curve, by liquids coming from original, total compositions x in the region $D_3P_3p_3$, when the tie line D_3L of the three-phase triangle for L on curve p_3P_3 comes to sweep through x, for at that point the solid A will have been consumed to leave D_3 as the sole solid phase.

(We shall speak of the transition curve as thus being "crossed" by the liquid in an equilibrium process, for x in a specified region. The word "crossing" will be used, for brevity, to mean that the liquid reaches the curve from one field, travels along the curve for a limited range, and then, when the original solid is consumed, leaves it before reaching an invariant point, to move across the adjacent field.)

While the liquid is on any one field, precipitating a single solid, it travels in a straight line extending from the separating solid, until it reaches one of the boundary curves of the field.

Except for the region between point C and the curve between p_1 and s, the relations in the subsystem A–C–D_2 are simple. Precipitation of a first solid leads to a boundary curve, and along the curve to one of the eutectics. Thus compositions in the region rsE_1m give D_1 as first solid, reach either curve sE_1 or curve mE_1, and finally point E_1, to end as D_1, C, and D_2.

But p_1s is a transition curve, and it is crossed, as explained for curve p_3P_3, by liquids originating in the region p_1D_1s. The curve p_1s is reached by liquids precipitating C, from the region between the curve and the corner C. Those coming from above the tangent line D_1s do not leave the curve, but stay on the curve up to the eutectic E_1. Along the section p_1s the quantity of C is decreasing at the expense of D_1, and between s and E_1 both solids are being precipitated.

For solutions from the region p_1D_1s, solid C is consumed when the tie line D_1L of the three-phase triangle passes through the fixed total composition, and the liquid then leaves the curve. For x in the region D_1p_1r, the liquid then reaches either curve e_2E_2 or curve mE_2 to end at point E_2; from the region D_1ry (y being on the line D_1E_1), the liquid reaches curve mE_1 and hence point E_1.

For x in region D_1ys, the liquid, having followed the odd curve ys for part of its length, leaves the curve, travels across the D_1 field, and then reaches the even part of the same curve, sE_1. These compositions then give the following sequence of events. The liquid precipitates C as the primary solid and moves on the C field on a straight line from the corner C, to reach the curve between p_1 and s. Along the curve, as L moves toward s,

$$L + C \rightarrow D_1 \quad ,$$

and C will have been completely redissolved or consumed when L reaches a point on the curve between y and s, on the straight line D_1x. The liquid now traverses the D_1 field, precipitating D_1, and reaches the same curve again between s and E_1, where it precipitates both D_1 and C. Finally, at point E_1,

$$L \rightarrow D_1 + C + D_2 \quad .$$

The primary solid phase C therefore disappears, but C reappears later as a secondary crystallization product together with D_1.

Finally, some of the relations in Fig. 5.3 will be shown on isothermal diagrams and vertical T vs c sections. Attending first to the isothermal solubility curve of D_1, we note that between p_1 and r its isothermal solubility curve (simply an isothermal temperature contour on the D_1 field in Fig. 5.3) is not cut by the line D_1D_2, while between r and m it is. The solid D_1 is then said to be incongruently soluble in D_2 in the temperature range between p_1 and r, but congruently soluble in D_2 between r and m. A solubility isotherm for this region between p_1 and r would be schematically as in Fig. 5.5. Between r and m, we have Fig. 5.6: just above m', below e_2, below e_6 but above e_5, above p_3, and below the freezing point of B. The isotherm shown in Fig. 5.7 is still above E_1 and E_2, below p_3 but still above P_3 and e_5. Figure 5.8 is at P_3 and below E_1, E_2, and e_5, but still above e_4. At the invariant P_3, the field of A in equilibrium with liquid shrinks to a line (AP_3) and vanishes, in the reaction:

$$L(P_3) + A \rightarrow D_3 + D_2 \quad .$$

The vertical T vs c sections through D_1D_2 and D_3D_2 are relatively simple, as shown in Figs. 5.9 and 5.10 (schematic, not in scale with Fig. 5.3). Figure 5.11 shows the vertical section through CD_3, and Fig. 5.12 the section through D_1B (both schematic).

UNCLASSIFIED
ORNL-LR-DWG 24763

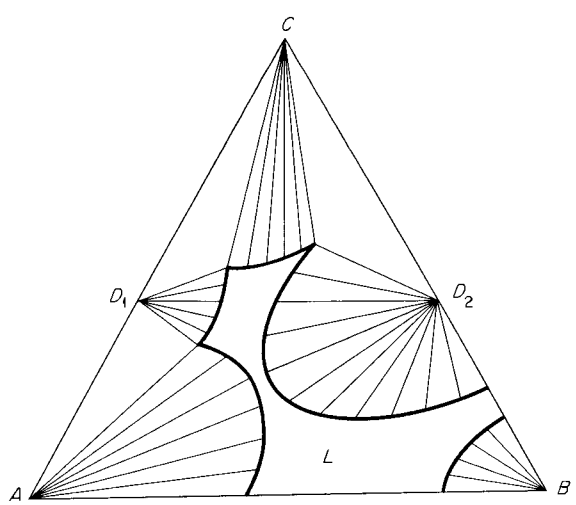

Fig. 5.6

UNCLASSIFIED
ORNL-LR-DWG 32574

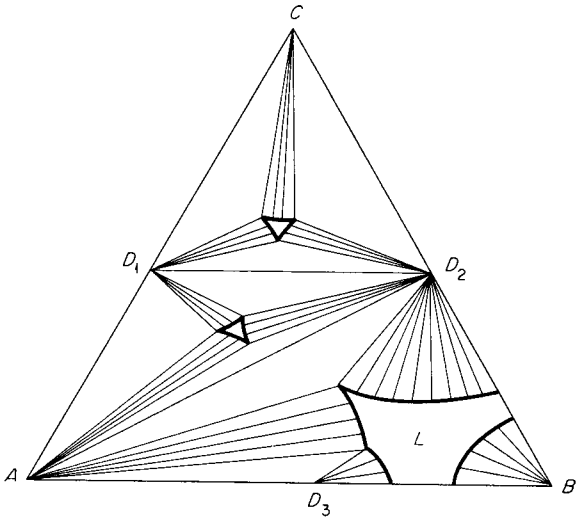

Fig. 5.7.

UNCLASSIFIED
ORNL-LR-DWG 24765

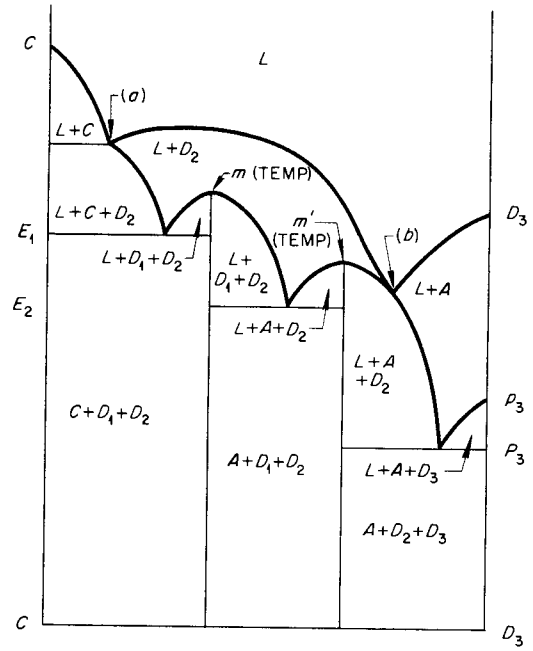

Fig. 5.11.

UNCLASSIFIED
ORNL-LR-DWG 24764

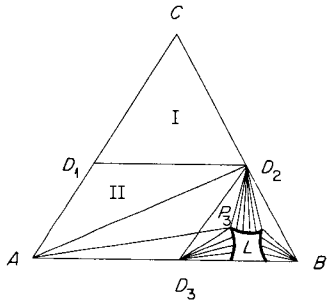

Fig. 5.8.

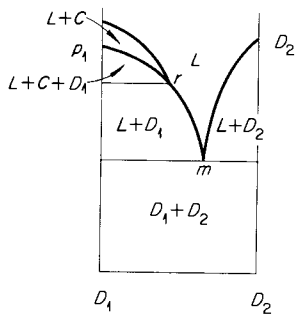

Fig. 5.9.

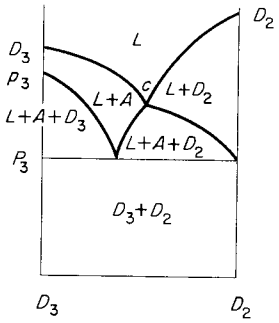

Fig. 5.10.

UNCLASSIFIED
ORNL-LR-DWG 24763

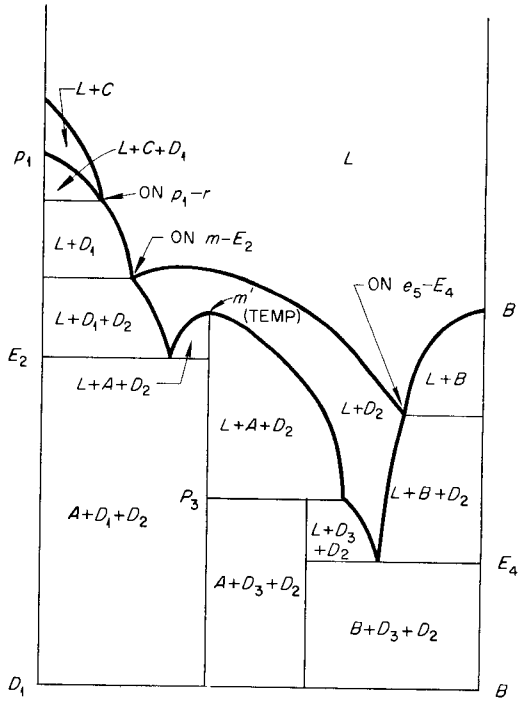

Fig. 5.12

6. CRYSTALLIZATION PROCESS WITH CONTINUOUS BINARY SOLID SOLUTION

The system of Fig. 6.1 involves two solid phases, pure C and the continuous binary solid solution A–B. The binary system has a minimum freezing point at m, Fig. 6.2. All ternary compositions must solidify to two solids, pure C and a binary A–B solid solution. Curve e_1e_2 represents liquid precipitating these two solids; M is a temperature minimum on this curve, and it is also the temperature minimum of the whole system. (Curve e_1e_2 may have either a minimum or a maximum or neither.) Liquids in the C field reach this curve on straight lines from the corner C; those in the solid solution field reach it along curves on the solid solution surface. In either case the liquid then travels toward M, but for complete equilibrium solidification is complete, leaving the two solids, before L reaches M, unless the total composition x lies on the straight line CMs. The three-phase triangles for L on the boundary curve start as the straight lines Ce_1A and Ce_2B and proceed, with falling temperature, toward M according to the configurations shown in Fig. 6.1, collapsing again, from either side, to the line CMs.

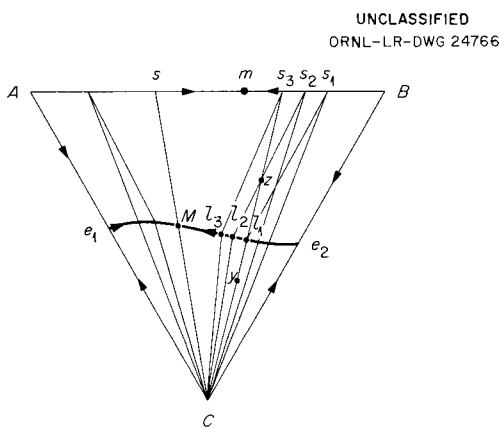

Fig. 6.1.

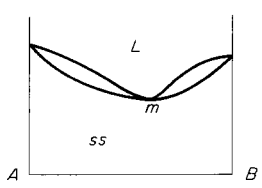

Fig. 6.2.

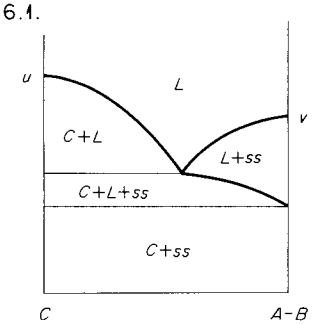

Fig. 6.3.

A vertical T vs c section from C to the side AB appears as in Fig. 6.3. Here the composition of the solid solution (ss) is not on the plane of the section. Even at point v the liquid of the section is not in equilibrium with solid solution of the same composition as the liquid (but point u of course is simply the melting point of pure C). Only for the section through Cm would v represent liquid and solid of the same composition, but the section through Cm would not pass through the ternary minimum M. The region $C + L + ss$ of Fig. 6.3 collapses to a horizontal (isothermal) line only for the section through M, CMs (and of course also at the binary sides Ce_1A and Ce_2B).

In an equilibrium process, any liquid of original composition x is completely solidified, while traveling on the curve, when the C–ss leg of the three-phase triangle passes through the point x, to leave C and a solid solution of composition on the extension of the line Cx. Solution y, moving on a straight line from C, reaches the curve at l_1 and there begins to precipitate s_1. As L travels on the curve toward M, more C and more solid solution will precipitate, but the solid solution changes in composition, leaving the solids C and s_3 when the last trace of liquid vanishes at l_3. Liquid z, moving on a curved equilibrium path, reaches the curve e_1e_2 at l_2, at which point the solid solution has the composition s_2. At l_2, C also begins to precipitate, and solidification is completed with liquid at l_3, leaving C and s_3.

The course of the liquid on the solid solution surface, however, is not shown by the "phase diagram" of Fig. 6.1. With a minimum m in the A–B binary equilibrium, this surface has two families of nonintersecting fractionation paths, as sketched in Fig. 6.4. All fractionation paths end, without intersection, at the boundary curve e_1e_2. The two families are separated by a limiting fractionation path originating at m. This path reaches the curve e_1e_2 at a point N which may be either on the left or on the right of M. Moreover, the path mN may be either convex toward B, as drawn, or convex toward A, and it may even have a point of inflection. With the arrangement assumed in Fig. 6.4, the fractionation paths on the A side are always convex toward B; those on the

UNCLASSIFIED
ORNL-LR-DWG 24767

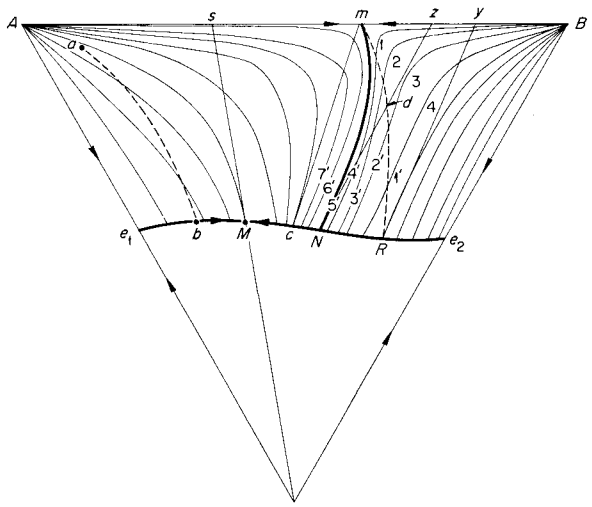

Fig. 6.4.

B side all start as convex toward A, but some of them have an inflection point and become convex toward B before they reach the boundary curve. These inflection points are joined by the locus curve mR.

6.1. FRACTIONATION PROCESS

As liquid follows one of the fractionation paths in a fractionation process, the composition of the layer of solid solution being deposited at any point is given by the tangent to the fractionation path through that point. Then, once the liquid reaches the curve e_1e_2, whether from the C field or from the solid solution field, it moves on the curve toward M as limit. For liquids traveling in the direction $e_1 \rightarrow M$, the outermost layers of solid solution being deposited have compositions increasing in B content, approaching s as the limit, from the A side. Those moving along the curve in the direction $e_2 \rightarrow M$ deposit layers increasing in A content, and also with s as limit.

The total process therefore varies according to the various regions of the surface. (In this discussion it must be remembered that the fractionation path is everywhere tangent to an equilibrium tie line. Hence the layer of solid being precipitated at the point where the fractionation path reaches the curve e_1e_2 is given by the tangent at that point, extended to the line AB. At M itself this tangent is the line CMs; at N the tangent goes to z, at R to y. Also, the word "solid" will here mean "the layer of solid being deposited.")

1. Region Ae_1M (i.e., between e_1 and the fractionation path AM): While L is still on the surface, the "solid" increases in B content, to a limit given by the tangent to the particular fractionation path involved at its intersection with the curve e_1M; and as L then travels on the curve (to M as limit), the "solid" increases still further in B (to s as limit).

2. Region between paths AM and mN: With L on the surface, the "solid" always increases in B, with z as the possible limit for fractionation paths reaching the boundary curve near N. The boundary is reached in the section MN, and then, as L moves toward M, the "solid" increases in A content, toward the limit s.

3. Region BRe_2: With L on the surface, the "solid" increases in A, with y as limit for the path BR itself; then, as L travels on the curve (to M as limit), the "solid" increases still further in A (to s as limit).

4. Region between paths BR and mN: The "solid" increases in A until the inflection point of the fractionation path is reached (intersection of fractionation path with curve mR), and the composition of the "solid" at that point is given by the tangent to the fractionation path at the inflection point. Now the "solid" begins to decrease in A content, to a limit given by the tangent at the end of the fractionation path at the boundary curve, reached in the portion NR. Then as L moves on the curve toward M as limit, the outermost layer of solid again moves to increasing A content, toward s as limit.

5. Path mN: For a solution on the path mN itself, the "solid" increases in B content (between limits $m \rightarrow z$), and then moves toward s as L, after reaching point N, moves on the curve toward M.

6.2. EQUILIBRIUM PROCESS

In a crystallization process with complete equilibrium between the total solid phase and the liquid, the liquid, such as point a in Fig. 6.4, follows an equilibrium path (dotted curve $a \ldots b$) in its course on the surface to the boundary curve e_1e_2. The relation of this equilibrium path to the fractionation paths which it crosses has been explained in connection with Fig. 2.4. The point b is fixed by a three-phase triangle with the ss–L leg passing through point a. Then as L moves on the curve toward M, solidification is complete when the ss–C leg of such a triangle passes through a.

The changes in the composition of the solid solution as the liquid follows its equilibrium path will depend on the region of the surface involved. Now the word "solid" will mean the total solid, assumed to be uniform in composition and in full equilibrium with the liquid. We note first that all equilibrium paths for solutions in the region $AsMe_1$ reach the boundary curve between e_1 and M; those for solutions in $BsMe_2$ reach the curve between e_2 and M. Point M is reached only for total compositions on the line CMs.

1. Region AMe_1: The equilibrium path does not cross the line sM on its way to the boundary curve. The solid increases in B both before and after L reaches the curve.

2. Region AMs: The equilibrium path crosses the line sM on its way to e_1M. The solid again increases in B both before and after L reaches the curve.

3. Region $smNM$: The equilibrium path does not cross the path mN; it ends on MN. The solid increases in B while L is on the surface, but the reverse change sets in when L begins to travel on the curve.

4. Region BRe_2: The equilibrium path does not cross the line Ry; it ends on e_2R; the solid increases in A both before and after L reaches the curve.

5. Region ByR: The equilibrium path crosses Ry; it ends on e_2R; the solid increases in A both before and after L reaches the curve.

6. Region $yzNR$: The equilibrium path does not cross the path mN; it ends on NR.

(*a*) Region $yzdR$: The solid increases in A until the equilibrium path crosses curve mR; then the solid increases in B until L reaches curve NR; then the solid increases again in A while L travels on the curve.

(*b*) Region dNR: The solid increases in B until L reaches curve NR; then it increases in A.

7. Region mzN: The equilibrium path crosses the path mN, to reach the boundary curve on the left of N (between c and N, curve cm being the $L-ss$ leg of a three-phase triangle for L at point c). The behavior for the regions above and below curve mR differs as described for region $yzNR$.

(The preceding discussion of Fig. 6.4 is based on the analysis by Osborn and Schairer.[1])

The composition of the equilibrium solid for original liquids in the region Rmy, as just stated, reverses its direction of change (increasing first in A, then in B) while the liquid is still on the surface. The equilibrium path for such a liquid first crosses fractionation paths which are convex with respect to A, in the order 1, 2, 3, 4, etc., and in this region the solid is becoming richer in A. But the rate of this composition change of the solid decreases as the equilibrium path meets fractionation paths of smaller and smaller convexity. When the equilibrium path finally reaches the locus curve mR, it has reached a fractionation path exactly at its inflection point, with no convexity at all at that point. This fractionation path will not be crossed by the equilibrium path, which here turns away and begins to recross the fractionation paths, which are now convex with respect to B; i.e., it now crosses the fractionation paths in the order 1′, 2′, 3′, ... , 7′, while the solid increases in B content.

It has been argued by Bowen[2] that when the equilibrium path just touches a fractionation path at the point of inflection of the latter (on curve mR), the equilibrium path undergoes an abrupt change in direction (a "corner"). This seems to be incorrect. The equilibrium path crosses fractionation paths only from their convex to their concave side. The sharper the curvature of a fractionation path, the greater is the angle of intersection where the equilibrium path crosses it. As the fractionation paths lose their curvature, approaching their inflection points, this angle of intersection diminishes; a zero angle of contact is approached (no longer an intersection) when the equilibrium path reaches a fractionation curve exactly at the latter's inflection point. If an equilibrium path has to cross the fractionation paths 1, 2, 3 before reaching path 4 at the inflection point of path 4, the intersection angle decreases as it crosses paths nearer and nearer to path 4, because the intersection is occurring nearer and nearer to an inflection point of a path.

[1] E. F. Osborn and J. F. Schairer, *Am. J. Sci.* **239**, 715 (1941).

[2] N. L. Bowen, *Proc. Natl. Acad. Sci. U.S.* **27**, 301 (1941).

The contact at such a point must therefore be tangential, and the equilibrium curve changes its course smoothly, without a cusp (Fig. 6.5). If i is the inflection point on the fractionation path Bf, and is is the tangent at i, then equilibrium paths for all total compositions (a, b, c) on the line is reach point i, changing their directions (with respect to the family of fractionation paths) as shown. The change in direction is more marked the farther the total composition is from the point i, but the equilibrium path is nevertheless tangent to Bf at i.

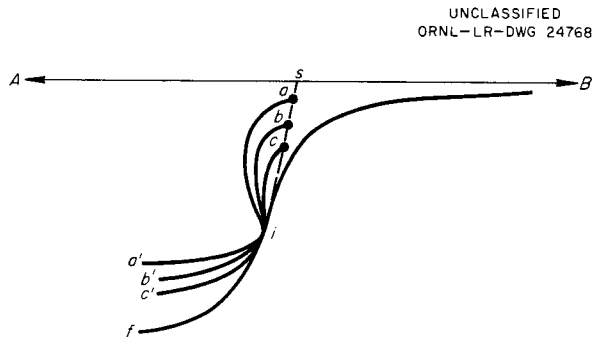

Fig. 6.5.

7. CRYSTALLIZATION PROCESS WITH SOLID SOLUTIONS AND SEVERAL INVARIANTS

7.1. THE PHASE DIAGRAM

In Fig. 7.1 the binary system A–B forms discontinuous solid solution with a eutectic at e_4, liquid saturated with solids whose compositions are S_e and S_e'. These points are to be compared with the binary diagram shown separately as Fig. 7.2. The other solid phases of the ternary system, C, D_1, D_2, are pure; D_1 is an incongruently melting binary compound, D_2 melts congruently. There are five fields – for C, D_1, D_2, A_s (the A-rich binary solid solution of A and B), and B_s (the B-rich binary solid solution of A and B) – and there are three invariant points, each pertaining to a three-solid triangle. From the directions of temperature fall, one is a peritectic, P_1, and two are eutectics, E_2 and E_3.

The curve E_2E_3 must have a saddle point m on it, and the A_s solid solution which (together with solid D_2) saturates the liquid at point m must lie on the extension of the straight line D_2m to the side AB, at S_m. The solid solutions saturating liquid E_3 are somewhere close to the points S_e and S_e'. Since the temperature of E_3 is lower than e_4, the compositions of the limiting solids of the A–B miscibility gap at E_3 will depend on the effect of temperature on the solid-solid solubility.

The three-solid triangles for any of the three invariant points, therefore, cannot be drawn in without the experimental determination of tie lines along the curves near the invariants, and ultimately of the solid solution compositions at the invariants. The invariant P_1, a peritectic, involves the solids C, D_1, and S_1 (a solid solution of composition somewhere near A) in the reaction:

$$L(P_1) + D_1 \rightarrow C + S_1 \quad ,$$

and P_1 is outside triangle I (CD_1S_1). The eutectic E_2 must be inside triangle II (CD_2S_2, where S_2 is another unknown solid solution composition); E_3 must be inside triangle III ($D_2S_3S_3'$). In the last case, S_3 and S_3' are known points if the solid solution limits in the binary system A–B are known for the temperature of E_3 (as in Fig. 7.2).

In Fig. 7.3, we assume that these key solid solution compositions have been determined and that the three-solid triangles may therefore be drawn. The solid miscibility gap in system A–B has been assumed to widen with falling temperature (Fig. 7.2) so that S_e and S_e' lie between the points S_3 and S_3'.

Since S_1, S_2, and S_3 are different compositions, the three-solid triangles are not adjacent. They do not have common sides, and they do not cover the whole of the diagram. Only original compositions x falling inside one of these three-solid triangles will, on cooling with complete equilibrium,

UNCLASSIFIED
ORNL-LR-DWG 24769

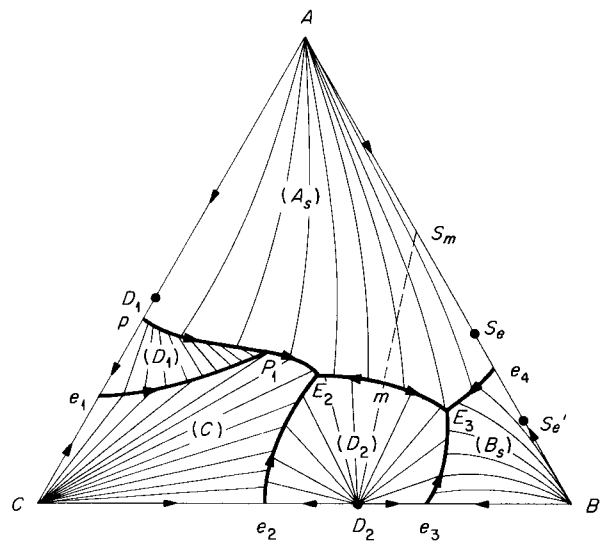

Fig. 7.1.

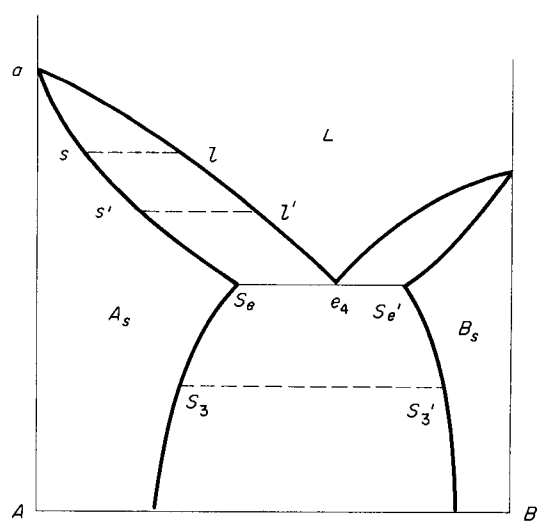

Fig. 7.2.

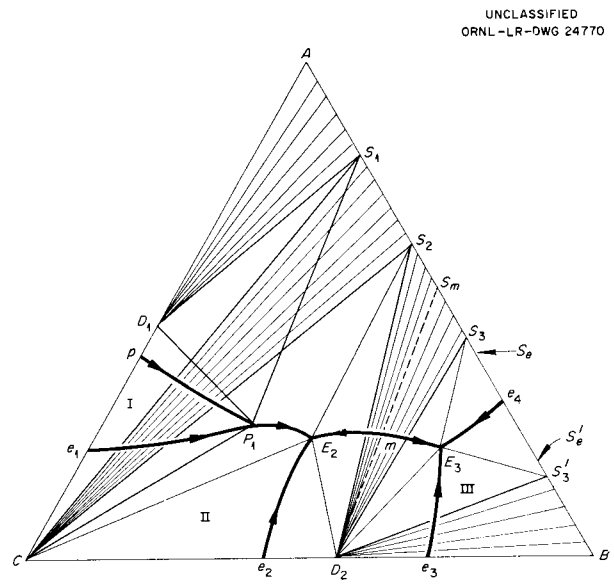

Fig. 7.3.

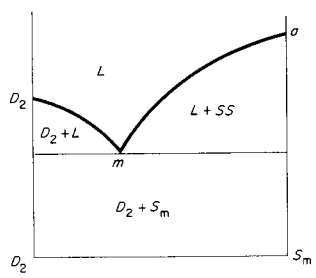

Fig. 7.4.

solidify to mixtures of three solids: those in triangle I solidify incongruently at P_1, those in triangle II and triangle III solidify congruently at E_2 and E_3, respectively. The areas not included in these triangles solidify to two-solid mixtures, and hence these areas are shown with tie lines: D_1 and a solid solution whose composition is between A and S_1 for the area D_1AS_1; C and a solid solution between S_1 and S_2 for the area CS_1S_2; D_2 and a solid solution between S_2 and S_3 for the area $D_2S_2S_3$; and D_2 and a solid solution between S_3' and B for the area $D_2S_3'B$.

The three-solid triangles do not overlap unless solid-phase interactions (here excluded) should occur at temperatures between the invariants. But when peritectic invariants are involved, the invariant planes (which include the liquid phase besides the three solids) may overlap, as is the case here for the invariant quadrangle $CD_1S_1P_1$, overlapping, on the polythermal projection, the invariant triangle CS_2D_2 (with E_2 as interior phase). These planes are at different temperatures; the P_1 plane is above the E_2 plane, which is above the E_3 plane.

Also, the solid solution compositions S_1 and S_2, it must be kept in mind, are not on the solidus curve aS_e of Fig. 7.2. They are simply compositions in the area of solid solution below this binary solidus curve. Liquids on the curve e_4E_3, including the points e_4 and E_3, are in equilibrium with conjugate solid solutions – solid solutions defined by the miscibility gap of Fig. 7.2. But the solid solutions involved along all other curves (pP_1, P_1E_2, E_2E_3, and e_3E_3, with the exception of just the point E_3) are simply compositions in the solid solution areas of Fig. 7.2.

7.2. EQUILIBRIUM CRYSTALLIZATION PROCESS

The reactions on curves e_1P_1 and e_2E_2 of Fig. 7.3 are simple precipitations of two pure solids; on e_1P_1:

$$L \rightarrow C + D_1 \quad ,$$

and on e_2E_2:

$$L \rightarrow C + D_2 \quad .$$

On curve e_4E_3, the liquid precipitates two solid solutions, starting as S_e and S_e' at e_4 and changing in composition to S_3 and S_3' at E_3. On curve e_3E_3, the liquid precipitates D_2 and a solid solution starting as pure B at e_3 and changing in composition to S_3' at E_3. For curve E_2E_3, the liquid is precipitating D_2 and a solid solution. If S_m is the composition of the solid solution for L at m (maximum of the curve), then along curve mE_3 the solid solution varies from S_m to S_3, and along curve mE_2 it varies from S_m to S_2. The vertical T vs c section on the line D_2mS_m is shown in Fig. 7.4. It looks like a quasi-binary section but it is not. The liquid on the curve am of Fig. 7.4 is in equilibrium, not with S_m, but with a solid solution of changing composition (not on the plane of the diagram) which is S_m only for L at point m itself.

Along curve P_1E_2, the liquid precipitates C and a solid solution changing from S_1 (at P_1) to

S_2 (at E_2). Curve pP_1 is a transition curve, along which the liquid reacts with solid solution and precipitates D_1. The three-phase triangle starts as the line pD_1A and ends as $P_1D_1S_1$, so that the solid solution in equilibrium with liquid on the curve varies from A at p to S_1 at P_1.

Since the solid solutions in the system are only binary, solidification cannot be complete while liquid is traveling on one of the surfaces; the liquid must reach either a curve involving a solid solution or one of the invariants. The course of the liquid on a surface precipitating a pure solid (C, D_1, or D_2) is clear: a straight line from the composition of the separating solid (Fig. 7.1). On the two surfaces for solid solution, the paths, whether for fractionation or for equilibrium crystallization, are curved. Fractionation paths are shown in Fig. 7.1; equilibrium paths cross these curves as explained under Fig. 2.4.

In the region D_2S_mB, only liquids from an original composition x in triangle III ($D_2S_3S_3'$) reach E_3, to solidify to three solids. Those for x in triangle $E_3S_3S_3'$ reach E_3 along curve e_4E_3, carrying two solid solutions, and these liquids do not solidify completely until they reach E_3, to produce D_2 as third phase. For x in the region $D_2E_3S_3'B$, the liquid reaches the curve e_3E_3, but if x is in triangle $D_2S_3'B$, the liquid is consumed (in complete equilibrium) before reaching the eutectic, to leave D_2 and a solid solution between B and S_3'. Liquids in the region $D_2S_mS_3E_3$ reach curve mE_3, and again those in triangle $D_2S_mS_3$ solidify completely on the curve, before reaching E_3, to leave D_2 and a solid solution between S_m and S_3. (Similar behavior is shown in the region $D_2S_mS_2E_2$.)

The curve pP_1 is reached by liquids originating in the region pAS_1P_1, after first precipitating a solid solution between A and S_1. For x in triangle D_1AS_1, the liquid is consumed on the curve pP_1, leaving D_1 and solid solution. For x in triangle pD_1P_1 the solid solution is consumed on the curve, leaving liquid and D_1; L then leaves the curve, crosses the D_1 field to curve e_1P_1, and travels to P_1. For x in triangle $D_1S_1P_1$, no phase is completely consumed along curve pP_1, and the liquid reaches P_1.

The peritectic P_1 is also reached for x in the D_1 field and for x in the region Ce_1P_1 – along curve e_1P_1; P_1 is thus reached only for x in the quadrangle $CD_1S_1P_1$. At P_1,

$$L + D_1 \rightarrow C + S_1 \quad .$$

Hence solidification is completed here for x in CD_1S_1 (triangle I), in an incongruent crystallization end point. Otherwise (for x in triangle CS_1P_1) D_1 is consumed and L begins to move along curve P_1E_2. This curve is also reached directly from the C field, for x in the region CP_1E_2, and from the A_s field for x in the region $P_1S_1S_2E_2$. As L travels on this curve, precipitating C and solid solution, it completes its solidification if the total original composition x is in triangle CS_1S_2; otherwise it reaches E_2, the crystallization end point for triangle II.

Some isothermal relations are shown in Figs. 7.5, 7.6, and 7.7. Figure 7.5 is still above the temperature of p, Fig. 7.6 just below p. Points s, l, s', and l' in these diagrams are related to the solidus and liquidus curves of the binary system A–B shown in Fig. 7.2. The points s'', s''' in Fig. 7.7 are between S_e and S_3 and between S_e' and S_3', respectively, of Fig. 7.2. The temperature of Fig. 7.7 is between m and the eutectics E_2, E_3, below all the binary eutectics, but still above P_1. At P_1 the tie-line region for D_1 in

UNCLASSIFIED
ORNL-LR-DWG 24771

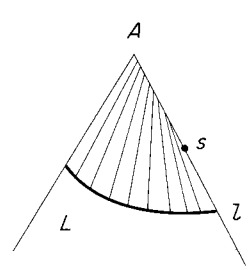

Fig. 7.5.

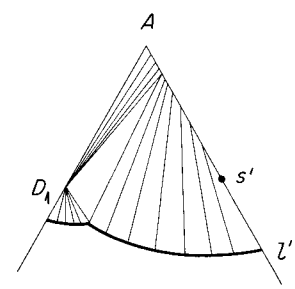

Fig. 7.6.

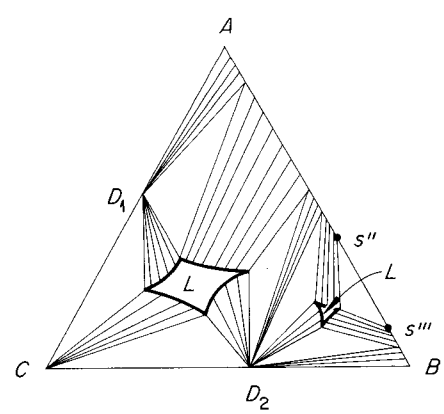

Fig. 7.7.

equilibrium with liquid shrinks to a line and vanishes.

Some vertical sections are shown in Figs. 7.8, 7.9, 7.10. The m in Fig. 7.9 is at the temperature of point m but does not represent its composition.

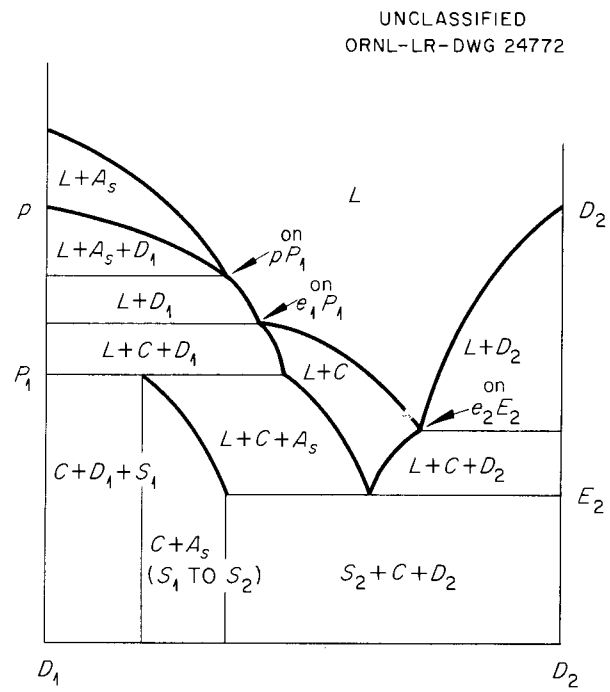

Fig. 7.8.

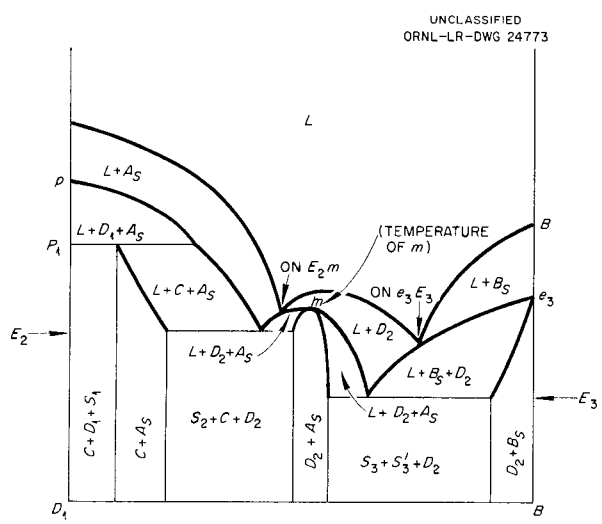

Fig. 7.9.

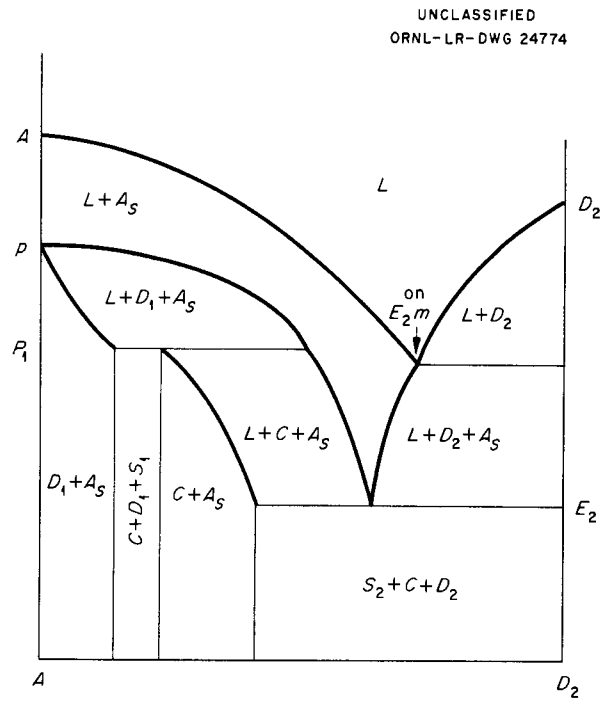

Fig. 7.10.

7.3. PROCESS OF CRYSTALLIZATION WITH PERFECT FRACTIONATION

The fractionation paths in the two solid solution fields (Fig. 7.1) are families of curves radiating from points A and B, respectively. Those in the A_s field are convex with respect to B, meaning that as L travels along such a path on cooling, in a fractionation process, it deposits successive solid solution layers always richer in B content; those in the B_s field are convex with respect to A, and the outermost solid solution layer here continually increases in A content while L is traveling on the surface.

In fractionation, a liquid in the region between e_3 and the path BE_3 reaches the curve e_3E_3, and on this curve the solid solution continues to increase in A content. Liquid between e_4 and the path BE_3 reaches curve e_4E_3, but now two solid solutions precipitate, and their outermost layers vary from S_e and S_e' to S_3 and S_3' in composition (Fig. 7.3). In an equilibrium process, the curve e_3E_3 is reached by all liquids below the line

E_3S_3', which is tangent, of course, to the fractionation path BE_3 at E_3, and e_4E_3 is reached only by liquids between e_4 and line E_3S_3'.

In a fractionation process on the A_s field, the curve P_1E_2 is reached by liquids between the fractionation paths AP_1 and AE_2, and the solid solution continues to increase in B content along this curve. Curve E_2m is reached by liquids between the paths AE_2 and Am, but in this case the outermost solid solution layer being deposited begins to increase in A content as L travels on this curve in the direction $m \rightarrow E_2$. The fractionation process for the region between the paths AP_1 and Am ends at E_2. The curve mE_3 is reached for liquids between paths Am and AE_3, with the solid solution increasing in B content both before and after L reaches the curve; and curve e_4E_3 is reached for liquids between e_4 and the path AE_3. In these regions the fractionation ends at E_3.

Liquid between p and the path AP_1 reaches the curve pP_1 and immediately crosses this curve to deposit D_1 on the solid solution already deposited before the curve was reached. The liquid then reaches curve e_1P_1, deposits a mixture of D_1 and C while traveling on this curve, reaches P_1, and without stopping at P_1 continues on curve P_1E_2, depositing C and a solid solution. The process ends at E_2. In this process the precipitation of the solid solution is interrupted while L is crossing the D_1 field and then returning to P_1 on the curve e_1P_1. There will consequently be a gap in the composition of the solid solution finally obtained.

In the fractionation process all liquids in the region bounded by the lines mD_2, D_2B, BA, and the fractionation path Am end at E_3, to leave three solids, A_s, B, and D_2. Liquids in the rest of the system end at E_2; of these, moreover, those in the region bounded by lines P_1C, CA, and the path AP_1 end as a mixture of four solids, A_s, D_1, C, and D_2, while the rest end as three solids, A_s, C, and D_2.

7.4. TERNARY SOLID SOLUTION IN COMPOUND D_1

Finally, we shall assume that the solid D_1 forms solid solution with both A and C in its binary system and with the third component B, to give at any temperature a small isothermal area of solid solution of ternary composition. This will affect all the equilibria involving solid D_1. The pertinent region of Fig. 7.3 becomes that shown in Fig. 7.11. Figures 7.6 and 7.7 change as shown in Figs. 7.12 and 7.13. A section like Fig. 7.8 now shows the region of homogeneous ternary solid at the D_1 side, labeled $D_1(s)$ in Fig. 7.14.

UNCLASSIFIED
ORNL-LR-DWG 24775

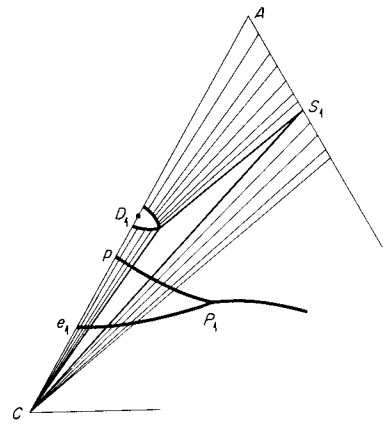

Fig. 7.11.

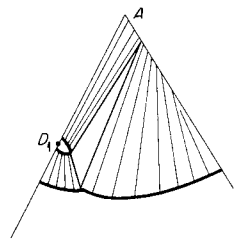

Fig. 7.12.

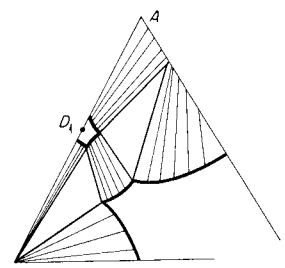

Fig. 7.13.

UNCLASSIFIED
ORNL-LR-DWG 24776

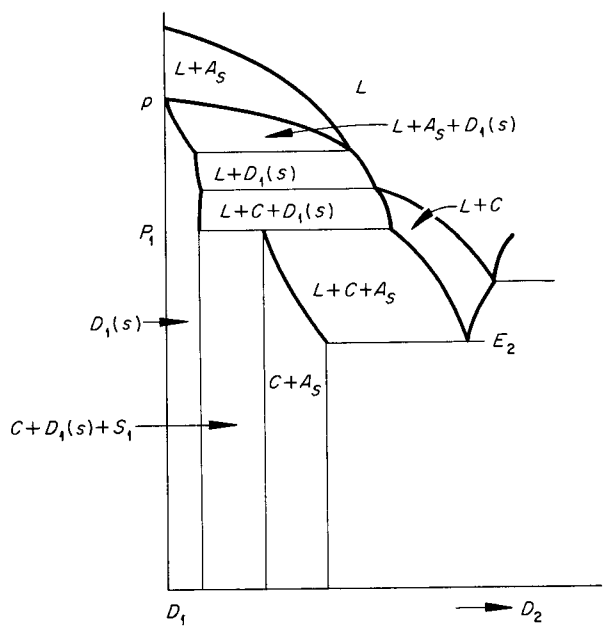

Fig. 7.14.

PART II

THE ACTUAL DIAGRAMS

The following sections will consider, one at a time, the ternary diagrams which have been constructed. For ease of drawing and for the sake of clarity, the diagrams used in these sections are not according to actual scale, but schematic in their quantitative relations. The formulas and the actual numerical values, including the temperatures, may be obtained from the experimental diagrams. For brevity and simplicity, moreover, single letters rather than chemical formulas have been used to represent the solid phases.

The following is the key for the letters regularly used for the components of all the systems:

Symbol	Component
R	RbF
U	UF_4
V	BeF_2
W	ThF_4
X	LiF
Y	NaF
Z	ZrF_4

The letters $A, B, \ldots, N$ will be used, as needed, for the various binary compounds in the binary systems. They do not represent the same compounds from one section (ternary system) to another, whereas the components are always referred to by the same letters.

The letter x will be used throughout to mean "the total original composition of a sample being cooled and solidified."

8. SYSTEM X–U–V: LiF–UF_4–BeF_2

The schematic phase diagrams for the binary systems of the first ternary system to be discussed, system X–U–V, are shown in Figs. 8.1, 8.2, and 8.3. No solid solution is involved, either in the binary systems or in the ternary system. Compound A in system X–U decomposes on cooling, at T_A, into the solids X and B; and compound E in system X–V forms on cooling, at T_E, from the solids D and V.

Every solid reaching equilibrium with liquid in its binary system must have its own primary phase field, bordering on the side of the triangle, in the ternary system. The field for compound A of the system X–U, however, will have T_A (designated P_A in the ternary system) as its lower temperature limit of stability, inasmuch as A decomposes on cooling to this temperature. At P_A the X and B surfaces of the ternary liquidus, separated above that temperature by the A field, will come into contact. The compound E of system X–V may or may not have a field (for liquid in equilibrium with solid E) in the ternary system. It will have a field only if the ternary liquid saturated with the two solids D and V exists down to the temperature T_E of Fig. 8.3, the temperature for the formation of E from D and V upon cooling.

The phase diagram of the ternary system is given in Fig. 8.4 (schematic). There are seven fields, identified by letters in parentheses, (U), (C), etc. The A field vanishes with falling temperature at P_A, at the temperature of decomposition of solid A in its binary system, T_A, but now in presence of ternary liquid. The temperature of

UNCLASSIFIED
ORNL-LR-DWG 25579

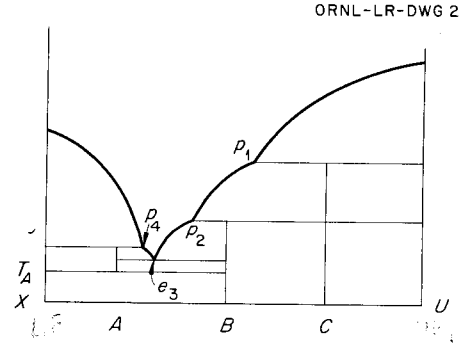

Fig. 8.1.

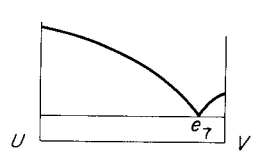

Fig. 8.2.

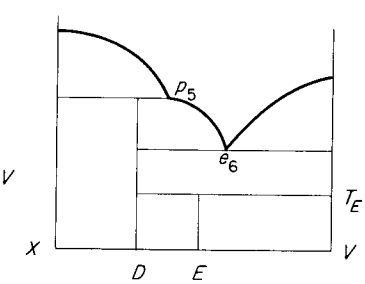

Fig. 8.3.

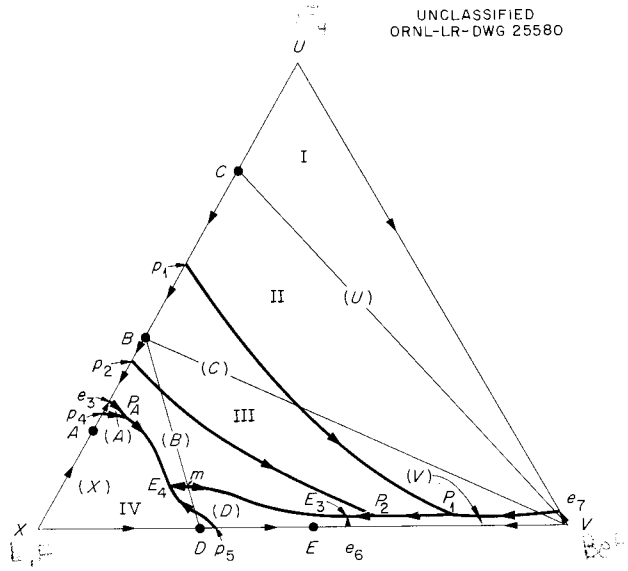

Fig. 8.4.

decomposition is unchanged, because the component V does not form solid solution with any of the three solids involved in the reaction. Since solid A decomposes before its field touches any field involving the component V, it is not part of one of the three-solid triangles of the system, of which there are only four, I, II, III, IV, with the corresponding invariant liquids P_1, P_2, E_3, E_4.

The reactions on the curves are as follows (all written as the reactions occurring upon cooling):

p_1P_1: $L + U \rightarrow C$.

p_2P_2: $L + C \rightarrow B$.

p_4P_A: $L + X \rightarrow A$.

e_3P_A: $L \rightarrow A + B$.

p_5E_4: $L + X \rightarrow D$. But this may change to:

$$L \rightarrow X + D$$

as the curve approaches E_4; it does change if the tangent to the curve comes to fall between X and D.

e_6E_3: $L \rightarrow D + V$.

e_7P_1: $L \rightarrow U + V$.

P_1P_2: $L \rightarrow C + V$.

P_2E_3: $L \rightarrow B + V$.

E_4E_3: $L \rightarrow B + D$. Accordingly, m is a saddle point, with temperature falling away both toward E_4 and toward E_3. But the line BD is not a quasi-binary section, for it includes the C field and the X field.

The invariant reactions are as follows:

P_1: $L + U \rightarrow C + V$. Point P_1 is reached along either of the two curves falling to it, for x in the quadrangle P_1CUV. It is the incongruent crystallization end point for triangle I (CUV). If x is in triangle P_1CV, the liquid continues, completing its solidification at P_2 for x in triangle II, or continuing still further and completing its solidification at E_3 for x in triangle III.

P_2: $L + C \rightarrow B + V$. Point P_2 is reached along either of the curves p_2P_2 or P_1P_2, for x in the quadrangle P_2BCV. It is the incongruent solidification end point for x in triangle II.

E_3: $L \rightarrow D + B + V$. Point E_3 is the congruent solidification end point for triangle III. The final equilibrium solids for this triangle, left at the lowest liquid reaction (E_3) of the region (triangle III), are therefore B, D, and V. However, at a still lower temperature (T_E of Fig. 8.3) the solids D and V react to form the compound E. Below T_E, therefore, the triangle III becomes two three-solid triangles, one for B, D, and E and one for B, E, and V.

E_4: $L \rightarrow X + B + D$. Point E_4 is the congruent solidification end point for triangle IV.

P_A: $A \rightarrow X + B$, in the presence of liquid P_A. The point P_A is reached by liquid for x in the triangle XBP_A, along either curve p_4P_A (as liquid in equilibrium with X and A) or curve e_3P_A (as liquid in equilibrium with A and B). At P_A the solid A decomposes to produce more X and B, and the liquid moves on along curve P_AE_4.

Four of the boundary curves are of odd reaction (transition curves). They are crossed by equilibrium crystallization paths as follows. (The expression "crossing of transition curves" is used with the meaning explained in Sec 5 in connection with curve p_3P_3 of Fig. 5.3. For restricted values of x, the liquid reaching a transition curve travels along the curve only for part of its length and then leaves it for another field.)

1. p_1P_1: Liquids reaching this curve for x in p_1CP_1 (i.e., in the region between C and the curve p_1P_1) travel along the curve only until all solid U is consumed, when the CL leg of the three-phase triangle passes through x; L then leaves the curve and crosses the C field.

2. p_2P_2: Similarly crossed by liquids reaching it from x in the region p_2BP_2, L proceeding onto the B field.

3. p_4P_A: Similarly crossed by L for x in the region p_4AP_A, L proceeding to travel upon the A field.

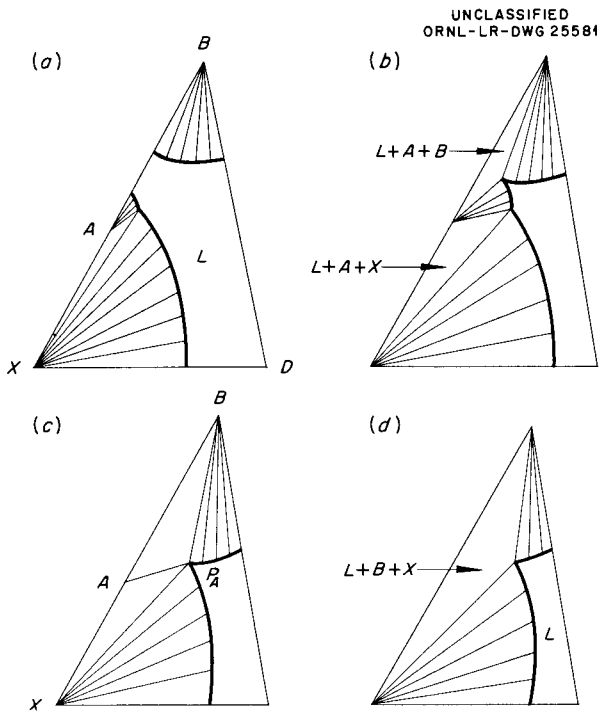

Fig. 8.5.

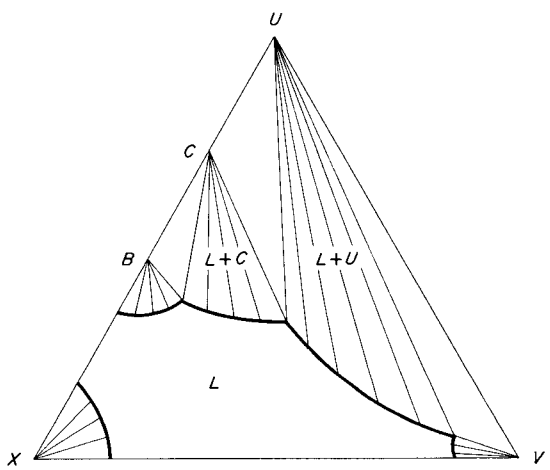

Fig. 8.6.

4. p_5E_4: Crossed for x in the region p_5Ds (s is the point of tangency of the LD leg of the three-phase triangle with curve p_5E_4). Then, for the region between the line Ds and the line DE_4, the primary X solid, which has been entirely consumed while L travels on the curve p_5s, appears again as a secondary crystallization product, mixed with D, when L, traversing the D field, reaches the curve sE_4 (cf. curve p_1E_1 of Fig. 5.3).

The isothermal relations for the A solid are shown in Fig. 8.5, (a) between p_4 and e_3, (b) between e_3 and P_A, (c) at P_A, and (d) below P_A.

Figure 8.6 is a schematic isotherm between e_3 and p_2, above P_2 and P_1, above p_4, and below e_7. The $L + U$ region will vanish as a line when the temperature falls to P_1, and the $L + C$ region vanishes similarly at P_2.

Some vertical T vs c sections are shown in Figs. 8.7, 8.8, 8.9, and 8.10.

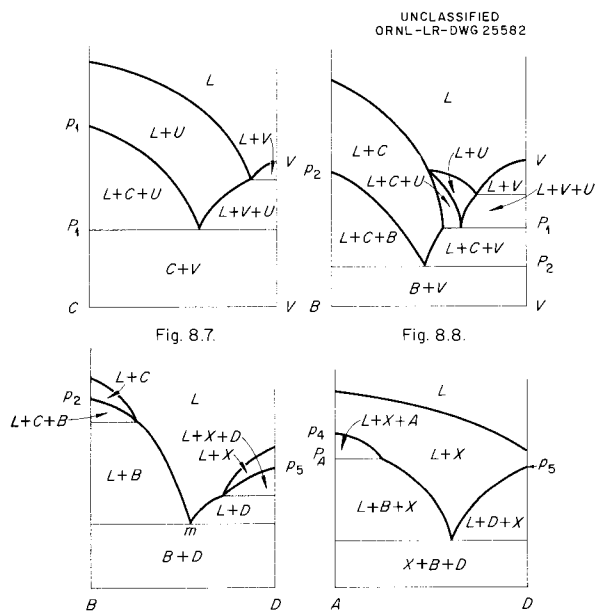

Fig. 8.7. Fig. 8.8.

Fig. 8.9. Fig. 8.10.

9. SYSTEM Y–U–V: NaF–UF_4–BeF_2

For the ternary system Y–U–V, we have the binary systems Y–U in Fig. 9.1 and Y–V in Fig. 9.2; the system U–V is as in Fig. 8.2, except that point e_7 is now designated e_9. The ternary diagram is given in Fig. 9.3.

The horizontal dotted lines in Figs. 9.1 and 9.2 represent polymorphic changes in pure phases: one in solid A, two in H, and one in G. Even when these transitions occur at liquidus temperatures, as in the transition T' for compound G, there is hardly any effect in the ternary diagram. Strictly, the freezing-point curve of G in the binary system Y–V has a slight break at t'. This break becomes an isothermal crease on the G surface in the ternary system. The crease starts at t' and enters the ternary diagram to look simply like an isothermal contour on the surface. It represents liquid in equilibrium with both forms of G. Above this temperature the surface is for liquid in equilibrium with G_α, and below this temperature it is the surface for liquid in equilibrium with G_β. This crease has been sketched in Fig. 9.3 as the curve $t't''$ across the G field.

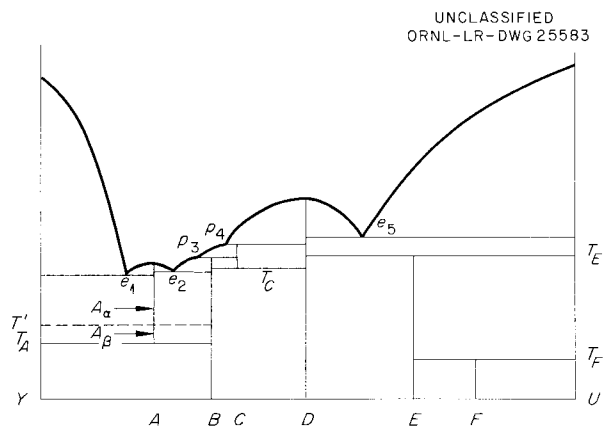

Fig. 9.1.

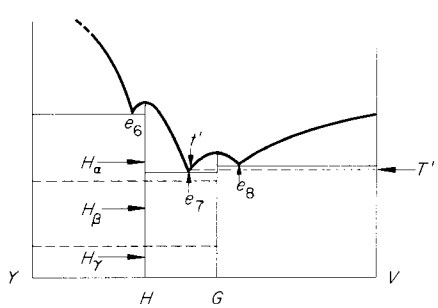

Fig. 9.2.

In the system Y–U, Fig. 9.1, we note two binary compounds, A and C, decomposing upon cooling and two, E and F, forming from other solids upon cooling. The first two decompose before reaching an invariant involving a solid containing component V; hence, as in the case of compound A in system X–U–V, these solids have primary phase fields but do not take part in the three-solid triangles of the ternary system. The compounds E and F of the present system, unlike the similar compound E of system X–U–V (Fig. 8.4), do have ternary fields in the system, because the curve for liquid in equilibrium with D and U extends down to the temperature T_E for the formation of E from D and U, and the resulting curve for liquid in equilibrium with E and U further extends down to the temperature T_F for the formation of F from E and U.

The ternary diagram thus has eleven fields and seven three-solid triangles (with corresponding invariant liquids). It also has four invariant points for liquids accompanying binary solid-phase reactions: P_A and P_C for the decompositions of solids A and C on cooling, and P_E and P_F for the formation of solids E and F on cooling.

The limited A field is divided into two regions by an isothermal crease, uv on Fig. 9.3. This crease is at the temperature T' of Fig. 9.1, the transition temperature for:

$$A_\alpha - \text{calories} \rightleftharpoons A_\beta \ .$$

The higher-temperature region of the field represents liquid in equilibrium with A_α, the lower region liquid in equilibrium with A_β; the form decomposing at P_A is A_β.

The similar transitions in the solid H are assumed to occur below the temperature of equilibrium with any ternary liquid, and hence are assumed to have no effect on the phase diagram.

Five curves are of odd reaction. (The even curves simply precipitate the solids of both adjacent fields.) The transition curves are as follows:

p_4P_C: $L + D \rightarrow C$; crossed by L for x in region Cp_4P_C.
p_3P_C: $L + C \rightarrow B$; crossed by L for x in region Bp_3P_C.
P_EP_F: $L + U \rightarrow E$; crossed for x in EP_EP_F.
P_FP_1: $L + U \rightarrow F$; crossed for x in FP_FP_1.
P_FP_2: $L + F \rightarrow E$; crossed for x in EP_FP_2.

UNCLASSIFIED
ORNL-LR-DWG 25584

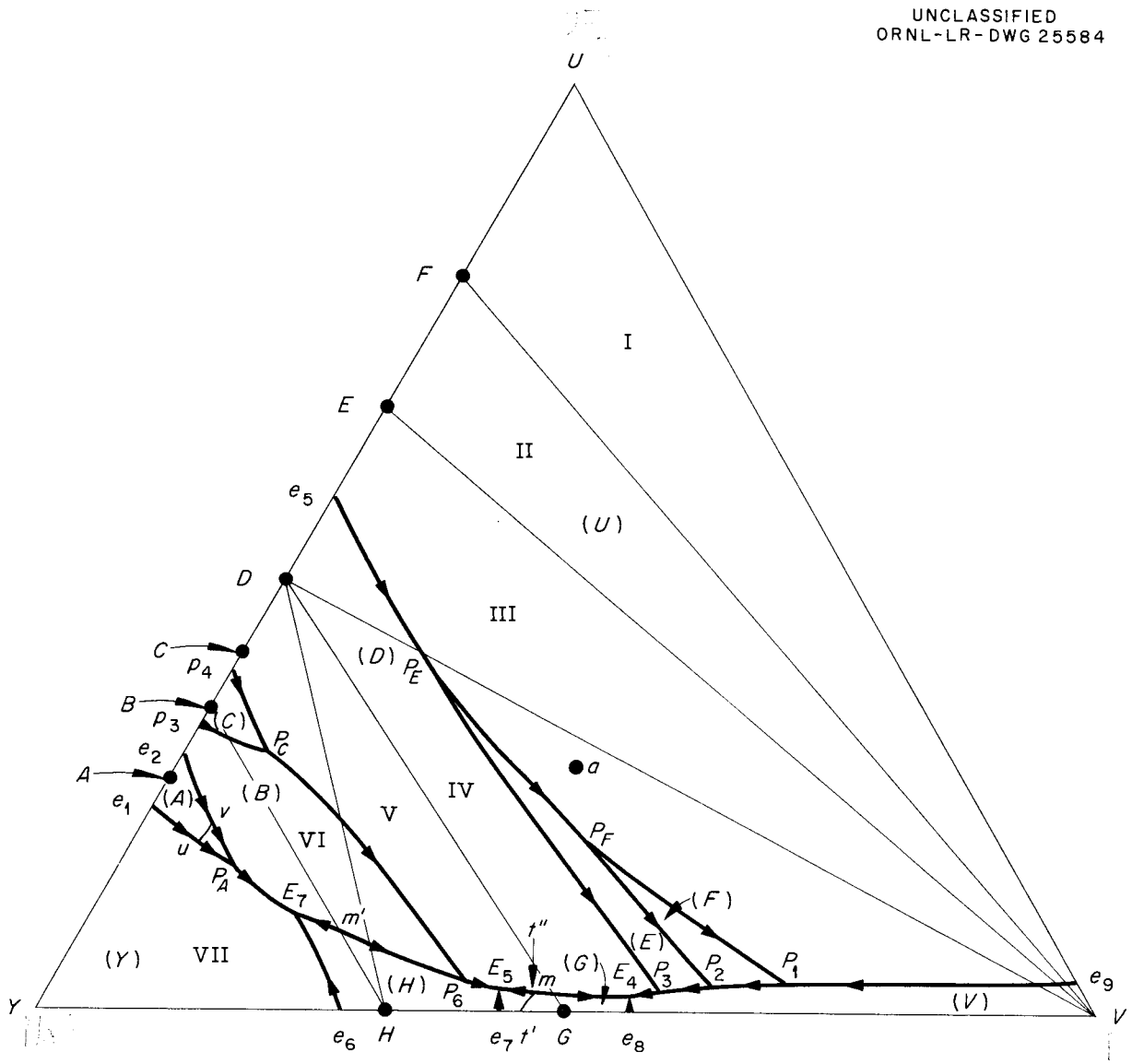

Fig. 9.3.

Invariant reactions are:

P_1: $L + U \rightarrow F + V$; incongruent crystallization end point for triangle I.

P_2: $L + F \rightarrow E + V$; same, for triangle II.

P_3: $L + E \rightarrow D + V$; same, for triangle III.

P_6: $L + B \rightarrow D + H$; same, for triangle VI.

E_4, E_5, E_7: eutectics for triangles IV, V, VII.

There are two saddle points: m on curve E_4E_5 and m' on curve P_6E_7. But only the line DG is a quasi-binary section, dividing the whole diagram into essentially independent subsystems. (Note: The composition diagram of a ternary system does not have to be a triangle. As long as it is a plane, with only two independent composition variables, it may have any shape.)

Some relations in the subsystem D–U–V–G may be illustrated by consideration of the equilibrium crystallization process for solution a, Fig. 9.3. This point is located on the left of line UP_F, in the region FP_FP_1, in the region EP_FP_2, in the quadrangle P_3DEV, and in triangle IV. The first solid on cooling is U, and the liquid travels on the

straight line Ua to the curve $P_E P_F$. With L on the curve,

$$L + U \rightarrow E \quad ,$$

but not all the U solid is consumed, and L reaches P_F. At this point all the E solid so far produced is consumed in reaction with U, to form F, and then the liquid, saturated with U and F, begins to travel on the curve $P_F P_1$. On this curve, the rest of the U solid is consumed, and L leaves the curve to traverse the F field on the straight line Fa. When L reaches the curve $P_F P_2$,

$$L + F \rightarrow E \quad ,$$

and now when all the F is consumed the liquid leaves this curve to traverse the E field, on the straight line Ea, until it reaches the curve $P_2 P_3$. Now precipitating E and V, the liquid reaches P_3, where

$$L + E \rightarrow D + V \quad .$$

Here E is consumed, and L moves on down the curve $P_3 E_4$, precipitating D and V. It reaches E_4 and there solidifies completely to G, D, and V. The original solution a thus gives only three solids upon solidification with complete equilibrium. If the phases are not given sufficient time for reaction during the cooling process, the liquid from the composition a would still reach E_4 before complete solidification, but the final mixture would contain all the solids of the subsystem: U, E, F, V, D, and G.

The point P_E is reached, in equilibrium crystallization, for x in the region $DP_E U$, by L on curve $e_5 P_E$ carrying solids D and U; at P_E these solids react to form E, leaving one of them in excess. Hence, if x is in the region DEP_E, U is consumed and L takes the curve $P_E P_3$; for x in the region EUP_E, D is consumed and L travels on curve $P_E P_F$. The point P_F is similarly reached, for x in the region $EP_F U$, by L on curve $P_E P_F$ carrying solids E and U. Then for x in the region EFP_F, U is consumed and L leaves on curve $P_F P_2$, while for x in FUP_F, E is consumed and L takes the curve $P_F P_1$.

Isotherms near P_F are shown in Fig. 9.4 (a) just above P_F and (b) just below P_F. At P_F the equilibrium area for liquid in equilibrium with F appears as the line FP_F.

Vertical T vs c diagrams for three sections of this subsystem are shown in Figs. 9.5, 9.6, and 9.7; and two T vs c sections for the subsystem Y–D–G are shown in Figs. 9.8 and 9.9.

UNCLASSIFIED
ORNL-LR-DWG 25585

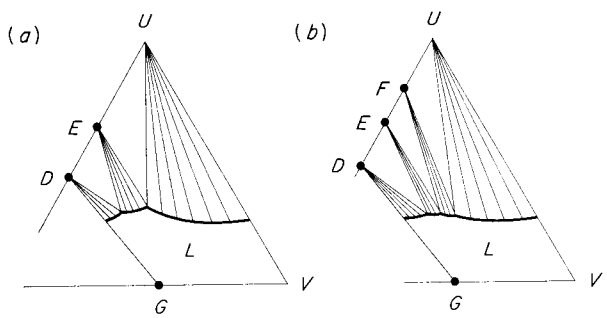

Fig. 9.4.

UNCLASSIFIED
ORNL-LR-DWG 25586

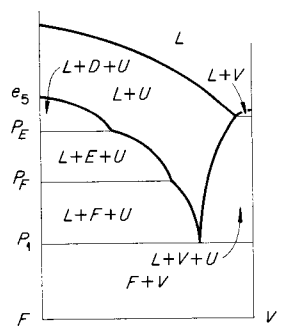

Fig. 9.5.

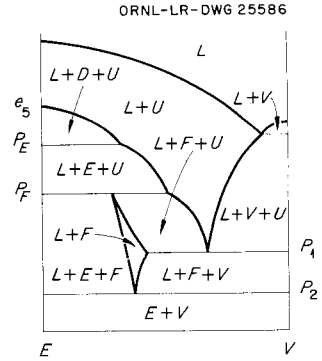

Fig. 9.6.

UNCLASSIFIED
ORNL-LR-DWG 25587

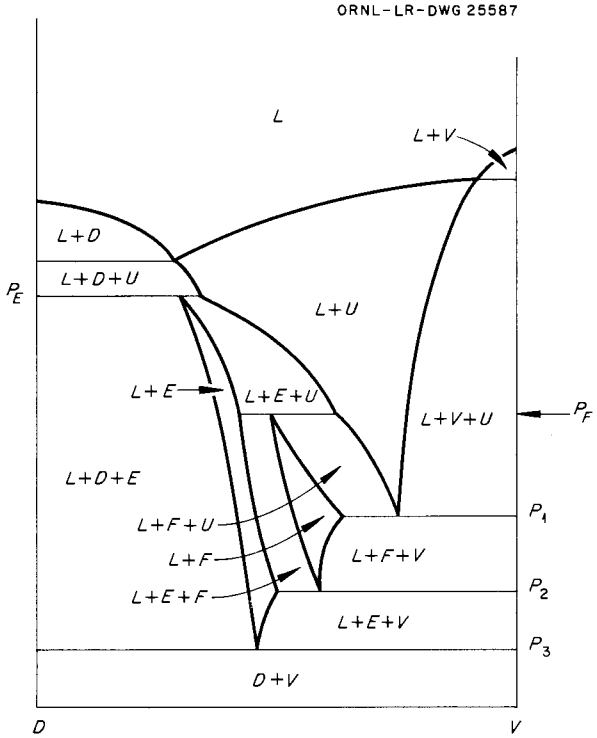

Fig. 9.7.

UNCLASSIFIED
ORNL-LR-DWG 25588

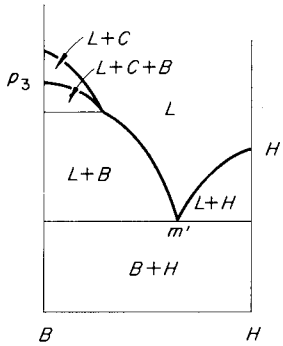

Fig. 9.8.

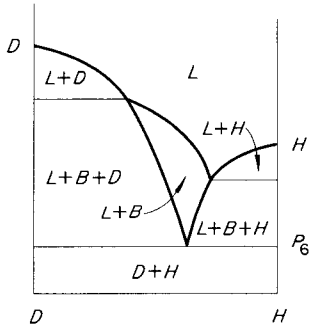

Fig. 9.9.

10. SYSTEM Y–U–R: NaF–UF_4–RbF

For the ternary system Y–U–R, Fig. 10.1 shows the binary system R–U, and Fig. 10.2 the system Y–R. The binary system Y–U is that of Fig. 9.1, with the same lettering.

Figure 10.3 is the ternary diagram.

We note first the restricted fields for the binary compounds A and C of the system Y–U, ending at points P_A and P_C, respectively, at the temperatures of decomposition of these solids on cooling (Fig. 9.1). The isothermal curve uv on the A field has been explained in connection with Fig. 9.3. The low-temperature compounds E and F of Fig. 9.1 do not appear at liquidus temperatures in Fig. 10.3, since the curve of liquid in equilibrium with D and U (e_5E_{11}) ends at a temperature higher than T_E of Fig. 9.1.

The new item in the present ternary system is the ternary compound Q, with $P_QP_3E_2P_4$ as its primary phase field. This compound is stable only below the temperature of P_Q. When heated to the temperature of P_Q it decomposes in a strictly binary solid-phase reaction, into the solids B and H. If the ternary compound Q is not pure, but is mixed either with a little Y or with a little R, it still decomposes as a solid phase into the same solids, B and H, at the same temperature, namely that of point P_Q, but now in the presence of the liquid P_Q. The invariant point P_Q is therefore entirely analogous to P_E in Fig. 9.3, where solid E decomposes, when heated, into D and U in the presence of the liquid P_E.

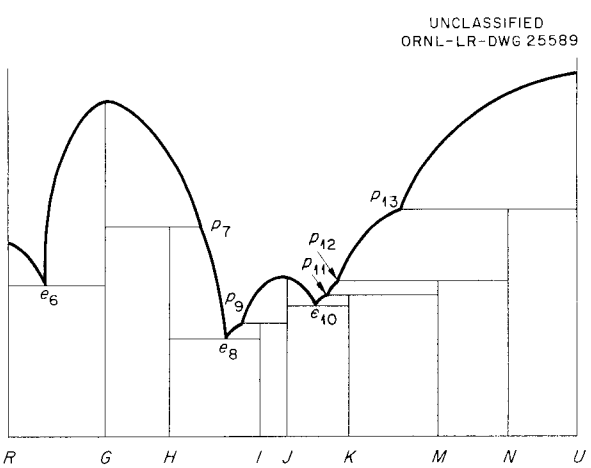

Fig. 10.1.

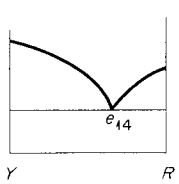

Fig. 10.2.

Figure 10.3 shows fifteen primary phase fields and eleven three-solid triangles with corresponding invariant liquids. There are five saddle points: m_1 on curve E_1E_2, m_2 on curve E_5P_Q, m_3 on curve P_6E_7, m_4 on curve E_7E_8, and m_5 on curve $P_{10}E_{11}$. Two of these saddle points, m_1 and m_4, are on quasi-binary sections, Ym_1G and Dm_4J; Fig. 10.3 therefore consists of three subsystems.

The subsystem D–U–J is relatively simple, with two eutectics, E_8 and E_{11}, and two peritectics, P_9 and P_{10}. Three of the curves are transition curves:

$p_{13}E_{11}$: $L + U \rightarrow N$; crossed by liquids originating in region $Np_{13}E_{11}$. This curve may become even in reaction close to point E_{11}.

$p_{12}P_{10}$: $L + N \rightarrow M$; crossed by liquids originating in region $Mp_{12}P_{10}$.

$p_{11}P_9$: $L + M \rightarrow K$; crossed by liquids originating in region $Kp_{11}P_9$.

Compositions in triangle XI solidify to D, U, and N, but at T_E of Fig. 9.1, D and U react to form E, and the triangle DUN is divided into two triangles of three coexisting solids, DEN and EUN. At a still lower temperature (T_F of Fig. 9.1), the triangle EUN divides into EFN and FUN.

In the middle subsystem, Y–D–J–G, there are the following transition curves:

p_3P_C: $L + C \rightarrow B$; crossed for x in Bp_3P_C.
p_4P_C: $L + D \rightarrow C$; crossed for x in Cp_4P_C.
p_7P_4: $L + G \rightarrow H$; crossed for x in Hp_7P_4.
p_9E_7: $L + J \rightarrow I$; crossed for x in Ip_9E_7.
P_QP_4: $L + H \rightarrow Q$; crossed for x in QP_QP_4.
P_CP_6: $L + D \rightarrow B$, up to point s (line Bs tangent to the curve). The relations along this curve are like those explained for curve p_1sE_1 in Fig. 5.3.

Point P_Q is reached by liquid from original compositions x in the triangle BP_QH. The liquid reaches the curve m_2P_Q either from the left side, carrying solid B, or from the right side carrying solid H. It then travels on the curve, precipitating both B and H, and reaches P_Q. At this point, B and H react to form solid Q, and one of the original

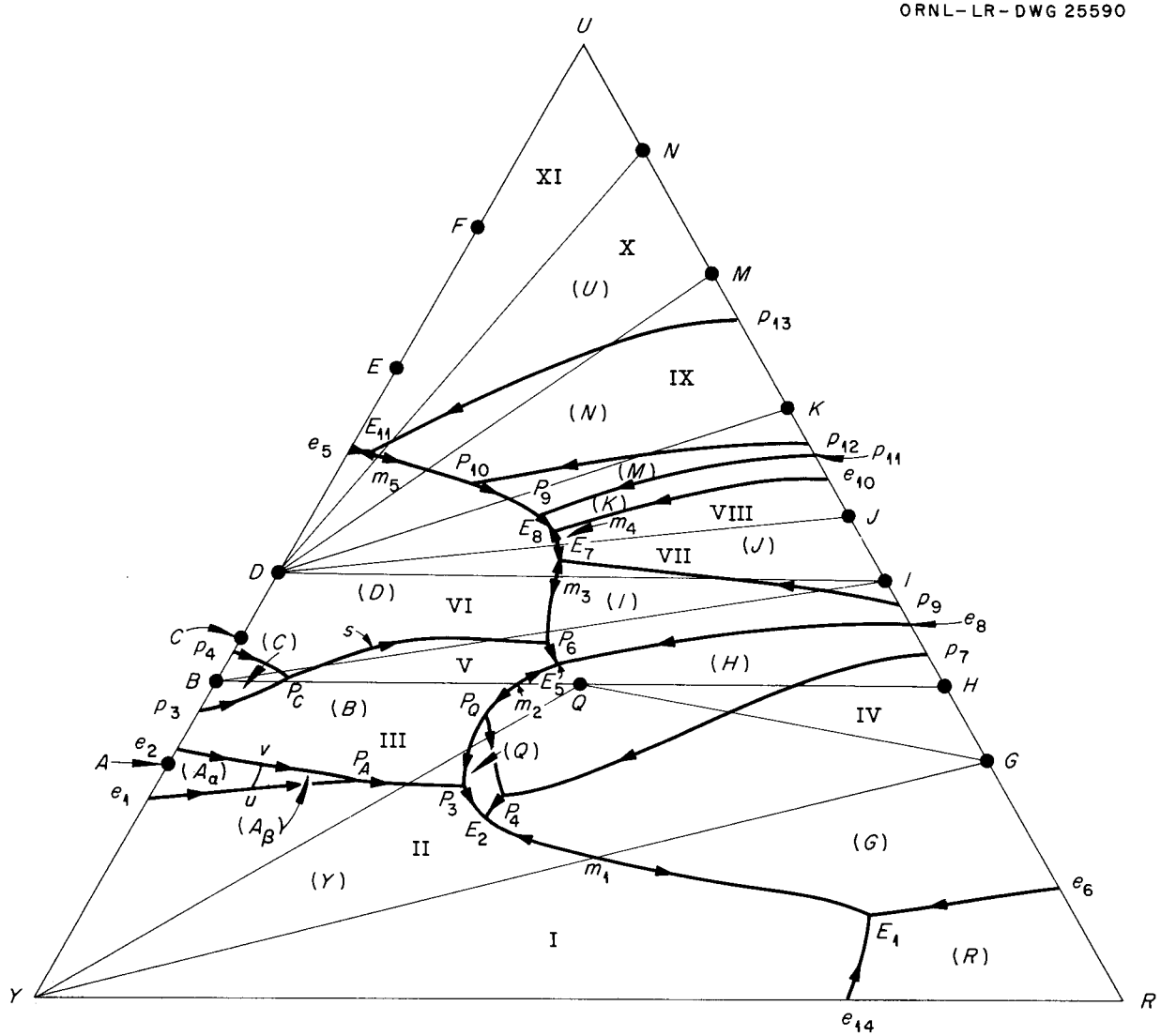

Fig. 10.3.

solids will be completely consumed. For x in the triangle P_QBQ, H is consumed and the liquid travels down the curve P_QP_3; for x in the triangle P_QQH, B is consumed and L moves onto curve P_QP_4.

Consider a total composition x in the region QP_QP_4. On cooling, the first solid is H, and L moves on a straight line from H to reach either curve P_QP_4 directly, or first curve $m_2P_{Q'}$ then point $P_{Q'}$ and then the curve P_QP_4. While L travels along this curve, H reacts with liquid to form Q, and eventually L leaves the curve, when all H is consumed, to enter the Q field. Traversing this field on a straight line from Q, it can reach any one of the three other boundaries of the Q field. These are all even curves, and liquid cannot leave them. If x is in triangle III, L will reach P_3 along curve P_QP_3 and complete its crystallization at P_3 to leave solids Y, B, and Q; for x in triangle II, L ends at E_2, leaving Y, Q, and G.

For a liquid with composition Q itself, the first solid is H, and L travels to the saddle point m_2, where the liquid solidifies completely into B and H, which solids will be present at the end in the exact proportions corresponding to Q. Then at the temperature of P_Q these solids combine to produce Q.

Compositions in triangle V complete their crystallization at E_5, into a mixture of B, H, and I. But on cooling further, B and H combine to produce Q, leaving, below the temperature of P_Q, either B, Q, and I or Q, H, and I.

Some T vs c vertical sections are shown in Figs. 10.4–10.10.

UNCLASSIFIED
ORNL-LR-DWG 25591

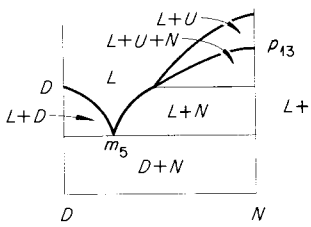

Fig. 10.4.

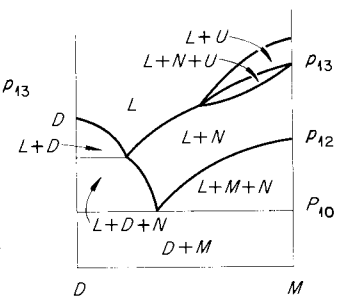

Fig. 10.5.

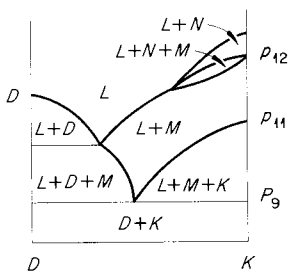

Fig. 10.6.

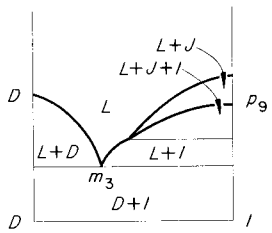

Fig. 10.7.

UNCLASSIFIED
ORNL-LR-DWG 25592

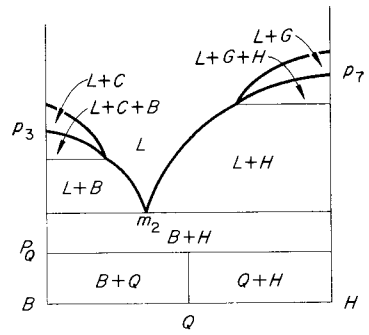

Fig. 10.8.

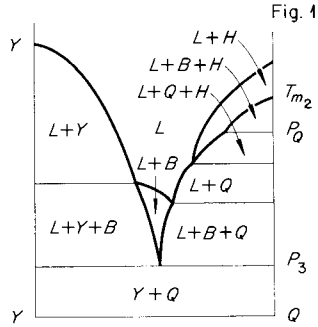

Fig. 10.9.

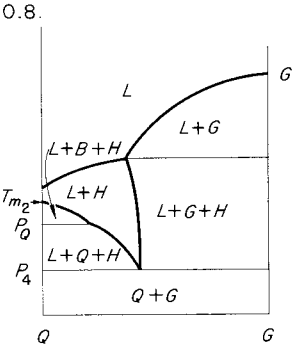

Fig. 10.10.

11. SYSTEM Y–Z–R: NaF–ZrF_4–RbF

For the ternary system Y–Z–R, the binary system Y–Z is shown (schematically) in Fig. 11.1 and R–Z in Fig. 11.2. The system Y–R is as in Fig. 10.2, but now with e_{13} in place of e_{14}.

In each of the first two compounds, A and B, of the system Y–Z, there is some solid solution on the Z side of the stoichiometric composition. In the case of B, solid solution is limited to the upper form, B_α, while the lower form, B_β, is pure. The transition temperature is accordingly lowered, from T' to T''. The compound E forms similar solid solution extending in the direction of the Y side. The subsolidus compound D, which forms from the solids C and E (a solid solution) at T_D, forms solid solution on the Z side. The compounds D and E, in other words, may be said to form a limited series of solid solutions with each other. The 1:1 compound will not be considered in connection with the ternary system. It is observed to be formed at relatively low temperature, but its relation to the established phase equilibria of the binary system has not been even tentatively clarified.

The phase diagram for the system R–Z shows some solid solution, on the Z side, for the two compounds G and H. At T' the compound H is shown as undergoing a polymorphic transition:

$$H_\alpha - \text{calories} \rightleftharpoons H_\beta \ ,$$

and the transition temperature is shown as being lowered to T'' as the result of the solid solution formation. The relations for compound H, however, are experimentally not clear. It seems possible that it may in fact be a pure solid phase, without any solid solution, and moreover, without any polymorphic transition.

The ternary diagram for the system is given in Fig. 11.3.

With regard to this diagram, which is shown as it has so far been worked out, we note the absence of any primary phase field for the incongruently melting compound B of the system Y–Z and for the subsolidus compound D of the same system. Both of these solids should have primary phase fields in the ternary system. The regions involved were investigated before the relations for these compounds were definitely established in the binary system, and they have not yet been reinvestigated.

We shall first discuss briefly the relations for the ternary system as reported in the diagram of Fig. 11.3, assuming, moreover, that the solids form no solid solution. This will serve as a basis, then, for a more detailed discussion of special regions of the system involving the missing solids, together with the solid solutions formed.

11.1. THE SYSTEM ACCORDING TO FIGURE 11.3 AND NEGLECTING SOLID SOLUTION

There are primary phase fields for three ternary compounds, M_1, M_2, and M_3, all with the same (1:1) ratio of the components Y and R, and varying only in Z content. They lie on a line with the corner Z. Both M_1 and M_3 have congruent melting points, with a temperature maximum in each field at the composition of the compound itself. Crystallization paths in each of these two fields radiate in all directions as straight lines from the maximum. Liquid can be in equilibrium with solid M_3 and any of seven other solids (the M_3 field has seven boundaries). The M_1 field has five boundaries (but the field for the here missing compound B will probably add a sixth boundary).

The ternary compound M_2 has a semicongruent melting point, at the temperature of point y on the boundary curve between the M_2 and M_1 fields (cf. Fig. 4.13). Instead of reaching a congruent melting point, the compound M_2, when heated to the temperature of y, decomposes, or melts incongruently, into compound M_1 and liquid y, collinear with M_2. The M_1 surface falls in temperature toward y, the M_2 surface falls away from y, and the temperature on the boundary curve P_5P_{16} falls away from y in both directions.

With saddle points (m' and m'') on each of the other two boundary curves crossed by the line $M_1M_2M_3Z$, this line is a quasi-binary section (from M_1 to Z) of the ternary system (Fig. 11.4); y is seen to be simply the incongruent melting point for the compound M_2 in this binary system.

Figure 11.3 shows fifteen primary phase fields and sixteen three-solid triangles with corresponding invariant liquids. There are ten saddle points (m-points), only one of which, with all solids assumed pure, is not on a quasi-binary section; this is on the curve $E_{14}E_{15}$. The nine quasi-binary sections divide the diagram into eight quite simple ternary subsystems, shown as the eight areas of Fig. 11.5.

UNCLASSIFIED
ORNL-LR-DWG 25643

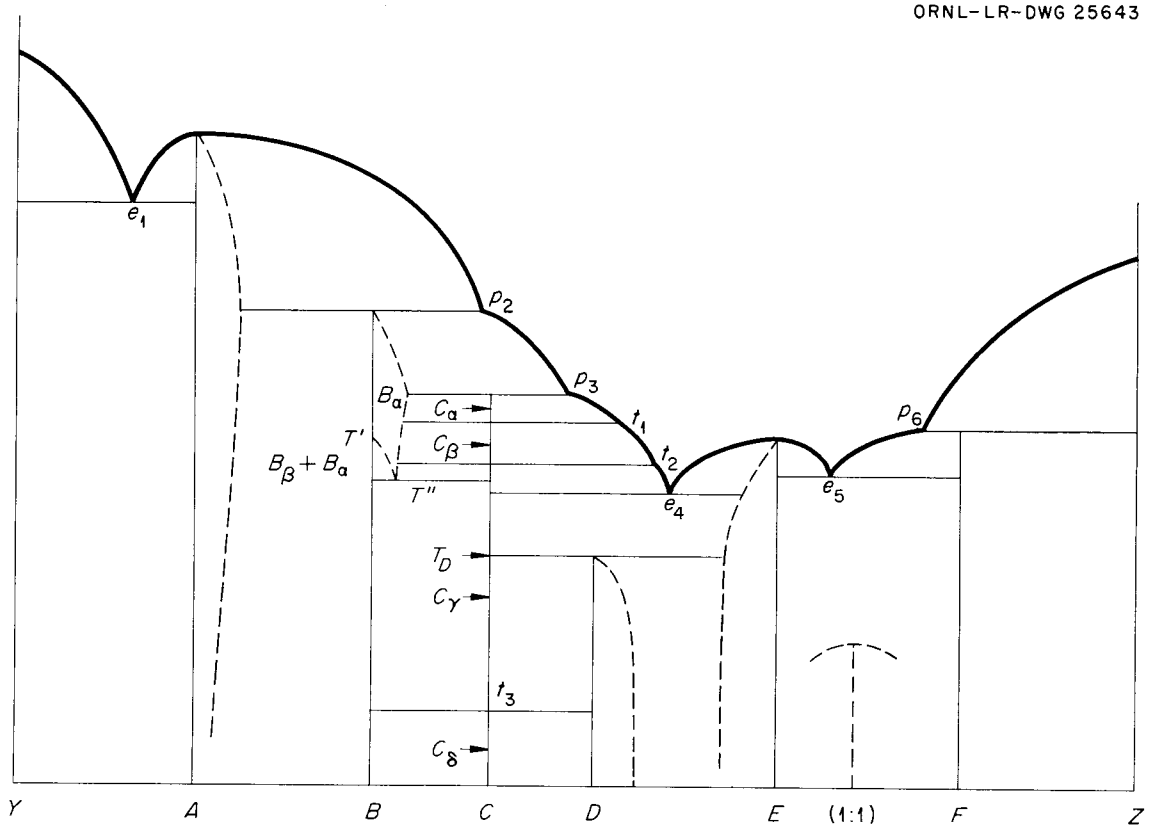

Fig 11.1.

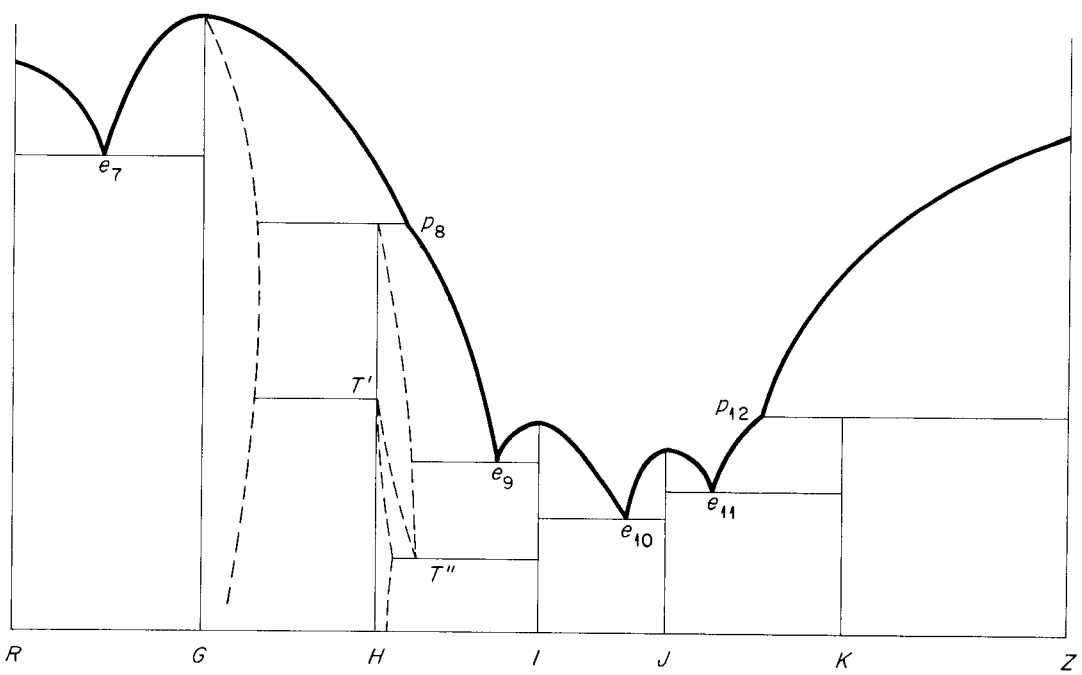

Fig. 11.2.

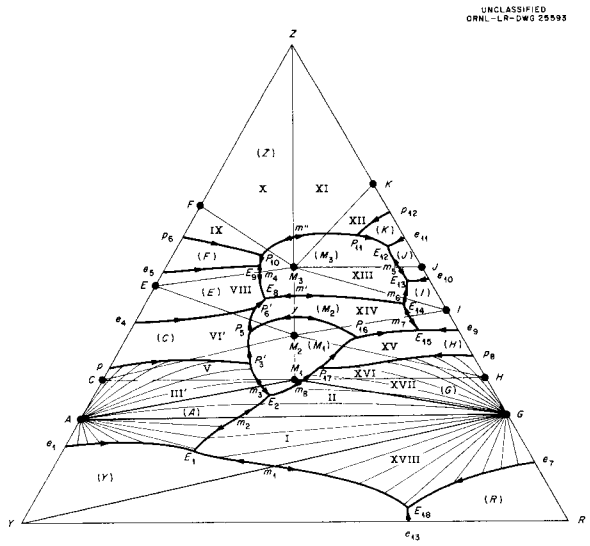

Fig. 11.3.

Only five of the boundary curves in Fig. 11.3 seem to be of odd reaction (pP_3', p_6P_{10}, $p_{12}P_{11}$, p_8P_{17}, and P_5P_{16}); all the others seem to be even. The curve P_5P_{16}, for

$$L + M_1 \rightarrow M_2 \ ,$$

is crossed by L for x between the curve and the lines P_5M_2 and $P_{16}M_2$.

The binary peritectic point p has been left unnumbered in Fig. 11.3, because it may represent either p_2 or p_3 of Fig. 11.1; and the invariant P_3' has been primed, because there must be two invariants here (P_3 and P_4) in place of just the one. Also, a primary field for compound D of Fig. 11.1 should make its appearance somewhere along the curve e_4P_6', the prime on P_6' being used because there should be two invariants here also, P_6 and P_7.

11.2. CONSIDERATION OF SOLID SOLUTION FORMATION

If the actual solid solutions in this system are considered, the phase diagram is no longer divided into as many independent subsystems as assumed in Fig. 11.5. Five of the areas of Fig. 11.5 remain simple, involving only pure solids: EZM_3 with just P_{10} and E_9 as invariants; M_3ZJ with P_{11} and E_{12}; M_3JI with E_{13}; YGR with E_{18}; and YAG with E_1.

However, although the solids A and G are present as pure solids in their equilibria below the line AG, they both form solid solutions, containing excess Z, in their binary systems. In other words, the liquid on curve $m_2 \rightarrow E_1$ precipitates pure A and pure G, but the liquid on the part $m_2 \rightarrow E_2$ (of the same curve) precipitates two solid solutions, starting as pure A and pure G at m_2 and ending as A_2 (on the side YZ) and G_2 (on the side RZ), for E_2. The A solid solution extends beyond A_2, toward Z, for the equilibrium with liquid on curve P_3E_2, and the saddle point m_3 is no longer on a quasi-binary section. At m_3, the liquid is in equilibrium with M_1 and a solid solution of composition A_{m_3}, between A_2 and A_3, the composition corresponding to L at P_3. Similarly, the saddle point m_8 is no longer on a quasi-binary section, since here the liquid is in equilibrium with M_1 and a solid solution of composition G_{m_8}, between G_2 and G_{17}, the composition for L at P_{17}. On the other hand, m_2, on the curve E_1E_2, is exactly on the line AG, a quasi-binary section.

The fractionation paths in the A field, then, originating from point A, are straight lines for the line Am_2 and below, but they are curves convex with respect to the Z corner above the line Am_2, with the limiting paths Ap and Am_2 both straight (sketched on Fig. 11.3). The paths for the G field are similar: straight lines from G below the line Gm_2, and curves, convex with respect to Z, above this line.

The region AEM_3IG, then, although it contains the quasi-binary line M_1M_3, is not subdivided into separate subsystems; the line M_1M_2 does not cut the region into two parts. For convenience, however, the right and left portions will be discussed separately.

11.3. THE REGION FOR COMPOUNDS G AND H OF SYSTEM R–Z

The Region As Shown in Figures 11.6 and 11.7

The relations for compounds G and H, as assumed in Fig. 11.2, are shown in schematic detail in Fig. 11.6. On the basis of these relations the region M_1M_2IG of the ternary system would be schematically as sketched in Fig. 11.7. For the H solid solution field the fractionation paths are curves, convex with respect to Z, originating by extension from the point H.

On the curve $m_8 \rightarrow P_{17}$, the liquid precipitates M_1 and solid solution on the binary side starting at G_{m_8} for L at m_8 and ending at G_{17} for P_{17}.

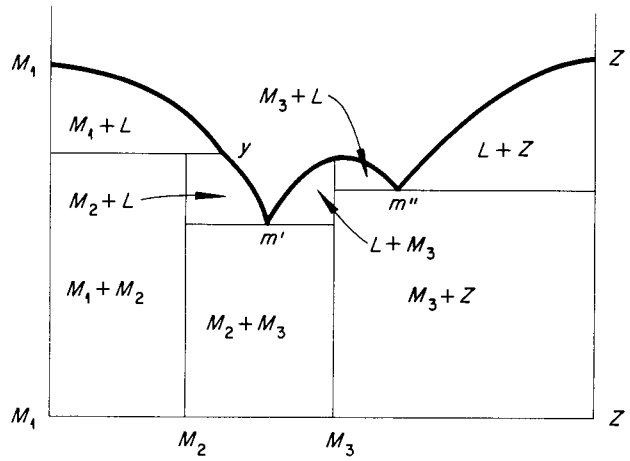

Fig. 11.4.

UNCLASSIFIED
ORNL-LR-DWG 25594

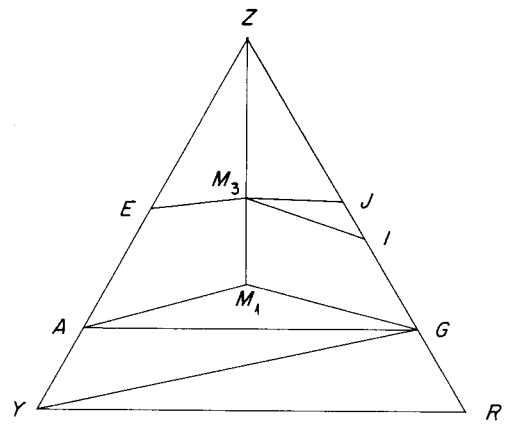

Fig. 11.5.

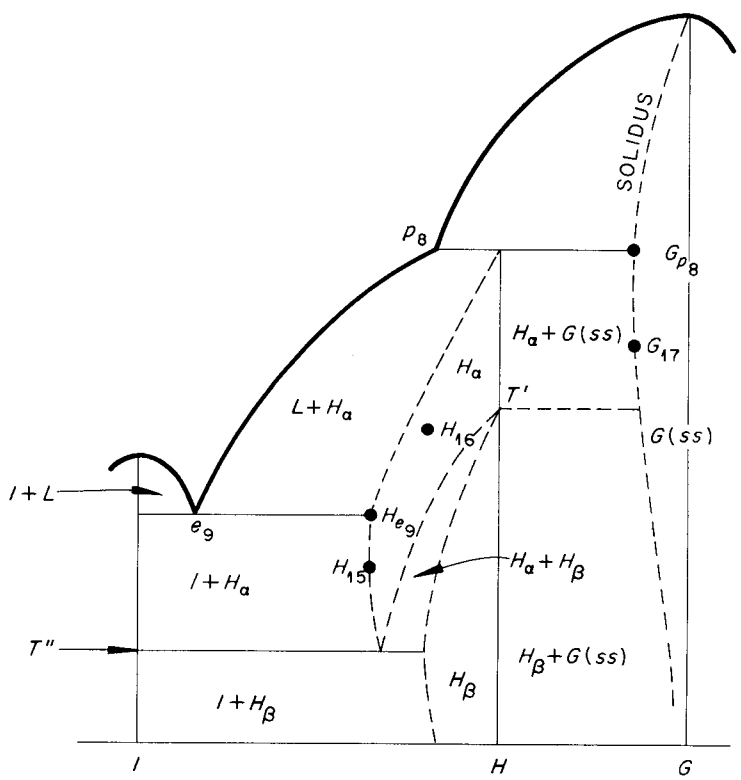

Fig. 11.6.

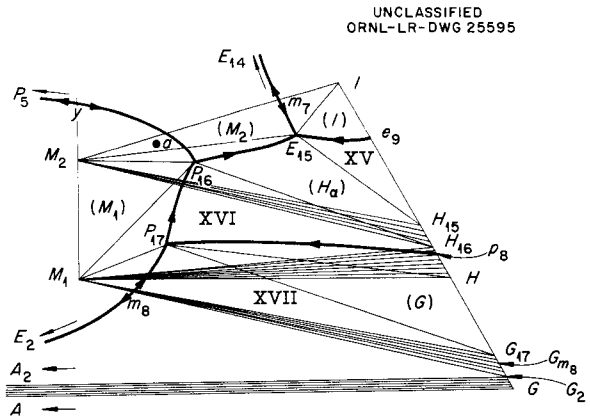

Fig. 11.7.

These solid solutions are not on the "solidus" curve of Fig. 11.6, but G_{17} itself is. On the curve $p_8 \rightarrow P_{17}$,

$$L + G \text{ (solid solution)} \rightarrow H_\alpha \text{ (pure)} \ .$$

The three-phase triangle starts as the line $p_8 H_\alpha G_{p_8}$ (see Fig. 11.6), and ends as the triangle $P_{17} H_\alpha G_{17}$. This curve is crossed for x in the region $H p_8 P_{17}$. The invariant reaction at P_{17} is

$$L + G_{17} \rightarrow M_1 + H_\alpha \ .$$

This is an incongruent crystallization end point for x in triangle XVII ($M_1 H G_{17}$); for x in $M_1 P_{17} H$, the liquid moves onto curve $P_{17} P_{16}$, precipitating M_1 and an H_α solid solution starting as pure H and ending as H_{16}. (As shown on Fig. 11.6, H_{16} is not on a solidus curve of the binary system.) On curve $y \rightarrow P_{16}$,

$$L + M_1 \rightarrow M_2 \ ;$$

this curve is crossed for x in the region $M_2 y P_{16}$. The point P_{16} is reached for x in the quadrangle $M_1 M_2 P_{16} H_{16}$; its reaction is

$$L + M_1 \rightarrow M_2 + H_{16} \ ,$$

and it is the incongruent crystallization end point for triangle XVI ($M_1 M_2 H_{16}$). For x in the region $M_2 P_{16} H_{16}$, L then travels on curve $P_{16} \rightarrow E_{15}$, precipitating M_2 and an H_α solid solution starting at H_{16} and ending at H_{15}. Along curve $e_9 \rightarrow E_{15}$, the liquid precipitates I and an H_α solid solution starting at H_{e_9} and ending at H_{15} (see Fig. 11.6). Along curve $E_{14} \rightarrow E_{15}$,

$$L \rightarrow M_2 + I \ .$$

The point E_{15} is reached for x in triangle XV ($M_2 I H_{15}$).

For x in the regions $M_1 G_{17} G$, $M_1 H_{16} H$, and $M_2 H_{15} H_{16}$, liquid is consumed, to leave two solids, while traveling on curves $E_2 P_{17}$, $P_{17} P_{16}$, and $P_{16} E_{15}$, respectively. The H solid solution produced in these processes, with compositions ranging from H to H_{15}, is the α form of H. As the temperature is lowered, however, the solid solution undergoes transition to the β form, starting at T' for pure H and ending at T'', as shown in Fig. 11.6; and these temperatures are unaffected by the coexistence with solid M_1 or solid M_2, since the H_α and H_β solid solutions are purely binary.

We have here assumed the order of decreasing temperature to be: $T' \cong P_{16} > e_9 > E_{15} > T''$. But if $T'' > E_{15}$, then there is an isothermal crease, at temperature T'', running across the H surface between curves $e_9 E_{15}$ and $P_{16} E_{15}$. The surface between this crease and E_{15} represents liquid in equilibrium with H_β solid solution; the rest of the H field represents liquid in equilibrium with H_α solid solution.

For the relations assumed in Fig. 11.7, liquid of composition a gives M_1 as first solid, and L moves on a straight line from M_1 (i.e., on the extension of the straight line $M_1 a$) to the curve $y P_{16}$. Here

$$L + M_1 \rightarrow M_2 \ ;$$

M_1 is consumed; L leaves the curve, traverses the M_2 field on a straight line from M_2, and reaches curve $m_7 E_{15}$. Here

$$L \rightarrow M_2 + I \ ,$$

and at E_{15}, H_{15} also precipitates.

The Region As Shown in Figures 11.8 and 11.9

The other possibility for the region $M_1 M_2 I G$ seems to be, as already stated, that H forms no solid solution, and has but one form. Then Fig. 11.6 becomes Fig. 11.8, and Fig. 11.7 becomes Fig. 11.9. In Fig. 11.9, the first solid for liquid

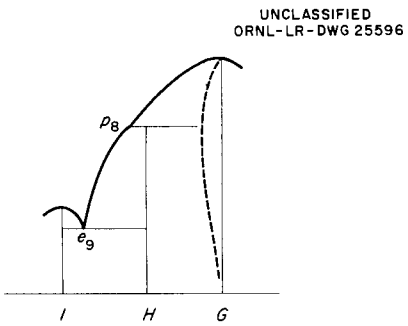

Fig. 11.8.

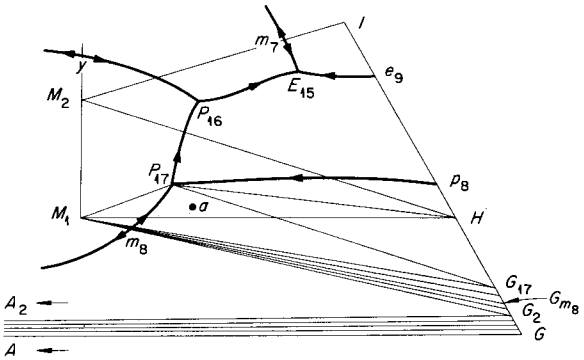

Fig. 11.9.

a is the G solid solution, between G_{m_8} and G_{17}. The liquid reaches the curve m_8P_{17}, traveling on a curved equilibrium path over the G surface. On the curve, the liquid precipitates M_1 and more solid solution, ending at G_{17}. At P_{17},

$$L + G_{17} \rightarrow M_1 + H \quad ;$$

G_{17} is consumed; the liquid travels on curve $P_{17}P_{16}$, precipitating M_1 and H, and reaches P_{16}, where the liquid is consumed in the reaction

$$L + M_1 \rightarrow M_2 + H \quad .$$

11.4. THE REGION INVOLVING COMPOUNDS *B* AND *D* OF SYSTEM Y–Z

Figure 11.10 shows a probable arrangement for the missing primary phase fields for compounds B and D of system Y–Z. Also, since four of the solids of system Y–Z form binary solid solutions, there must be various two-solid areas reached upon complete solidification in this region, whenever one of these solids crystallizes together with a solid involving the third component R; i.e., for every case of a boundary curve involving one of these solids and a solid containing component R. These areas are shown with tie lines, the relations being essentially as already explained schematically for Fig. 7.3.

The field for compound B is introduced as $p_2p_3P_4P_3$, and that for compound D as $P_DP_6P_7$. There are now two more three-solid triangles, for the two added ternary invariants. The composition represented by P_D is simply the ternary solution present when the compound D forms on cooling from solids C and E (a solid solution); it is similar to P_E and P_F in Fig. 9.3, where, however, only pure solids are involved.

As explained for the solid phase H under Fig. 11.7, the solid form of B involved on the B field and along its boundaries is the solid solution in the upper polymorphic form B_α, ranging in composition from pure B to the solid solution limit indicated in Fig. 11.10. As the temperature is lowered, however, the B_α phase undergoes transition to the pure β form, starting at T' for pure B_α and ending at T'' for the solid solution (Fig. 11.2). As in the case of compound H these temperatures are unaffected by the coexistence with solid M_1.

Wherever the compound C is involved as a solid phase, its form is C_α above the temperature of t_1 (Fig. 11.1), C_β between t_1 and t_2, C_γ between t_2 and t_3, and C_δ below t_3. The C surface, (C), is, strictly, divided into four parts, by the special isothermal contours at t_1, t_2, and t_3. These contours constitute slight creases in the surface, defining the regions for liquid in equilibrium with C_α, C_β, C_γ, and C_δ, respectively.

Since A, B, D, and E are binary solid solutions, the fractionation paths on the fields for these solids are curved. Those for the E field are are similar to those on the A field: above the line Em_4 they are straight lines from E, and below this line they are curves convex with respect to the corner Y. For the B and D fields the paths originate by extension from the points B and D respectively, and they are convex toward Z in both cases.

Along the binary curve Ee_4 (from the congruent melting point of E to e_4), the liquid precipitates a solid solution starting as pure E at the melting point of E and ending at E_s for L at e_4. Along the ternary curve e_4P_D, the liquid precipitates C and a solid solution of E, strictly varying in composition between the temperatures of e_4 and P_D, but practically constant because the solidus

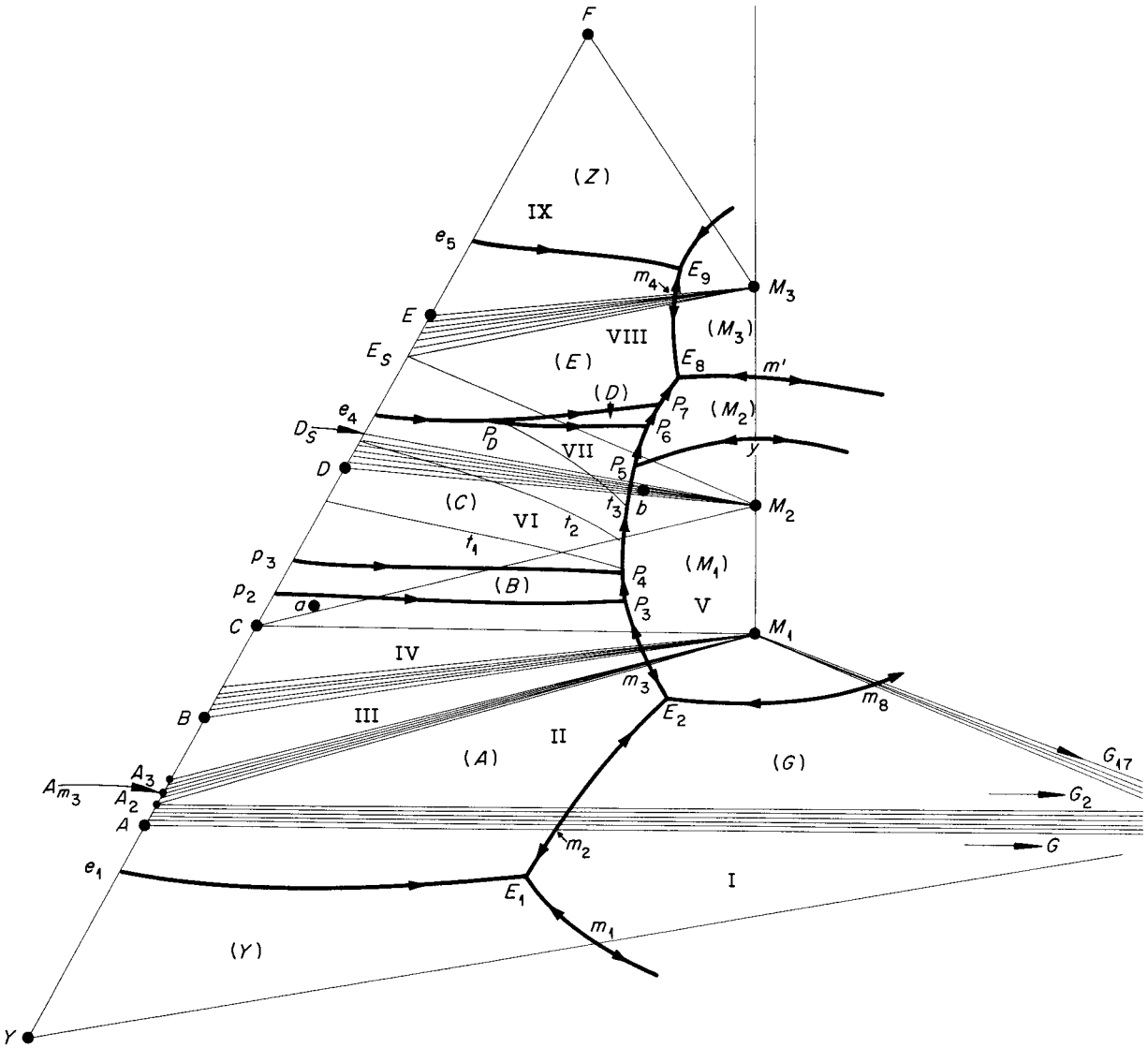

Fig. 11.10.

(Fig. 11.1) is practically vertical. At P_D, therefore,

$$C + E_s - \text{calories} \rightarrow D \ .$$

For x in the region CDP_D, E_s is consumed, and L travels on curve P_DP_6, precipitating D in the reaction

$$L + C \rightarrow D \ .$$

For x in the region DE_sP_D, C is consumed, and L travels on curve P_DP_7, precipitating two solid solutions, conjugate solid solutions of the compounds D and E. The D solid starts as pure D at P_D and ranges to D_s when P_7 is reached, and the E solid, already at E_s, changes slightly but is still practically constant at E_s. The point P_7 is then the invariant liquid for the solids D_s, E_s, and M_2, in the reaction

$$L + D_s \rightarrow E_s + M_2 \ .$$

For x in the region $E_sP_7M_2$, D_s is consumed, and L moves along curve P_7E_8, precipitating M_2 and

E_s (still practically constant, we are assuming).

The saddle points m_1, m_2, m_4, and m' involve liquid saturated with two pure solids, as does also the special point y; m_3 and m_8, as already discussed, involve M_1 and a solid solution (A_{m_3} and G_{m_3}, respectively).

For liquid of composition a in Fig. 11.10 the first solid on cooling is a solid solution of A, between A_{m_3} and A_3. The liquid reaches curve p_2P_3, where

$$L + A(ss) \rightarrow B \quad .$$

The A solid solution is consumed; L leaves the curve, traverses the B field precipitating solid solution B, and reaches the curve p_3P_4. Here

$$L + B(ss) \rightarrow C \quad .$$

The B solid solution is consumed; L leaves the curve, traverses the C field on a straight line from C, and reaches curve P_4P_5. Here

$$L \rightarrow C + M_1 \quad .$$

At P_5,

$$L + M_1 \rightarrow C + M_2 \quad ,$$

M_1 is consumed, and L moves to P_6, where D also precipitates to leave C, D, and M_2. The path of the liquid on the solid solution fields (A and B) is curved, convex with respect to the corner Z.

Liquid b gives M_1 as first solid, reaches curve P_4P_5, precipitates C and M_1, and reaches P_5, where M_1 is consumed in the reaction

$$L + M_1 \rightarrow C + M_2 \quad .$$

Now L moves on P_5P_6 to P_6, where C is consumed in the reaction

$$L + C \rightarrow D + M_2 \quad .$$

The liquid now starts out on curve P_6P_7, precipitating M_2 and solid solution, but the liquid vanishes on the curve to leave a two-solid mixture of M_2 and a solid solution between D and D_s, on a straight line through b and M_2.

12. SYSTEM Y–Z–X: $NaF–ZrF_4–LiF$

For the ternary system $Y–Z–X$, the diagram of the binary system $Y–Z$, already considered under Fig. 11.1, is used here with the same lettering. The binary systems $X–Z$ and $Y–X$ are shown, schematically, in Figs. 12.1 and 12.2. Two of the compounds of the system $X–Z$ decompose on cooling, one of them, G, also showing a polymorphic transition, at T'.

The ternary diagram, as far as it has been worked out, is shown in Fig. 12.3. Like Fig. 11.3, the diagram does not show the primary phase fields for compounds B and D of the $Y–Z$ system, which should appear.

This system involves several series of solid solutions. It has not only the binary solid solutions of the system $Y–Z$ (Fig. 11.1), but also solid solutions, with compositions on straight lines (crosshatched on Fig. 12.3) across the diagram, formed between corresponding binary compounds of the systems $Y–Z$ and $X–Z$. The compound A of system $Y–Z$ ($3Y{\cdot}1Z$) forms solid solution with G (also 3:1 in composition) of system $X–Z$. The solid solution is not continuous, but has a miscibility gap. Since both compounds have congruent melting points and since the section Am_2G of Fig. 12.3 is quasi-binary, it is clear that the ternary system may immediately be divided at this point into separate subsystems. With m_2 a temperature minimum between A and G, the binary system $A–G$ is eutectic in nature.

Solid A, however, also forms solid solution (with excess Z in its composition) in the binary $Y–Z$ system. The solid solution originating at point A of Fig. 12.3 is therefore actually ternary in composition, occupying an area of the diagram, and one edge of this area is the straight line from point A to point G.

The corresponding compounds F and I, both 3:4 in composition, also form solid solution with a miscibility gap. Both have incongruent melting points, however, and the section FI of Fig. 12.3 is of course not quasi-binary, even though the solutions formed are strictly on the line FI. The quasi-binary section EH, however, through the saddle point m_3 on the curve $E_6'E_8$, divides the upper part of Fig. 12.3 into two independent subsystems. This is so since E forms solid solution with D (Fig. 11.1) but not with F, and H is pure.

We shall therefore discuss this system part by part, for it consists of three practically independent subsystems: $Y–A–G–X$, $A–E–H–G$, and $E–Z–H$. (Note: This independence holds at least to just below liquidus temperatures, but not all the way, since compounds G and I of system $X–Z$ decompose at low temperature.)

We shall first describe the fractionation paths for the solid solution surfaces. The field for the A-rich solid solution of A and G, i.e., the surface for liquid in equilibrium with A_s, is $e_1ApP_4'P_3E_2E_1$. The maximum of this surface is point A itself, since this compound melts congruently. The fractionation paths therefore radiate as curves from point A, and they may be said to consist of two families of paths, divided by the straight-line fractionation path running from A to m_2. All the paths, diverging from this line, are convex with respect to point G. A similar arrangement holds for the G_s field (field for liquid in equilibrium with G-rich solid solution), $e_7Ge_8P_3E_2$, with a straight-line path running from G to m_2 and all other paths diverging from this line and convex with respect to the point A. For the surface $e_5p_6P_{10}P_9$, for liquid in equilibrium with F_s (F-rich solid solution of F and I), the temperature maximum for the origin of the fractionation paths is the metastable congruent melting point of F.

UNCLASSIFIED
ORNL-LR-DWG 25598

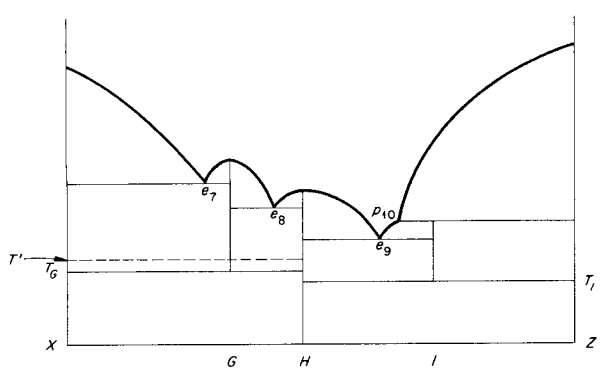

Fig. 12.1.

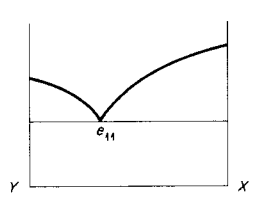

Fig. 12.2.

UNCLASSIFIED
ORNL-LR-DWG 25599

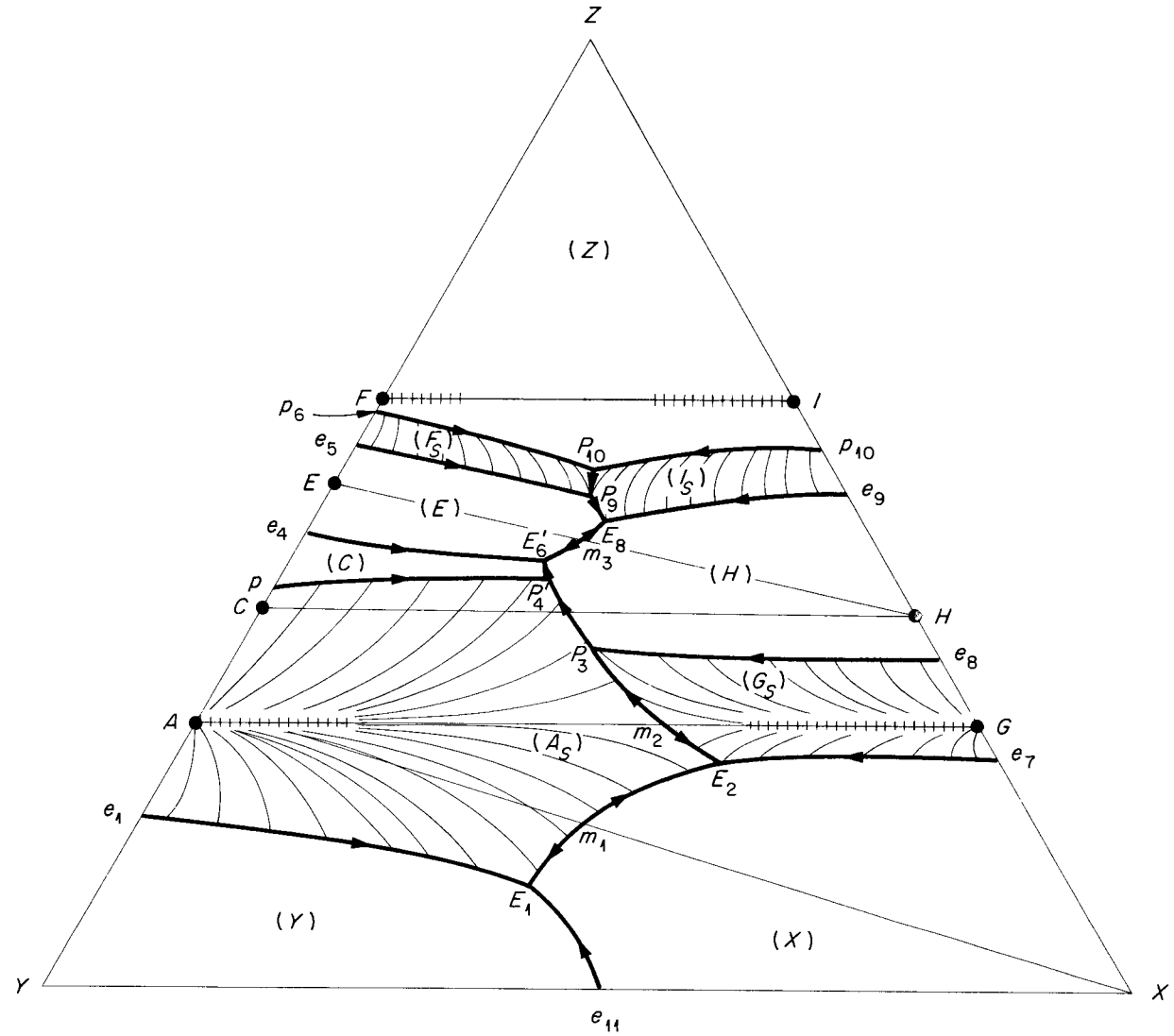

Fig. 12.3.

Hence the fractionation paths do not show a common origin on the field itself, but radiate, as curves convex toward I, from point F. The fractionation paths for the I_s surface, $e_9p_{10}P_{10}P_9E_8$, similarly radiate, as curves convex toward F, from the submerged maximum at point I.

The fractionation paths for the fields for solid solutions of the compounds B, D, and E of system Y–Z, to be considered later, will be as described for the same fields in the preceding system (Sec 11.4).

12.1. SUBSYSTEM Y–A–G–X

The region $YAGX$ is shown in Fig. 12.4, and the vertical T vs c section AG is given, schematically, in Fig. 12.5.

Liquid on the curve m_2E_2 precipitates two mutually saturating solid solutions, with conjugate compositions starting as s_{m_2} and s'_{m_2} at the temperature of m_2 and ending as s_2 and s'_2 at the temperature of E_2. These limiting solid solutions may be identified on the miscibility gap in

UNCLASSIFIED
ORNL-LR-DWG 25600

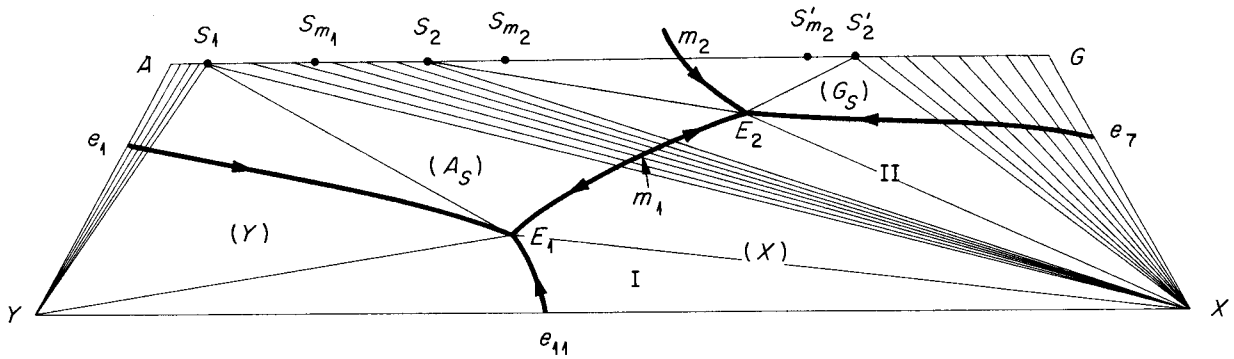

Fig. 12.4.

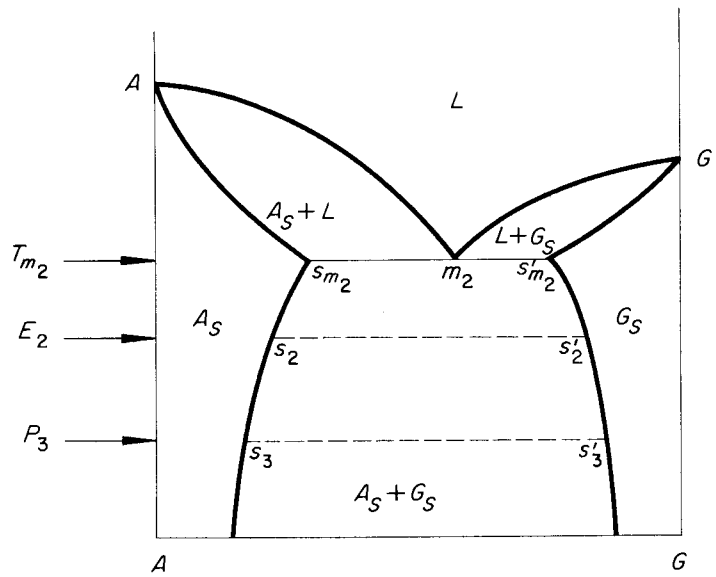

Fig. 12.5.

Fig. 12.5, which shows the solid-solid solubility as diminishing with decreasing temperature. On curve e_1E_1, liquid precipitates Y and solid solution A_s ranging from pure A at e_1 to s_1 at E_1; similarly, liquid on curve e_7E_2 precipitates X and solid solution G_s ranging from G to s'_2. Liquid on curve E_1E_2 precipitates X and A_s solid solution starting at s_{m_1} for solution m_1 and ranging to s_2 for liquid following curve m_1E_2 and ranging to s_1 for liquid following curve m_1E_1. The solid solution compositions s_1 and s_{m_1} are not related to the miscibility gap of Fig. 12.5; they are merely points in the A_s solid solution area of that diagram. Also, as explained under Fig. 7.3, the line $s_{m_1}m_1X$ is not a quasi-binary section.

Liquids with original composition x in the region s'_2GX reach the curve e_7E_2 and solidify completely before reaching E_2, to leave X and G_s. Similarly, liquids from x in the $s_{m_1}s_2X$ solidify on the curve m_1E_2 to leave A_s and X. Only liquids for x in the triangle $s_2s'_2X$ reach E_2 to give the three solids s_2, s'_2, and X. Similarly, only liquids for x in the triangle Ys_1X reach E_1 to form the three solids of triangle I.

Summarizing the equilibrium crystallization process for the curves: curve e_1E_1 is reached for x in region YAs_1E_1, but the liquid vanishes on the curve for x in Yas_1; curve e_7E_2 is reached for x in $XGs_2'E_2$, but the liquid is consumed for x in XGs_2'; curve E_1E_2 is reached for x in $s_1s_2E_2XE_1$, but the liquid is consumed for x in s_1s_2X; curve $e_{11}E_1$ is reached for x in YE_1X, and curve m_2E_2 for x in $s_2s_2'E_2$, but on these curves the liquid does not vanish.

12.2. SUBSYSTEM *E–Z–H*

The region EZH is shown in Fig. 12.6, and the vertical T vs c section FI is shown in Fig. 12.7. The miscibility gap in the F–I solid solution is shown as widening with falling temperature. The three invariant planes in Fig. 12.6 are seen to overlap. The quadrangle $P_{10}s_{10}Zs_{10}'$ is the highest in temperature. Below it is the quadrangle $P_9Es_9s_9'$. The lowest in temperature is the triangle for E_8, Es_8H. (This diagram has certain similarities to the hypothetical case of Fig. 7.3.)

UNCLASSIFIED
ORNL-LR-DWG 25601

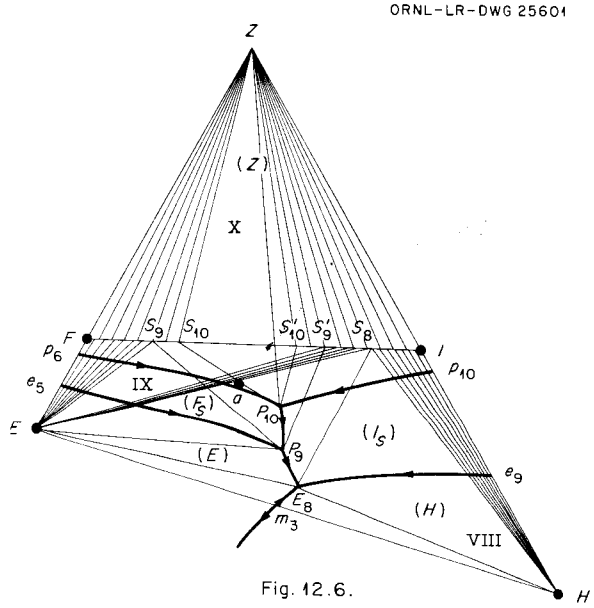

Fig. 12.6.

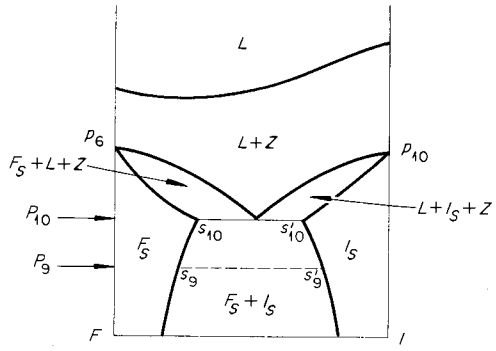

Fig. 12.7.

In the relations as assumed in these figures, liquids in the field $p_6Zp_{10}P_{10}$ give pure Z as primary solid, and travel on a straight line from Z to one of the transition curves p_6P_{10} and $p_{10}P_{10}$. On the curve p_6P_{10},

$$L + Z \rightarrow F_s \ ,$$

the F-rich solid solution. The three-phase triangle for this equilibrium starts as the line p_6FZ and ends as the triangle $P_{10}s_{10}Z$. For x in the region FZs_{10}, the liquid vanishes on the curve, leaving Z and F_s (between F and s_{10}). For x in the region $p_6Fs_{10}P_{10}$, Z is consumed while L is on the curve, and the liquid then leaves the curve to travel, on a curved path, across the F_s field. Similar relations hold on the I side, with respect to curve $p_{10}P_{10}$, with the reaction

$$L + Z \rightarrow I_s \ .$$

For x in the region IZs_{10}', the liquid vanishes on the curve, leaving Z and I_s (between I and s_{10}'), and for x in $p_{10}Is_{10}'P_{10}$, L leaves the curve when all Z is consumed, to travel, on a curved path, across the I_s field. Only liquids for x in the quadrangle $s_{10}Zs_{10}'P_{10}$ reach P_{10}, where the reaction is

$$L + Z \rightarrow s_{10} + s_{10}' \ .$$

For x in $s_{10}Zs_{10}'$, therefore, the liquid is consumed at P_{10} to leave the three solids of triangle X, s_{10}, s_{10}', and Z; and otherwise, with Z consumed, L moves down along curve $P_{10}P_9$, precipitating two conjugate solid solutions with compositions changing from s_{10} and s_{10}' to s_9 and s_9', according to the miscibility gap in Fig. 12.7.

The curve $P_{10}P_9$ may also be reached directly from either the F_s field or the I_s field, for x in the regions $s_9s_{10}P_{10}P_9$ and $s_{10}'s_9'P_9P_{10}$, respectively. Point P_9 is reached by liquids for x in the quadrangle $Es_9s_9'P_9$, and with the reaction

$$L + s_9 \rightarrow E + s_9' \ ,$$

this is the incongruent crystallization end point for triangle IX, Es_9s_9'. If s_9 is consumed in the P_9 reaction, the liquid moves down on curve P_9E_8,

precipitating E and I_s solid solution ranging from s_9' to s_8. (With reference to Fig. 12.7, s_8 is in the I_s area but not on the solidus edge of the miscibility gap.) Also, liquids reaching curve e_9E_8 travel on it precipitating H and I_s (between I and s_8). For x in Hs_8I, the liquid vanishes on the curve to leave H and I_s. The point E_8, then, is reached for x in triangle VIII, Es_8H, for which it is the eutectic.

Finally, liquid traveling on curve e_5P_9, but with x in the region EFs_9, vanishes on the curve to leave E and F_s; liquid traveling on the curve P_9E_8 and with x in $Es_9's_8$ vanishes to leave E and I_s between s_9' and s_8.

As an example of some of the relations we consider point a in Fig. 12.6. For liquid of this composition, the first solid on cooling is Z, and L reaches curve p_6P_{10} on a straight line from Z. On the curve,

$$L + Z \rightarrow F_s \ ,$$

starting between F and s_{10} and moving toward s_{10}. But before the composition of the solid solution reaches s_{10}, Z is consumed; L leaves the curve and travels on a curved path, convex with respect to I, across the F_s field. While L is on the F_s surface, the solid solution continues to become richer in I. When L reaches curve $P_{10}P_9$ the I-rich solid solution begins to precipitate together with F_s, the compositions of the solid solutions being given at each temperature by the miscibility gap of Fig. 12.7. When L reaches P_9,

$$L + s_9 \rightarrow E + s_9' \ ,$$

and s_9' vanishes. The liquid then travels on the curve P_9E_8, while s_9 changes toward s_8. Crystallization is completed at E_8, to leave the solids E, s_8, and H.

12.3. SUBSYSTEM A–E–H–G

The phase diagram as constructed in Fig. 12.3 omits fields for the binary compounds B and D of the system Y–Z (Fig. 11.1). We shall, however, discuss the region $AEHG$, not as shown in Fig. 12.3, but as it might probably appear with the necessary fields for B and D (Fig. 12.8), as was done for the system Y–Z–R in Fig. 11.10.

The points s_{m_2}, m_2, and s_{m_2}' of Fig. 12.8 are the same as those so labelled in Fig. 12.4. The

UNCLASSIFIED
ORNL-LR-DWG 25602

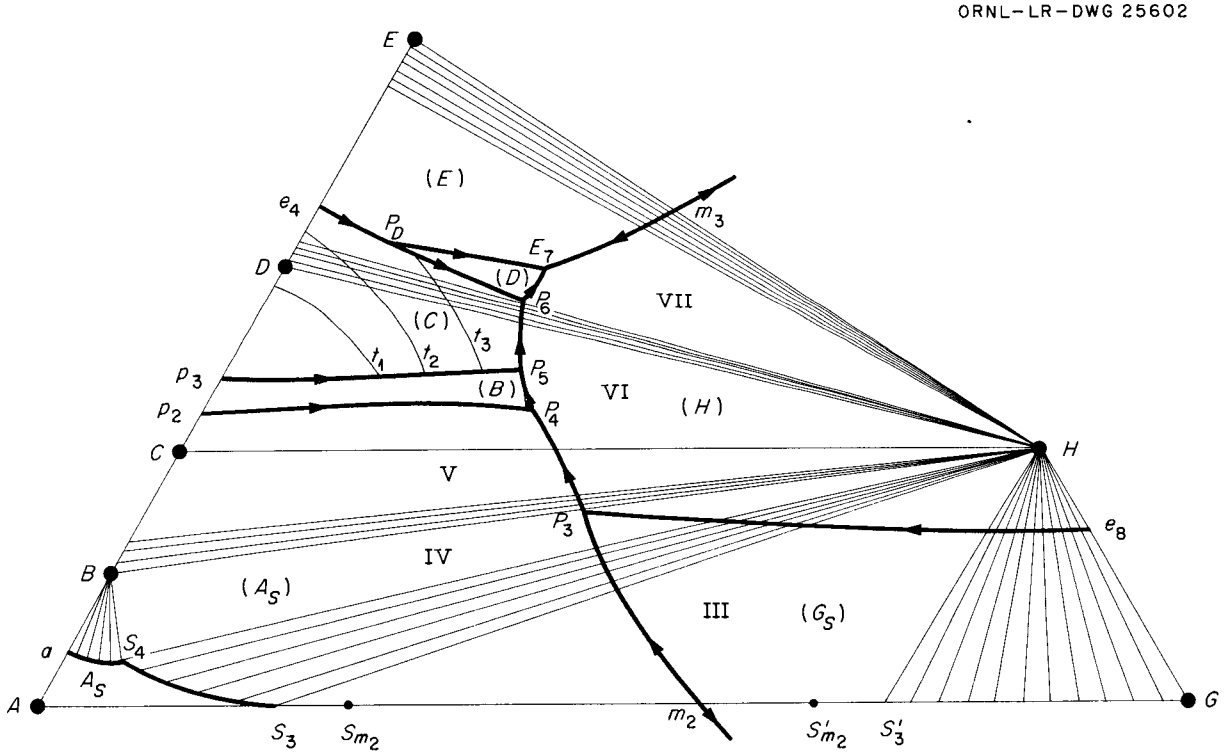

Fig. 12.8.

solid solutions s_3 and s_3' (like s_2 and s_2' in Fig. 12.4) are also conjugate solid solutions of the A–G solid solution miscibility gap, identifiable in Fig. 12.5.

As liquid travels on the curve $m_2 \rightarrow P_3$, it precipitates solid solutions beginning as s_{m_2} and s_{m_2}' and ending as s_3 and s_3'. The solids of triangle III, s_3, s_3', and H, are in equilibrium with the invariant liquid P_3, where the reaction is

$$L + s_3' \rightarrow s_3 + H \ .$$

If s_3' is consumed in this reaction, the liquid moves down the curve P_3P_4, precipitating A_s solid solution and H. The A_s solid solution, however, is here shown as ternary in composition, and it has the composition s_4 when L reaches P_4. Point a is the limiting composition in the binary system Y–Z at the temperature of p_2.

Compositions x in the area Aas_4s_3 would solidify (in full equilibrium) to a single ternary solid solution phase while the liquid is traveling on the A_s field, before the liquid reaches any boundary curve (cf. Fig. 2.3). For x in the region aBs_4, L reaches the transition curve p_2P_4, along which

$$L + A_s \rightarrow B \ ,$$

and the liquid vanishes while on that curve, to leave A_s (on the curve as_4) and B.

The rest of the relations in this diagram are altogether similar to those in Fig. 11.10, with H, so to speak, in place of the various ternary compounds of that diagram.

12.4. SUBSOLIDUS DECOMPOSITIONS OF COMPOUNDS G AND I

As shown in Fig. 12.1, for the binary system X–Z, the compounds G and I undergo solid-phase decompositions at the temperatures T_G and T_I, respectively. In the ternary system Y–Z–X, both of these compounds form solid solution with the third component, Y, while their products of decomposition do not. The decomposition temperature is therefore lowered, in both cases, and we shall say to T_G' and T_I', respectively. The compound I is considered first.

Decomposition of Compound I

The changes in the two- and three-solid equilibria accompanying the low-temperature decomposition of compound I are shown in the successive isotherms of Fig. 12.9. Isotherm (a) is just below E_8 of Fig. 12.6, and it represents the various two- and three-solid mixtures which will be obtained

UNCLASSIFIED
ORNL-LR-DWG 25603

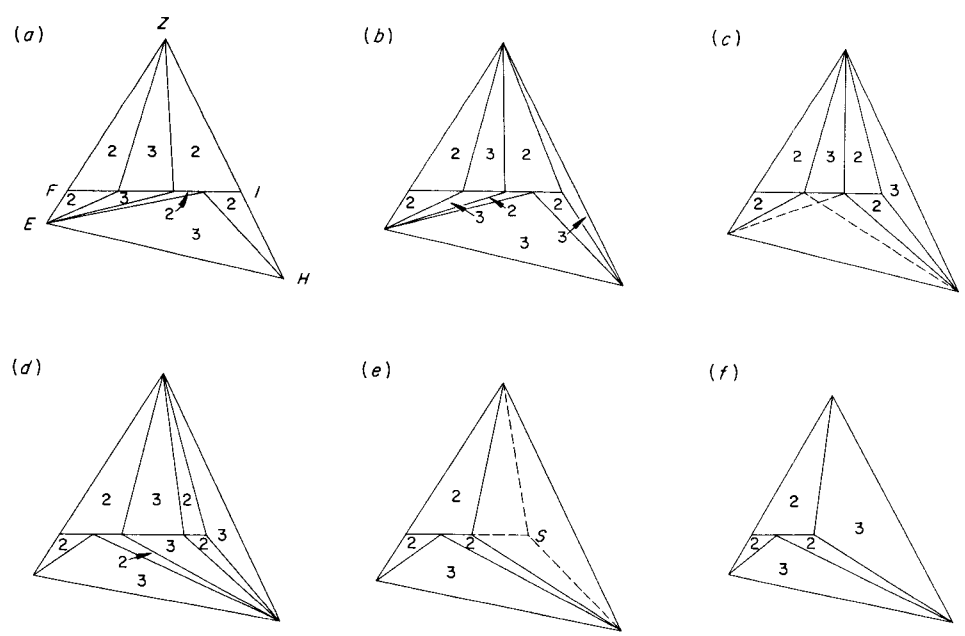

Fig. 12.9.

upon complete solidification of any composition in this subsystem. Only the number of phases is shown in the figure; the phases may be identified, if necessary, from Fig. 12.6. Figure 12.9 (*b*) is just below T_I of Fig. 12.1, where the three-solid area for Z, H, and I_s appeared on cooling. Figure 12.9 (*c*) is at the temperature of a four-solid invariant, for the reaction

$$E + I_s \rightarrow F_s + H$$

on cooling, and Fig. 12.9 (*d*) is just below this invariant. Figure 12.9 (*e*) is at the temperature T_I', the lowest temperature for the existence of the I_s solid phase (point *s*). Figure 12.9 (*f*) is below this temperature. The T vs c section FI (Fig. 12.10) shows little of all these changes.

Decomposition of Compound G

According to Fig. 12.1, the compound G undergoes a transition on cooling, at T', from G_α to G_β, before the β form decomposes at T_G. In the successive solid-phase isotherms of Fig. 12.11 it is assumed that, as in the case of the decomposition temperature itself, the transition temperature is also lowered, from T' to T'', as the result of the presence of the third component in solid solution. The temperature-composition relations assumed, then, for the section AG are shown in Fig. 12.12.

The first isotherm, (*a*), of Fig. 12.11 represents the two- and three-solid combinations for equilibrium just below the temperature of point P_4 of Fig. 12.8, for the region $YBHX$ (the ternary solid solution area for A_s is omitted). At T' there appears a length of G_β solid solution, with four new equilibria for H and $(G_s)_\beta$; X and $(G_s)_\beta$; H, $(G_s)_\alpha$, and $(G_s)_\beta$; and X, $(G_s)_\alpha$, and $(G_s)_\beta$. Figure 12.11 (*b*) shows these new combinations, at a temperature between T' and T''. Figure 12.11 (*c*) is at T'', the lowest temperature for existence of the ternary G_α solid solution. Figure 12.11(*d*) is between T'' and T_G, where the β form begins to decompose (into H and X) in the binary system. Figure 12.11(*e*) is between T_G and T_G'. Figure 12.11(*f*) is at T_G', the lowest temperature of existence of the G_β solid solution in the ternary system. Figure 12.11(*g*) is below T_G'.

UNCLASSIFIED
ORNL-LR-DWG 25604

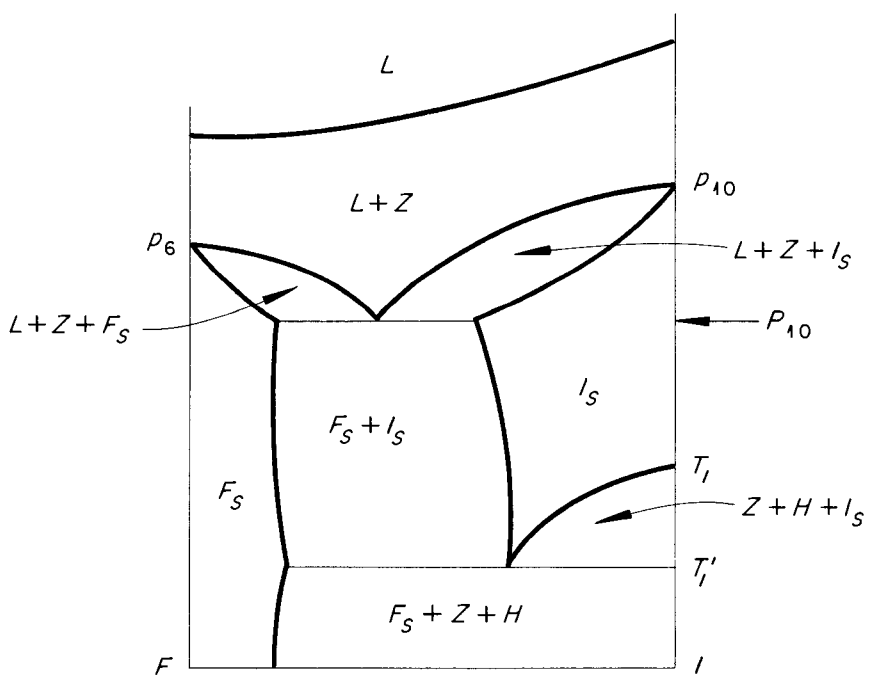

Fig. 12.10.

UNCLASSIFIED
ORNL-LR-DWG 25605

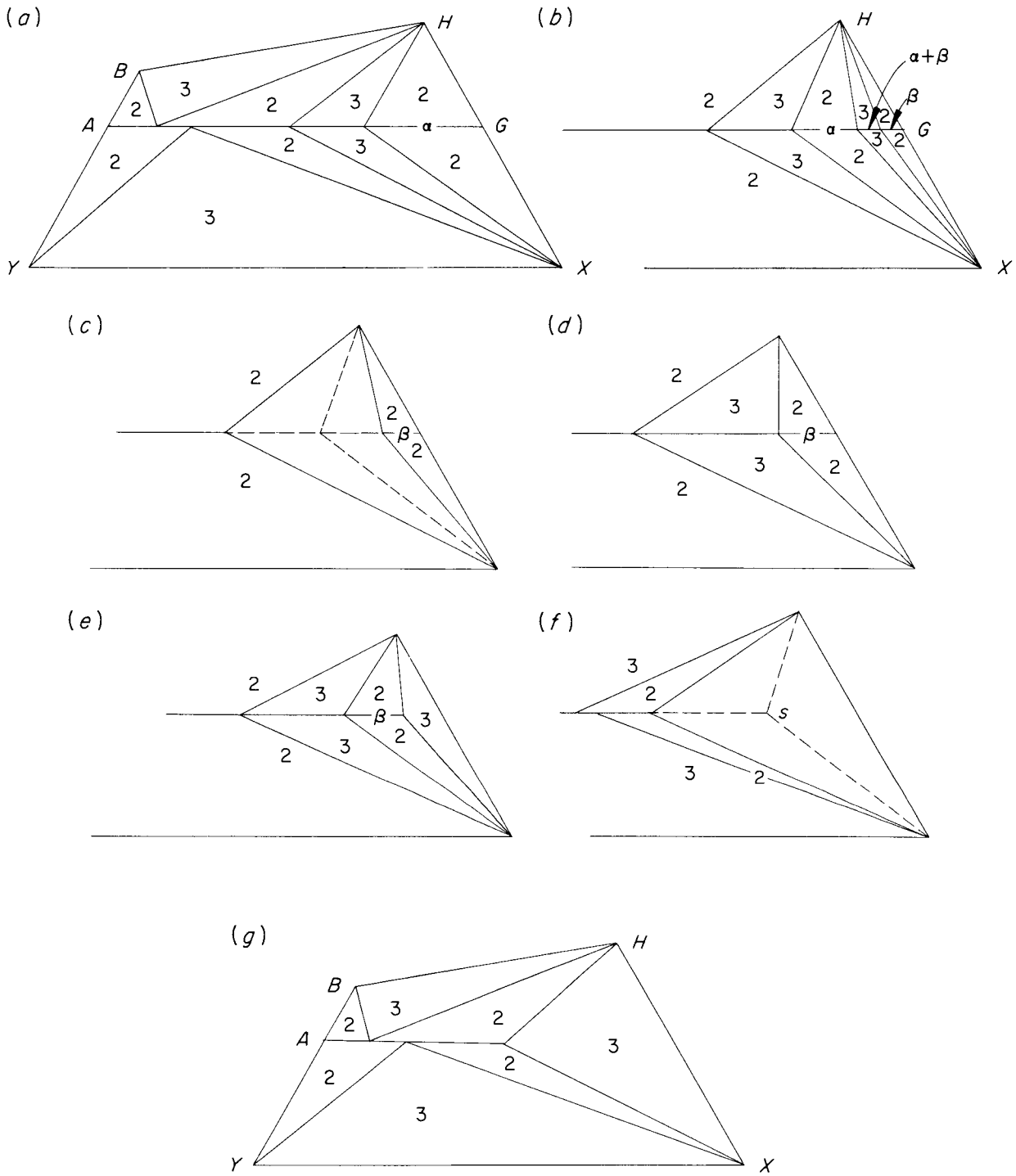

Fig. 12.11.

UNCLASSIFIED
ORNL-LR-DWG 32522

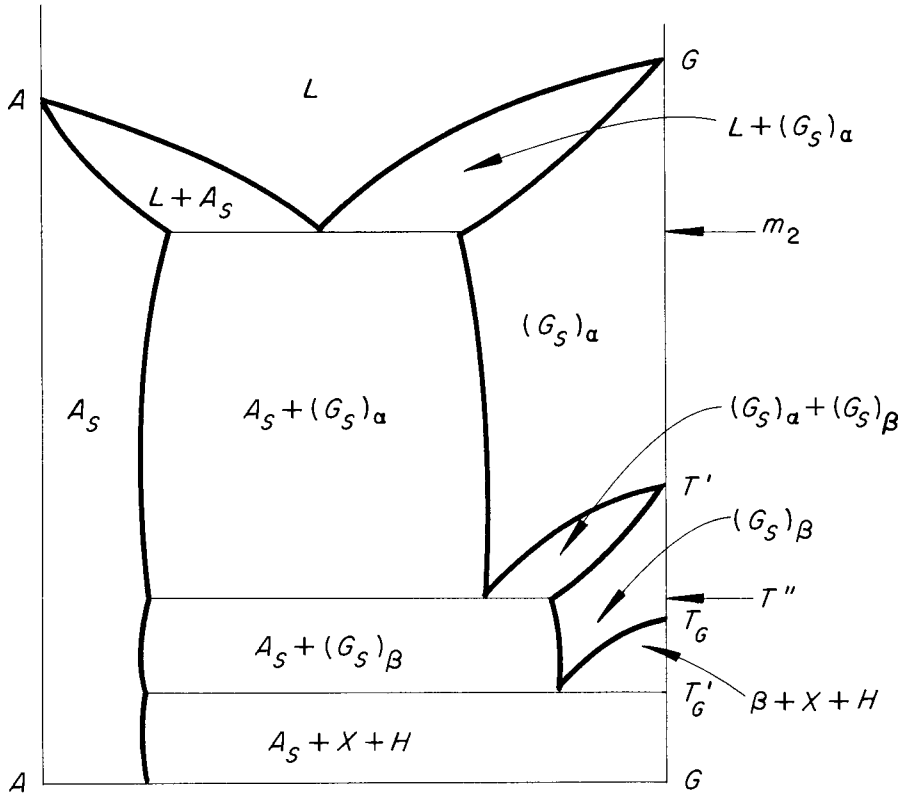

Fig. 12.12.

13. SYSTEM Y–U–X: NaF–UF_4–LiF

For the ternary system Y–U–X, the binary system Y–U is used with the lettering shown on Fig. 9.1. The binary system Y–X is that of Fig. 12.2, with e_{10} now in place of e_{11}. The binary system X–U, already given in Fig. 8.1, is repeated here in Fig. 13.1 to show the new lettering required in the present section. We note the binary compounds A and C of system Y–U and G of system X–U, decomposing on cooling. The system Y–U also has two compounds, E and F, which form below the liquidus temperature.

UNCLASSIFIED
ORNL-LR-DWG 25606

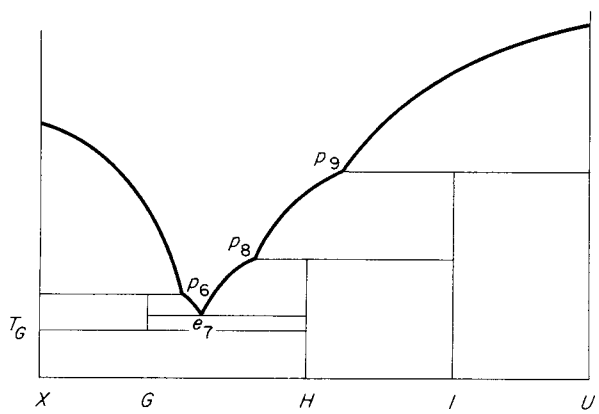

Fig. 13.1.

The ternary diagram is given in Fig. 13.2. There are no binary solid solutions involved in this system, but there are two large primary phase fields for solid solutions formed across the diagram by corresponding 7:6 compounds D and H. These compounds form discontinuous solid solution with a considerable miscibility gap. The primary phase fields for D_s (the D-rich solid solution) and for H_s (the H-rich solid solution) are in contact along the boundary curve E_3E_4, and the point m_3 on this curve is a saddle point, being on the line DH. However, compound D has a congruent melting point, while compound H melts incongruently, so that the line Dm_3H is not a quasi-binary section. The system has three saddle points but no quasi-binary section at all. The line Dm_2X looks like one but is not, because of the solid solution in the D solid phase. The extent of solid-solid solubility at the liquidus temperatures, across the section DH, is suggested by the crosshatching on this line in Fig. 13.2.

The fractionation paths on the D_s surface originate at point D and radiate, on either side of the straight-line path Dm_3, as curves convex with respect to point H. The paths on the H field must be imagined as radiating by extension from point H (the submerged, metastable maximum of the field); they curve similarly on either side of the straight-line path Hm_3 (of which only the portion $r \rightarrow m_3$ is on the stable surface for liquid in equilibrium with H_s) and are convex with respect to point D.

The vertical T vs c relations for the section DH of the ternary system are shown in Fig. 13.3. The point r is on curve p_8P_5 of Fig. 13.2, and s_r is the composition of the solid solution in equilibrium with liquid r. The solids s_{m_3} and s'_{m_3} are the conjugate solid solutions in equilibrium with liquid m_3, the minimum of the section. The compositions below this temperature on Fig. 13.3 correspond to liquids at the ternary eutectics E_4 and E_3, and will be referred to later.

The system (Fig. 13.2) has ten primary phase fields and ten invariant points. Four of these invariants, however, involve simply the decomposition or formation of binary compounds. There are consequently only six three-solid triangles for ultimate combinations of solids on complete solidification, related to two ternary peritectics and four ternary eutectics. We shall consider first the four special invariant points for appearance or disappearance of binary compounds and then the relations involved in the principal invariants.

13.1. THE INVARIANTS P_A, P_C, P_G, AND P_E

The Invariant P_A

The decomposition of compound A involves pure solids:

$$A \rightarrow Y + B \quad ,$$

and the temperature of the invariant P_A is therefore the same as T_A in Fig. 9.1. (The changes in isothermal relations near P_A are entirely similar to those shown in Fig. 8.5.) The curves e_1P_A and e_2P_A are both curves of even reaction,

$$L \rightarrow A + Y$$

and

$$L \rightarrow A + B \quad ,$$

respectively; the first is reached by liquid for total composition x in the region YAP_A, the second for x in ABP_A. At P_A, solid A decomposes, and the

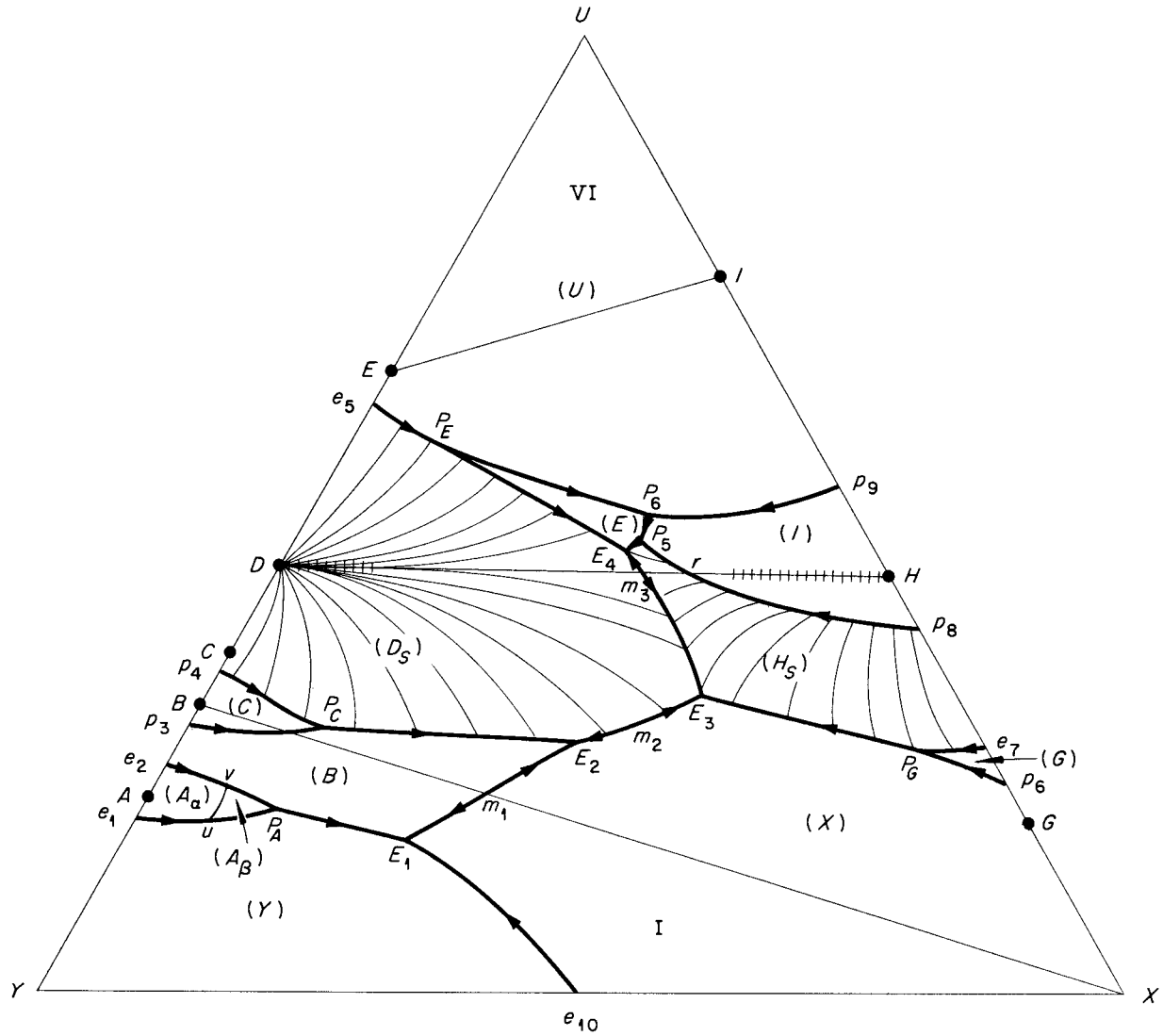

Fig. 13.2.

liquid travels on curve $P_A E_1$ precipitating B and Y. The isothermal curve uv represents liquid in equilibrium with A_α and A_β and divides the A field into regions for liquid in equilibrium with A_α and for liquid in equilibrium with A_β. Its temperature is T' in Fig. 9.1.

The Invariant P_C

The temperature of the invariant P_C, for the decomposition of compound C in the presence of ternary liquid, is higher than T_C of Fig. 9.1, because C is here decomposing not into pure solids but into B and a solid solution of D and H. The isothermal relations involving P_C are shown in Fig. 13.4: (*a*) between p_3 and P_C, (*b*) at P_C, (*c*) between P_C and T_C, and (*d*) below T_C. The reaction on curve $p_4 P_C$ is

$$L + D_s \rightarrow C \ ,$$

the three-phase triangle starting as line $p_4 CD$ and ending as $P_C Cy$ (isotherm *b*). This curve is reached for x in the region $p_4 DyP_C$. For x in CDy, the liquid is consumed on the curve to leave

UNCLASSIFIED
ORNL-LR-DWG 25608

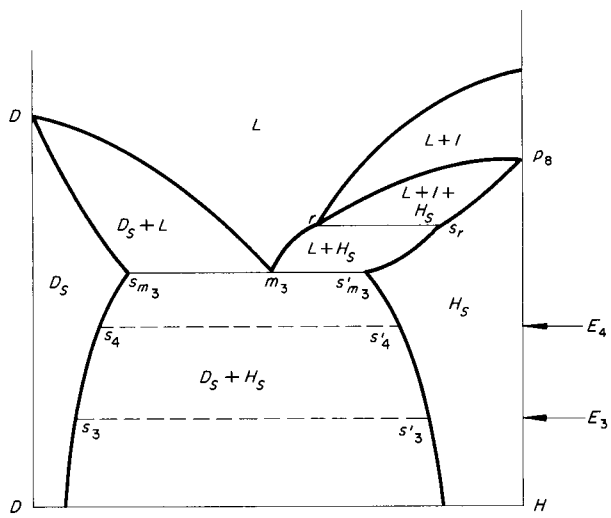

Fig. 13.3.

C and D_s (between D and y). For x in $p_4CP_{C'}$ D_s is consumed on the curve, and L then traverses the C field on a straight line from C, to reach curve $p_3P_{C'}$. For curve $p_3P_{C'}$

$$L + C \rightarrow B \quad .$$

The curve is reached for x in $p_3CP_{C'}$; then for x in $p_3BP_{C'}$ C vanishes on the curve and L leaves the curve to travel on the B field. The point $P_{C'}$ with the invariant reaction

$$L + C \rightarrow B + y \quad ,$$

is reached only for x in the quadrangle $BCyP_C$. For x in the triangle BCy, the liquid is consumed to leave the three solids, while for x in $ByP_{C'}$ C is consumed and the liquid moves away on curve P_CE_2, precipitating B and D_s, the solid solution ranging from point y at P_C to s_2 (Fig. 13.9) at E_2.

At P_C the equilibrium between C and liquid, shown in isotherm (a), is replaced by the equilibrium between B and D_s, shown in isotherm (c), with the D_s composition ranging between limits y' and y''. The limit y' reaches pure D at T_C and the limit y'' reaches s_2 at E_2.

As the temperature begins to fall below $P_{C'}$ compositions in the region BDy have already been completely solidified, either as C and D_s (from D to y) or as B, C, and y. Now as the tie line By' of Fig. 13.4 (c) moves to the left, the C vanishes from the three-solid mixtures to leave B and D_s, and the two-solid (C and D_s) mixtures first change to B, C, and y' and then lose the C phase to leave B and D_s. The lowest temperature for coexistence of C with liquid is $P_{C'}$ but C finally vanishes from coexistence with solids B and D_s at $T_{C'}$ to leave Fig. 13.4 (d).

The Invariant P_G

The relations at P_G are similar, except that one of the boundaries of the G field is a curve of even reaction. At $P_{G'}$ the decomposition of G involves pure X and H_s solid solution, and the temperature is higher than T_G of Fig. 13.1. The isothermal relations are shown in Fig. 13.5: (a) between e_7 and $P_{G'}$ (b) at $P_{G'}$ (c) between P_G and $T_{G'}$ and (d) below T_G. The reaction on curve p_6P_G is

$$L + X \rightarrow G \quad ;$$

the curve is reached for x in $Xp_6P_{G'}$ and crossed for x in Gp_6P_G. On curve $e_7P_{G'}$

$$L \rightarrow G + H_s \quad ,$$

the solid solution starting as pure H and ending at z [Fig. 13.5 (b)]. The curve is reached for x in P_GzHG. For x in zHG, the liquid vanishes on the curve to leave G and H_s. The point $P_{G'}$ for the reaction

$$L + G \rightarrow z + X \quad ,$$

is reached for x in the quadrangle P_GzGX. For x in the triangle zGX, the liquid vanishes to leave the three solids; for x in P_GzX, G is consumed, and the liquid travels on curve P_GE_3 precipitating X and H_s solid solution ranging from z to s'_3 (Fig. 13.9) at E_3.

In the two- and three-solid mixtures containing G, left in region zHX as the temperature falls below $P_{G'}$ solid G vanishes to leave simply X and H_s, as the tie line $z'X$ of Fig. 13.5 (c) moves to the side of the diagram, which it reaches at $T_{G'}$ to leave the isotherm of Fig. 13.5 (d).

The Invariant P_E

The invariant P_E represents the formation of the binary compound E in the presence of ternary liquid, not from pure solids but from U and D_s solid solution; the temperature of P_E is therefore lower than T_E in Fig. 9.1. The pertinent isothermal relations are shown in Fig. 13.6: (a) between e_5 and $T_{E'}$ (b) between T_E and $P_{E'}$ (c) at $P_{E'}$ and (d) below P_E. Curve $e_5P_{E'}$ with the reaction

$$L \rightarrow U + D_s \quad ,$$

is reached for x in the region e_5UP_E by liquid

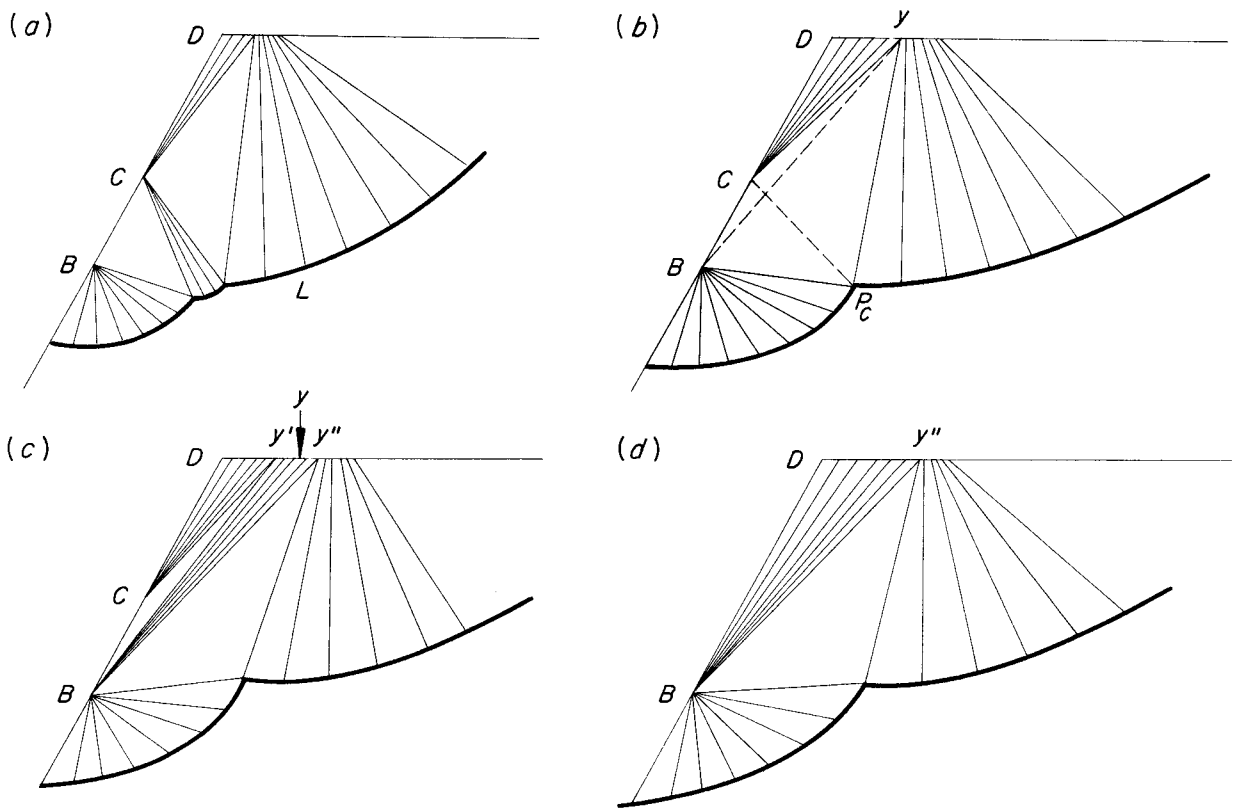

Fig. 13.4.

precipitating U or for x in De_5P_Ed by liquid precipitating D_s solid solution which starts as pure D at e_5 and ends as d at P_E [Fig. 13.6 (c)].

For x in the region DUd, the liquid vanishes while on the curve between e_5 and P_E, when the tie line $d'U$, moving from DU at e_5 to dU at P_E, comes to pass through x, to leave D_s and U. At T_E, however (between e_5 and P_E in temperature), the tie lines $d''E$ and $d''U$ also begin to enter the diagram [Fig. 13.6 (b)]. When x comes to be swept by the line $d''U$, solid E appears in the mixture, and the two-solid mixture of D_s and U becomes a mixture of D_s, E, and U. Moreover, if x is in the region DEd [Fig. 13.6 (c)], it comes next to be swept by the line $d''E$, when solid U vanishes from the mixture, to leave D_s and E.

Mixtures in the region DUd are therefore completely solidified before L reaches P_E, and at that temperature, when d'' and d' meet to give point d of the invariant quadrangle in Fig. 13.6 (c), and when the region for D_s and U has shrunk to the line dU, the solids present are either D_s and E in DEd, or D_s (of composition d), E, and U in dEU.

Liquids traveling on the curve e_5P_E reach P_E only if x is in the triangle dUP_E.

The reaction at the temperature of P_E, however, is

$$D_s(d) + U \rightarrow E + L(P_E) \ ;$$

it requires simply the solids d and U, and proceeds whether or not the liquid phase is present. Hence

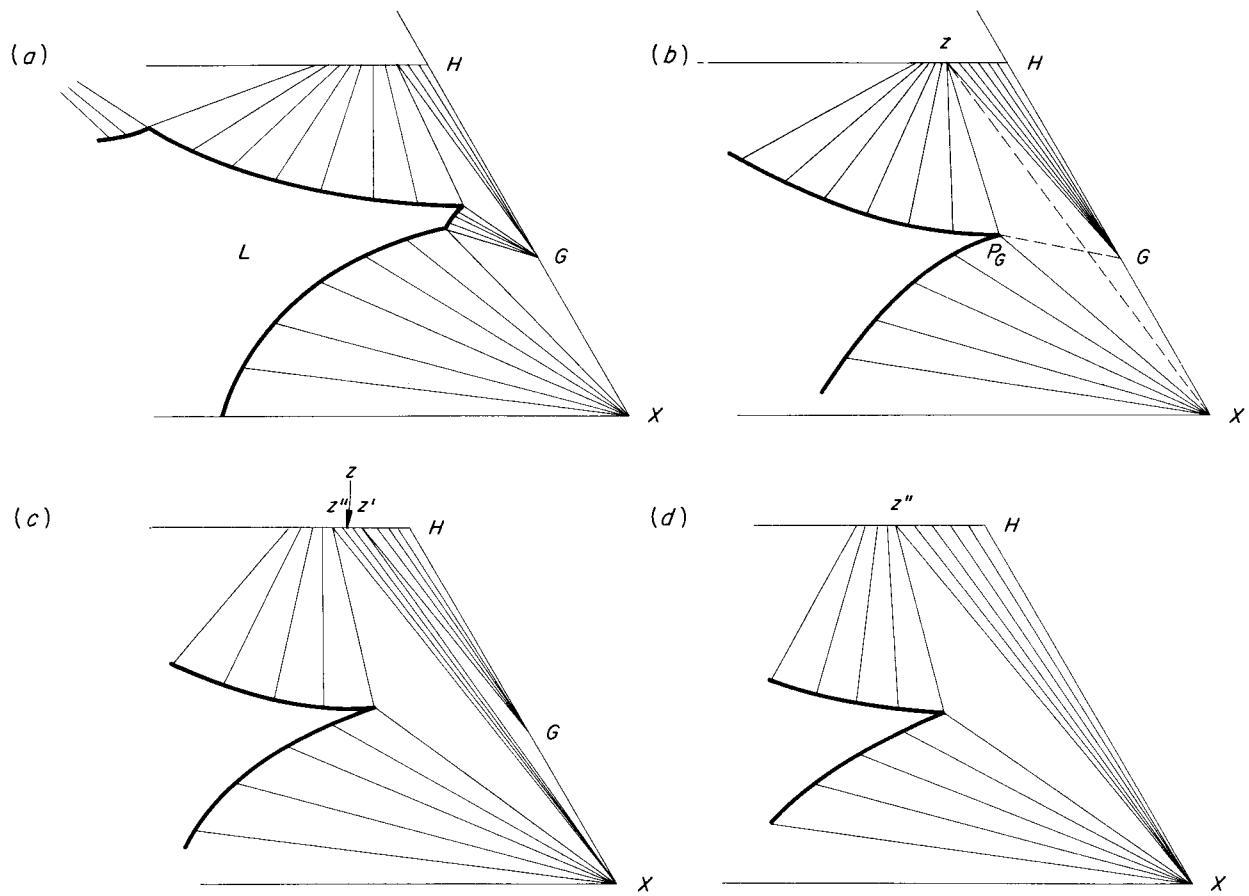

Fig. 13.5.

those mixtures which had already solidified to E, d, and U now produce liquid of the composition P_E again, in the invariant reaction. The invariant P_E is an example of the type of invariant discussed as case (b) under Fig. 4.12.

Now for x in the region EUP_E, the solid solution d is consumed and L travels away on curve $P_E P_6$, along which

$$L + U \rightarrow E \quad ;$$

and for x in dEP_E, U is consumed and L moves onto curve $P_E E_4$, for

$$L \rightarrow E + D_s \quad ,$$

the solid solution starting at d and ending at s_4 (Fig. 13.7).

13.2. THE REGION *DUH*

Figure 13.7 gives the schematic arrangement for the reactions involving the invariant points in the upper half of the ternary system, the region DUH. The invariant quadrangle pertaining to P_E is shown by dashed lines. The invariant planes are seen to overlap in various ways. The order of temperature is $P_E > P_6 > P_5 > E_4$. The planes are $dEUP_E$, $EUIP_6$, EIs_5P_5, and s_4Es_4' (for E_4).

The transition curve $P_E P_6$, for the reaction

$$L + U \rightarrow E \quad ,$$

is reached, directly or indirectly, by liquids for x in the region $P_E EUP_6$; but for x in $P_E EP_6$, L then leaves the curve when U is consumed, to

UNCLASSIFIED
ORNL-LR-DWG 25611

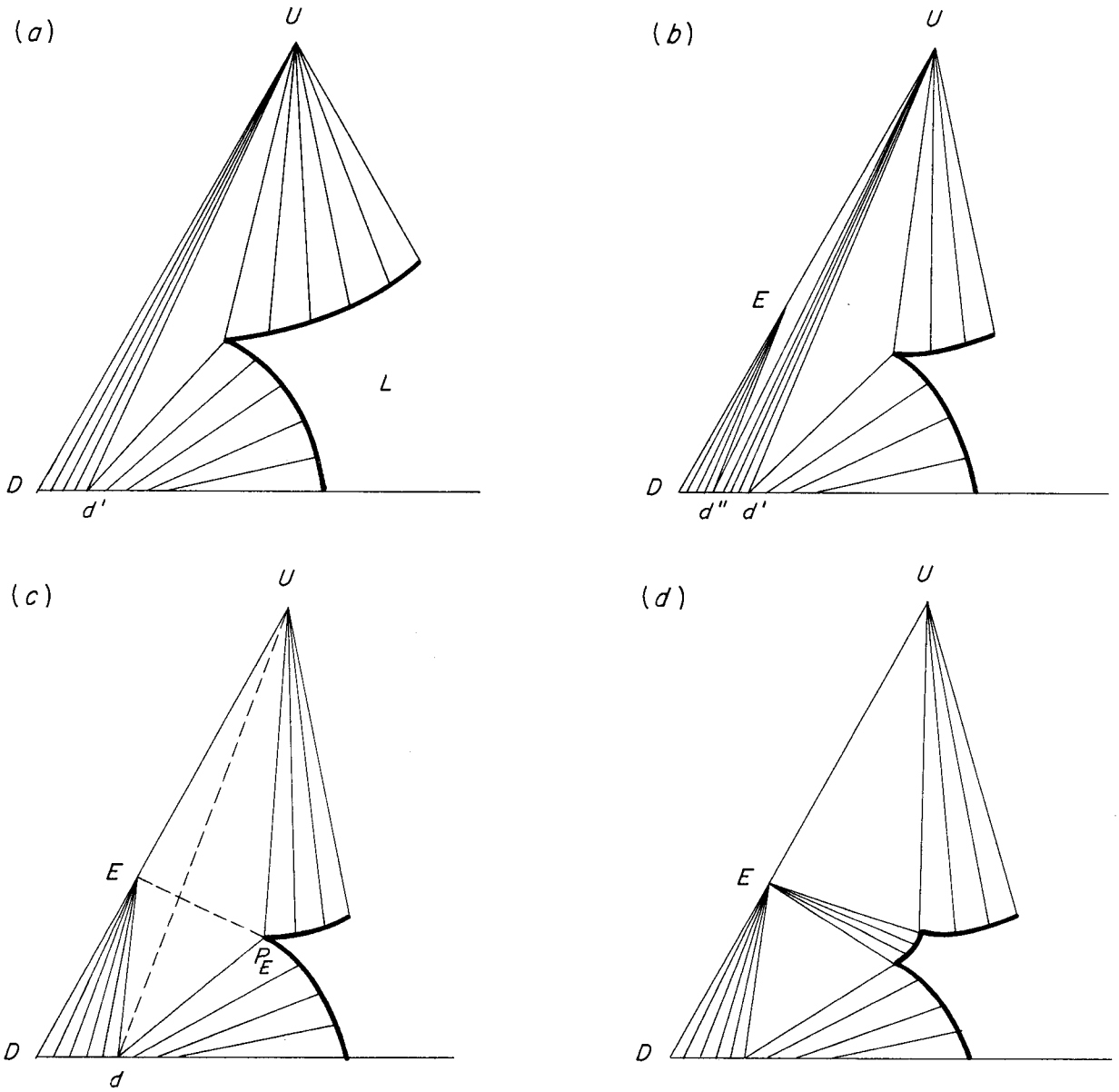

Fig. 13.6.

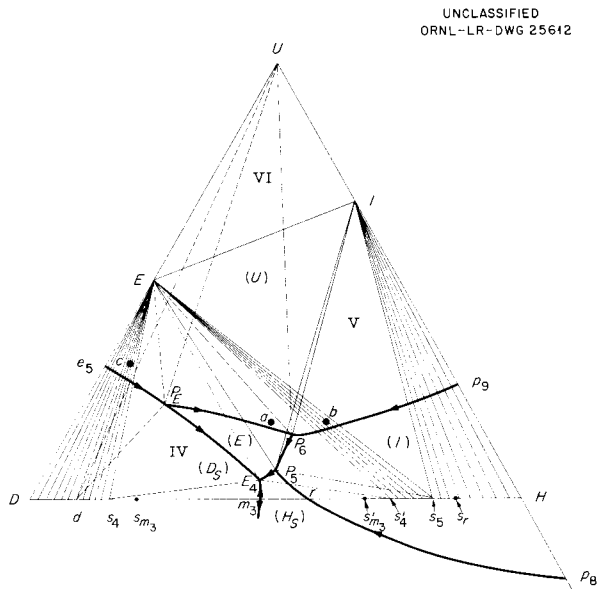

Fig. 13.7.

travel across the E field. The transition curve $p_9 P_6$, for the reaction

$$L + U \rightarrow I \ ,$$

is reached from the region $p_9 UP_6$, and it is left by liquid for x in $p_9 IP_6$. The point P_6 is reached only for x in $P_6 EUI$; its reaction is

$$L + U \rightarrow E + I \ ,$$

and it is the incongruent solidification end point for triangle VI (EUI). At a still lower temperature, solid F of system Y–U forms from the solids E and U, and then we have either E, F, and I or F, U, and I.

The reaction on curve $P_6 P_5$ is odd,

$$L + E \rightarrow I \ ,$$

if, as assumed in Fig. 13.7, its tangent extends to the right of I. In this case the curve is reached either from P_6 (for x in the region $P_6 EI$) or directly from the E field for x in $P_5 EP_6$. But for x in $P_5 IP_6$ the curve is left by the liquid when E is consumed, when the liquid, saturated only with I, moves onto the I field.

Next, the transition curve $p_8 P_5$ is reached, directly or indirectly, for x in the region $IP_5 p_8$. The reaction on this curve is

$$L + I \rightarrow H_s \ .$$

The three-phase triangle for liquid in equilibrium with H_s and I starts as the straight line $p_8 HI$ and extends into the diagram to end as $P_5 s_5 I$. Consequently either the liquid or the solid I may be completely consumed while L is on the curve. For x in $s_5 IH$, the liquid is consumed when the H_s–I leg of the three-phase triangle sweeps through the point x, to leave I and H_s (between H and s_5). For x in the region $p_8 rP_5 s'_5 H$, solid I is consumed when the L–H_s leg passes through x; this leg starts as the line $p_8 H$ and sweeps around to become rs_r for L at r, and finally $P_5 s_5$. When I has vanished, L leaves the curve to travel upon the H_s field, on a curved path (a straight path only between r and m_3, but otherwise curving always away from this line). The invariant P_5 is reached only for x in the quadrangle $P_5 EIs_5$. Its reaction is

$$L + I \rightarrow E + s_5 \ ,$$

and it is the incongruent crystallization end point for triangle V (EIs_5).

For x in the region $P_5 Es_5$ the liquid moves on down the curve $P_5 E_4$, precipitating E and solid solution H_s, beginning at s_5 and ending at s'_4. The curve $P_5 E_4$ is also reached directly, from the E field for x in $E_4 EP_5$, and from the H_s field for x in $s_5 P_5 E_4 s'_4$. For x in $Es'_4 s_5$, the liquid vanishes on the curve to leave E and a solid solution (between s'_4 and s_5). The curve $P_E E_4$ is reached from the E field for x in $P_E EE_4$, from P_E itself for x in dEP_E (d shown in Fig. 13.6); and from the D_s field for x in $dP_E E_4 s_4$. Liquid on the curve $P_E E_4$ precipitates E and D_s, starting at d and ending at s_4. Compositions in dEs_4 solidify completely on the curve to leave E and D_s. (It will be recalled that compositions in DEd solidify completely on the curve $e_5 P_E$.) The invariant E_4 is also reached along curve $m_3 E_4$, with the liquid precipitating two mutually saturated solid solutions ranging from s_{m_3} and s'_{m_3} at m_3 to s_4 and s'_4 (cf. Fig. 13.3). From the D_s side, $m_3 E_4$ is reached for x in $s_4 E_4 m_3$; from the H_s side, directly or indirectly, for x in $m_3 E_4 s'_4$. The invariant E_4, a eutectic, is therefore reached for x in triangle IV ($s_4 Es'_4$).

The vertical T vs c section through EH is shown schematically in Fig. 13.8.

Solution of composition a, in Fig. 13.7, gives U as first solid, and L reaches curve $P_E P_6$ on a straight line from U. On the curve,

$$L + U \rightarrow E \ .$$

The solid U is consumed; L leaves the curve,

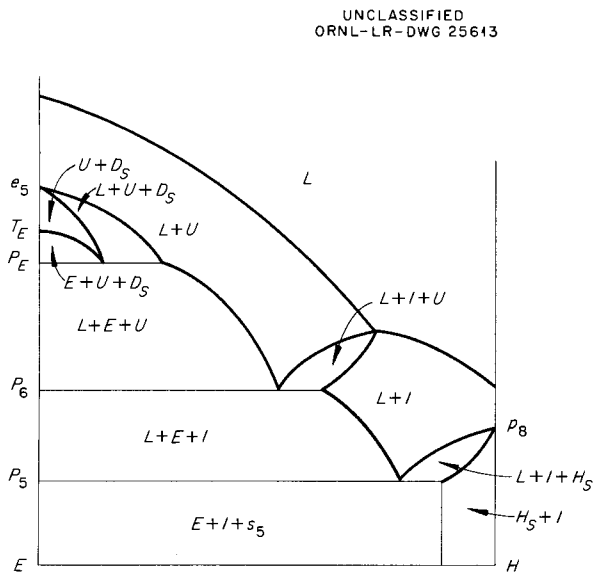

Fig. 13.8.

travels on a straight line from E, and reaches curve P_6P_5. On this curve

$$L + E \rightarrow I \ .$$

The liquid reaches P_5, where

$$L + I \rightarrow E + s_5 \ .$$

The compound I is consumed, and the liquid follows curve $P_5 \rightarrow E_4$, precipitating E and a solid solution ranging from s_5 to s_4'. At E_4, s_4 also precipitates, and the liquid vanishes to leave s_4, E, and s_4'.

Liquid b gives U as first solid and reaches curve p_9P_6. On the curve,

$$L + U \rightarrow I \ .$$

The solid U is consumed; L leaves the curve, crosses the I field, and reaches curve p_8P_5. On this curve

$$L + I \rightarrow H_s \ ,$$

the solid solution starting with composition just to the right of s_r and reaching s_5 when L is at P_5. Now

$$L + I \rightarrow E + s_5 \ .$$

The compound I is consumed, and L starts out on curve P_5E_4, but the liquid is consumed before reaching E_4, to leave E and a solid solution between s_5 and s_4'.

Liquid c gives U as first solid and reaches curve e_5P_E. On the curve

$$L \rightarrow U + D_s \ ,$$

and the liquid vanishes, on the curve, to leave U and a solid solution between D and d, fixed by the straight line Uc. As the temperature continues to fall, solid E forms to give E, U, and D_s, the composition of the solid solution moving toward point d. The D_s solid reaches point d at the temperature of P_E. Here

$$U + d \rightarrow E + L(P_E) \ .$$

The solid U is consumed, and liquid reappears, therefore, with composition P_E. Now the liquid travels along curve P_EE_4, precipitating E and D_s, with D_s starting at d; but the liquid vanishes while on this curve to leave E and a solid solution between d and s_4, fixed by the line Ec.

Finally, consider a liquid of composition x on the line DH. The first solid is I, and liquid reaches curve p_8P_5, for the reaction

$$L + I \rightarrow H_s \ .$$

If x is between r and s_r, then when L reaches point r, I will just have been consumed, and the solid solution has the composition s_r. Now the liquid leaves the curve and travels to m_3, where it vanishes to leave the conjugate solid solutions s_{m_3} and s_{m_3}'. But for x between s_r and H, the liquid and I vanish simultaneously, leaving H_s as sole solid phase, before L reaches point r on the curve, when the H_s corner of the L–H_s–I three-phase triangle passes through point x.

13.3. THE REGION *YDHX*

The lower part of the ternary system is represented in Fig. 13.9. The relations involving the fields of the decomposing solids A, C, and G have already been discussed. The Y, B, and X fields involve pure solids, with straight-line crystallization paths radiating from the points Y, B, and X, respectively. The transition curve p_8P_5 was discussed under Fig. 13.7. Liquids reach this curve on straight-line paths from the point I (Fig. 13.7), but for x in the portion of the I field included in Fig. 13.9, I is completely consumed while L is still on the curve. On leaving the curve, L then travels across the H_s field, on a curved path, to reach one of its boundaries m_3E_3, P_GE_3, or e_7P_G.

UNCLASSIFIED
ORNL-LR-DWG 25614

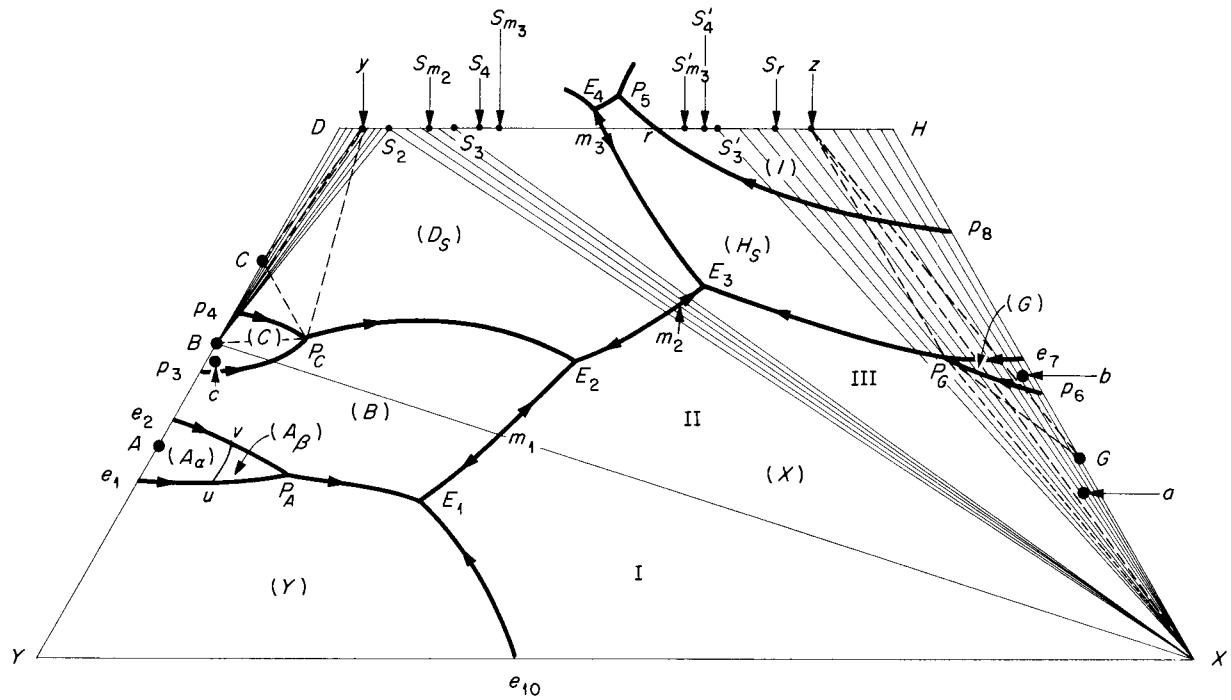

Fig. 13.9.

The eutectic E_1 is reached for x in triangle (YBX). The reaction on the curve $E_1 m_1 E_2$ is

$$L \rightarrow B + X \ ,$$

in both directions. The reaction for curve $E_2 m_2 E_3$ is

$$L \rightarrow X + D_s \ ,$$

the solid solution ranging from s_{m_2} for L at m_2, to s_3 at E_3 and to s_2 at E_2. For x in the region $s_2 s_3 X$, the liquid is consumed on the curve, before reaching a eutectic, to leave X and D_s (between s_2 and s_3). The point m_2 is a saddle point, but the section $s_{m_2} m_2 X$ is not quasi-binary; the liquid with composition s_{m_2} is in equilibrium with a solid solution not of composition s_{m_2} but between D and s_{m_2}.

The reaction on curve $P_C E_2$ is probably of even sign,

$$L \rightarrow B + D_s \ ,$$

along its whole length. The solid D_s for this curve starts as point y (see Fig. 13.4) for L at P_C and ranges to s_2 for L at E_2. For x in the region CDy, solidification is complete on curve $p_4 P_C$ to leave C and D_s; compositions in BCy solidify at P_C to leave B, C, and y. As the temperature falls further, C then begins to vanish from these solid mixtures, disappearing completely on the binary side of the system at T_C. For x in Bys_2, solidification is complete on the curve $P_C E_2$ to leave B and D_s. The point E_2 is reached only for x in triangle II $(Bs_2 X)$.

Similarly, compositions in the region zHG solidify completely on curve $e_7 P_G$ to leave G and H_s, and those in zGX solidify at P_G to leave G, X, and z. Then as the temperature falls further, G begins to decompose in these solid mixtures, vanishing last on the binary side at T_G. For x in $s'_3 zX$, the liquid vanishes on the curve $P_G E_3$ to leave X and H_s. On curve $m_3 E_3$, the liquid precipitates conjugate solid solutions ending at s_3 and s'_3. The point E_3 is reached for x in triangle III $(s_3 s'_3 X)$.

The vertical T vs c section BG is shown in Fig. 13.10.

UNCLASSIFIED
ORNL-LR-DWG 25615

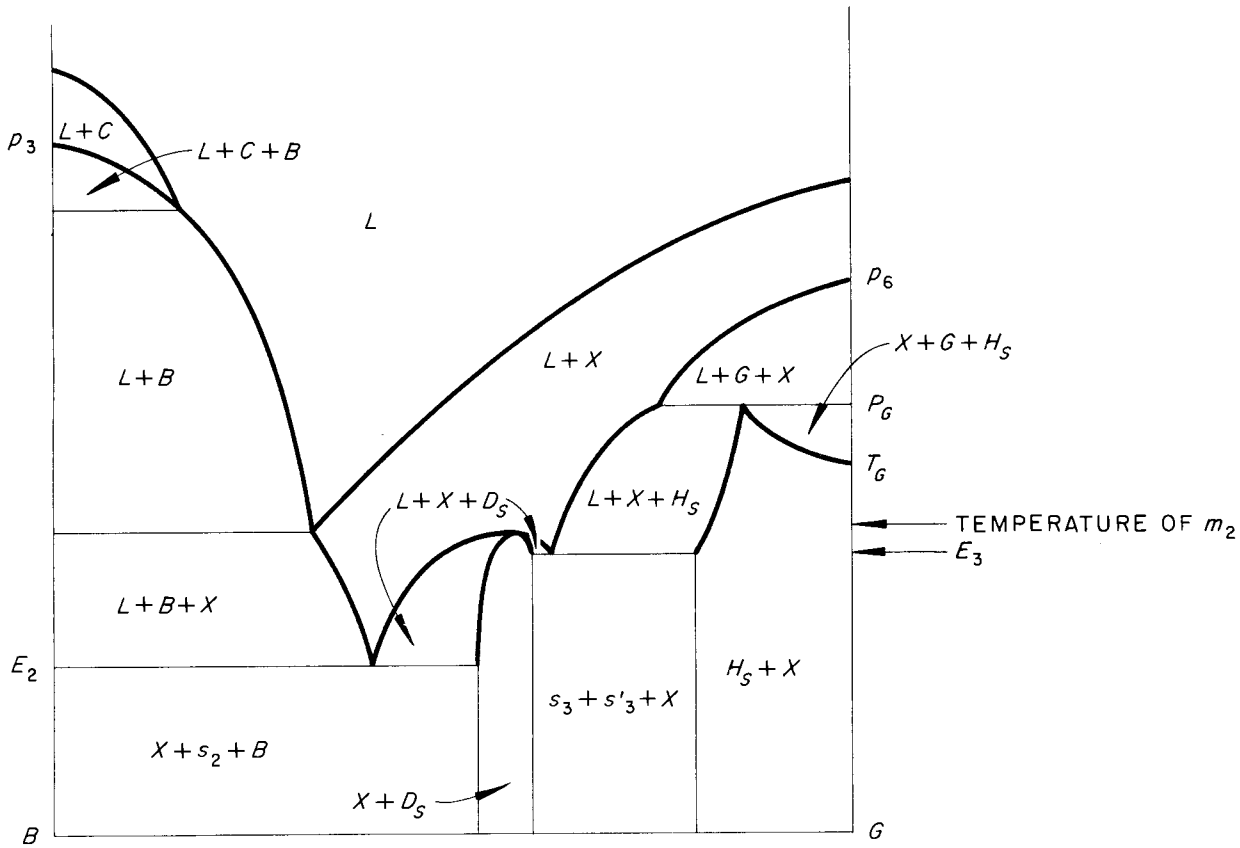

Fig. 13.10.

Liquid a in Fig. 13.9 gives X as first solid, reaches curve p_6P_G, reaches P_G carrying G and X, and there solidifies to G, X, and z. With falling temperature, the composition of the solid solution moves to the right from z, and G vanishes to leave X and a solid solution fixed by the line Xa.

Liquid b gives G as first solid, reaches curve e_7P_G, and solidifies on this curve to leave G and a solid solution z' [Fig. 13.5 (c)] between z and H. Then as the temperature falls further and z' moves to the right, X appears as third solid when the line Gz' passes through b, and finally G vanishes when the line Xz' passes through b.

Liquid c gives C as first solid, reaches curve p_3P_C, leaves this curve when C is consumed, reaches curve e_2P_A on the left of v, and begins to precipitate A_α together with B. At v, A_α changes to A_β. At P_A, A_β decomposes, and the liquid travels on curve $P_A \rightarrow E_1$ to solidify at E_1 to Y, B, and X.

13.4. FRACTIONATION PROCESS ON THE SOLID SOLUTION FIELDS

In a fractionation process, L follows one of the fractionation paths to a boundary of the field; the solid increases in H on the D_s field and increases in D on the H_s field. The fractionation end point is E_4 above the line DH. Liquids starting in the region between e_5 and the path DP_E end as four solids, D_s, U, E, and H_s, but all others starting in the solid solution fields above line DH end as D_s, E, and H_s.

Below the line DH the fractionation process for the H_s field ends at E_3, leaving H_s, X, and D_s;

the same holds for the D_s field above the path Dm_2. The rest of the D_s field is divided by the fractionation path Dq of Fig. 13.11; q is the intersection of p_4P_C with line Ct, and t is the intersection of curve p_3P_C with line Bm_1. Liquid in the region between p_4 and the path Dq reaches curve p_4q. Without stopping on the curve, L crosses it and traverses the C field in a straight line from C to reach curve p_3t. Without stopping on this curve, L crosses it and traverses the B field to one of its boundaries, e_2P_A, P_AE_1, and m_1E_1. The process ends at E_1 to leave D_s, B, Y, and X, since solids C and A will have decomposed. The fractionation end point for the D_s field between the paths Dq and Dm_2 is E_2, the final solids being D_s, B, and X. For the region between the paths Dq and DP_C, the precipitation of the solid solution is interrupted while L crosses the C field and then the B field between curve tP_C and curve m_1E_2, finally reaching E_2, where D_s begins to precipitate again with the composition s_2. Consequently, there is then a gap in the composition of the D_s solid solution finally obtained.

UNCLASSIFIED
ORNL-LR-DWG 25616

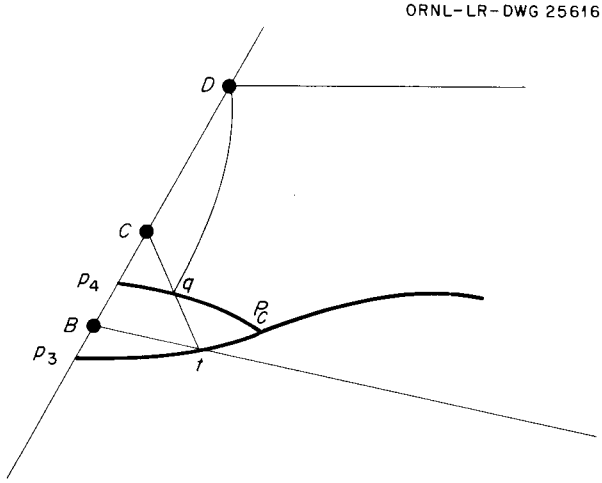

Fig. 13.11.

14. SYSTEM Y–U–Z: NaF–UF_4–ZrF_4

For the ternary system Y–U–Z, the binary system Y–U appears in Fig. 9.1, and it is here used with the same lettering. The Y–Z binary diagram was given in Fig. 11.1, but it is redrawn here (Fig. 14.1) to show the different lettering necessary in the present section. The system U–Z is given in Fig. 14.2.

14.1. GENERAL CHARACTERISTICS

The phase diagram of the ternary system is given schematically in Fig. 14.3.

The principal feature in this system is the existence of three continuous series of solid solutions: that between the components U and Z, with a minimum at m', that between the congruently melting corresponding 7:6 compounds D and K, and that between the congruently melting corresponding 3:1 compounds A and G. For brevity these solid solutions will be called U_s, D_s, and A_s, respectively. The primary phase fields for these solid solutions are the three largest fields of the diagram.

Moreover, each of the sections AG and DK constitutes a quasi-binary section of the system (Figs. 14.4 and 14.5). At least as far as the equilibria involving the liquidus are concerned, therefore, the system as a whole may be divided into three independent subsystems, Y–A–G, A–D–K–G, and D–U–Z–K, which will thus be considered separately.

In the subsystem Y–A–G, with only two fields (pure Y and A_s), there is only one boundary curve ($e_6 \rightarrow e_1$), and the temperature on this curve falls in the same direction as for the quasi-binary section $G \rightarrow A$ itself. In the subsystem D–U–Z–K the liquidus pertains almost entirely to the primary fields for two continuous (effectively binary) solid solutions. The boundary curve is slightly complicated by the field for compound M, but it has no minimum of temperature. The temperature of the boundary curve falls continuously from the YU to the YZ side, as in the section DK itself, despite the minimum m' in the U–Z system. The middle subsystem, however, is unusual in having opposite directions of falling temperature in its bounding quasi-binary solid solution systems, $D \rightarrow K$ and $A \leftarrow G$. No "normal" behavior can be predicted for the boundary curve between the solid solution fields. This boundary curve is complicated by the minor fields of the four other solids of this subsystem, but essentially it falls in temperature from the AD to the GK side, with a slight maximum m near point e_2.

The A–G and D–K solid solutions, moreover (as shown in exaggerated form in Fig. 14.6), are actually ternary in composition on the YZ side. They occupy small areas of ternary composition near points G and K, respectively, not lying simply on the straight lines AG and DK. This is so because the compounds G and K form solid solutions in the Y–Z system itself, besides forming the continuous solid solutions with the analogous compounds of the Y–U system.

The only invariant points (for liquid in equilibrium with three solids) in the entire system are five peritectic points. There is no eutectic, nor is there a minimum on any curve of liquid in equilibrium with two solids.

The vertical T vs c section of the system from the corner Y to a point midway between U and Z is merely a section passing successively through the three adjacent but independent subsystems (Fig. 14.6). Details of this diagram will be mentioned later.

14.2. SUBSYSTEM Y–A–G

The relations in the subsystem Y–A–G (Figs. 14.7 and 14.8) are similar to those discussed under Figs. 6.1 to 6.4, but simpler, since there is here no minimum either in the binary edge AG or in the boundary curve $e_1 e_6$.

All mixtures in the system solidify to two solids, Y and A_s. The reaction on the curve $e_1 e_6$ is

$$L \rightarrow Y + A_s \ ,$$

and the three-phase triangle, starting as the line Ye_6G, moves, with the configuration shown in Fig. 14.7, across the diagram to end as the line Ye_1A. All liquids reach the boundary curve, and they are completely solidified on that curve when the total composition x is swept by the leg YA_s of the three-phase triangle. Liquid a (Fig. 14.7) gives Y as first solid and reaches the curve on a straight line from Y. On the curve, the liquid precipitates Y and a solid solution starting with composition s_1. The liquid vanishes on the curve, while moving toward e_1, when the solid solution reaches a composition on the extension of the straight line Ya. Liquid b precipitates a solid solution beginning between G and s_1. The liquid reaches the curve on a curved equilibrium path

UNCLASSIFIED
ORNL-LR-DWG 25617

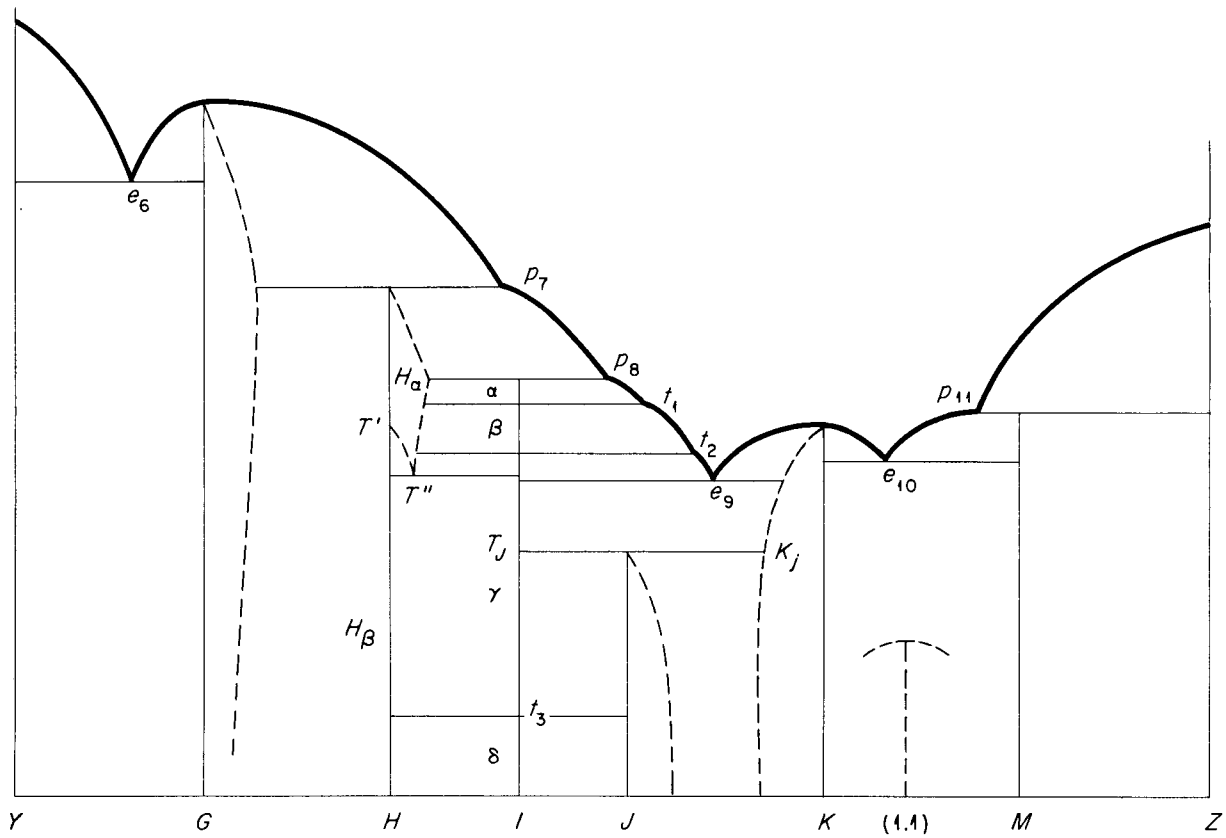

Fig. 14.1.

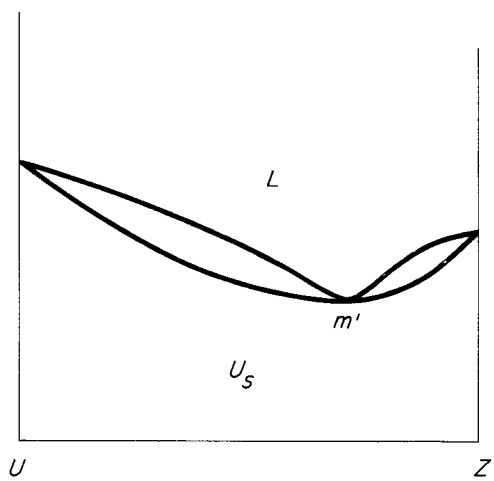

Fig. 14.2.

UNCLASSIFIED
ORNL-LR-DWG 25618

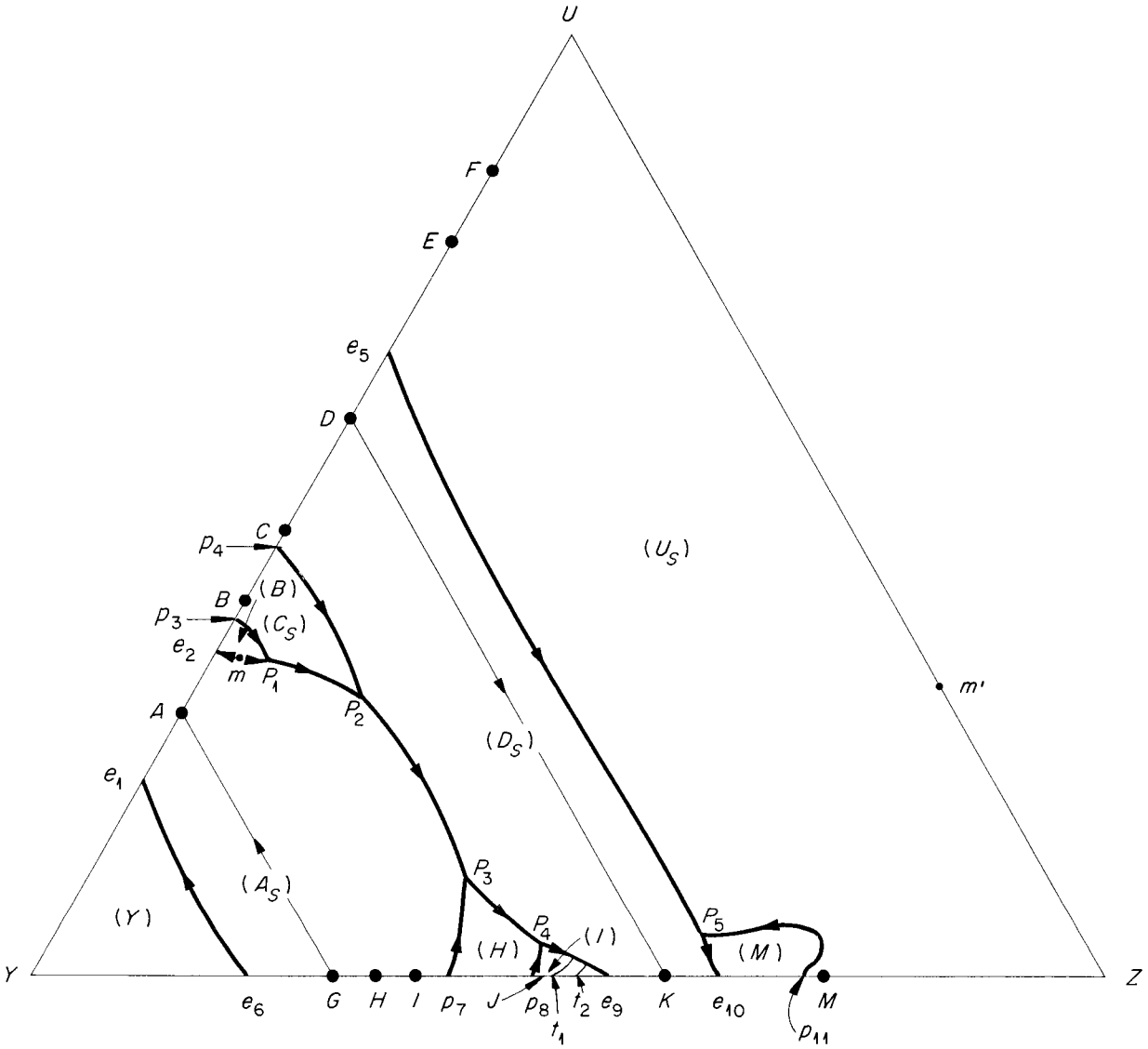

Fig. 14.3.

UNCLASSIFIED
ORNL-LR-DWG 25619

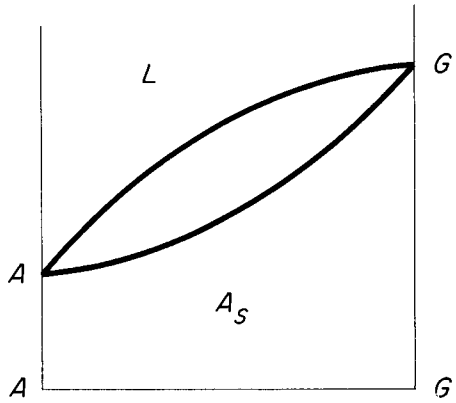

Fig. 14.4.

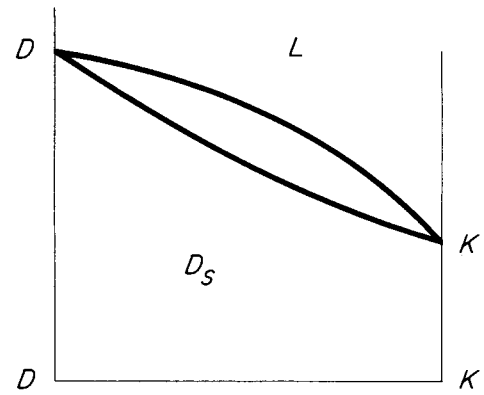

Fig. 14.5.

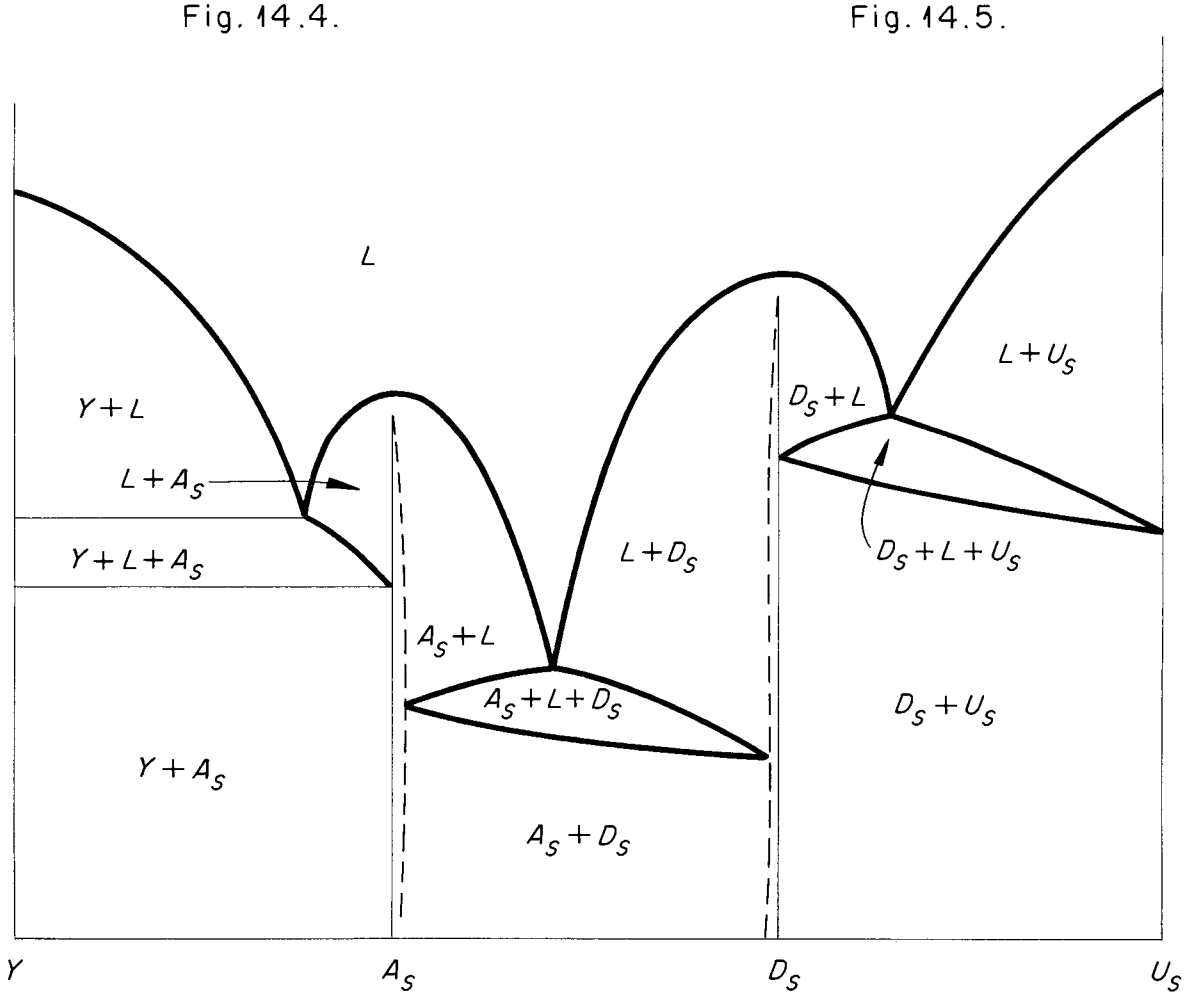

Fig. 14.6.

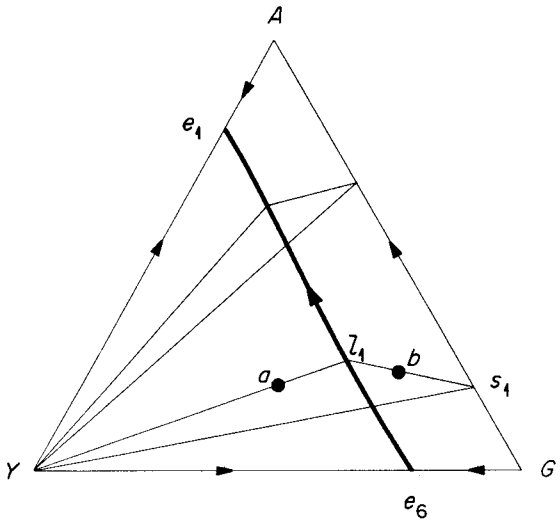

Fig. 14.7.

UNCLASSIFIED
ORNL-LR-DWG 25620

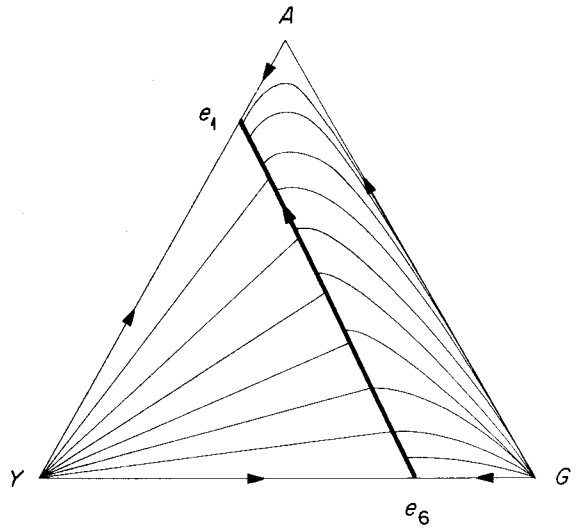

Fig. 14.8.

(as discussed in Sec 6) convex with respect to point A. When it reaches the curve, the liquid is at l_1 and the solid at s_1. Now Y begins to precipitate with the solid solution; the liquid moves toward e_1, and vanishes when the solid solution reaches a composition on the extension of line Yb.

The vertical T vs c section (first third of Fig. 14.6) is similar to Fig. 6.3; but in the present case the area for liquid in equilibrium with Y and A_s collapses to a line only at e_6 and at e_1, since there is no minimum in the boundary curve.

Crystallization paths in the Y field are straight lines from Y. Fractionation paths in the A_s field are a family of curves originating at G, diverging from the line $G \rightarrow A$, convex with respect to A, and each ending at the boundary curve (Fig. 14.8).

14.3. SUBSYSTEM A–D–K–G

The two large fields in the subsystem A–D–K–G (Fig. 14.9) pertain to solid solutions A_s and D_s. Part of the A_s field is in the subsystem Y–A–G already discussed, and part of the D_s field is in the subsystem D–U–Z–K. The line $G \rightarrow A$ is simply the line of maximum temperature running from G to A, and it is the limiting fractionation path of the field dividing the curved paths of the two subsystems. The line $D \rightarrow K$ is a similar

UNCLASSIFIED
ORNL-LR-DWG 25621

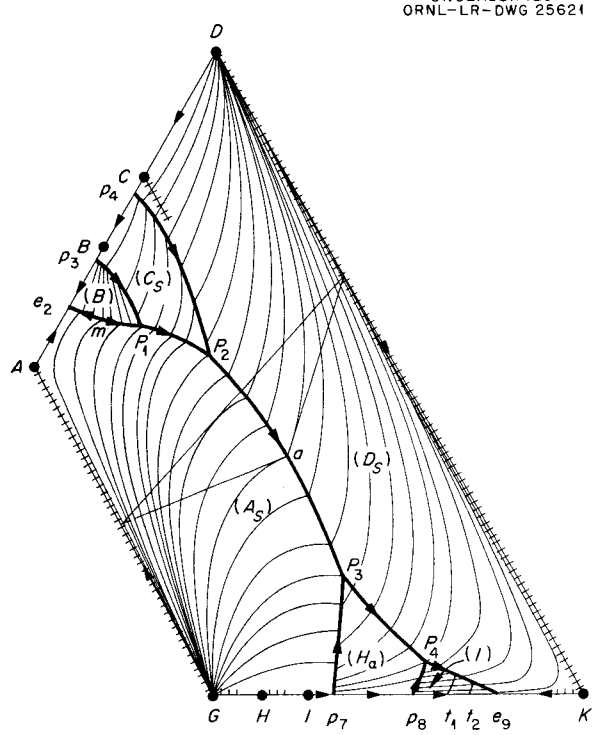

Fig. 14.9.

limiting straight-line fractionation path running from the melting point of D to the melting point of K, and dividing the curved families of fractionation paths of the two adjacent subsystems. The fractionation paths in the A_s field (on either side of the line AG – i.e., both in Fig. 14.8 and in Fig. 14.9) are convex with respect to point A, and those in the D_s field are convex with respect to point K. The tangents for the two fractionation curves meeting from two sides at the curve P_2P_3 must be such that the three-phase triangle for this curve points toward P_3 (direction of falling temperature), as shown for point a in Fig. 14.9.

The vertical T vs c section across the curve P_2P_3 is shown as the middle part of Fig. 14.6. There is theoretically a single-phase ternary solid solution band reaching very slightly into the section both from the AG line and from the DK line; the dimensions are exaggerated in order to show the schematic relations. The region "A_s + L + D_s" is a cut through the space generated by the moving three-phase triangles of curve P_2P_3. The coexisting phases are not on the plane of the diagram. The order of temperature for the three corners of this cut ($L > A_s > D_s$) results from the fact that the section involved, from Y to the 1:1 ratio on the UZ side, is reached, with falling temperature, first by the L corner of the three-phase triangle, next by the A_s corner, and last by the D_s corner, according to the configuration of the triangle drawn on Fig. 14.9.

The solid H_α of system Y–Z forms some binary solid solution on the side of compound I, and hence the fractionation paths in the H_α field are curved and are convex with respect to K. The common origin of these paths, extended back, is the metastable congruent melting point of H_α in the Y–Z binary system. The transition from H_α solid solution to pure H_β, all occurring below liquidus temperature, will be discussed later. The compound C, as will be explained shortly, also forms solid solution with composition extending into the diagram toward the GK side; hence the paths on the C field are also curved, are convex with respect to K, and originate by extension from the point C. Only the solids B and I are pure, in Fig. 14.9. The I field is divided into three portions, by isothermal creases at the temperatures t_1 and t_2 of Fig. 14.1; the portions represent, with falling temperature, liquid in equilibrium with I_α, liquid in equilibrium with I_β, and liquid in equilibrium with I_γ. The t_3 transition, to I_δ, occurs at a low temperature and does not affect the liquidus surfaces.

The crosshatched lines in Fig. 14.9 indicate where the solid solution compositions are found.

The Region Involving A, B, C, and D

With regard to the evidence for solid solution formation by compound C, we note that this incongruently melting 5:3 compound decomposes on cooling, at T_C(630°), into the pure solids B and D in the binary system Y–U. But its primary phase field in the ternary system Y–U–Z extends down to the temperature of P_2 (610°). Since D is known to form solid solution with K in the ternary system, the decomposition temperature of C is expected to be raised in the ternary system unless the solid phase C itself forms a solid solution containing the third component. This solid solution, which the compound C must therefore form, may be imagined as involving the hypothetical corresponding 5:3 compound in the Y–Z system, so that the composition of the solid phase to be called C_s (solid solution of 5:3 compounds originating at point C) probably extends on a line into the diagram parallel to the edges AG and DK.

Moreoever, the point P_2 may either represent the lowest temperature of existence of this solid phase in the ternary system; or it may represent simply the lowest temperature for its equilibrium with ternary liquid, while the lowest temperature for its existence may be still lower (in subsolidus relations). In absence of the information required for deciding between these alternatives, we shall consider both relations for this region of the system, referring to the first as Scheme I and to the second as Scheme II.

Scheme I. – The point P_2 is here assumed to be the lowest temperature of existence of the C_s solid solution, with the third component, in other words, continually lowering the decomposition temperature of C. The schematic relations for the invariant four-phase planes would be as shown in Fig. 14.10. There are three such planes. The highest-temperature plane is the quadrangle for P_1, involving B, C_1, A_1, and $L(P_1)$; the next, in dashed lines, which will be referred to as the invariant Q_z, is a quadrangle involving B, A_z, D_z, and C_z; the lowest is the triangle for P_2, for the phases A_2, D_2, $L(P_2)$, and C_2 as the interior phase.

The order of decreasing temperature for the fixed points involved is assumed to be:

$$p_4 > p_3 > m > e_2 > P_1 > T_C > Q_z > P_2 \ .$$

A series of isotherms relating these points is given in Fig. 14.11: (a) between p_4 and p_3;

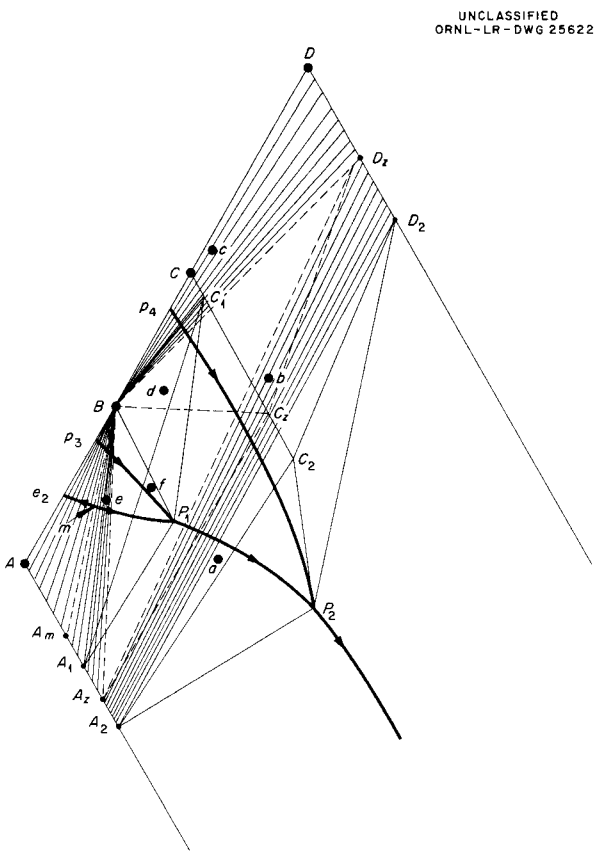

Fig. 14.10.

(*b*) between p_3 and m; (*c*) between m and e_2; (*d*) at P_1; (*e*) between P_1 and T_C; (*f*) between T_C and Q_z; (*g*) at Q_z; (*h*) between Q_z and P_2; (*i*) at P_2; (*j*) below P_2.

The reactions on the curves (of liquid in equilibrium with two solids) and at the invariants are as follows:

1. $p_4 \rightarrow P_2$: $L + D_s \rightarrow C_s$. The three-phase triangle, triangle 1 in Fig. 14.11(*a*), starts as the line p_4CD and ends as $P_2C_2D_2$. This curve is reached by liquids from the region $p_4DD_2P_2$, precipitating D_s. But for original, total composition x in the region CDD_2C_2, the liquid vanishes while traveling on the curve, before reaching P_2, to leave C_s and D_s when the C_s–D_s leg of the three-phase triangle comes to pass through x. (The appearance and disappearance of phases to be considered in this section will most easily be visualized through the sequence of isotherms in Fig. 14.11. The disappearance of the liquid phase is not necessarily the end of the phase changes.) For x in the region $p_4CC_2P_2$, the D_s phase vanishes while L is still on the curve, when the L–C_s leg of the triangle passes through x. Then the liquid, saturated only with C_s, traverses the C_s field to reach one of its other boundaries, p_3P_1 or P_1P_2.

2. $p_3 \rightarrow P_1$: $L + C_s \rightarrow B$. The three-phase triangle, [triangle 2 in Fig. 14.11(*b*)], starts as line p_3BC and ends as P_1BC_1. The curve is reached for x in $p_3CC_1P_1$, by liquid precipitating C_s. For x in BCC_1, the liquid vanishes on the curve to leave B and C_s when the leg B–C_s passes through x; for x in p_3BP_1, C_s vanishes on the curve when the L–B leg passes through x, and then L traverses the B field.

3. $m \rightarrow e_2$: $L \rightarrow B + A_s$. Point m is the temperature maximum on the curve e_2P_1. For this section, $m \rightarrow e_2$, the three-phase triangle starts as the line A_mmB and ends as Ae_2B [triangle 3′ in Fig. 14.11(*c*)]. The curve is reached from the B field for x in me_2B or from the A_s field for x in Ae_2mA_m. The liquid always vanishes before reaching e_2, to leave B and A_s (between A and A_m) on a line passing through x.

4. $m \rightarrow P_1$: $L \rightarrow B + A_s$. The three-phase triangle [triangle 3 in Fig. 14.11(*c*)] starts again as the line A_mmB and ends as A_1BP_1. The curve is reached from the B field, by liquid precipitating B, for x in mBP_1; and it is reached from the A_s field by liquid precipitating A_s, for x in $A_mmP_1A_1$. Now if x is in A_1A_mB, the liquid vanishes on the curve to leave B and A_s (between A_m and A_1) on a line passing through x.

Invariant P_1: The triangles 2 and 3 are seen, in Fig. 14.11(*c*), to be separated by a region in which B is in equilibrium with liquid. This equilibrium shrinks to a line at P_1, in the invariant reaction

$$L(P_1) + B \rightarrow A_1 + C_1 \ ,$$

and it is replaced by the equilibrium between A_s and C_s which now separates two new three-phase triangles [4 and 5 in Fig. 14.11(*e*)] for B, C_s, and A_s and for liquid, A_s, and C_s. Point P_1 represents a type B diagonal invariant reaction, the triangles 2 and 3 being replaced by 4 and 5. The point P_1 is reached for x in the quadrangle $A_1BC_1P_1$. For x in A_1BC_1, the liquid is consumed in the reaction to leave A_1, B, and C_1 (triangle 4); for x in $A_1C_1P_1$, the solid B is consumed, and L travels on the curve $P_1 \rightarrow P_2$, representing the traveling of triangle 5 (L–A_s–C_s).

5. $P_1 \rightarrow P_2$: $L \rightarrow A_s + C_s$. The three-phase triangle (triangle 5) starts, as just explained, as

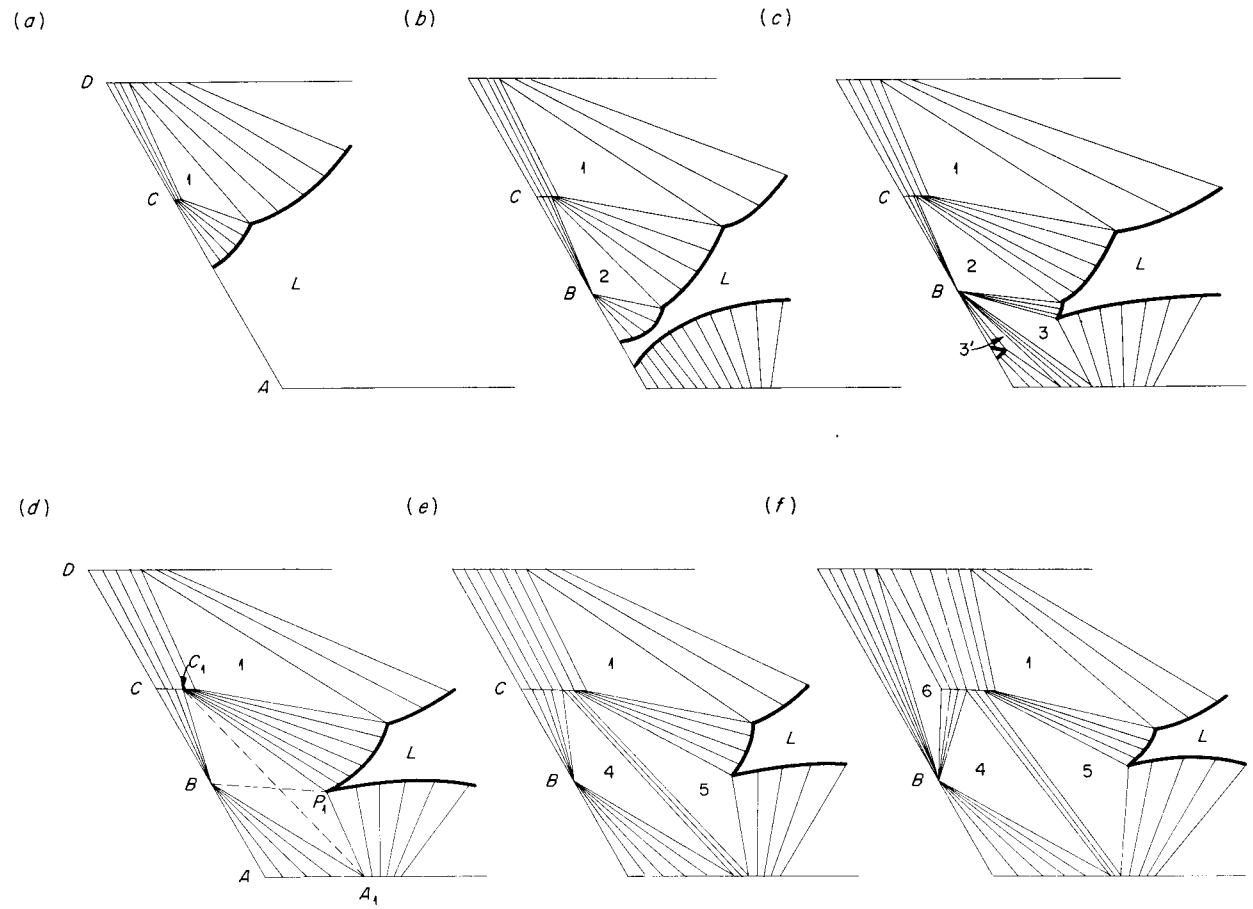

Fig. 14.11. (part 1)

$A_1C_1P_1$ and ends as $A_2C_2P_2$. This curve is reached from the C_s field for x in $P_1C_1C_2P_2$, and from the A_s field for x in $A_1P_1P_2A_2$. For x in $A_1C_1C_2A_2$, the liquid vanishes on the curve to leave A_s and C_s when the A_s–C_s leg of the triangle passes through x.

Between the temperatures of P_1 and P_2, however, at T_C (the decomposition temperature of C in the binary system) the equilibrium between B, C_s, and D_s appears as a three-phase triangle [triangle 6 in Fig. 14.11(f)]. It starts as the line BCD at T_C and ends as the triangle BC_zD_z at the invariant temperature Q_z.

The invariant Q_z involves four solid phases (three of them variable) in another quadrangular or diagonal invariant reaction of type B. As the Q_z temperature is approached, the region for the equilibrium between B and C_s [which is seen, in Fig. 14.11(f), to separate triangles 4 and 6] shrinks to a line, the two triangles come into contact, and we have the reaction

$$B + C_z \rightarrow A_z + D_z \ .$$

The equilibrium between B and C_s is replaced by one between A_s and D_s, now separating the two new triangles originating at Q_z: triangles 7 and 8 of Fig. 14.11(h), for B, A_z, and D_z and for A_s, D_s, and C_s.

In all the three-phase triangles of Fig. 14.11, the corners representing variable phases (C_s, A_s, D_s, L) move continually to the right with falling temperature. Triangle 7, however, will be assumed to remain constant with further decrease of temperature; at any rate it will not be involved in any more of the phase changes now under discussion.

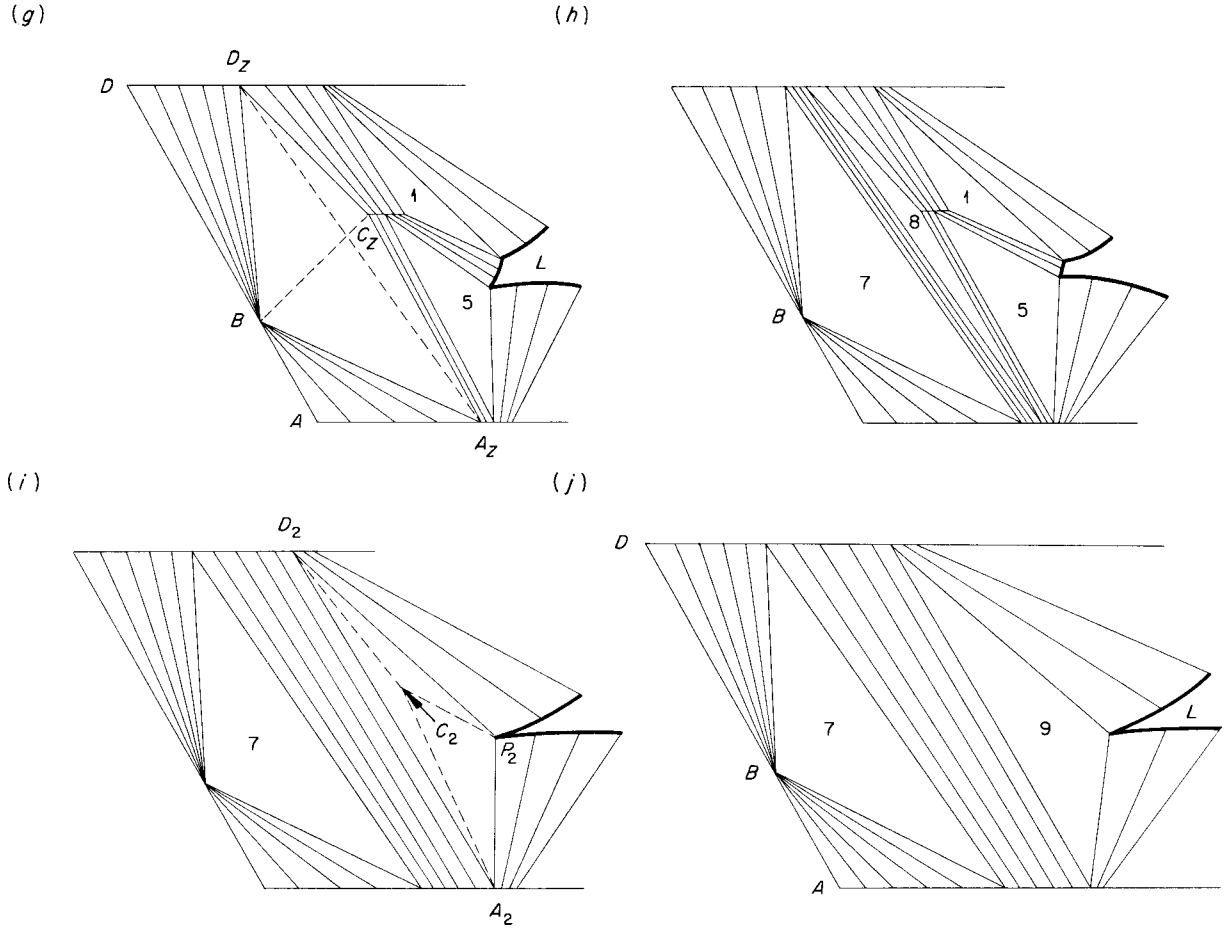

Fig. 14.11. (part 2)

The invariant reaction Q_z will occur for x in the quadrangle $BD_zC_zA_z$, leaving B, D_z, and A_z for x in triangle BD_zA_z, and otherwise A_s, D_s, and C_s, as triangle 8, which continues to move to the right.

Finally, the three remaining moving triangles, 1, 5, and 8, come together at P_2. The range of existence of the C_s solid phase, in other words, here shrinks to a point, C_2. The invariant P_2, then, is of type A, triangular, with C_2 as interior phase; it is terminal for the phase C_s. It is an example of the case c invariant discussed under Fig. 4.11. It may be said to be the decomposition point, on cooling, for the C_s solid solution in the ternary system. The reaction is

$$C_2 \rightarrow D_2 + A_2 + L(P_2) \ ,$$

whereupon the liquid then travels down the curve $P_2 \rightarrow P_3$, with its three-phase triangle 9 [Fig. 14.11(j)].

Some of the relations may be shown, in different fashion, in the T vs c vertical section of Fig. 14.12, between C in system Y–U and the 5:3 ratio in system Y–Z. This section cuts triangles 1, 6, 7, 8, and 9 of the foregoing discussion.

The sequence of phase changes upon cooling, for complete equilibrium, starting with a liquid of specified composition in Fig. 14.10 may be followed

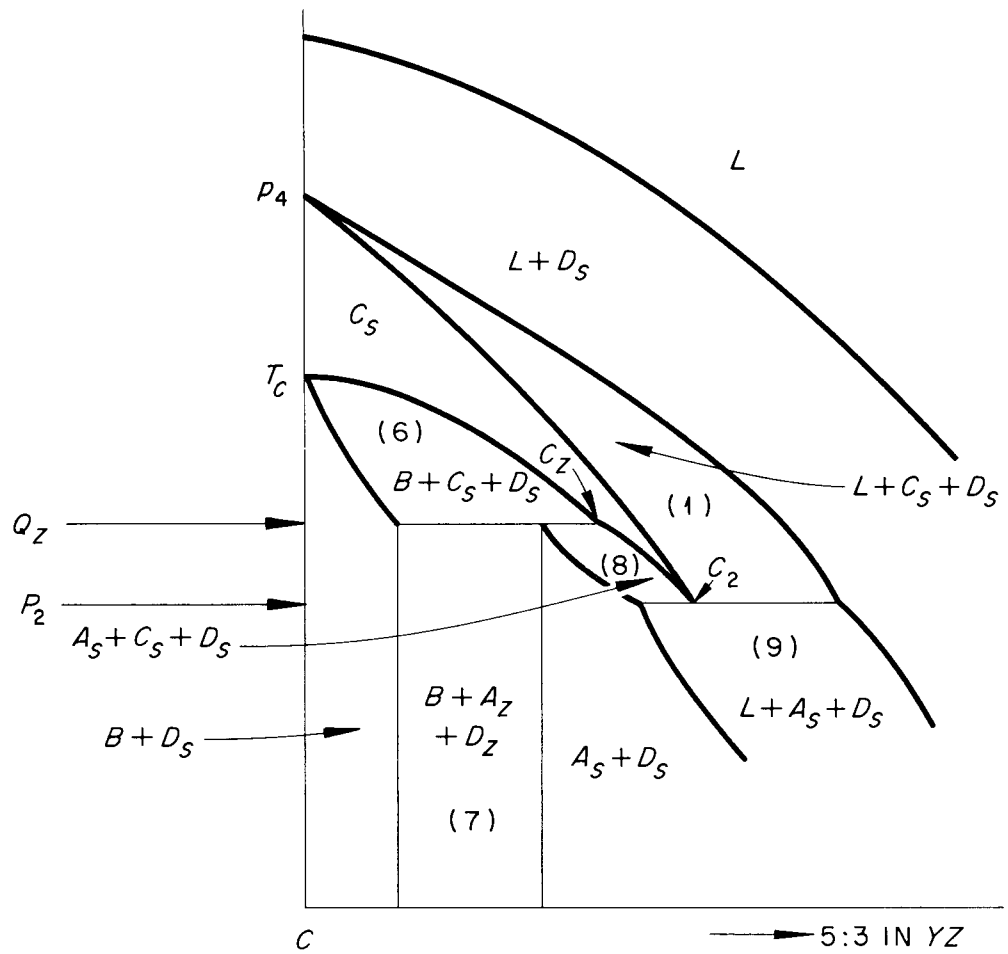

Fig. 14.12.

with the aid of Fig. 14.11. The fixed composition point x will fall successively in the various two-phase regions (tie line areas) and three-phase triangles (numbered and explained above) as these move through the point with falling temperature. A few particular compositions will be considered, for illustration.

Point a (Fig. 14.10): The first solid on cooling is A_s, starting between A_1 and A_2. The liquid reaches curve P_1P_2 and precipitates A_s and C_s (C_s starting between C_1 and C_2). The liquid vanishes before reaching P_2, leaving A_s and C_s on a line through point a. Point a, in other words, finds itself in the two-solid region between triangles 8 and 5 of Fig. 14.11(b). With further cooling, this region moves to the right, and point a enters triangle 8, with three solids, A_s, C_s, and D_s. The solid C_s thus decomposes into A_s and D_s on cooling, and the residual C_s approaches C_2 in composition. When the temperature reaches P_2, liquid reappears, in the invariant reaction:

$$C_2 - \text{calories} \rightarrow L(P_2) + A_2 + D_2 \quad .$$

[This reaction is case (c) of Sec 4, Fig. 4.11, but now with solids of variable composition.] When all C_2 is consumed, the liquid starts out on curve P_2P_3, vanishing to leave A_s and D_s on a line through point a.

Point b: The first solid is D_s, between D and D_2. The liquid reaches curve p_4P_2. Here

$$L + D_s \rightarrow C_s \ ,$$

C_s starting between C and C_2. The liquid is consumed on the curve, leaving C_s and D_s on a line through b. Point b now comes to be in the region for C_s and D_s, between triangles 6 and 1. When triangle 6 reaches b, B appears as a solid phase. Then at Q_z,

$$B + C_z \rightarrow A_z + D_z \ ,$$

B is consumed, and b ends as A_s and D_s, in the region between triangles 7 and 8 [Fig. 14.11(b)].

Point c: As in the case of point b, the liquid reaches curve p_4P_2 and vanishes to leave C_s and D_s. But below T_C, C begins to decompose; point c comes to be in triangle 6, and finally into the area for B in equilibrium with D_s as triangle 6 moves on.

Point d: The first solid is C_s, between C and C_1. The liquid reaches curve p_3P_1, where

$$L + C_s \rightarrow B \ .$$

At P_1, A_1 appears, and

$$L + B \rightarrow A_1 + C_1 \ .$$

The liquid is consumed, and point d finds itself in triangle 4. Next, A_s vanishes, leaving B and C_s. Then D_s appears, and point d enters triangle 6. At Q_z,

$$B + C_z \rightarrow A_z + D_z \ ,$$

leaving B, A_z, and D_z, d being in triangle 7.

Point e: The first solid is B, and L reaches curve mP_1, where

$$L \rightarrow B + A_s \ ,$$

the solid solution being between A_m and A_1. At P_1,

$$L + B \rightarrow A_1 + C_1 \ ,$$

the liquid is consumed, and point e is now in triangle 4. As this triangle moves on, however, the C_s phase vanishes, to leave B and A_s, on a line through point e.

Point f: The first solid is C_s, L reaches curve p_3P_1, C_s is consumed on the curve, and L traverses the B field to reach curve mP_1. At P_1,

$$L + B \rightarrow A_1 + C_1 \ ,$$

B is consumed, and the liquid travels on curve P_1P_2, precipitating A_s and C_s (triangle 5). The liquid vanishes, however, to leave A_s and C_s, between triangles 4 and 5, and point f next comes to be in triangle 4, as B, A_s, and C_s. Then at Q_z,

$$B + C_z \rightarrow A_z + D_z \ ,$$

leaving the solids of triangle 7.

Scheme II. – The point P_2 is here assumed not to be the lowest temperature of existence of the C_s solid solution (with composition C_2). The C_s phase is assumed to vanish, on cooling, at some intermediate composition (C_y, between C and C_2), at a still lower temperature, that of a four-solid invariant to be called Q_y. The relations would be those shown schematically in Fig. 14.13. The highest-temperature invariant plane is again the P_1 quadrangle, assumed to be identical with that in Scheme I (Fig. 14.10). Next is the P_2 plane, now a quadrangle, an example of the case (d) invariant discussed under Fig. 4.10. Below these is the triangular plane of the Q_y invariant reaction, terminal for C_y, the interior phase. We now have the temperature order:

$$P_1 > T_C > P_2 > Q_y \ .$$

The first six isotherms of Fig. 14.11 apply to Scheme II as they are. The subsequent isotherms are given in Fig. 14.14, and to preserve continuity these will be lettered as follows: (g) at P_2, (h) between P_2 and Q_y, (i) at Q_y, (j) below Q_y.

Except for the positions of the compositions A_2, C_2, and D_2 involved at P_2, the crystallization processes on the liquidus surfaces and on the curves of twofold saturation are the same in both schemes. The schemes differ only in the reactions of the solid phases left after complete solidification.

Triangles 1–6 originate as in Scheme I, and they again move to the right with falling temperature. The relations in the isotherm (f) (which is between T_C and P_2 in Scheme II and between T_C and Q_z in Scheme I) are topologically the same for both schemes. This is now followed by isotherm (g), at P_2. The triangles 1 and 5, separated in (f) by the equilibrium between C_s and liquid, here come into contact, in the reaction

$$L(P_2) + C_2 \rightarrow A_2 + D_2 \ ,$$

giving rise to the equilibrium between A_s and D_s, separating the two new triangles 8′ and 9′. These involve the same phases as the triangles of the same number in Scheme I, but the compositions are different. Also, while triangle 9′, like triangle 9

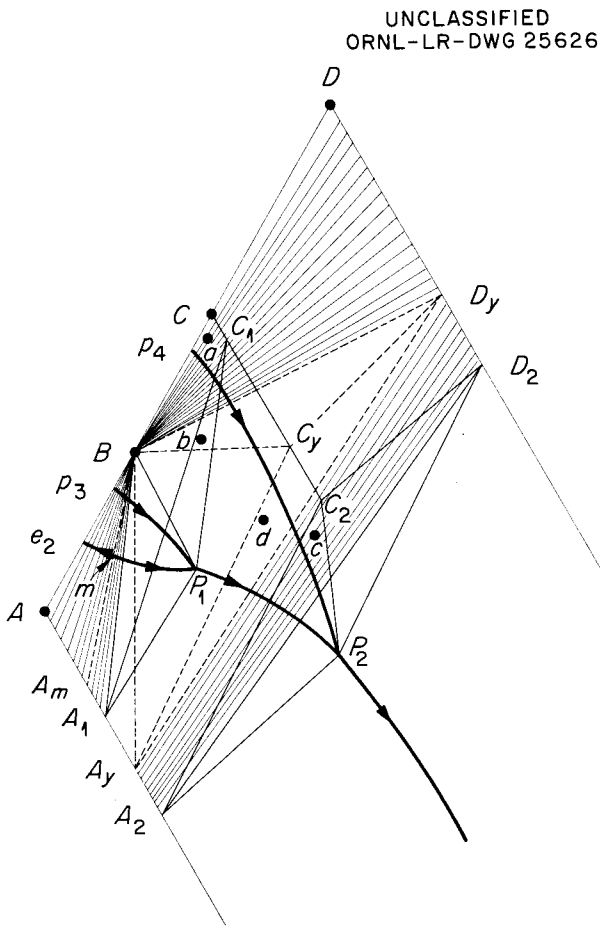

Fig. 14.13.

in Scheme I, now continues to move to the right as the liquid travels on the curve P_2P_3 precipitating A_s and D_s, the triangle 8′ begins to move to the left with falling temperature. Eventually it makes contact with triangles 6 and 4, in the Q_y invariant reaction, in the arrangement shown in Fig. 14.14(*i*). The ternary C solid solution, the interior phase of the triangular, type A invariant reaction, simply decomposes into the solids B, A_y, and D_y, leaving triangle 7′, which corresponds to triangle 7 of Scheme I.

The vertical T vs c section through C and the 5:3 ratio in the system Y–Z is shown in Fig. 14.15, which is to be compared with Fig. 14.13. In both cases there are two solid-state decomposition reactions for C_s:

$$C_s \rightarrow B + D_s$$

and

$$C_s \rightarrow A_s + D_s \quad .$$

In Scheme I, the decomposition into B and D_s extends from the binary temperature T_C to the invariant Q_z, and the decomposition into A_s and D_s falls in temperature from Q_z to the invariant P_2. In Scheme II, the decomposition into B and D_s falls in temperature from T_C to Q_y, and the decomposition into A_s and D_s rises in temperature from Q_y to P_2.

Point a (Fig. 14.13): The first solid is D_s. The liquid reaches curve p_4P_2, where

$$L + D_s \rightarrow C_s$$

(triangle 1), and the liquid vanishes on the curve to leave C_s and D_s. Below T_C, the point a is reached by triangle 6 (for B, C_s, and D_s), and finally remains as B and D_s when it is left behind by triangle 6.

Point b: The first solid is C_s. The liquid reaches curve p_3P_1, where

$$L + C_s \rightarrow B$$

(triangle 2). At P_1,

$$L + B \rightarrow A_1 + C_1 \quad .$$

The compound B is consumed, and the liquid moves on curve P_1P_2, precipitating A_s and C_s (triangle 5). The liquid vanishes on the curve to leave A_s and C_s, and point b is next reached by triangle 4 (for B, C_s, and D_s). At Q_y, the C_s phase decomposes to leave B, A_y, and D_y (triangle 7′).

Point c: The first solid is D_s. The liquid reaches curve p_4P_2, where

$$L + D_s \rightarrow C_s$$

(triangle 1). At P_2,

$$L + C_2 \rightarrow A_2 + D_2 \quad .$$

The liquid is consumed, and point c is left in triangle 8′ (for A_s, C_s, and D_s). But this triangle moves to the left with falling temperature, and before the temperature of Q_y is reached, C_s will have vanished to leave A_s and D_s.

Point d: The first solid is C_s. The liquid reaches curve P_1P_2, where $L \rightarrow A_s + C_s$ (triangle 5). The liquid vanishes on the curve to leave A_s and

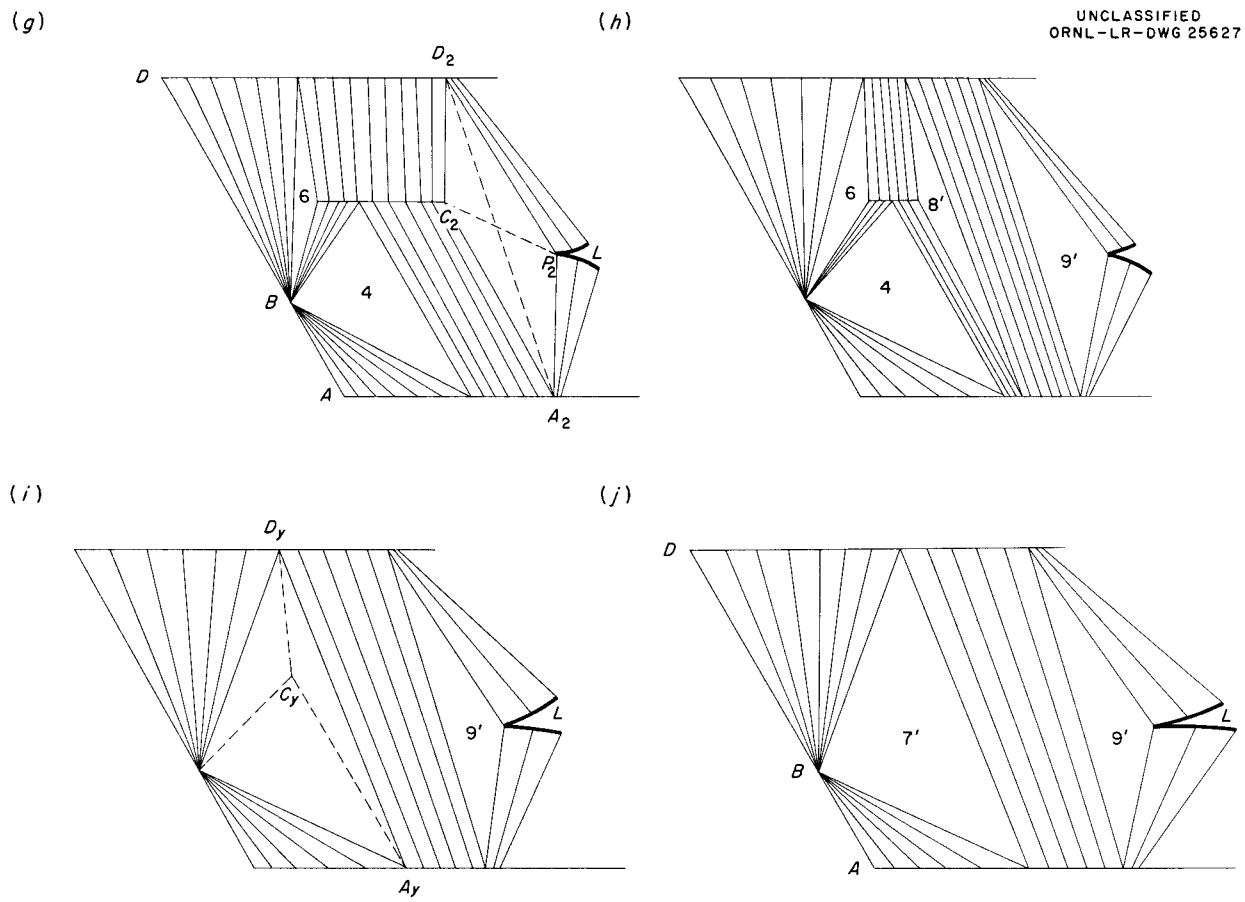

Fig. 14.14.

C_s. But point d is next reached by triangle 8′, from the right, to give A_s, C_s, and D_s. At Q_y the C_s phase decomposes to leave the three solids of triangle 7′ (B, A_y, and D_y).

The Region Involving G, H, I, and K

The lower part of the subsystem A–D–K–G is shown in Fig. 14.16. Liquids on curve P_2P_3 precipitate the solid solutions A_s and D_s, solidifying completely, while on the curve, for x above the line A_3D_3 (joining the solid solution compositions for liquid at P_3). (We continue here to call the A–G solid solution A_s and the D–K solid solution D_s, even down to the limits G and K.) As the composition of G is approached, the A_s solid solution is shown as occupying an area in composition, since G also forms solid solution in the binary system Y–Z, varying from G to the composition G_7 at the temperature of p_7. The same situation holds at K, which forms solid solution in the binary system Y–Z, extending from K to the limit K_9 at the temperature of e_9.

For the curve p_7P_3, which is reached for x in the region $p_7G_7A_3P_3$, the reaction is

$$L + A_s \rightarrow H_\alpha \ .$$

The solid solution starts at G_7 for L at p_7 and ends at A_3 for L at P_3. The three-phase triangle starts as the line G_7Hp_7 and ends as A_3HP_3. Hence liquid on the curve is completely solidified, leaving H_α and A_s (between G_7 and A_3), for x in HG_7A_3. For x in the area of the ternary solid solution, ss, solidification is complete with L still on the A_s surface, before any curve is reached. The curve p_7P_3, moreover, is crossed for x in HP_3p_7, when, after the A_s phase has been consumed, the liquid leaves the curve to travel across the H_α field, but now precipitating not pure H_α but the H_α solid solution ranging from H to H_4.

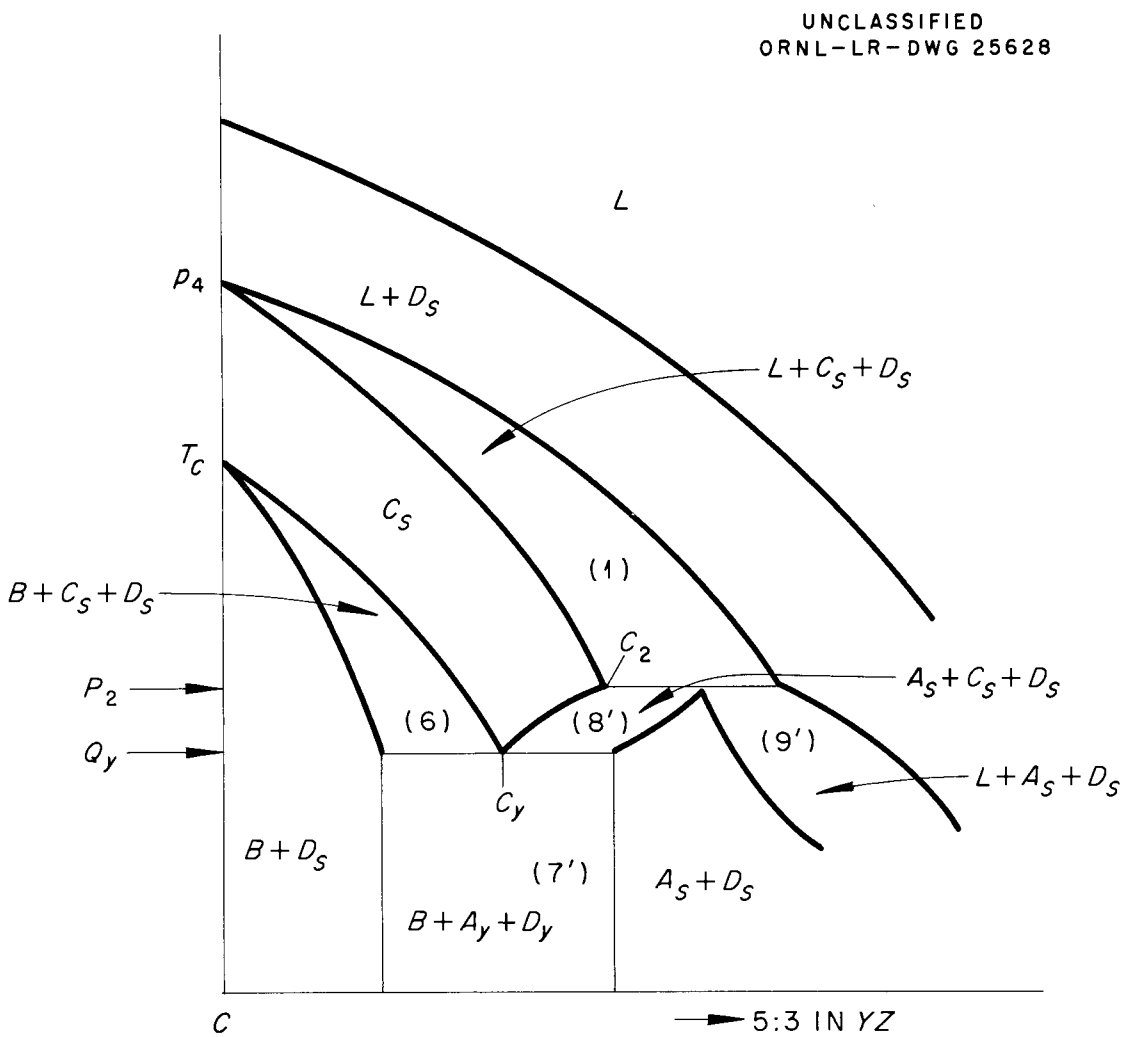

Fig. 14.15.

The point P_3 is reached for x in the region $HA_3D_3P_3$, by way of either curve P_2P_3 or curve p_7P_3. Liquids with x in the triangle A_3D_3H then solidify completely in the reaction

$$L(P_3) + A_3 \rightarrow H_\alpha + D_3 \quad ,$$

while the others travel down the curve $P_3 \rightarrow P_4$, precipitating two solid solutions, one of H_α (H to H_4) and one of D_s (D_3 to D_4). Complete solidification is therefore effected on this curve for x in $HD_3D_4H_4$. The curve is reached from the H_α field for x in $HP_3P_4H_4$ and from the D_s field for x in $P_3D_3D_4P_4$.

On the transition curve p_8P_4,

$$L + H_\alpha \rightarrow I_\alpha \quad .$$

The H_α solid solution in equilibrium along this curve is, strictly, variable in composition, starting just to the right of H_4 at p_8 and ending at H_4. (Since P_4 is below p_8 in temperature, the composition of H_4 must be just to the left of that for the binary peritectic p_8 of Fig. 14.1.) Since the variation is probably very slight, we have here assumed this solid to be constant at H_4 for the whole curve. This curve is reached for x in $H_4P_4p_8$, and it is crossed for x in IP_4p_8. The point P_4 is thus reached, either from curve P_3P_4 or from curve p_8P_4, for x in the quadrangle $H_4D_4P_4I$. The reaction is

$$L(P_4) + H_4 \rightarrow I_\alpha + D_4 \quad ,$$

so that liquidus for x in the triangle H_4D_4I here

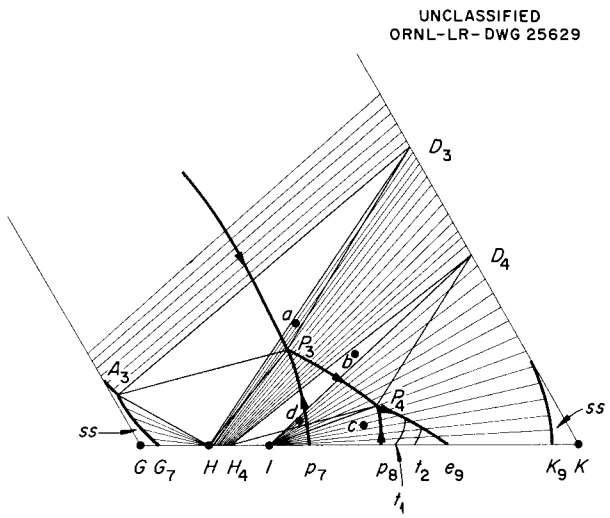

Fig. 14.16.

solidify completely. The rest move on down the curve P_4e_9, precipitating I and D_s (between D_4 and K_9); the form of the compound I deposited will be I_α down to temperature t_1, then I_β to temperature t_2, and I_γ to the temperature e_9. All liquids reaching curve P_4e_9 solidify completely before reaching e_9. The curve is reached from the I field for x in IP_4e_9 and from the D_s field for x in $P_4D_4K_9e_9$. Liquids with x in the ss area near K solidify completely while L is still on the D_s surface.

For composition a in Fig. 14.16 the first solid to form on cooling is D_s. The liquid reaches curve P_2P_3, where

$$L \rightarrow A_s + D_s \quad .$$

At P_3,

$$L + A_3 \rightarrow H + D_3 \quad ;$$

A_3 is consumed, and L starts out on curve P_3P_4; on this curve the liquid vanishes, to leave H_α and D_s solid solutions on a line through point a.

Point b: The first solid is D_s. The liquid reaches curve P_3P_4, where it precipitates a solid solution between H and H_4 and a solid solution between D_3 and D_4. At P_4,

$$L + H_4 \rightarrow I_\alpha + D_4 \quad ,$$

leaving the three solids H_4, I_α, and D_4.

Point c: The first solid is H_4 (strictly slightly to the left of H_4). The liquid reaches curve p_8P_4, where

$$L + H_4 \rightarrow I_\alpha \quad .$$

The solid H_4 is consumed, and L crosses the I field to curve P_4e_9. Here

$$L \rightarrow I + D_s \quad ,$$

and the liquid vanishes to leave I and D_s on a line through point c; the polymorphic form of I depends simply on the temperature.

Point d: The first solid is A_s, between G_7 and A_3. The liquid reaches curve p_7P_3, where

$$L + A_s \rightarrow H_\alpha \quad .$$

The solid A_s is consumed; L leaves the curve, crosses the H field, and reaches curve P_3P_4. Here

$$L \rightarrow H_\alpha + D_s \quad .$$

At P_4,

$$L + H_4 \rightarrow I_\alpha + D_4 \quad ;$$

H_4 is consumed; the liquid starts out on curve P_4e_9, and vanishes to leave I and D_s on a line through point d.

Fractionation Processes in the Subsystem A–D–K–G

The phase changes so far discussed have been those for crystallization with complete equilibrium. We shall now consider crystallization with perfect fractionation, as explained in Sec 6, simply for the two principal solid solution fields of Fig. 14.9.

In a fractionation process, the liquid on a surface follows a single fractionation path (as sketched in Fig. 14.9). These paths are here curves in every case except for the B and I fields, where they are straight lines radiating, by extension, from points B and I, respectively. When the liquid, following such a fractionation path, whether curved or straight, reaches a boundary curve of even reaction (one on which the liquid precipitates two solids on cooling), the liquid travels along this curve. But if it reaches a curve of odd reaction (transition curve), it immediately crosses the curve and begins to travel along a fractionation path – curved or straight – on the next field. (See Sec 4-D for the behavior at invariant points.)

In the fractionation process, the outermost layer of solid solution being deposited by liquid on the

D_s field continually increases in K content. It continues to change in the same direction, moreover, whichever of the four boundary curves is reached, while L travels on the boundary curve. But the boundary curve p_4P_2 is a transition curve; L does not travel on it but immediately crosses it. Hence the ultimate mixture of solids (non-equilibrium mixture) produced by liquid in a fractionation process varies according to the various regions into which the D_s surface may be divided.

There is first a very narrow region, close to the p_4D side, from which L will cross the curve p_4P_2, traverse the C_s field, cross the curve p_3P_1, traverse the B field, and reach curve $m \rightarrow e_2$. The final mixture of solids obtained therefore contains D_s, C_s, B, and A_s (although C_s may have decomposed on cooling).

Next to this region there is one from which L will traverse the same curves and fields but end on the boundary $m \rightarrow P_1$ of the B field. The liquid then follows boundary curves all the way to e_9, to leave a mixture of all six solids of the subsystem: D_s, C_s, B, A_s, H_α solid solution, and I_α. The next region will send L to curve P_1P_2, missing the B field, and now solid B will be missing in the final five-solid mixture, except as formed by decomposition of C_s For these two regions the composition of the D_s solid solution finally obtained will have a discontinuity (a gap), since precipitation of D_s is interrupted between the point when L reaches and crosses the curve p_4P_2 and the point when it reaches P_2 along curve P_1P_2 (as explained also in Sec 7.3).

The next region, between the fractionation paths DP_2 and DP_3, will miss the C_s field entirely and end as four solids: D_s, A_s, H, and I. The region between paths DP_3 and DP_4 will give only D_s, H, and I, and that between the path DP_4 and the corner K only D_s and I.

On the A_s field the outermost layer of solid solution continually increases in A content while L is still on the surface. For the region between A and the fractionation path Gm, the solid deposited continues to increase in A content while L moves on the curve $m \rightarrow e_2$, ending as a mixture of B and A_s. For the region between the paths Gm and GP_3 the depositing solid reverses its direction (of composition change) and moves toward G as L travels on the boundary curves $m \rightarrow P_1 \rightarrow P_2 \rightarrow P_3$. The liquid then follows the curves $P_3 \rightarrow P_4 \rightarrow e_9$, and finally leaves a mixture of all six solids of the subsystem (counting C_s, which, however, may have decomposed). For the region between p_7 and the path GP_3, L crosses the curve p_7P_3 but ultimately reaches either P_3P_4 or P_4e_9, to approach, in either case, e_9 as the limit of the process; the final mixture consists of A_s, H_α solid solution, I_α, and D_s.

Subsolidus Reactions Involving Compounds A, H, and J

The two- and three-solid regions left on complete solidification in the two subsystems so far considered, below the temperatures of all the phase reactions discussed, are shown in Fig. 14.17. There are also two single-phase regions ss near points G and K.

At T_A (Fig. 9.1), the compound A of the system Y–U (after changing from A_α to A_β at T') decomposes on cooling into Y and B. Because A forms ternary solid solution (A_s, with G), the decomposition temperature is lowered in the ternary system. This decomposition involves changes in the upper part of Fig. 14.17, and the pertinent isotherms are shown in Fig. 14.18: (a) just below T_A; (b) at a four-solid invariant of type B, where

$$B + S_1 \rightarrow Y + S_2 .$$

on cooling; and (c) below this invariant.

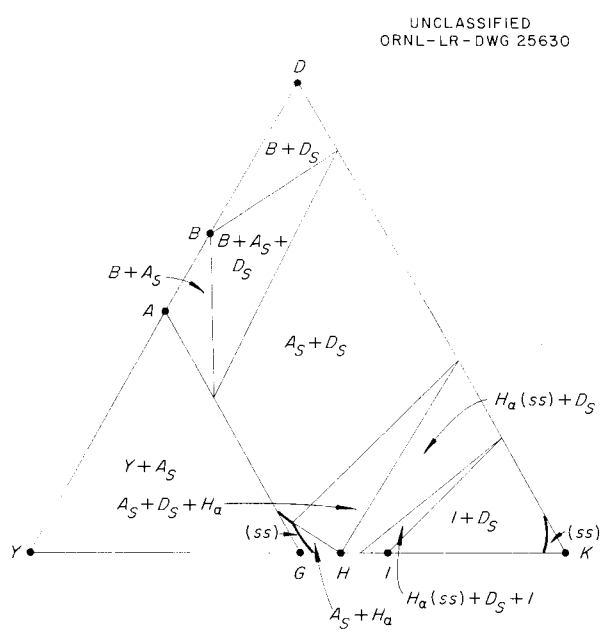

Fig. 14.17.

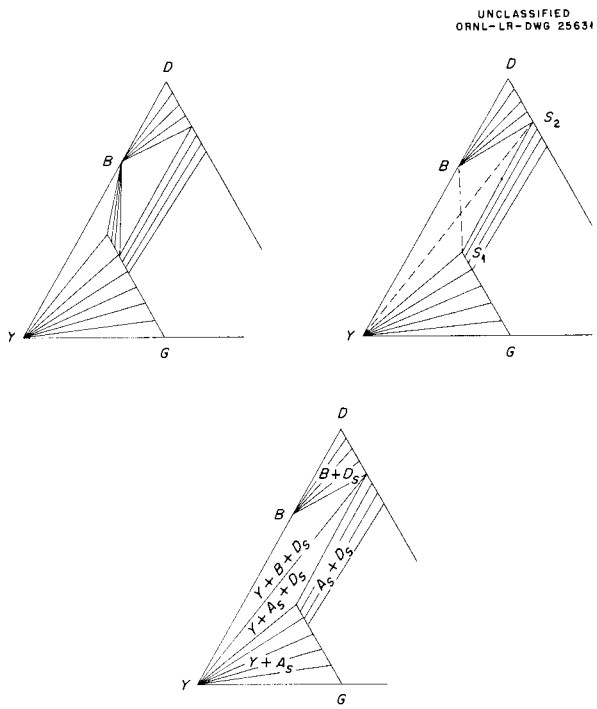

Fig. 14.18.

At T' (Fig. 14.1), H_α undergoes transition to H_β, which is a pure solid instead of a binary solid solution, and the binary transition temperature is lowered to T''. Since the solid solution is not ternary, these temperatures are not changed in the ternary system. Figure 14.19 shows the accompanying changes in the solid phase combinations: (*a*) above T', (*b*) between T' and T'', (*c*) below T''.

At T_J (Fig. 14.1), the compound J of system Y–Z appears on cooling, forming from I and K_j (the binary solid solution composition for K at the temperature of T_J). Because K forms ternary solid solution (D_s, with D), the formation temperature is lowered in the ternary system. The changes affecting Fig. 14.17 are shown in the isotherms of Fig. 14.20: (*a*) just at T_J, where the point J appears as pure J in equilibrium with I and K_j; and (*b*) below T_J. With decreasing temperature the three-phase equilibrium of $I + J + D_s$ moves into the diagram as the triangle IJK''. The two-phase equilibrium between J and K_j (Fig. 14.1) becomes the two-phase tie-line band $J_s + D_s$ of Fig. 14.20(*b*), with tie lines running from the binary solid J–J' to the ternary solid K''–K'. The solids J' and K' vary with temperature according to the miscibility gap in the J–K solid solutions shown in Fig. 14.1.

14.4. SUBSYSTEM D–U–Z–K

Equilibrium Crystallization Along Curves

The relations for complete equilibrium solidification in the subsystem D–U–Z–K are shown, schematically, in Fig. 14.21, and Fig. 14.22 shows approximate temperature contours for this region.

There are three primary phase fields: one for the D–K solid solution D_s, one for the U–Z solid solution U_s, and one for the incongruently melting, pure compound M. The reaction on the curve e_5P_5 is $L \rightarrow D_s + U_s$, the three-phase triangle starting as the line De_5U and ending as the triangle $D_5P_5U_5$. This curve is reached from the D_s field for total composition x in the region $De_5P_5D_5$, and from the U_s field for x in $e_5UU_5P_5$. Solidification is complete on the curve for x in DUU_5D_5.

The third part of Fig. 14.6 shows the vertical T vs c section through this part of the system. It is similar to the middle part of Fig. 14.6 except that the solid solutions are strictly on vertical lines, D_s being on a vertical line through DK and U_s on a vertical line through UZ.

On the curve $p_{11}P_5$, from p_{11} to t, the reaction is one of transition,

$$L + U_s \rightarrow M \ ,$$

with U_s ranging from pure Z at p_{11} to U_t at t. For the section of the curve from t to P_5, the reaction is even:

$$L \rightarrow M + U_s$$

(ranging from U_t to U_5). The three-phase triangle L–M–U_s starts as the line $p_{11}MZ$ and ends as P_5MU_5. The sign of the reaction changes at point t, where the L–M leg of the triangle is tangent to the curve.

The odd-reaction section of the curve, $p_{11}t$, is reached only from the U_s field, for x in the region $p_{11}tU_tZ$, by liquids precipitating U_s as primary crystallization product. Then if x is in the region $p_{11}tM$, U_s is consumed while L is traveling on the curve, between p_{11} and t, and the liquid leaves the curve to traverse the M field, on a straight line from M. Compositions for x in $p_{11}yM$ (y being on the line P_5M) then reach the curve P_5e_{10}, while those for x in ytM reach the curve tP_5, where U_s,

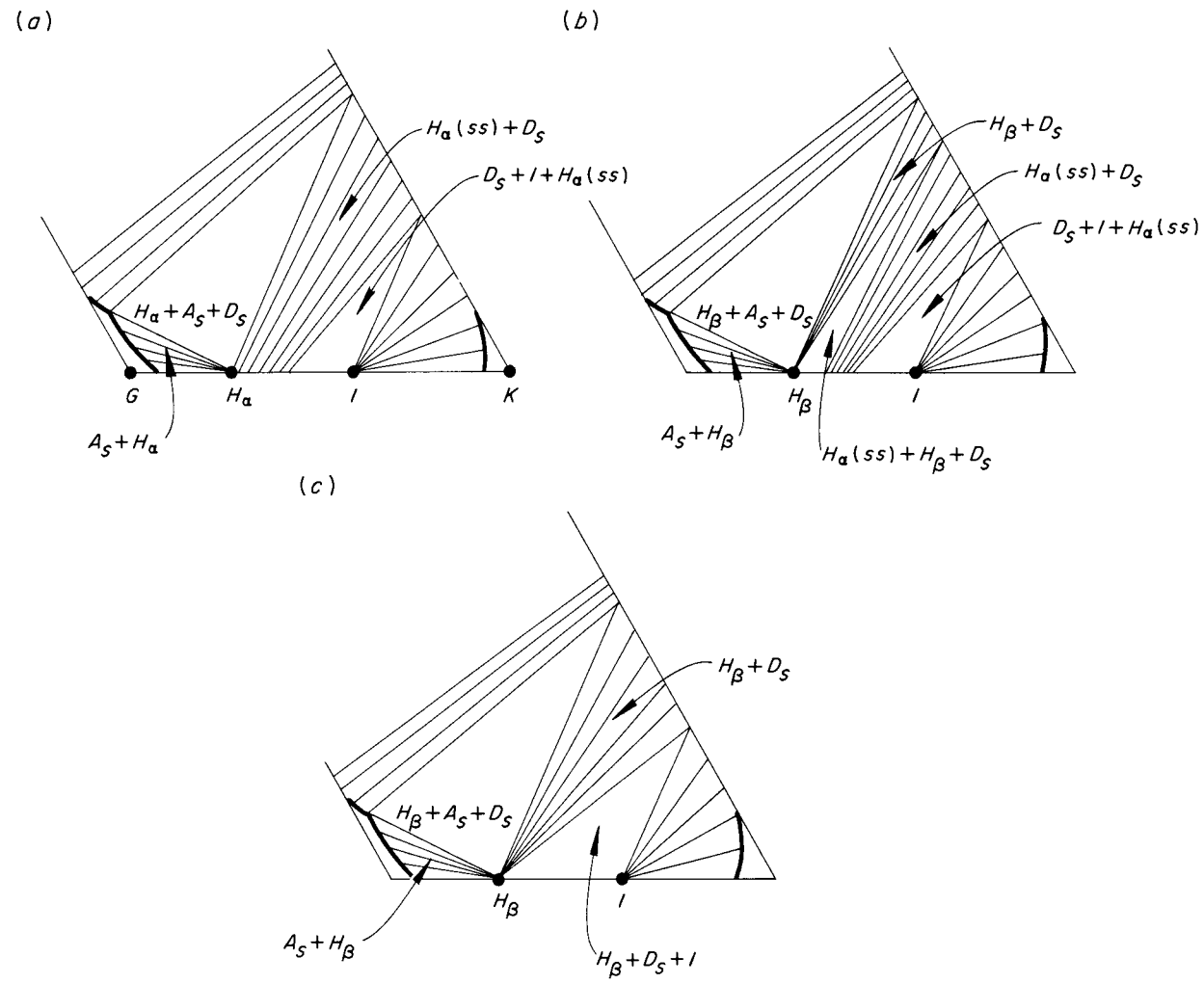

Fig. 14.19.

now richer in U, appears again as a secondary crystallization product mixed with M.

The even portion of the curve, tP_5, is reached from either side: from the U_s field directly for x in the region $tP_5U_5U_t$, and from the M field for x in MP_5t, either directly or after the crossing of the yt curve.

Liquids for x in the region MU_5Z solidify completely while traveling on this curve, somewhere between p_{11} and P_5, when x comes to be swept by the M–U_s leg of the three-phase triangle.

The point P_5 is therefore reached only for x in the quadrangle $D_5U_5MP_5$, and, with the reaction

$$L + U_5 \rightarrow D_5 + M \ ,$$

it is the incongruent crystallization end point for x in the triangle D_5U_5M, to leave the three solids D_5, U_5, and M. For x in P_5D_5M, U_5 is consumed, and L travels down the curve P_5e_{10} to solidify completely, before reaching e_{10}, into M and D_s solid solution between D_5 and K. The curve P_5e_{10}, along which

$$L \rightarrow M + D_s \ ,$$

is reached from the D_s field directly for x in $KD_5P_5e_{10}$ and from the M field for x in $e_{10}P_5M$, either directly or after the crossing of the $p_{11}y$ curve.

The compositions of points D_5, U_5, and U_t are hypothetical.

UNCLASSIFIED
ORNL-LR-DWG 25633

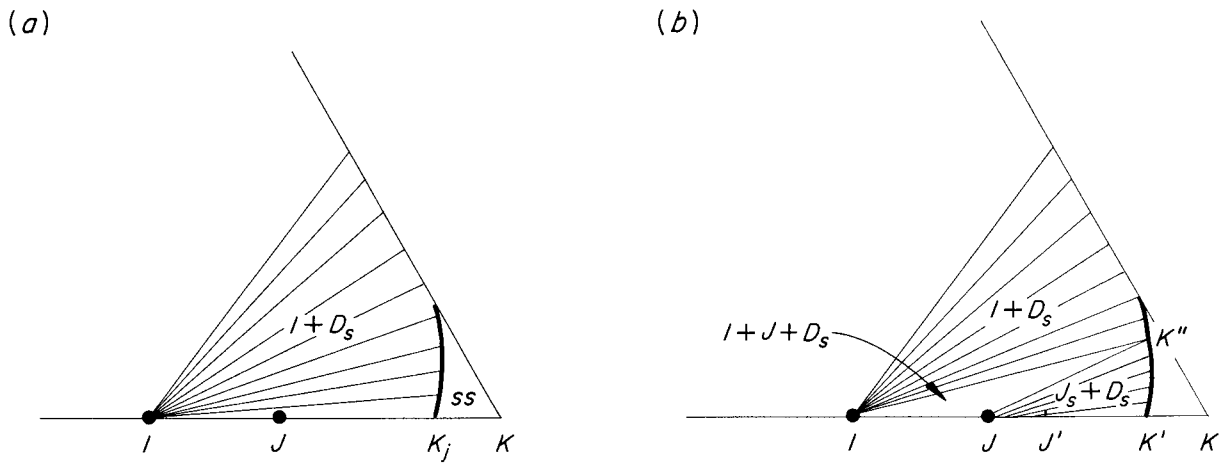

Fig. 14.20.

UNCLASSIFIED
ORNL-LR-DWG 25634

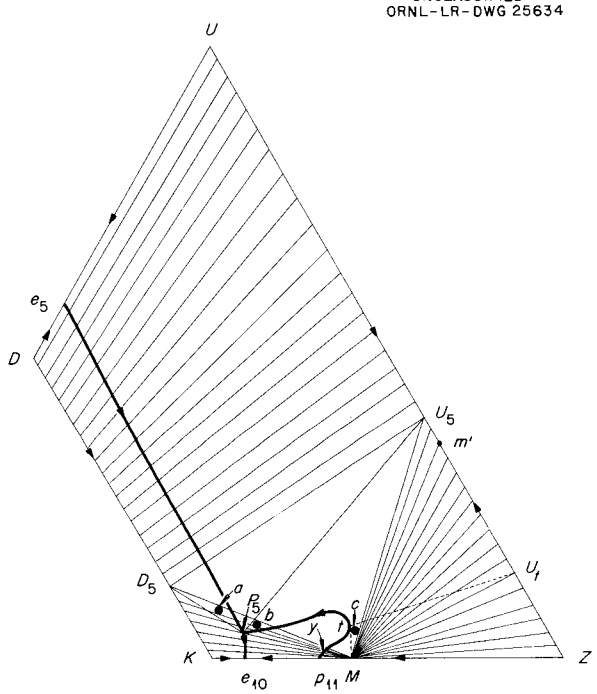

Fig. 14.21.

UNCLASSIFIED
ORNL-LR-DWG 25635

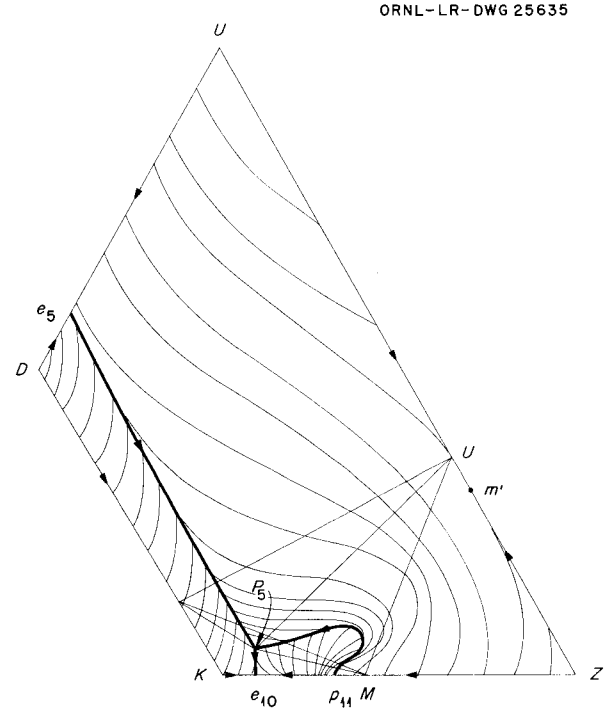

Fig. 14.22.

The minimum m' of the U–Z binary system is not involved in any of these considerations, for the points U_5 and U_t involve temperatures and compositions not on the solidus curve of Fig. 14.2.

Point a: For liquid with original composition at point a in Fig. 14.21, the first solid on cooling is D_s, with composition between D and D_5. The liquid reaches curve e_5P_5, where

$$L \rightarrow D_s + U_s$$

(between U and U_5). At P_5,

$$L + U_5 \rightarrow D_5 + M \ .$$

The solid U_5 is consumed; the liquid moves onto curve P_5e_{10} and vanishes to leave M and D_s on a line through a.

Point b: The first solid is U_s (below U_5). The liquid reaches curve $p_{11}P_5$, where

$$L \rightarrow M + U_s \ .$$

The solid U_s now moves up to reach U_5 when L reaches P_5. Thereafter, the solidification occurs as for point a.

Point c: The first solid is U_s (below U_t). The liquid reaches curve $p_{11}P_5$. As L follows this curve, the quantity of U_s first diminishes – until L reaches t – and then increases as L moves from t to P_5. But all the while the composition of U_s is moving toward U_5. At P_5, the liquid is consumed to leave D_5, U_5, and M.

Point d: (This point is not shown on the diagram; it is in the area between M and curve $p_{11}P_5$, between the lines MP_5 and MD_5.) The first solid is U_s, near Z. The liquid reaches curve $p_{11}P_5$, and U_s is now entirely consumed in the reaction

$$L + U_s \rightarrow M \ ,$$

while L is moving on the curve, before it reaches point t. The liquid then leaves the curve, travels across the M field precipitating more M, and reaches the same curve again near P_5. Here

$$L \rightarrow M + U_s$$

(now near U_5 in composition). At P_5, U_5 is consumed; the liquid moves onto curve P_5e_{10} and vanishes to leave M and D_s on a line through point d.

Fractionation Processes in the Subsystem *D–U–Z–K*

Figure 14.23 shows schematic fractionation paths in the subsystem D–U–Z–K. These are hypothetical, for we have no information on the

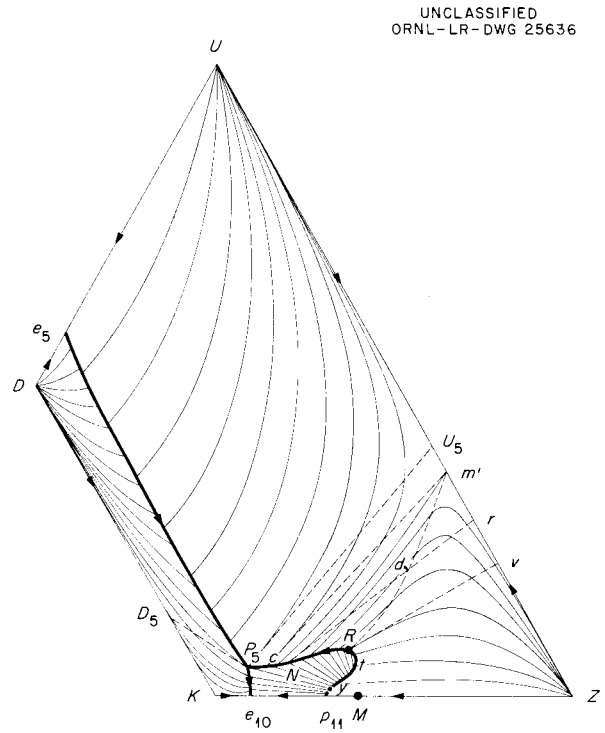

Fig. 14.23.

liquid-solid tie-line directions for points on the surfaces (and we can make only uncertain inferences for the directions of tie lines at the boundary curves). However, we shall assume the relations shown schematically in Fig. 14.23 and discuss them along the lines followed under Figs. 6.1 to 6.4.

The paths on the M field are simply straight lines originating by extension from point M. Those on the D_s surface originate from the maximum D and diverge from the straight line DK, always convex with respect to K. This means that when a liquid is traveling over this surface, whether in complete equilibrium with the whole solid phase or in a fractionation process, the solid solution is always changing in composition toward K. Moreover, the same direction of change in the solid continues here when either of the boundary curves is reached: e_5P_5 or P_5e_{10}.

The U_s surface, with two maxima (U and Z), has two families of fractionation paths, separated by a limiting fractionation path originating at the binary minimum m'. This path, $m'N$, must reach one of the two boundary curves, e_5P_5 or $p_{11}P_5$. We assume that it reaches the curve $p_{11}P_5$ at the point N between P_5 and t, and that it is convex with respect to the corner Z. Accordingly, the

paths on the U side of $m'N$ are convex with respect to Z through their entire length, but some of those on the Z side, while starting out as convex with respect to U, pass through a point of inflection and become convex with respect to Z before reaching the boundary curve. The dashed curve $m'R$ is the locus of these inflection points, and R is assumed to be between N and t. The paths between ZR and Zp_{11} have no inflection point and are simply convex with respect to U.

For further orientation we note that the line P_5U_5 of Fig. 14.21 is tangent at P_5 to the fractionation path UP_5, Nr is tangent at N to the path $m'N$, and Rv is tangent at R to the path ZR. Point y is on the line P_5M.

The sequence of changes in the fractionation process varies according to the regions into which the U_5 surface is divided by the lines and curves just defined. The outermost layer of U_s solid solution being deposited will be referred to as "solid."

1. Region e_5UP_5 (meaning between e_5 and the fractionation path UP_5): While L is still on the U_s surface, the "solid" increases in Z content to a limit given by the tangent to the particular fractionation path involved at the curve e_5P_5. At the same point of the curve, the tangent to the D_s fractionation path gives the initial composition of the D_s "solid" precipitated, together with U_s, while L follows the curve $e_5 \rightarrow P_5$. Then, as L travels on the curve, the "solids" reach D_5 and U_5 when L reaches P_5. Then L follows curve P_5e_{10} towards e_{10} as limit, depositing M and D_s ranging from D_5 to an outermost layer approaching pure K.

2. Region between paths UP_5 and $m'N$: The "solid" increases in Z while L is on the surface, reaching a point between U_5 and r when L reaches the curve between P_5 and N. Then, as the liquid moves toward P_5, precipitating M and U_s, the outermost "solid" reverses its direction, reaching U_5 when L reaches P_5. Thereafter the solidification occurs as for region 1. (Note: Once L reaches P_5 in fractionation, it continues onto curve P_5e_{10}.)

3. Region $p_{11}Zy$: The "solid" increases in U content while L is on the surface, to a limit, fixed by the tangent to the fractionation path, when L reaches the curve between p_{11} and y. The liquid crosses the curve at once in a straight line from M, precipitating M, to reach curve P_5e_{10}. Thereafter the solidification occurs as for region 1.

4. Region between paths Zy and Zt: The "solid" increases in U for L on the surface, to a limit, fixed by the fractionation path, when L reaches the curve between y and t. The liquid crosses the curve at once on a straight line from M, precipitating M, to reach the curve again along tP_5. This curve is followed to P_5, with the liquid precipitating M and U_s again, the "solid" starting at a higher U content than when its precipitation ceased on the curve yt. Its composition reaches U_5 when L reaches P_5; thereafter the solidification occurs as for region 1.

5. Region between paths Zt and ZR: The "solid" increases in U both before and after L reaches the curve. The limit is U_5 at P_5. Thereafter the solidification occurs as for region 1.

6. Region between paths ZR and $m'N$: The "solid" increases in U until the inflection point of the fractionation path is reached (intersection of path with curve $m'R$), and the "solid" at that point is given by the tangent to the path at its inflection point. Now the "solid" begins to decrease in U content, to a limit, given by the tangent to the end of the fractionation path at the boundary curve, reached between N and R. Then, as L follows the curve to P_5, the "solid" again moves to higher U content, reaching U_5 for L at P_5. Thereafter the solidification occurs as for region 1.

7. Path $m'N$: For a liquid on the path $m'N$ itself, the "solid" increases in Z (between the limits $m' \rightarrow r$), and then moves, in reverse, to U_5 as L moves on the curve from N to P_5. Thereafter the solidification occurs as for region 1.

Equilibrium Crystallization in the U_s Field

We finally consider the behavior of liquid on the U_s surface under conditions of complete equilibrium with the whole of the solid phase. For such crystallization with complete equilibrium, involving equilibrium paths crossing the fractionation paths, the behavior for the various regions would be as follows (all entirely analogous to the discussion of the regions in Fig. 6.4). When the liquid reaches a boundary curve, of liquid in equilibrium with two solids, it proceeds according to the equilibrium relations already considered above for Fig. 14.21. We are here dealing only with L on the surface itself.

1. Region between e_5 and the fractionation path UP_5: The equilibrium solid always increases in Z content. The equilibrium path does not

cross the line P_5U_5. The liquid reaches the boundary curve e_5P_5. (It reaches it at a point where the L–U_s leg of the three-phase triangle for L on the curve passes through the total original composition x.)

2. Region between path UP_5 and line U_5P_5: The solid always increases in Z. The equilibrium path crosses the line U_5P_5 on its way to the boundary curve, which is reached between e_5 and P_5.

3. Region between line U_5P_5 and path $m'N$: The solid always increases in Z. The equilibrium path does not cross the fractionation path $m'N$, and it reaches the boundary curve between P_5 and N.

4. Region between p_{11} and the path ZR: The solid always increases in U content. The equilibrium path does not cross the line Rv, and it reaches the boundary curve between R and p_{11}.

5. Region between the path ZR and the line Rv: The solid always increases in U. The equilibrium path crosses the line Rv, and it reaches the boundary curve between R and p_{11}.

6. Region between line Rv and line Nr: The equilibrium path does not cross the path $m'N$, and it ends on the curve between N and R.

(*a*) Region $rvRd$: The solid increases in U until the equilibrium path crosses the curve $m'R$; then the solid increases in Z content until L reaches the boundary curve.

(*b*) Region dNR: The solid always increases in U content for L on the surface.

7. Region between path $m'N$ and line Nr: The equilibrium path crosses the fractionation path $m'N$, to reach the boundary curve on the left of N, between N and a point c, where cm' is the L–U_s leg of the three-phase triangle for the curve with U_s at composition m'. The behavior above and below the curve $m'R$ differs as under region 6.

Subsolidus Compounds *E* and *F*

The solid equilibria after complete solidification of liquid will be affected, with further fall of temperature, by the appearance of the subsolidus compounds E and F of the system Y–U (Fig. 9.1). The pertinent isothermal relations are shown schematically in Fig. 14.24: (*a*) above T_E (temperature of formation of E from D and U in the binary system); (*b*) between T_E and T_F; (*c*) below T_F (temperature of formation of F from E and U in the binary system). Only the upper part of Fig. 14.21 is involved.

UNCLASSIFIED
ORNL-LR-DWG 25637

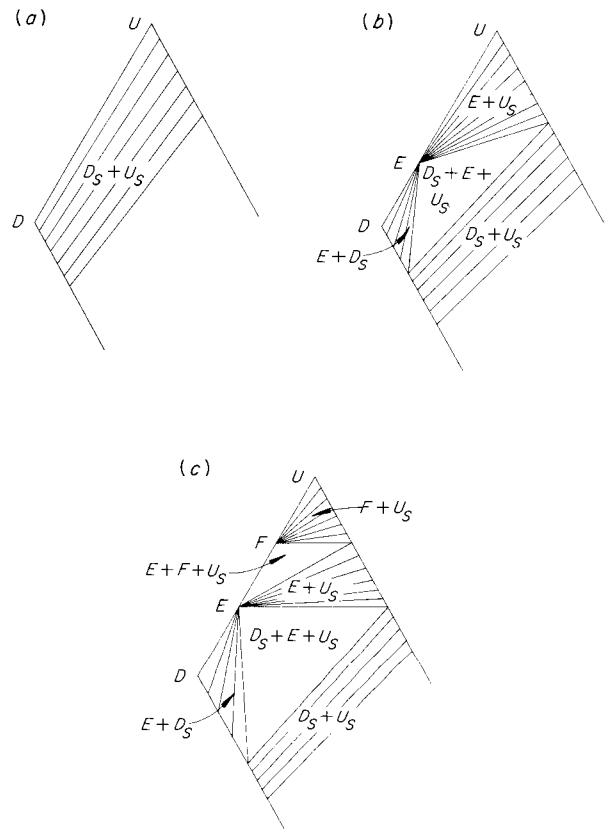

Fig. 14.24.

15. SYSTEM Y–W–Z: $NaF–ThF_4–ZrF_4$

The binary system $Y–W$ is shown schematically in Fig. 15.1, and $W–Z$ in Fig. 15.2. We note compound G in Fig. 15.1, decomposing on cooling at T_G. System $W–Z$ forms continuous solid solution with a minimum at m. The diagram for the system $Y–Z$ is used with the same lettering as shown in Fig. 11.1. It has the subsolidus compound D, solid solution in four compounds (A, B, D, and F), and transitions in two compounds (B and C).

The ternary diagram, as at present reported, is that of Fig. 15.3.

Despite the continuous solid solution in the $W–Z$ system there seems to be no solid solution formed across the diagram between the corresponding 2:1 compounds H and C.

The phase diagram as represented in Fig. 15.3 has two principal items of uncertainty. The first is the absence of a field for compound B of system $Y–Z$. The field now attributed to compound C pertains, actually, practically entirely to the 5:2 compound B, and only a small region of the "C field" of Fig. 15.3, near the boundary curve e_4E_6, pertains to the 2:1 compound C. There must be another three-solid triangle in the diagram, and another invariant point between m_2 and E_6. The second uncertainty concerns the invariant point E_8, reported as eutectic. If a temperature maximum definitely exists on the curve P_7E_8, then E_8 must be a eutectic. This temperature maximum, however, if it does exist (and its existence seems to be experimentally uncertain, actually), will not be, as now drawn, on the line WE, for the solid phase in the large field is not pure W but a continuous solid solution of W and Z. The curve P_7E_8, then, may or may not have a maximum on it, and if it does, the maximum must be on the right of the line WE. The mere position of E_8 in the triangle EWZ does not tell us whether it is a peritectic or a eutectic, for it is necessary to know its position in relation to the particular solid solution composition saturating the liquid at E_8.

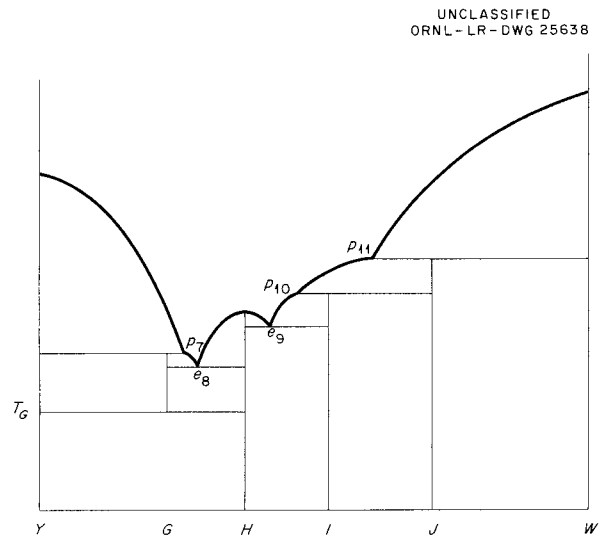

Fig. 15.1.

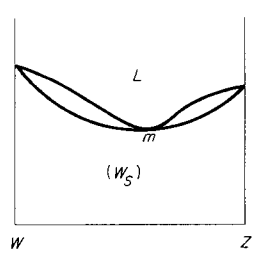

Fig. 15.2.

In Fig. 15.4 we assume, principally for the sake of clarity of discussion, that this invariant, now called E_9, is a eutectic; and an additional field is introduced between those for A and E, so that both B and C are now represented with primary fields.

In this schematic diagram, then, there are eleven fields and nine three-solid triangles (not all shown in Fig. 15.3) with corresponding invariant liquids. There are only two saddle points, m_1 between the A and the H fields, and m_3 between the fields for E and W_s (solid solution of W and Z).

Because of the binary solid solutions formed by the solid phases A, B, and F, the triangles in Fig. 15.4 are not drawn for the actual compositions of the solid phases involved at the invariant solutions. The probable relations will be discussed separately for the two principal regions of the system, shown in Figs. 15.5 and 15.7.

We shall assume that the saddle point m_1 is exactly on the line HA, although compound A forms solid solution in the direction of B. With this assumption, the line Hm_1A becomes a quasi-binary section (the only one in the system), and the region YHA an independent, simple subsystem, with two invariants, P_1 and E_2, involving pure solid phases. The final solids are either Y, G,

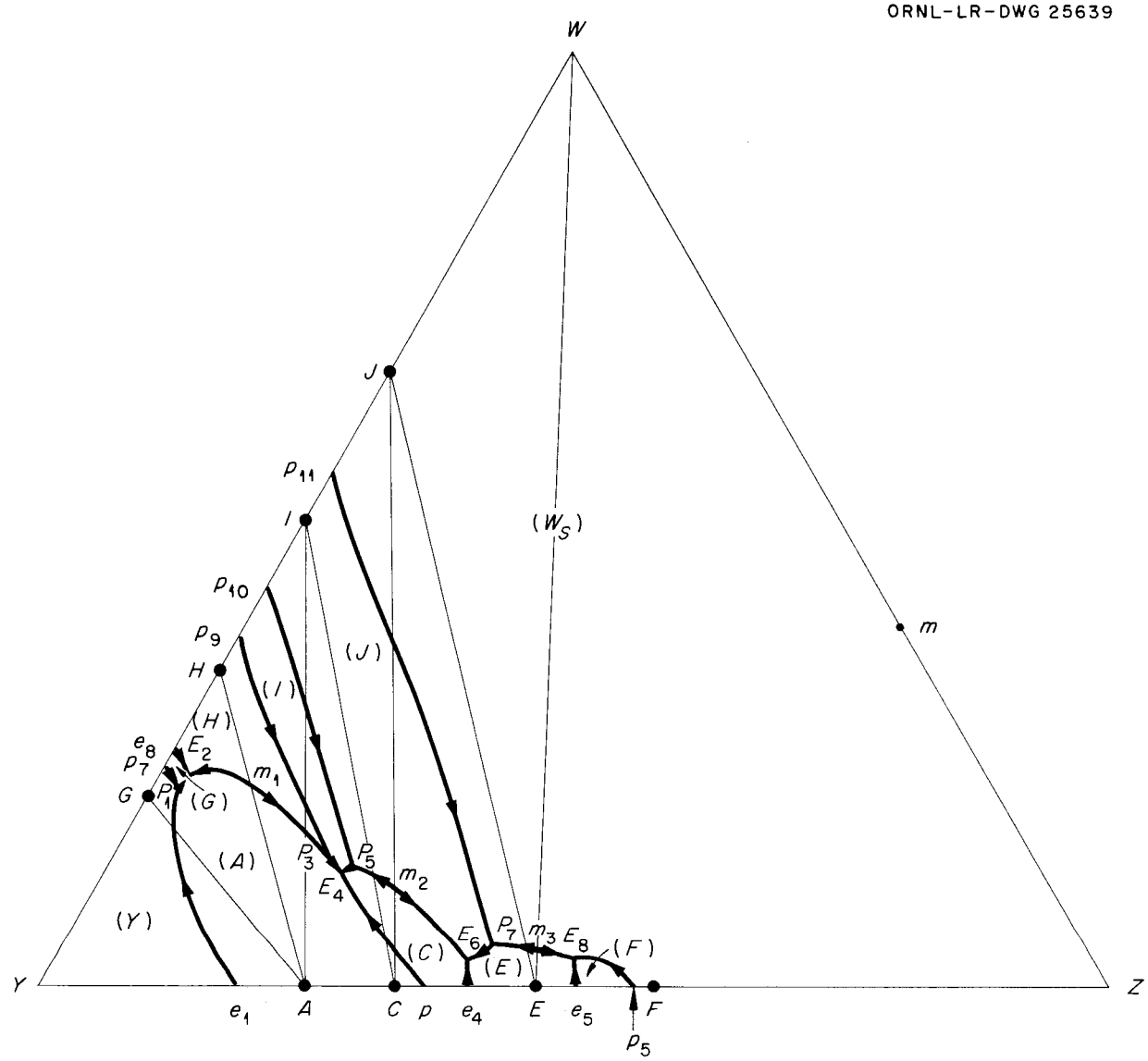

Fig. 15.3.

and A or G, H, and A; but below T_G of Fig. 15.1, G decomposes into Y and H, leaving Y, H, and A for the whole corner.

Some solid solution is involved at each of the other invariants of the system.

The region between the section HA and roughly JE is shown in detail, in Fig. 15.5, schematically, and distorted for clarity. The reactions along the curves are as follows:

1. m_1P_3: $L \rightarrow H + A$, the A solid starting as pure A and ranging to A_3 at P_3.
2. e_9P_3: $L \rightarrow H + I$.
3. $p_{10}P_5$: $L + J \rightarrow I$.
4. p_2P_4: $L + A \rightarrow B$, the A solid starting with the composition given by Fig. 11.1 at temperature p_2 and ranging to A_4 at P_4.
5. P_3P_4: $L \rightarrow I + A$, the A solid ranging from A_3 to A_4.
6. P_4P_5: $L \rightarrow I + B$, the B solid starting as pure B and ranging to B_5.
7. P_5P_6: $L \rightarrow J + B$, the B solid ranging from B_5 to B_6.

UNCLASSIFIED
ORNL-LR-DWG 25640

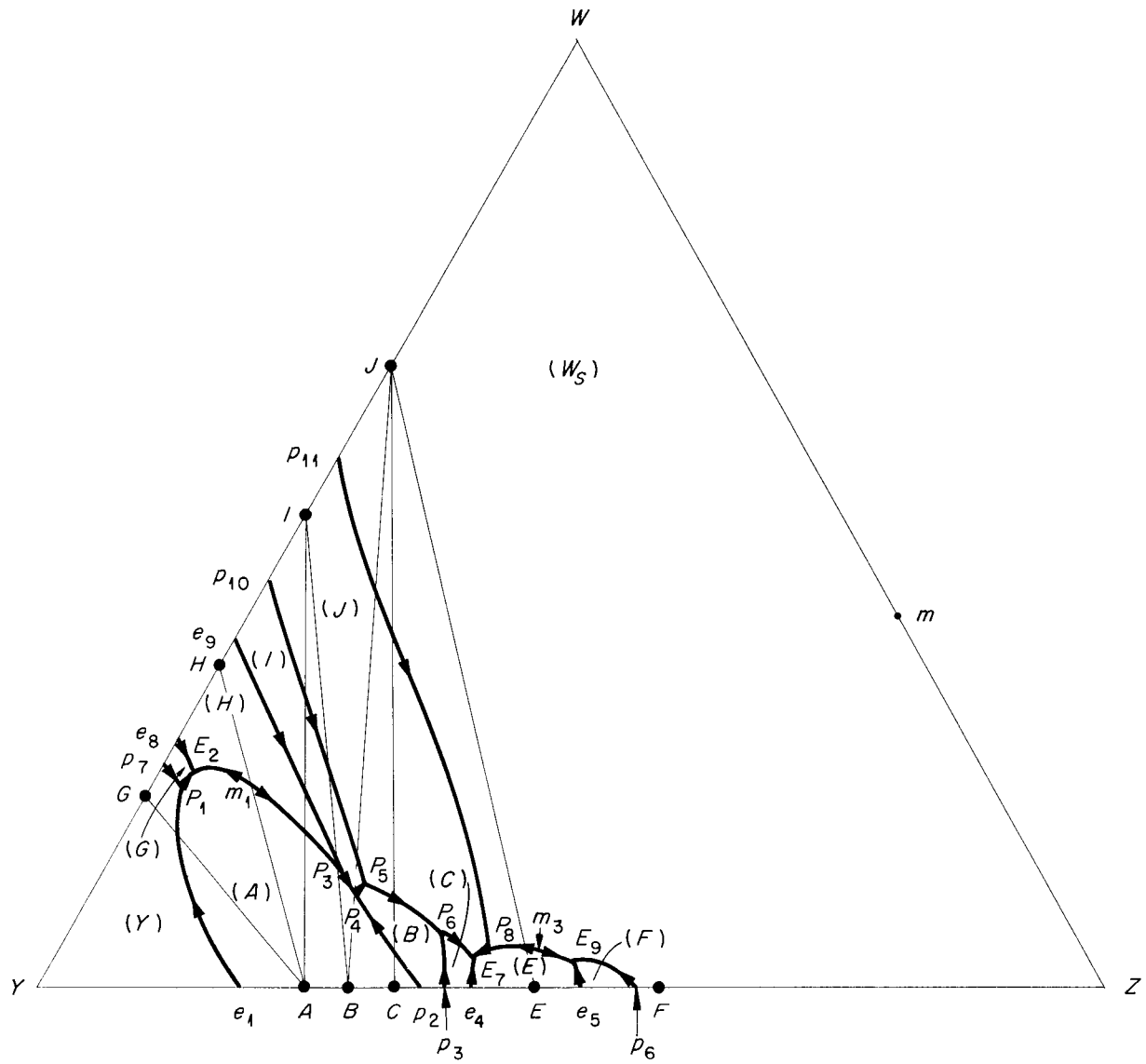

Fig. 15.4.

8. p_3P_6: $L + B \rightarrow C$, the B solid starting with the composition given by Fig. 11.1 at temperature p_3 and ranging to B_6 at P_6.

9. e_4E_7: $L \rightarrow C + E$, the E solid starting with the composition given by Fig. 11.1 at temperature e_4 and ending at $E_{(7)}$ (not to be confused with the eutectic point E_7).

10. P_6E_7: $L \rightarrow J + C$. (Note: the solid for the C field is C_α above the isothermal curve at t_1 and C_β below it.)

11. $p_{11}P_8$: $L + W_s \rightarrow J$, the W_s solid starting as pure W and ranging to W_8 (of Fig. 15.7).

12. P_8E_7: $L \rightarrow J + E$, the E solid starting as pure E and ending at $E_{(7)}$. (But the compositions of the solids at P_8 will be discussed further under Fig. 15.7.)

The invariant reactions are as follows:

P_3: $L + H \rightarrow A_3 + I$; incongruent crystallization end point for triangle III (HA_3I).

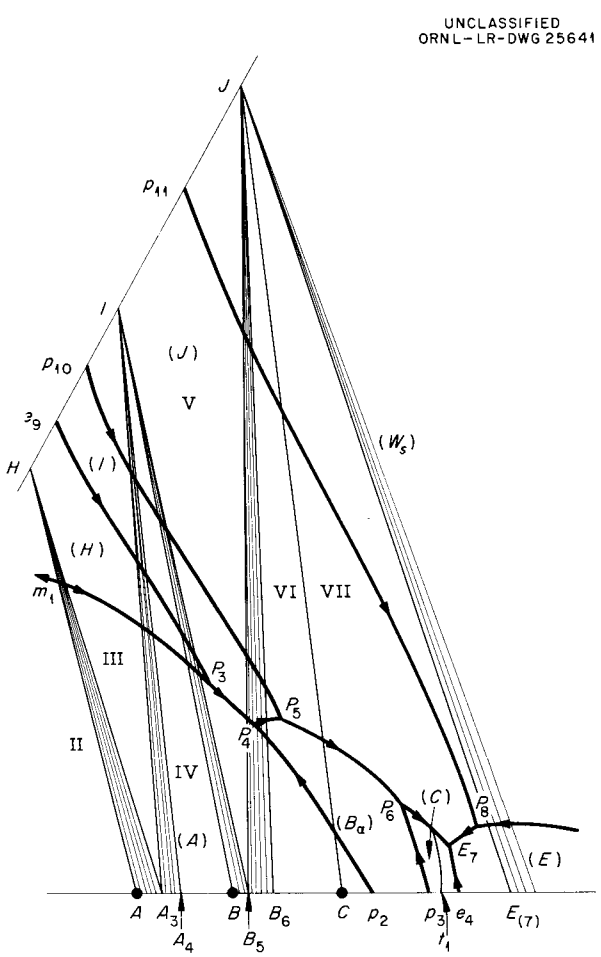

Fig. 15.5.

P_4: $L + A_4 \rightarrow \bar{I} + B$; incongruent crystallization end point for triangle IV (A_4IB).

P_5: $L + I \rightarrow B_5 + J$; incongruent crystallization end point for triangle V (B_5IJ).

P_6: $L + B_6 \rightarrow C_\alpha + J$; incongruent crystallization end point for triangle VI ($B_6C_\alpha J$).

E_7: $L \rightarrow C_\beta + J + E_{(7)}$; congruent crystallization end point for triangle VII [$C_\beta JE_{(7)}$].

Liquids with original compositions in the tie-line areas of Fig. 15.5 complete their crystallization on the various curves, leaving two-solid mixtures of one pure compound and one solid solution.

The B solid involved in the liquid equilibria of Fig. 15.5 is the B_α form. Figure 11.1 shows this form undergoing transition to the pure B_β between the temperatures T' and T'' in the binary system Y–Z. These temperatures are unaffected by the third component W. The changes in the solid-phase combinations brought about by this transition are shown in the series of schematic isotherms of Fig. 15.6: (*a*) between P_6 and T; (*b*) between T' and Q; (*c*) at Q; (*d*) between Q and T''; (*e*) below T''. The point Q is a four-solid invariant of type B, the reaction being:

$$I + B_\alpha(ss) - \text{calories} \rightleftharpoons J + B_\beta \ .$$

The two-solid equilibrium between I and $B_\alpha(ss)$ here shrinks to a line on cooling, to be replaced by the two-solid equilibrium between J and B_β (a line). At T'', between isotherms (*d*) and (*e*), the equilibrium between J and $B_\alpha(ss)$ shrinks to a line and vanishes.

Also, at temperature T_D of Fig. 11.1, below E_7 of Fig. 15.5, the compound D of system Y–Z appears, forming from C and $E_{(7)}$ (more exactly it forms from compound E of the composition given by Fig. 11.1 at the temperature T_D). This simply divides the triangle VII [which involves, at this temperature, C_γ, J, and $E_{(7)}$] into two triangles: one for C_γ, J, and D (pure D), and one for J and conjugate solid solutions of D and E, with compositions given in Fig. 11.1. At t_3 of Fig. 11.1, C_γ further changes to C_δ.

The remaining region of the system is shown schematically in Fig. 15.7, with a temperature maximum m_3 assumed to occur in the curve P_8E_9, and E_9 therefore a eutectic. The point E_9 therefore lies in a three-solid triangle (IX) involving the solids E, F, and a W–Z solid solution assumed to have the composition shown as W_9. The W_s composition in equilibrium with liquid at m_3, W_{m_3}, is, of course, on a line with m_3 and E. Although m_3, then, is a saddle point, the section $Em_3W_{m_3}$ is not quasi-binary, since the point W_{m_3} does not represent liquid and solid of the same composition in equilibrium. The point W_8 represents the W_s composition for triangle VIII, for the peritectic point P_8, together with the two solids J and E. It is assumed that the solid phase E is pure for liquids along the whole length of the curve P_8E_9, and that the binary solid solution of E (in the direction of C) enters only beyond P_8, on curve P_8E_7. It seems possible, however, that the E solid phase may begin to vary in composition even before P_8 is reached. In this case the line W_8E would end slightly to the left of E, as would also the line $W_{m_3}m_3E$. We assume, therefore, that the spread in the composition of solid E is insignificant along the curve P_8E_9.

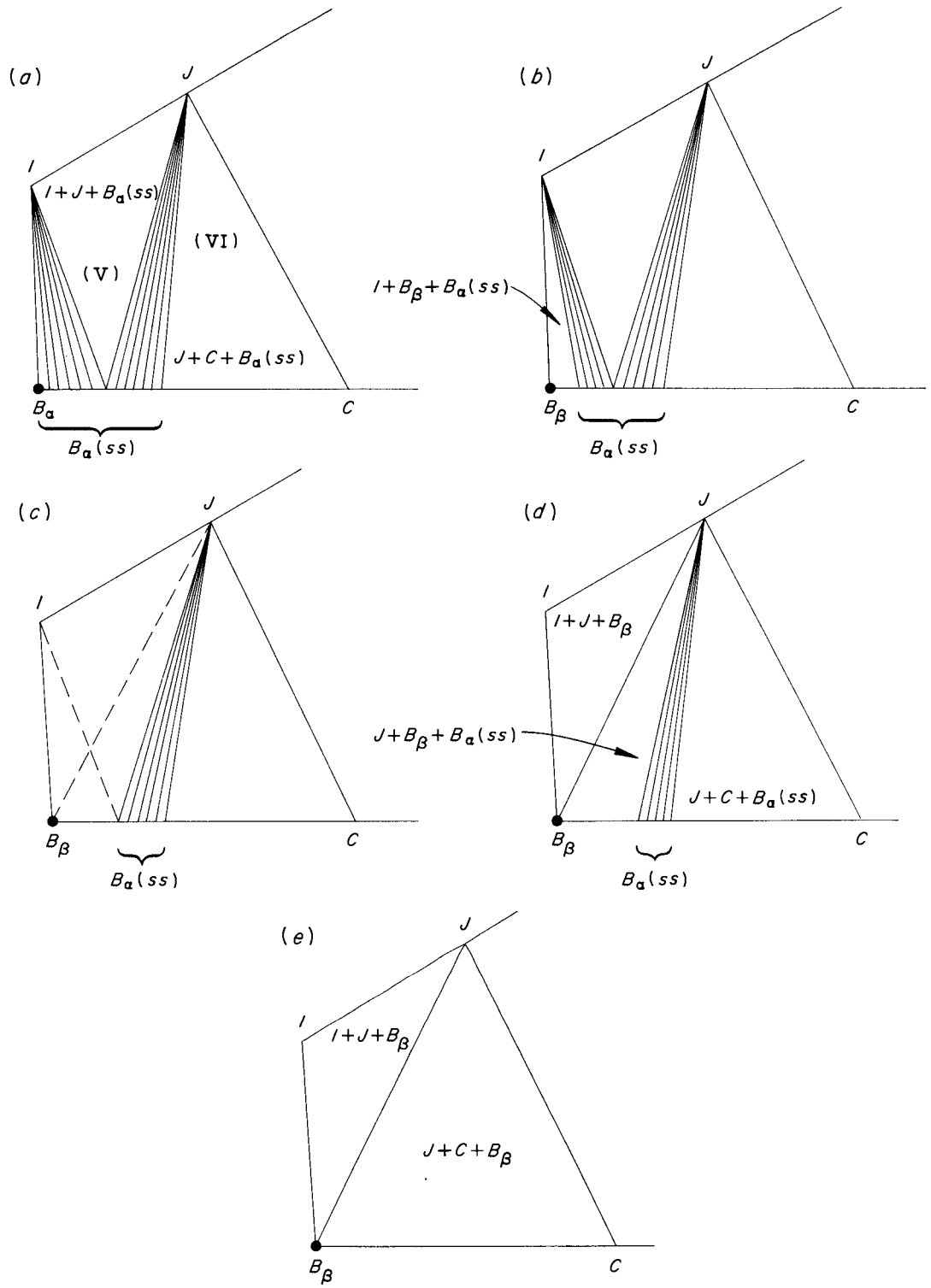
(a)
J
I
I+J+Bα(ss)
(VI)
(V)
J+C+Bα(ss)
Bα
C
Bα(ss)
(b)
J
I
I+Bβ+Bα(ss)
Bβ
C
Bα(ss)
(c)
J
I
Bβ
C
Bα(ss)
(d)
J
I
I+J+Bβ
J+Bβ+Bα(ss)
J+C+Bα(ss)
Bβ
C
Bα(ss)
(e)
J
I
I+J+Bβ
J+C+Bβ
Bβ
C

Fig. 15.6.

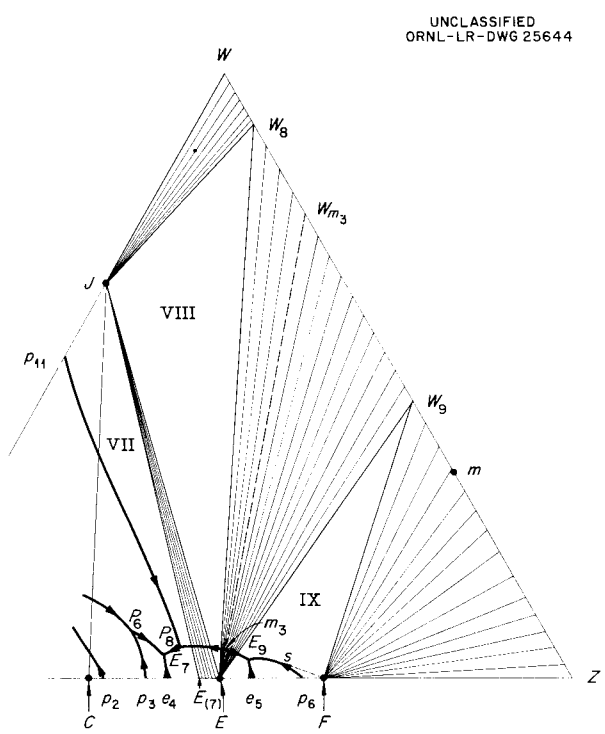

Fig. 15.7.

We consider this region, then, on the basis of the relations as drawn in Fig. 15.7.

The reaction on curve $p_{11}P_8$ is

$$L + W_s \rightarrow J \ ,$$

and the three-phase triangle starts as the line $p_{11}JW$ and ends as p_8JW_8. The curve is reached by liquids for original composition x in the region $p_{11}WW_8P_8$. For x in JWW_8, the liquid vanishes on the curve to leave J and W_s. For x in $p_{11}JP_8$, W_s vanishes on the curve, and L leaves the curve to traverse the J field on a straight line from J.

On the curve m_3P_8,

$$L \rightarrow E + W_s \ ,$$

the three-phase triangle starting as $Em_3W_{m_3}$ and ending as EP_8W_8. For x in the region $EW_8W_{m_3}$, the liquid vanishes on the curve to leave E and W_s. The curve is reached from the W_s field for x in $P_8W_8W_{m_3}m_3$ and from the E field for x in EP_8m_3. The point P_8 is reached for x in the quadrangle P_8JW_8E; the invariant reaction is

$$L + W_8 \rightarrow J + E \ .$$

This is the incongruent crystallization end point, then, for triangle VIII (JW_8E); but for x in EP_8J, L moves onto curve P_8E_7. Along this curve,

$$L \rightarrow J + E \ ,$$

with the three-phase triangle starting as JP_8E and ending as $JP_8E_{(7)}$, so that for x in $E_{(7)}JE$ the liquid vanishes on the curve to leave J and a solid solution between E and $E_{(7)}$.

Along curve m_3E_9,

$$L \rightarrow E + W_s \ ,$$

the W_s solid ranging between W_{m_3} and W_9. For x in the triangle $EW_{m_3}W_9$, the liquid vanishes on the curve to leave E and W_s. Along curve e_5E_9,

$$L \rightarrow E + F \ .$$

Curve p_6E_9 starts as

$$L + W_s \rightarrow F \ ,$$

from p_6 to point s, where the line Fs is tangent to the curve; between s and E_9,

$$L \rightarrow F + W_s \ .$$

The three-phase triangle starts as the line p_6FZ and ends as the triangle FE_9W_9. For x in FW_9Z, the liquid vanishes on the curve to leave F and W_s between Z and W_9. For x in the region Fp_6s, W_s vanishes on the curve, and L traverses the F field to reach either curve e_5E_9 or the even section of the original curve, sE_9, when W_s appears again, but as a secondary crystallization product mixed with F. The point E_9 is reached only for x in triangle IX, with the reaction

$$L \rightarrow E + W_9 + F \ .$$

Compositions in the region covered in Fig. 15.7, then, upon cooling in complete equilibrium, solidify either to a mixture of three solids (the corners of one of the triangles VII, VIII, and IX) or to mixtures of two solids, in the tie-line areas for J and W_s, for J and E, for E and W_s, and for F and W_s.

The fractionation paths on the surface for liquid in equilibrium with W_s are sketched in Fig. 15.8, on the basis of the assumptions made in Fig. 15.7. Line W_8P_8 is tangent to the fractionation path ending at P_8, $W_{m_3}m_3$ is tangent to the path Wm_3,

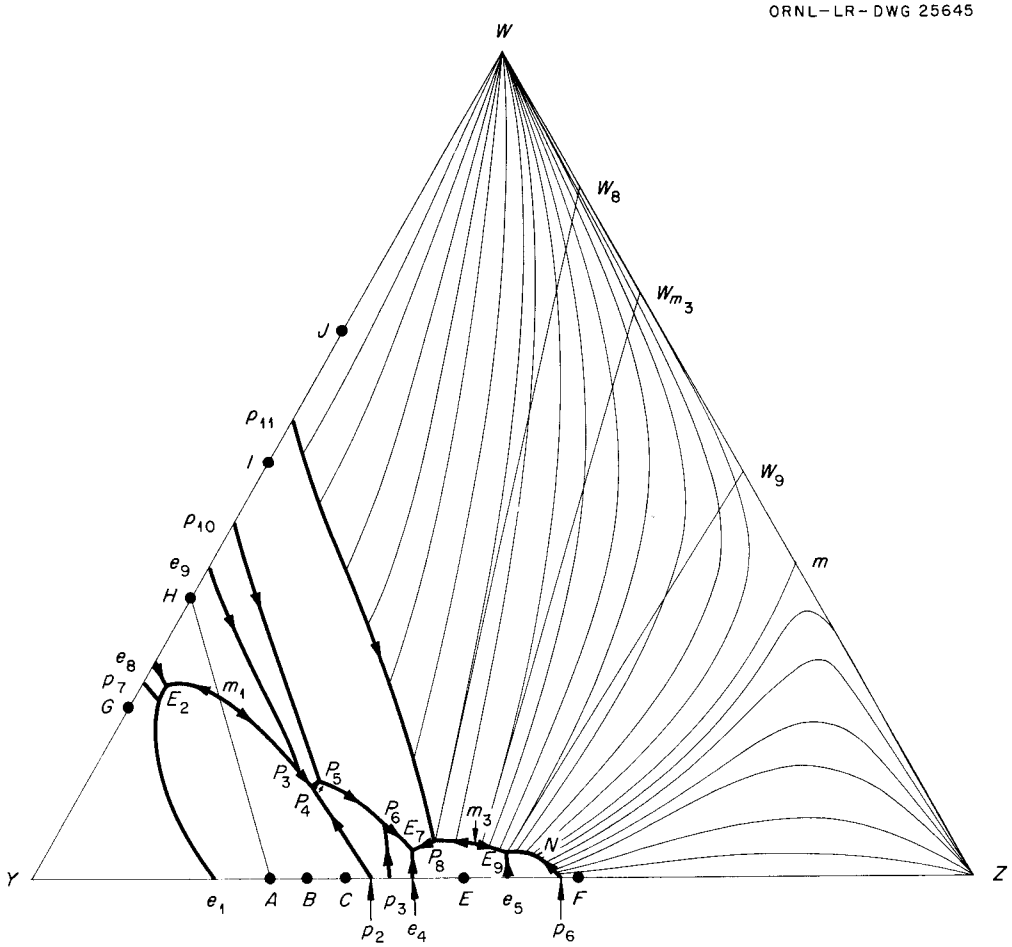

Fig. 15.8.

and W_9E_9 is tangent to the path WE_9. Curve mN is the limiting fractionation path dividing the separate families of paths originating at W and at Z. The path mN is assumed to be convex with respect to Z and to end (at N) on the curve p_6E_9. The paths on the W side of mN are convex, throughout, toward Z; the solid solution being precipitated on this surface continually increases in Z content. Those on the Z side start as convex with respect to W, but some of them (nearing mN) pass through an inflection point before reaching the boundary curve between p_6 and N. For these paths the solid solution precipitated by liquid traveling on the surface first increases and then decreases in W content before reaching the curve.

The complete fractionation process tends toward one of the eutectics E_7 and E_9 as limit. It must be remembered that on reaching a transition curve in such a process L does not travel on the curve but immediately crosses it. This occurs, therefore, in a narrow region between Z and the curve p_6E_9, where the odd section of the curve (p_6s) would be crossed. Liquids reaching the boundary curves between m_3 and p_6 all end at E_9, however, whether or not they cross the transition curve, and the final solids consist of E, F, and W_s.

The curves $p_{11}P_8$ and $p_{10}P_5$ are also crossed in the fractionation process. Consequently in a narrow region between W and the beginning of the curve $p_{11}P_8$, liquids will end on the curve e_9P_3, then proceeding to E_7 as limit, leaving W_s, J, I, H, A, B, C, and E in the final nonequilibrium mixture. For liquids a little farther out from the YW side, the curve e_9P_3 will just be missed, and the solid H will not be present at the end. If the curve $p_{10}P_5$ is just missed, then both A and I will also be absent. If the liquid misses the curve P_5P_6, and ends to the right of P_6, then the final solids will be W_s, J, C, and E; this will be the mixture obtained for liquids up to the fractionation path Wm_3.

INTERNAL DISTRIBUTION

1. C. E. Center
2. Biology Library
3. Health Physics Library
4–5. Central Research Library
6. Reactor Experimental Engineering Library
7–26. Laboratory Records Department
27. Laboratory Records, ORNL R.C.
28. A. M. Weinberg
29. L. B. Emlet (K-25)
30. J. P. Murray
31. J. A. Swartout
32. E. H. Taylor
33. E. D. Shipley
34. S. C. Lind
35. M. L. Nelson
36. C. P. Keim
37. J. H. Frye, Jr.
38. R. S. Livingston
39. H. G. MacPherson
40. F. L. Culler
41. A. H. Snell
42. A. Hollaender
43. M. T. Kelley
44. K. Z. Morgan
45. C. F. Weaver
46. A. S. Householder
47. C. S. Harrill
48. C. E. Winters
49. H. E. Seagren
50. D. Phillips
51. F. C. VonderLage
52. D. S. Billington
53. J. A. Lane
54. M. J. Skinner
55. W. H. Jordan
56. G. E. Boyd
57. C. J. Barton
58. J. P. Blakely
59. M. Blander
60. F. F. Blankenship
61. C. M. Blood
62. S. Cantor
63. R. B. Evans
64. H. A. Friedman
65. R. A. Gilbert
66. W. R. Grimes
67. H. Insley
68. F. Kertesz
69. S. Langer
70. R. E. Meadows
71. R. E. Moore
72. G. J. Nessle
73. R. F. Newton
74. L. G. Overholser
75. J. D. Redman
76. J. H. Shaffer
77. R. J. Sheil
78. N. V. Smith
79. R. A. Strehlow
80. B. J. Sturm
81–90. R. E. Thoma
91. W. T. Ward
92. G. M. Watson
93. M. A. Bredig
94. S. Datz
95. R. E. Minturn
96. A. S. Dworkin
97. G. P. Smith
98. M. T. Robinson
99. A. J. Miller
100. L. G. Alexander
101. R. R. Dickison
102. G. W. Keilholtz
103. W. D. Manly
104. A. P. Fraas
105. L. E. Mann
106. F. R. Bruce
107. E. S. Bettis
108. R. P. Milford
109. R. A. Charpie
110. W. K. Ergen
111. R. B. Lindauer
112. J. C. White
113. A. S. Meyer
114. W. F. Vaughn
115. D. E. Ferguson
116. R. E. Blanco
117. J. T. Long
118. G. I. Cathers
119. W. H. Carr, Jr.
120. H. E. Goeller

121. J. O. Blomeke
122–141. J. Ricci (consultant)
142. C. E. Larson (consultant)
143. P. H. Emmett (consultant)
144. H. Eyring (consultant)
145. G. T. Seaborg (consultant)
146. ORNL – Y-12 Technical Library, Document Reference Section

EXTERNAL DISTRIBUTION

147. Division of Research and Development, AEC, ORO
148. W. W. Grigorieff, Oak Ridge Institute of Nuclear Studies
149–151. University of Cincinnati (1 copy each to H. S. Green, J. W. Sausville, and T. B. Cameron)
152. E. F. Osborn, Pennsylvania State University, University Park, Pennsylvania
153–713. Given distribution as shown in TID-4500 (14th ed.) under Chemistry-General category (75 copies – OTS)